BARC-P--1 (Vol. 2)

PROCEEDINGS OF THE

CHEMISTRY SYMPOSIUM 1969

VOLUME II
CONTRIBUTED PAPERS

ORGANISED BY
THE CHEMISTRY & METALLURGY COMMITTEE OF THE
DEPARTMENT OF ATOMIC ENERGY
GOVERNMENT OF INDIA
1970

PROCEEDINGS OF THE CHEMISTRY SYMPOSIUM

Sept. 23-26, 1969

VOLUME II
CONTRIBUTED PAPERS

ORGANISED BY
THE CHEMISTRY & METALLURGY COMMITTEE OF THE
DEPARTMENT OF ATOMIC ENERGY
GOVERNMENT OF INDIA

CONTENTS

ELECTRIC POLARIZATION AND STRUCTURE OF MOLECULAR COMPLEXES OF SILVER PERCHLORATE WITH AROMATIC HYDROCARBONS

V. N. Krishnamurthy and S. Soundararajan
Department of Inorganic and Physical Chemistry,
Indian Institute of Science, Bangalore 12

The infra-red spectra of a polycrystalline sample of silver perchlorate-benzene complex shows the absence of any intense band near 1000 cm^{-1}, typical of π-complexes of benzene with centrosymmetrical arrangement for the metal atom[1]. In the ultra-violet absorption spectra of silver perchlorate in benzene[2, 3], the benzene band doubles in intensity but is unchanged in energy. Also, a new band appears at 2300 Å (ϵ = 1500) which has been attributed to charge transfer transition. The charge transfer transition energy has been calculated to be ~15.7 kcal/mole.[4]

The gross geometrical features of the silver perchlorate benzene has been predicted by Mulliken[5, 6] and Dewar[7] and verified by Smith and Rundle[4] from X-ray investigations. According to these authors, the silver atom is situated approximately above one of the C-C bonds of the ring.

Measurements of electric polarization have, therefore, been made on a few of the aromatic hydrocarbon-silver perchlorate complexes using benzene as solvent and interpreted in terms of Mulliken's theory.[5, 6]

PREPARATION OF THE COMPLEXES

The complexes of toluene and tetralin were prepared by dissolving silver perchlorate in toluene and tetralin respectively and the complexes were isolated using dry petroleum ether dried over silica gel in a vacuum desiccator for an hour. All the operations were carried out inside a dry box in a dark room.

Apparatus and Methods of Measurement

The dielectric constant measurements were made with a.c. mains operated heterodyne beat apparatus. Densities of solutions were obtained using an Ostwald-Sprengel pyknometer. The molar polarization of the solute at infinite dilution was calculated using the mean values of the Hedestrand's constants α and β. The molar refraction of silver perchlorate in aqueous solution was determined for the sodium D line using Brice-Phoenix differential refractometer at 35°C. Molecular weights of these complexes were determined cryoscopically in dry benzene.

Calculation of Ionic Character Using Mulliken's Theory

Mulliken's[5, 6] theory can be applied to a wide variety of donor(D) and acceptor(A) entities. The amount μ_N which is equal to the experimentally determined μ_{AD} of the molecular compound is given by the equation

$$\mu_N = \int \psi_N M \psi_N \, d\nu$$

$$= a^2\mu_O + b^2\mu_1 + abS(\mu_1 - \mu_O) + 2abS\mu_O$$

where μ_O is the vector sum of the component moments of A and D, μ_1 = e. γ_{AD} (e, the electronic charge and γ_{AD}, the equilibrium distance between Ag^+ and the benzene ring. From the values of μ_1, μ_O, μ_N and S, the coefficients a and b have been calculated. The values $b^2/(a^2 + b^2)$ may be taken as corresponding to the ionic character of the compound as defined by Mulliken.

RESULTS AND DISCUSSION

The observed moments of silver perchlorate in benzene (5.36D) and in toluene (4.41D) are comparable with those reported for silver perchlorate in benzene (4.70D)[8] and for aluminium bromide in benzene (5.2D)[9], indicating the presence of molecular complexes in line with other physical measurements.[10] This moment is less than that calculated for uncomplexed silver perchlorate, suggesting that the bond involve a strong π-type bond superposed on a weak π-type bond, as suggested by Dewar.

For the application of Mulliken's theory to the complexes, the silver ion has been taken as the donor and the benzene ring as the acceptor in view of the above discussion. From the values of a^2 and b^2 it is seen that $a^2 > b^2$ for both the complexes and the ionic character for benzene and toluene complexes are respectively 15.55% and 32.95%.

In line with the above dipole moment, data are the observations of Turner and Amma[11] on the crystal data of silver perchlorate-benzene complex. According to them, if the acceptor were a 5s orbital or sp^3 hybrid orbital, the most advantageous position would be at the point of greatest electron density of the ring directly above one of the carbon atoms. On the other hand, using the inner d-orbitals of the metal as donor, the most likely position would be above and symmetrically between two carbon atoms of the ring. The closest carbon-metal distances of 2.50 and 2.63 Å observed by Smith and Rundle[4] indicate a compromise between the acceptor and the donor properties of the silver ion.

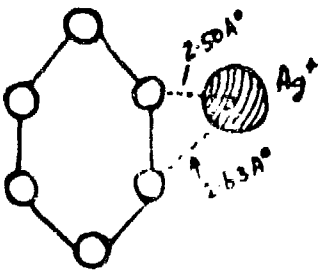

Determinations of molecular weight of toluene and tetralin complexes of silver perchlorate in benzene show a dissociation of the complexes into more or less two species (observed molecular weight being $\frac{1}{2}$ of that calculated) as follows:

$$AgClO_4.Ar \xrightarrow[\text{solvent}]{C_6H_6} AgClO_4.C_6H_6 + Ar.$$

i. e., the benzene molecule displaces the aromatic hydrocarbon from the coordination sphere. So, the observed polarization values for toluene and tetralin complexes agree with those calculated applying the mixture rule.

Polarization Data for Silver Perchlorate and its Complexes in Benzene at 35 - 0.02°C

	$AgClO_4$ in benzene	$AgClO_4$ in toluene	$AgClO_4$-Toluene		$AgClO_4$-Tetralin	
Total polarization(cm^3)	585.38	400.56	604.86		645.29	
Polarization of the ligands(cm^3)	-	-	33.50	618.88	50.63	636.0
Polarization of $AgClO_4$ in benzene(cm^3)	-	-	585.38		585.38	

Ionic Character of the Complexes*

Molecular compound	Moment of the complex	a	b#	$b^2/(a^2+b^2)$
Silver perchlorate-benzene	5.36	0.8588	0.3685	0.1555
Silver perchlorate-toluene	4.41	0.7518	0.5258	0.3295

* The value of the overlap integral S is taken to be 0.2. μ_0 = 6.08 D and μ_1 = e x 2.57 Å = 12.34 D.

Mainly because of its strong dependence on the uncertain quantity S, the value of b can only be relative.

REFERENCES

1. L. W. Daasch; Spectrochim. Acta 9, 726 (1959)
2. B. G. Torne-Mori, D. Janjic and B. P. Susz; Helv. Chim. Acta 47, 1172 (1964).
3. J. N. Murrell and S. Carter; J. Chem. Soc. 6185 (1964)
4. H. G. Smith and R. E. Rundle; J. Am. Chem. Soc. 80, 5075 (1958)
5. R. S. Mulliken; J. Am. Chem. Soc. 74, 811 (1952)
6. R. S. Mulliken; J. Phys. Chem. 56, 801 (1952)
7. M. J. S. Dewar; Bull. Soc. Chim. France 18, C 79 (1951)
8. J. W. Williams and R. J. Allgeier; J. Chem. Soc. 49, 2416 (1927)
9. A. L. McClellan; "Tables of dipole moments", W. H. Freeman and Co., San Francisco (1963)
10. D. F. R. Gilson and C. A. McDowell; J. Chem. Phys. 39, 1825 (1963)
11. Turner and E. L. Amma; J. Am. Chem. Soc. 88, 1877 (1966)

A STUDY OF BERYLLIUM 2-METHYL OXINATE PRECIPITATED FROM HOMOGENEOUS SOLUTION

T. P. Prasad* and M. N. Sastri
Department of Chemistry, Andhra University, Waltair

In this paper, we report our observations on some aspects of the beryllium-2-methyl oxinate complex obtained from homogenous solutions using the well-known urea hydrolysis and mixed solvents technicques.

EXPERIMENTAL

Beryllium nitrate solution was prepared from analytical reagent grade sample and was standardized gravimetrically.

A 5% solution of 2-methyl oxinate (reagent grade) was prepared in acetone.

1% triethanolamine (reagent grade) (W/V) in water.

All other reagents were of reagent grade.

Apparatus

Thermogravimetric analysis was carried out in air at atmospheric pressure with the Stantan Model TR-1 thermobalance. The balance has a sensitivity of 1 mg., a linear heating rate of 4°C per minute, and a chart speed of 6" per hour.

The infra-red spectra were taken as mujol mulls using Perkin Elmer-237 Spectrophotometer.

X-ray spectra were taken with a Philips 114.6 mm Camera.

Precipitation of the Complex

Priliminary investigations showed that the complex cannot be precipitated from acetic acid medium. Hence, the precipitations were carried out from ammonical medium. A large excess of the reagent was found to be necessary to get a well crystallized complex and the precipitation was incomplete under all the experimental conditions studied. The procedures described here give the maximum yield.

*Present Address: Regional Research Laboratories, Bhubaneswar-4 Orissa.

a) Urea Hydrolysis Method

To the solution containing not more than 9.0 mg. beryllium (25.0 mg. BeO) in a 100 ml. beaker, were added 8 ml. of the reagent followed by 5.0 gms. of urea. The volume was adjusted to 50 ml. The beaker was immersed in a hot water bath at 70°C until the precipitation started and then the temperature was raised to 90 to 100°C. The solution was kept at this temperature until the precipitate settled down leaving the supernatent solution clear. (Total time of precipitation is approximately 90 to 100 mins.). The solution was filtered hot through a sintered glass crucible of porosity 3, and washed several times with small portions of hot distilled water. The precipitate remaining in the beaker was removed by a jet of hot water. The precipitate was then dried at 110°C to constant weight and weighed as $Be(C_{10}H_8NO)_2$. The filtrate showed a pH of 8.0 to 8.5. The results are shown in Table I.

b) Mixed Solvents Method

To the solution containing not more than 9.0 mg. beryllium in a 100 ml. beaker, were added 8 ml. of the 2-methyl oxinate reagent, 25 ml. acetone and 2 ml. of triethanol amine (1% W/V) in water. The volume was adjusted to 50 ml. with water. The beaker was immersed in a hot water bath maintained at 70°C. The volume of the solution lost during heating was replaced by the addition of hot water. When the precipitation was complete as indicated by the clear orange-yellow supernatent solution (total time is 90 mins.), the filtration was carried out while hot through a sintered glass crucible of porosity 3. The precipitate remaining in the beaker was removed by a jet of hot water. The precipitate was washed several times with small portions of hot water, dried at 110°C to constant weight and weighed as $Be(C_{10}H_8ON)_2$. The results are given in Table II.

Thermogravimetric, X-ray, and IR studies were carried out on samples dried at 110°C.

RESULTS AND DISCUSSION

The results of Tables I and II clearly show that the precipitation of the complex as represented by the formula, $Be(C_{10}H_8ON)_2$, is not quantitative. The precipitate obtained by urea hydrolysis technique is in the form of shining green crystals, the shape of which is not clear to the naked eye. The complex obtained by mixed solvents method was in the form of shining green needles. However, under microscope both of them appeared as large euhedral crystals. The

precipitates obtained by both the methods showd yellow-green fluorescence under ultra-violet light. It was observed that a thin white layer remains on the walls of the beaker. This layer, on dissolving in acid and testing gave positive test for beryllium. Thus, it appears that first beryllium hydroxide is formed which in turn reacts with the precipitating agent to give the complex. The hydroxide formed on the walls loses its capacity to react with the reagent and hence remains unattacked. This leads probably to the incomplete precipitation. Freshly precipitated beryllium hydroxide when mixed with the solid reagent and kept under ultra-violet light, at first shows no yellow-green fluorescence. But, in a few minutes, the yellow-green fluorescence can be noticed. Aged beryllium hydroxide fails to show such fluorecence.

The analysis of the precipitate clearly shows that the complex confirms strictly to the formula, $Be(C_9H_8NO)_2$.

The complex easily dissolves in common organic solvents as chloroform, acetone and alcohol.

The differential thermogravimetric curves of the substances obtained from homogeneous solution, together with that obtained Motojima's procedure, are given in Figures 1, 2 and 3. It can be seen that all the curves are more or less similar. The complex is stable upto about 220°C showing a sharp maximum in the 450-460°C region (that obtained by Motojuma's procedure[4] shows at 410°C). The decomposition above 460°C is complex, and probably represents oxidation of carbonaceous matter with simultaneous adsorption and desorption of the gaseous products on the solid phase. The complexes obtained from homogeneous solution are converted to oxide at 700°C whereas that obtained by the direct addition method[4] is converted to oxide at 760°C.

The complex was found to have a melting point at 250 ± 1°C. The thermogravimetric curves show that the complex undergoes some loss before the melting point is reached. When a small amount of the compound was taken in an ignition tube and heated slowly, it melted, first giving highly viscous oily liquid which on further heating decomposed. During melting, a pale yellow liquid condensed on the mass on cooling. This crystalline mass melted at 72°C, indicating that it is 2-methyl oxine.

In view of the absence of coordinated water in the complex, the formation of free reagent from the complex seems to be peculiar and cannot be explained on the lines we suggested for the case of Be oxinate complex[1].

Infra-red spectrum always indicated the presence of moisture in the complex. It is presumed that water is present only in trace amounts as micro-analysis does not indicate any deviation from the formula. In fact our attempts to get IR spectrum of perfectly dry compound failed. It is noteworthy that the complex takes only trace amounts of water from atmosphere (or probably retains) irrespective of the time of preservation (that is, the mcro-analysis shows the same result even after one month).

On this basis, an attempt is made to explain the evolution of free reagent from the complex on heating. It is suggested that the complex undergoes solid state hydrolysis utilizing moisture from the atmosphere which is initiated by the traces of adsorbed or retained moisture already present in the complex (as indicated by the IR spectrum), according to the reaction:

$$Be(C_{10}H_8NO)_2 + H_2O = Be(C_{10}H_8NO)\,OH = + C_{10}H_9NO \quad \ldots\ldots \quad 1$$

the hydroxy complex further undergoes decomposition at higher temperature to give beryllium oxide and carbondioxde etc., according as

$$Be(C_{10}H_8NO)_2OH = BeO + \text{Decomposition products of the complex.} \quad \ldots\ldots \quad 2$$

The reaction 1 is represented by peak I of the thermogravimetric analysis while the peak II indicate the reaction 2.

X-ray examination was carried out using Philips 114.6 mm. camera. On analysis of the X-ray results, it was found that the unit cell containing four molecules is primitive ortho-rhombic with a = 9.348 Å, b = 13.03 Å and c = 15.12 Å. X-ray and pyknometric densitives were 1.17 and 1.10 respectively.

REFERENCES

1. T. P. Prasad and M. N. Sastri; Talanta 14,481 (1967)

TABLE I

Precipitation of Beryllium 2-methyl Oxinate by Urea Hydrolysis technique

Theoretical weight mg.	Weight obtained mg.
109.70	95.6
109.70	100.3
109.70	97.8
165.49	150.5
165.49	155.6
165.49	155.2

TABLE II

Precipitation of Beryllium 2-methyl Oxinate Complex from Mixed Solvents (Acetone-Water)

Theoretical weight mg.	Weight obtained mg.
109.70	104.6
109.70	105.2
109.70	105.0
109.70	104.8
165.49	161.6
165.49	161.6
165.49	157.5
165.49	157.2

FIG. 1

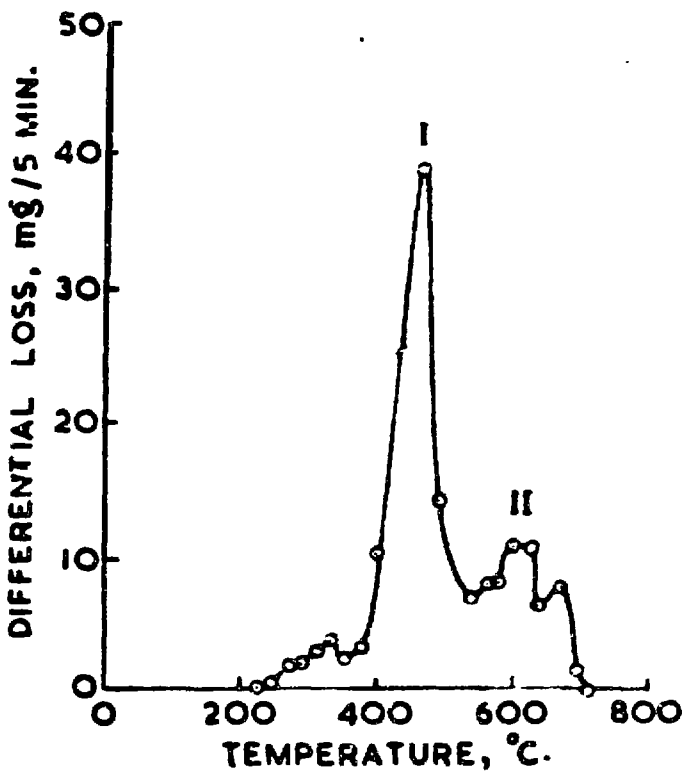

D.T.G. CURVE FOR THE COMPLEX BY UREA HYDROLYSIS METHOD.

FIG. 2

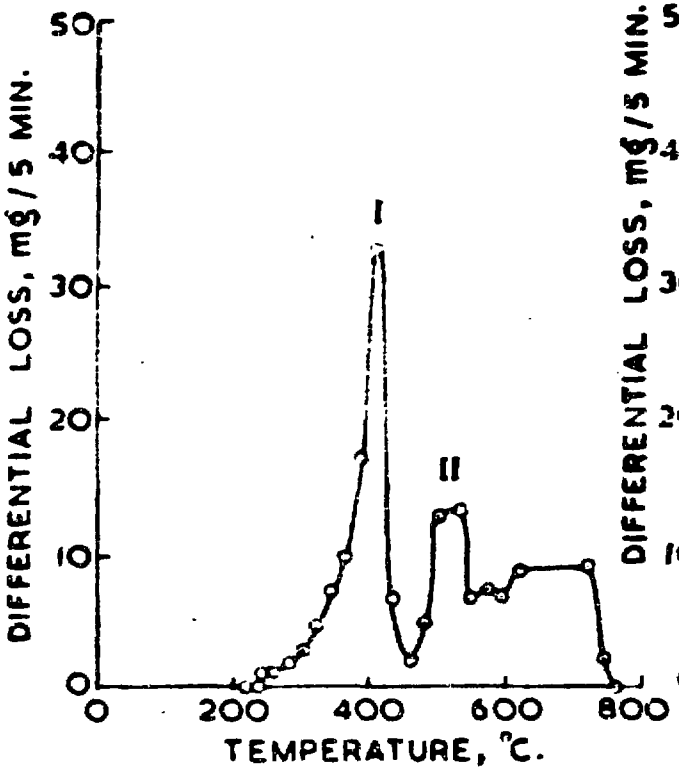

D.T.G. CURVE FOR THE COMPLEX BY MOTOJIMA'S METHOD

FIG. 3

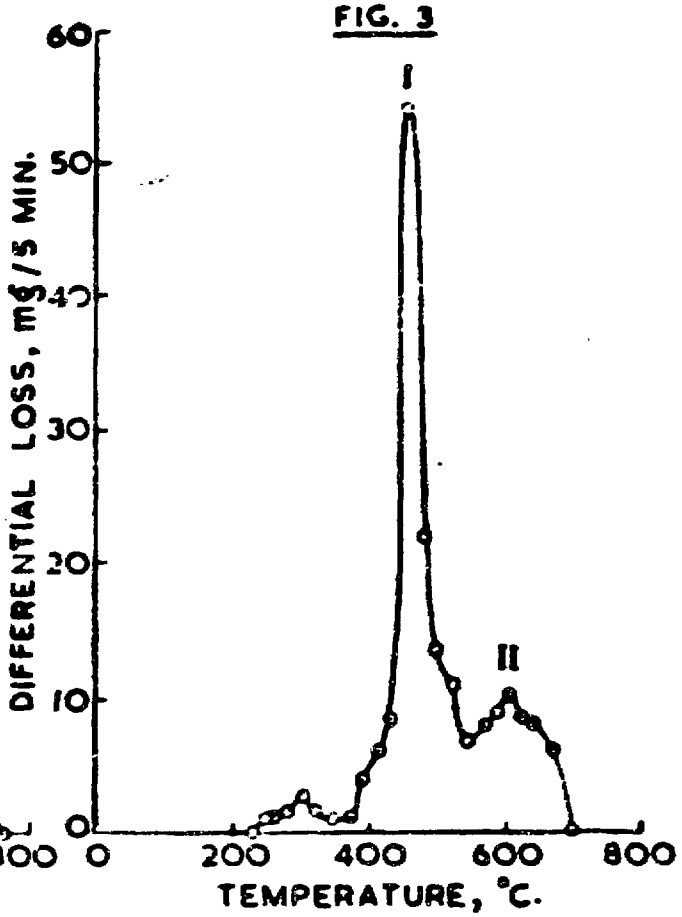

D.T.G. CURVE FOR THE COMPLEX BY MIXED SOLVENTS METHOD.

ADDITION COMPOUNDS OF ALDEHYDES WITH SOME GROUP (IV) HALIDES

Ram Chand Paul, Hem Raj and S. L. Chadha
Department of Chemistry, Punjab University, Chandigarh

INTRODUCTION

Literature records the preparation of a few addition compounds of aldehydes with some group (IV) halides.[1-3] However, not much has been indicated regarding the structure of these adducts. Instead, there appears some discrepency regarding the nature of bonding based on the lowering of carbonyl stretching frequency of aldehyde on co-ordination. Terenin et al.[4] have suggested a strong coordination between tin (IV) halides and acetaldehyde while Schwartz and Bernd[5] pointed out a very weak force present between titanium (IV) halides and benzaldehyde. The present study, therefore, has been undertaken to throw some light on the nature of the adducts of aldehydes such as naphthaldehydes, phthalaldehyde, benzaldehyde, salicyldehyde and furanaldehyde with some group (IV) halides, by examining their infra-red spectra (4000-250 cm^{-1}), dipole moment, molecular weight, molar conductance and heat of formation.

EXPERIMENTAL

Purification of aldehydes[6] and metal halides[7, 8] has already been described. The addition compounds have been prepared by a method similar to one already described for analogous antimony (V) chloride adducts.[6] The details for the physical measurements have also been described already.[6]

RESULTS AND DISCUSSIONS

Group (IV) halides such as tin (IV) chloride and bromide, titanium (IV) chloride and bromide and zirconium (IV) chloride form solid addition compounds with aldehydes having 1:2 stoichiometry except for phthalaldehyde which forms adducts having 1:1 composition. The analytical data suggest that possibly the coordination number six is attained by tin, titanium and zirconium in these adducts. The molar conductance of milimolar solutions of these adducts in nitrobenzene is between 2-5 cm^2 ohm^{-1} $mole^{-1}$ which suggests them to be predominently covalent.[9] Molecular weight determination of some of these adducts in benzene or nitrobenzene indicate them to be monomolecular in these solvents.

Infra-red spectra of the adducts reveal the lowering by 50-150 cm^{-1} of the carbonyl stretching frequency of pure aldehyde on complex formation which indicates the coordination of carbonyl oxygen of aldehyde to the metal atom. It may be mentioned that the carbonyl stretching frequency of naphthaldehyde at 1700 cm^{-1} shifts to 1550 cm^{-1} in its adduct with titanium (IV) chloride and such a large shift does not agree with the earlier work by Schwartz and Bernd.[5] New bands in 400-460 cm^{-1} spectral region in these adducts are associated with the oxygen $\longrightarrow$ metal vibrations.[7, 8] Strong intensity bands present in 300-330 cm^{-1} spectral region in tin (IV), titanium (IV) and zirconium (IV) chloride adducts, respectively are due to metal-halogen vibrations and they compare well with those of other hexacoordination compounds of these metal chlorides.[10-12]

Dipole moment of a few tin (IV) halide adducts have been determined. The dipole moment of pure tin (IV) chloride is nearly zero while that of aldehydes lie between 2 - 3.5D.[13] The dipole moment of the adducts of tin (IV) chloride and bromide with naphthaldehyde is zero, while those of phthalaldehyde, benzaldehyde and furanaldehyde is of the order of 6 - 7.5D. It is suggested by Beattie et al.[14] that bulky ligands prefer to acquire a trans-position and small ligands a cis-position in six coordination adducts of tin (IV) chloride and the zero dipole moment of naphthaldehyde adducts justifies its trans-octabedral structure.

The thermogravimetric analysis of a few adducts have been carried out and the data indicate that the adducts start decomposing between 200-250°C. From the relative initial decomposition temperatures, it appears that the adducts of chlorides are more stable than those of bromides. Nothing definite could be said about the mode of decomposition of these adducts since the process of decomposition appears to be continuous one and metal oxide is left as the final product in some of the adducts while in a few others, it appears that the maxima in the temperature versus percentage weight loss curve, indicate the loss of component of the adduct leaving behind the residue to correspond to SnO_2X_2 (X = halogen) in tin (IV) halide adducts.

Heats of formation of tin (IV) chloride and bromide with naphthaldehyde and cinnamaldehyde have been found to be (27.6 $\pm$ 0.2 and 22.2 $\pm$ 0.2) and (23.1 $\pm$ 0.6 and 20.3 $\pm$ 0.4) k.Cal. /Mole, respectively. This data establishes that the chlorides are stronger acceptor than bromides and naphthaldehyde is stronger donor than cinnamaldehyde.

REFERENCES

1. P. Pfeiffer et. al; Zurich Chem. Unit. Lab. Ann. 376, 285. C.A. 5, 4602 (1911)

2. G.I. Conteanu; Ber. 60, 2223 (1927); C.A. 21, 3168.

3. H.J. Emeleus and G.S. Rao; J. Chem. Soc., 4245 (1958)

4. A. Terinin, W. Filiminov and D. Bystrov., Izvest. Akad. Nauk. SSSR, Set. F. 12, 22, 1100 (1958)

5. D. Schwartz and P. Bernd; J. Less Comm. Metals. 7, 108 (1964)

6. R.C. Paul, Hem Raj and S.L. Chadha; J. Chem. Soc. A, 1849 (1969)

7. R.C. Paul and S.L. Chadha; J. Inorg. Nucl. Chem. 31, 1679 (1969)

8. R.C. Paul, B.R. Sreenathan, and S.L. Chadha; J. Inorg. Nucl. Chem. 28, 1225 (1966)

9. M.E. Foss and G.S. Gibson; J. Chem. Soc. 3063 (1949)

10. C.I. Wilkins and H.M. Heendlir; J. Chem. Soc. 3174 (1965)

11. R.C. Paul and S.L. Chadha; Aust. J. Chem. 22, 1381 (1969)

12. R.C. Paul and S.L. Chadha; J. Inorg. Nucl. Chem. (In press)

13. A.L. McClellan; 'Tables of Experimental Dipole Moments' W.H. Freeman and Co. San Francisco. Calif. (1963)

14. I.R. Beattie, R. Hulme and L. Rule; J. Chem. Soc. 1581 (1965)

DISCUSSION

S. Soundararajan : What will be the order of the strength of the metal oxygen bond in terms of the heats of formation and I. R. shifts?

S. L. Chadha : The order of strength of O-M bond (where M= Sn) from I. R. data is:

Naphthaldehyde > Benzaldehyde > Phthalaldehyde > Furanaldehyde > Cinnamaldehyde

While from heat of formation, data collected is only for two aldehydes which may be arranged as Naphthaldehyde > Cinnamaldehyde

COORDINATION COMPOUNDS OF TRIBUTOXYSILYLAMINES

Ram Chand Paul and Suraj Prakash Narula
Department of Chemistry, Panjab University, Chandigarh

The formation of addition complexes of some organosilyl-amines has already been reported[1-3]. However, addition compounds with organoxysilylamines have not so far been studied. Addition compounds of tributoxysilylamines with tin (IV) and titanium (IV) chlorides have been isolated and their structures studied with the help of infra-red spectroscopy.

When equimolar quantities of tributoxysilylamine or ethyl, tributoxysilylamine in dry carbon tetrachloride was added to the ice cold solution of tin (IV) or titranium (IV) chlorides in the same solvent, a white precipitate separated out. It was filtered in the atmosphere of dry nitrogen, repeatedly washed with dry carbon tetrachloride, dried in vacuo and analysed. Molar conductance of these compounds was measured in nitrobenzene. All the relevant data are recorded in Table I.

TABLE I

Complex	Sn/Ti		Cl		Molar conductance
	Calculated	Found	Calculated	Found	
$(C_4H_9O)_3Si\,NH_2.SnCl_4$	22.8	22.50	27.9	26.8	14.0
$(C_4H_9O)_3Si\,NH_2.TiCl_4$	10.6	10.66	31.4	30.6	7.5
$(C_4H_9O)_3Si\,NHC_2H_5.SnCl_4$	21.5	22.00	25.7	25.3	17.0

Infra-red spectra were recorded on Perkin Elmer model 337 having sodium chloride optics.

DISCUSSION

N-H Stretching vibrations in organosilylamines[4] generally occur between 3550-3280 cm^{-1}. Occurrence of a doublet at 3350 and 3100 cm^{-1}.

for tributoxysilylamines shows that the amino group is bonded. From the structure of these compounds, the existence of hydrogen bond may be expected. Frequencies assigned to different bonds in tributoxysilylamines mines and their addition compounds are recorded in Table II.

TABLE II

Assignment	$(BuO)_3SiNH_2$ A	$(BuO)_3SiNHC_2H_5$ B	$SnCl_4$. A	$TiCl_4$. A	$SnCl_4$. B
	cm.$^{-1}$	cm.$^{-1}$	cm.$^{-1}$	cm.$^{-1}$	cm.$^{-1}$
N - H	3355 w	3350 w	3350 w	-	3197 w
	3110 m	-	3107 m	3150 m	-
C - H	2925 s	2920 s	2915 s	2910 s	2950 s
	2900 s	2895 s	2880 s	2875 s	2870 s
	2810 s	2800 s	2850 s	2850 s	2850 s
CH_3	1440 s	1440 s	1445 s	1440 s	1440 s
CH_2	1350 s	1350 s	1352 m	1350m	1352 m
Si-O-C	1080 vs	1075 b	1060 b	1050 b	1060 b
	1030 s	1040 s	1020 b	-	-
Si-N	980 s	975 s	950 b	950 b	940 b

The characteristic frequencies of NH_2 group normally experience shift in lower spectral region in infra-red spectra on coordination. On the other hand, hydrogen bonds in a donor molecule break on coordination and the characteristic frequencies of the group appear in the higher spectral region than in the original base molecule[5]. In coordination compounds of the hydrogen bonded ligand, the spectral shift of the donating group, therefore, may be the net result of two opposing

phenomena.

In tributoxysilylamine, tin (IV) chloride complex, there is a slight negative shift (~5 cm.$^{-1}$) in the stretching vibrations of the NH_2 group from the original silylamine. In a similar complex with titanium (IV) chloride, the stretching modes appear in the higher spectral region (40 cm.$^{-1}$). It may be concluded that while in the first case both positive and negative shifts mostly cancel each other, in the second case positive shifts is more than the negative shift. In ethyl tributoxysilylamine, the extent of hydrogen bonding is small and the tendency to shift to higher spectral region on account of the breaking of hydrogen bond will, threfore, be small. As expected, the stretching modes of NH_2 group suffer a negative shift of the order of 153 cm.$^{-1}$. It is thus clear that coordination is through amino group.

Si-N bond is known to absorb between 900-1000 cm.$^{-1}$ in organosilylamines[6]. The bands between 970-980 cm.$^{-1}$ in the present silylamines may, therefore, be assigned to Si-N bond. These bands also suffer negative shift of the order of 35 to 40 cm.$^{-1}$ these compounds. This further supports the formation of N $\longrightarrow$ M dative bond.

The absorption band assigned to Si-O-C bond[7] (1050-1100 cm.$^{-1}$) shifts to lower frequencies in the complex formation which suggests the presence of O $\longrightarrow$ M bond, as well. Since relatively stronger Lewis acids were used, the $p\pi - d\pi$ bonding between oxygen and silicon may be broken, leaving oxygen atoms comparatively free to donate the lone pairs of electrons.

Tin (IV) and titanium (IV) chlorides are known to form hexacoordinated compounds. Moreover, the compounds formed are solids and insoluble in common organic solvents which may suggest that these compounds are polymeric in natture. Molar conductances reveal that these are non-electrolytes. On the basis of the above data, the compounds may be assigned the following structure:

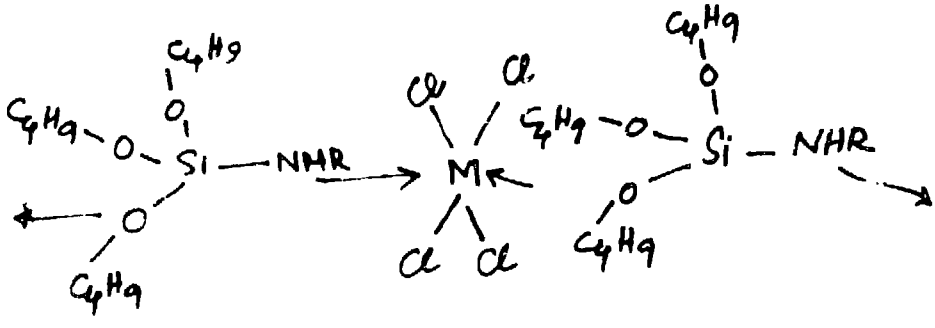

REFERENCES

1. S. Sujishi and S. Witz, J. Am. Chem. Soc. 76, 4631 (1954)

2. B.J. Aylett and L.K. Peterson; J. Chem. Soc. 4043 (1965)

3. S. Sujishi and S. Witz; J. Am. Chem. Soc. 79, 2447 (1957)

4. R. Fessenden, J. Org. Chem. 25, 2191 (1960)

5. R.C. Paul, S.L. Chadha and R. Dev, Ind. J. Chem. 3, 364 (1965)

6. U. Wannagat in H.J. Emeleus and A.G. Sharp; 'Advances in Inorganic and Radio Chemistry' Vol. 6, Academic Press, New York, 1964, page. 225

7. K. Nakamoto; " Infra-red Spectra of Inorganic Compounds", John Wiley and Sons, New York, 1962, p. 298

COORDINATION COMPOUNDS OF ORGANO-TIN HALIDES WITH BASES ADDUCTS OF PHENYL ETHYL TIN DICHLORIDE WITH AMINES

K. L. Jaura, N. S. Khurana and V. K. Verma
Department of Chemistry, Punjab University, Chandigarh

Tin in the hexa coordination state involving $sp^3 d^2$ hybridised orbitals has been studied quite extensively during the recent years[1-6]. In the present communication, phenyl ethyl tin dichloride has been reported to form 1:2 addition compounds with organic bases such as pyridine, quinoline, isoquinoline, α, β and γ-picolines, morpholine, piperidine and aniline. The stoichiometry of these complexes has been established from their halogen and tin contents. Their molar conductance studies have been carried out in nitro-benzene at 25°C and the i. r. data mainly in the region (600-200) cm^{-1} have been utilised to establish their possible structure.

EXPERIMENTAL

Triphenyl ethyl tin employed for the preparation of phenyl ethyl tin dichloride was prepared by the method of E. Krause and M. Schmitz[7] with some modifications[8]. Dry hydrochloric acid gas was bubbled through a refluxing solution of triphenyl ethyl tin in benzene for about an hour[9], benzene was distilled off and the resulting phenyl ethyl tin dichloride was recrystallised from petroleum ether (60-80°). It was reacted slowly with freshly distilled amines and the adducts mainly solids were separated out in some cases instantaneously and in some by chilling.

RESULTS AND DISCUSSION

Infrared Spectra

As is evident from the work of Poller[10] on phenyl tin compounds and of Berghe and coworkers[11] on ethyl tin compounds that phenyl ethyl tin dichloride should give two tin-carbon stretching frequencies corresponding to phenyl and ethyl groups in the region below 600 cm^{-1}. The strong absorption bands detected at 255 cm^{-1} and at 520 cm^{-1} (Table III) may thus be assigned to $Sn-C_6H_5$ and $Sn-C_2H_5$ respectively. The changes in the Sn-C frequencies on the formation of adducts are not significant (Table III), and therefore, are in agreement with the observation of Poller et al.[10] and Clark and Williams[12] in the sense that the Sn-C stretching frequencies are almost insensitive to complex formation. The Sn-Cl absorption frequencies have been reported to fall in the region 300-360 cm^{-1} (6, 10, 13). A strong absorption band at 320 cm^{-1} and a shoulder at 305 cm^{-1} in the spectrum of diorgano-tin dichloride may thus be assigned to the Sn-Cl stretching frequencies. On coordination through nitrogen

in these adducts, lengthening of the Sn-Cl bond and subsequently a fall in the Sn-Cl stretching frequencies to about 100-110 cm^{-1} is observed. A medium intensity band followed by other weak bands almost in all the adducts indicates splitting of the Sn-Cl band.

N-H stretching frequencies in case of piperidine, morpholine and aniline on coordination with phenyl ethyl tin dichloride also fall (Table II). This may also be the effect of coordination through nitrogen.[14]

Stereo Chemistry

Phenyl ethyl tin dichloride has been found to form 1:2 coordination compounds with amines. Tin, in all these adducts, appears in the hexa-coordinated state involving sp^3d^2 hybridisation and the compounds possess octahedral structure as has been reported earlier.[5, 13, 15] The splitting of the Sn-Cl bands in the region (200-230) cm^{-1} provides evidence that the two chlorines are in the cis configuration. Beattie[13] in his work on $(CH_3)_2SnCl_2 . 2Pyridine$ has reported that the complex possesses an octahedral structure with methyl groups in the trans position. In the present case, both the organic groups being different and quite bulky, their tendency to exist in the trans position is expected to be far greater than that in the methyl complex. Appearance of absorption bands around 500 cm^{-1}, which may be assigned to $Sn-C_2H_5$ symmetric stretching frequencies, further suggests that C-Sn-C is a non-linear arrangement[15] as is expected because of the different sizes of the organic groups, phenyl and ethyl. Concluding therefrom a distorted octahedral structure as

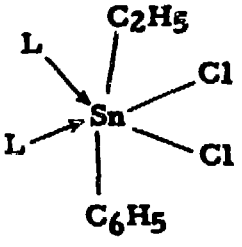

may be proposed for these adducts.

The molar conductance values determined in nitro-benzene being invariably below 20 cm^2 ohm^{-1} $mole^{-1}$ suggest that these complexes cannot be classified as true electrolytes.

REFERENCES

1. R.K. Ingham, S.D. Rosenberg and H. Gilman; Chem. Rev. 60, 459 (1960)

2. I.R. Beattie and L. Rule; J. Chem. Soc. 3267 (1964)

3. I.R. Beattie; Quart. Rev. 17, 382 (1963)

4. J.E. Fergusson, W.R. Roper and C.J. Wilkins; J. Chem. Soc. 3716 (1965)

5. T. Tanka, Y. Matsumra and R. Okawara and Y. Musya and S. Kinumaki; Bull. Chem. Soc. (Japan) 41, 1497 (1968)

6. R.J.H. Clark, Alwyn G. Davies and R.J. Puddephatt; J. Chem. Soc.(A) 1828 (1968)

7. E. Krause and M. Schmitz; Ber. 52, 2150 (1919)

8. K.L. Jaura, L.K. Churamani and K.K. Sharma; Ind. J. Chem. 4, 329 (1966)

9. H. Ralph, Bullard and Francis R. Holden; J. Am. Chem. Soc. 53, 3150 (1931)

10. R.C. Poller and D.L.B. Tolley; J. Chem. Soc. (A), 1578 (1967)

11. E.V. Vanden Berghe, L. Verdonck and G.P. Vanderkelen; J. Organometal. Chem. 497 (1969)

12. R.J.H. Clark and C.S. Williams; Spectrochimacta 21, 1861 (1965)

13. I.R. Beattie and G.P. Mcquillan; J. Chem. Soc. 1519 (1963)

14. N.N. Greenwood and K. Wade; J. Chem. Soc. 1130 (1960)

15. Gen-Etsu Matsubayashi Toshio Tanka and Rokuro Okawara; J. Inorg. Nucl. Chem. 30, 1831 (1968)

TABLE I

Complexes of $Ph(C_2H_5)SnCl_2$ with Nitrogeneous Bases

Complexes (m. pt.) °C	Molar conductance $cm^2\ ohm^{-1}\ mole^{-1}$	% of Cl		% of Tin	
		Found	Required	Found	Required
$Ph(C_2H_5)SnCl_2$. 2 Pyridine (88-90)	3.89	15.25	15.60	25.82	26.21
$Ph(C_2H_5)SnCl_2$. 2 Quinoline (95-96)	9.08	12.62	12.81	22.05	21.48
$Ph(C_2H_5)SnCl_2$. 2 Iso-quinoline (114-116)	3.85	13.10	12.81	21.03	21.48
$Ph(C_2H_5)SnCl_2$. 2 α-Picoline (64-65)	10.88	15.12	14.73	25.12	24.68
$Ph(C_2H_5)SnCl_2$. 2 β-Picoline (88)	4.73	15.21	14.73	24.23	24.68
$Ph(C_2H_5)SnCl_2$. 2 γ-Picoline (102)	3.51	14.92	14.73	24.17	24.68
$Ph(C_2H_5)SnCl_2$. 2 Morpholine (112-114)	6.52	15.00	15.11	24.93	25.32
$Ph(C_2H_5)SnCl_2$. 2 Piperidine (decomposed at 162-165)	2.59	15.56	15.23	25.09	25.53
*$Ph(C_2H_5)SnCl_2$. 2 Aniline (90)	--	14.43	14.73	24.06	24.68

* Molar conductance could not be determined as the complex was sparingly soluble in nitro-benzene.

TABLE II

Amine	ν (N-H)cm^{-1}	Adduct	ν (N-H) cm^{-1}
Piperidine	3290 s	$Ph(C_2H_5)SnCl_2$. 2 Piperidine	3120 m
Morpholine	3340 s	$Ph(C_2H_5)SnCl_2$. 2 Morpholine	2910 m
Aniline	3390 s 3315 s 3180 m	$Ph(C_2H_5)SnCl_2$. 2 Aniline	(2875-2900)s. br.

where x = strong m = medium, s. br. =strong broad.

TABLE III

I. R. spectra of the adducts of $Ph(C_2H_5)SnCl_2$ with amines

Compound	$\nu(Sn-C_6H_5)$ cm.$^{-1}$	$\nu(Sn-C_2H_5)$ cm^{-1}. Asy.	$\nu(Sn-C_2H_5)$ cm^{-1} Sym.	Unassigned stretching frequencies.	$\nu(Sn-Cl)$ cm^{-1}
$Ph(C_2H_5)SnCl_2$	255 v. s.	520 s			320 s.
$Ph(C_2H_5)SnCl_2$. 2 Pyridine	250 v. s.	560 m 555 m	508 m 500 w	400 m	218 sh 212 m 207 w
*$Ph(C_2H_5)SnCl_2$. 2 Quinoline		540 m	515 m		
$Ph(C_2H_5)SnCl_2$. 2 Isoquinoline	255 v. s.	530 s	510 m	410 s	210 w 202 m
*$Ph(C_2H_5)SnCl_2$. 2 α-Picoline		540 s	505 m		
*$Ph(C_2H_5)SnCl_2$. 2 β-Picoline		530 m	500 m	405 m	
$Ph(C_2H_5)SnCl_2$. 2 γ-Picoline	255 v. s.	540 m	512 w	410 s	220 w 212 m 208 w
$Ph(C_2H_5)SnCl_2$. 2 Morpholine	255 v. s. 244 w.	540 s	505 w	408 s	230 m 225 w 220 w 210 w 200 w
$Ph(C_2H_5)SnCl_2$. 2 Piperidine	253 v. s.	520 m	-	400 s	225 w 215 w 210 w 205 w 200 m
*$Ph(C_2H_5)SnCl_2$. 2 Aniline		540 m	-		

where v. s. = very strong, s = strong, m = medium w = weak and sh = shoulder

*the i. r. spectrum was not studied below 400 cm^{-1}.

THE ELECTRONIC SPECTRA OF TRIGONAL BIPYRAMIDAL VANADOUS COMPLEXES

M. N. Sankarshana Murthy and A. P. B. Sinha
National Chemical Laboratory, Poona

A strong-field treatment of the vanadous ion in D_{3h} symmetry is lacking at present, though weak-field treatments of the subject have been given.(1) The five-fold manifold of d-electrons in a free ion breaks up in a field of D_{3h} symmetry into the following terms in the order of decreasing energy:

a_1^1 spanned by d_z2 (which we will call a_1)

e' spanned by d_{xy} and $d_x2_{-y}2$ (α and β say)

e'' spanned by d_{yz} and $d_x2_{-y}2$ (ξ and η)

let Δ_1 be the energy interval e' to e'' and Δ_2 that between a_1^1 and e''.

Table I gives the allowed strong-field terms resulting from the d^2 configuration in D_{3h} symmetry, as also their basis functions. Table II gives the corresponding matrices of electrostatic and orbital energy. From these matrices, we get energy level diagrams of the type of Fig. (1) for the V^{3+} ion in D_{3h} symmetry. We draw these energy level diagrams as a series of constant energy contours for each set of degenerate terms, with Δ_1/B and Δ_2/B shown on the abscissa and ordinate respectively. We mark the energies on the contours, taking the energy of the ground state, $^3A_2^1$ as zero and in units of the Racah parameter B.

On the basis of such energy level diagrams, we interpret the absorption spectrum(2) of $VCl_3.2N(CH_3)_3$ as per Table III assuming $\Delta_1/B = 8$, $\Delta_2/B = 21$, $B = 732$ (i.e. 15% reduction in the free ion value for V^{3+}).

ACKNOWLEDGEMENT

The authors are very grateful to Dr. A. S. Apte of the Central Water and Power Research Station, Khadakwasla, Poona, for his kind help at the computer.

REFERENCES

1. J. S. Wood; Inorg. Chem. 7, 853 (1968)

2. M. W. Duckworth, G. W. A. Fowles and P. T. Greene; J. Chem. Soc. A, 1593 (1967)

Also quoted and discussed by J. S. Wood. (Ref. 1. above)

TABLE I

Strong-field basis functions for d^2 in D_{3h} symmetry

Configuration	Term	Basis functions
$(e'')^2$	$^3A_2'$	$\lvert\xi^+\eta^+\rangle$
	$^1E'$	$(\lvert\xi^+\xi^-\rangle - \lvert\eta^+\eta^-\rangle)1/\sqrt{2}$; $(\lvert\xi^+\eta^-\rangle - \lvert\xi^-\eta^+\rangle)1/\sqrt{2}$
	$^1A_1'$	$(\lvert\xi^+\xi^-\rangle + \lvert\eta^+\eta^-\rangle)1/\sqrt{2}$
$(e'')(e')$	$^3E''$	$(-\lvert\xi^+\beta^+\rangle + \lvert\eta^+\alpha^+\rangle)1/\sqrt{2}$; $(\lvert\xi^+\alpha^+\rangle + \lvert\eta^+\beta^+\rangle)1/\sqrt{2}$
	$^3A_2''$	$(\lvert\eta^+\alpha^+\rangle + \lvert\xi^+\beta^+\rangle)1/\sqrt{2}$
	$^3A_1''$	$(\lvert\xi^+\alpha^+\rangle - \lvert\eta^+\beta^+\rangle)1/\sqrt{2}$
	$^1E''$	$\{(\lvert\eta^+\alpha^-\rangle - \lvert\eta^-\alpha^+\rangle)1/\sqrt{2} - (\lvert\xi^+\beta^-\rangle - \lvert\xi^-\beta^+\rangle)1/\sqrt{2}\}1/\sqrt{2}$ $\{(\lvert\xi^+\alpha^-\rangle - \lvert\xi^-\alpha^+\rangle)1/\sqrt{2} + (\lvert\eta^+\beta^-\rangle - \lvert\eta^-\beta^+\rangle)1/\sqrt{2}\}1/\sqrt{2}$
	$^1A_2''$	$\{(\lvert\eta^+\alpha^-\rangle - \lvert\eta^-\alpha^+\rangle)1/\sqrt{2} + (\lvert\xi^+\beta^-\rangle - \lvert\xi^-\beta^+\rangle)1/\sqrt{2}\}1/\sqrt{2}$
	$^1A_1''$	$\{(\lvert\xi^+\alpha^-\rangle - \lvert\xi^-\alpha^+\rangle)1/\sqrt{2} - (\lvert\eta^+\beta^-\rangle - \lvert\eta^-\beta^+\rangle)1/\sqrt{2}\}1/\sqrt{2}$
$(e'')(a_1')$	$^3E''$	$\lvert a_1^+\xi^+\rangle$; $\lvert a_1^+\eta^+\rangle$
	$^1E''$	$(\lvert a_1^+\xi^-\rangle - \lvert a_1^-\xi^+\rangle)1/\sqrt{2}$; $(\lvert a_1^+\eta^-\rangle - \lvert a_1^-\eta^+\rangle)1/\sqrt{2}$
$(a_1')^2$	$^1A_1'$	$\lvert a_1^+ a_1^-\rangle$
$(a_1')(e')$	$^1E'$	$(\lvert a_1^+\alpha^-\rangle - \lvert a_1^-\alpha^+\rangle)1/\sqrt{2}$; $(\lvert a_1^+\beta^-\rangle - \lvert a_1^-\beta^+\rangle)1/\sqrt{2}$
	$^3E'$	$\lvert a_1^+\alpha^+\rangle$; $\lvert a^+\beta^+\rangle$
$(e')^2$	$^1A_1'$	$(\lvert\alpha^+\alpha^-\rangle + \lvert\beta^+\beta^-\rangle)1/\sqrt{2}$
	$^3A_2'$	$\lvert\alpha^+\beta^+\rangle$
	$^1E'$	$(\lvert\alpha^+\beta^-\rangle - \lvert\alpha^-\beta^+\rangle)1/\sqrt{2}$ $(\lvert\alpha^+\alpha^-\rangle - \lvert\beta^+\beta^-\rangle)1/\sqrt{2}$

TABLE II

Energy matrices for d^2 in D_{3h} symmetry

$^1E'$	$(e'')^2$	$(a_1')(e')$	$(e')^2$
$(e'')^2$	A+B+2C	0	0
$(a_1')(e')$	0	$A+2C+(\Delta_1+\Delta_2)$	0
$(e')^2$	0	0	$A+4B+2C+2\Delta_1$

$^3E''$	$(e'')(e')$	$(e'')(a_1')$
$(e'')(e')$	$A-2B+\Delta_1$	$B3\sqrt{6}$
$(e'')(a_1')$	$B3\sqrt{6}$	$A+B+\Delta_2$

$^1A_1'$	$(e'')^2$	$(a_1')^2$	$(e')^2$
$(e'')^2$	A+7B+4C	$(B+C)\sqrt{2}$	2(3B+C)
$(a_1')^2$	$(B+C)\sqrt{2}$	$A+4B+3C+2\Delta_2$	$(4B+C)\sqrt{2}$
$(e')^2$	2(3B + C)	$(4B + C)\sqrt{2}$	$A+4B+4C+2\Delta_1$

$^3A_2'$	$(e'')^2$	$(e')^2$
$(e'')^2$	A-5B	6B
$(e')^2$	6B	$A+4B+2\Delta_1$

$^1E''$	$(e'')(e')$	$(e'')(a_1')$
$(e'')(e')$	$A-2B+2C+\Delta_1$	$-B\sqrt{6}$
$(e'')(a_1')$	$-B\sqrt{6}$	$A+3B+2C+\Delta_2$

$(e')(e'')$ < $^3A_1''$; $^3A_2''$ with energy $A-8B+\Delta_1$

$^1A_1''$, $^1A_2''$ with energy $A+4B+2C+\Delta_1$

$(e')(a_1')$ $^3E'$ with energy $A-8B+(\Delta_1+\Delta_2)$

TABLE III

Assignments of the electronic spectrum of $VCl_3 . 2N(CH_3)_3$

Transitions from $(e'')^2\ ^3A_2'$ to		Calculated frequency in cm^{-1} (to the nearest integral multiple of ten)	Observed frequency in cm^{-1} (max)
$(e')(e'')\ ^3A_1''\ ^3A_2''$		6.37 x 732 = 4660	4800(60)
$(e')(e'')\ ^3E''$		9.5 x 732 = 6950	7000(16)
$(e'')^2\ ^1E'$		17.05 x 732 = 12,480	12,700(W)
$(e')(e'')\ ^1E''$	§	21.72 x 732 = 15,900	16,600(10)
$(e'')^2\ ^1A_1'$	§	22.25 x 732 = 16,290	
$(e')^2\ ^3A_2'$	§	27.74 x 732 = 20,310	19,700(60)
$(a_1')\ (e')\ ^3E'$	§	27.32 x 732 = 20,030	

Fig I

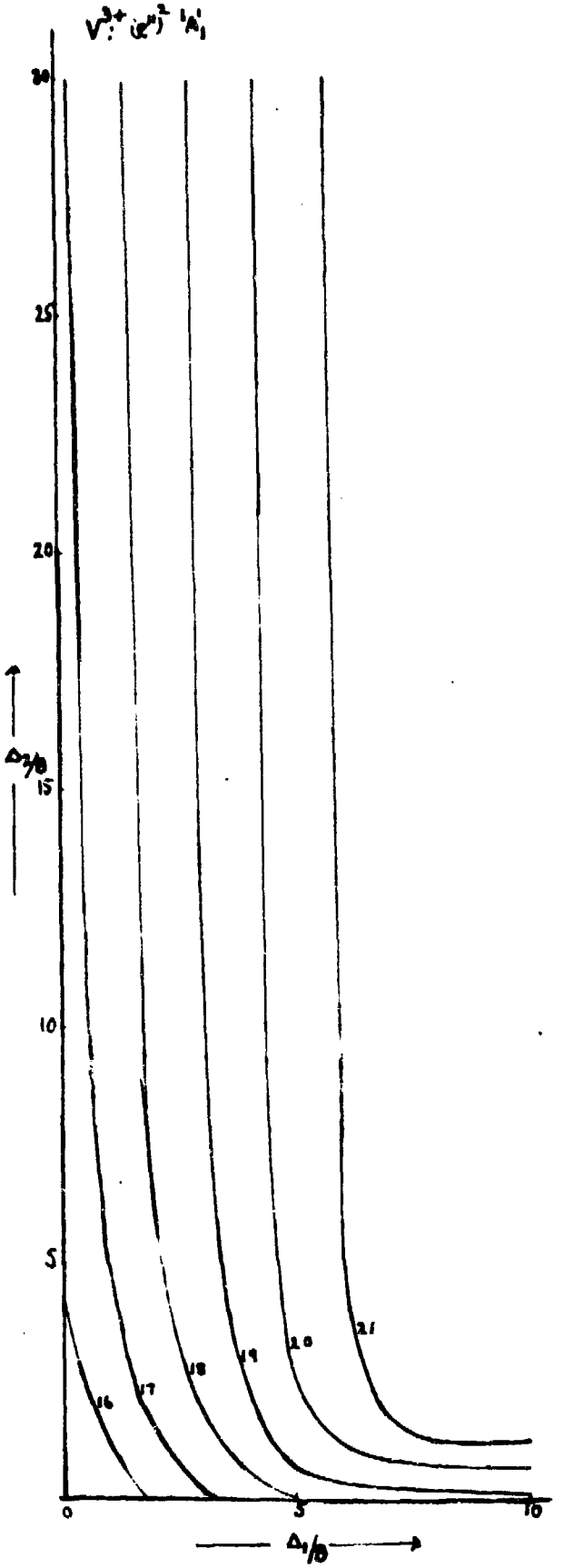

IR STUDY OF Cr (III) COMPLEXES WITH AMINOPYRIDINES

P. S. Relan, S. L. Chopra and I. S. Bhatia
Department of Chemistry and Biochemistry,
Punjab Agricultural University, Ludhiana.

Chromium (III)[1-3] is known to form a number of complexes with many ligands. In the present investigation, some of the complexes of aminopyridines with Cr (III) salt have been given.

The complexes of aminopyridines with chromium chloride have been synthesised by taking equimolar ethanolic solutions of ligand and metal salt and refluxing for 3-4 hours. The solutions were concentrated on a water bath and then crystalized in vacuum. The crystals were washed with absolute alcohol and again dried in vacuum. The purity of the complexes was tested by estimation of Cr, N and Cl. The structure was determined by IR- studies.

RESULTS

The results of analysis of the complexes of aminopyridines are given in Table I.

TABLE I

ANALYSIS OF AMINOPYRIDINE COMPLEXES

1.	Penta-aquo-2 ampy chromium (III) chloride	% of metal 15.03 % of nitrogen 8.15 % of halogen 31.04	Reqd. " "	15.18 8.17 31.09
2.	Penta-aquo-3 ampy chromium (III) chloride	% of metal 15.08 % of nitrogen 8.15 % of halogen 31.08	" " "	15.18 8.17 31.09
3.	Penta-aquo-4 ampy chromium (III) chloride	% of metal 15.08 % of nitrogen 8.15 % of halogen 31.09	" " "	15.18 8.17 31.09

TABLE II

IR DATA OF COMPLEXES OF AMINOPYRIDINES WITH Cr (III)

Ligand 2 ampy	Complex	Ligand 3 ampy	Complex	Ligand 4 ampy	Complex
3478 (S)	3374 (B)	3454	3450 (B)	3492	3490 (S)
3190	3175 (B) 2924 (B)	3375	-	3405	-
1619 (S)	1666 (B) 1626 (B)	3340	-	3216	2898 (B)
			1640 (B)		1640 (B)
1570 (S)	1545	1623	1629 (B)	1626	1628 (B)
1487	1487	1586	1552 (V)	1601	-
1340	1483 (S)	1485	1485 (W)	1572	1515 (W)
1290 (W)	1243 (W)	1290	-	1508	1449 (B)
1170 (S)	1165	1170	-	1340	1369 (B)
1005 (S)	1025	1005	-	1170	1197 (B)
-	870	-	850	-	870
755 (S)	770	755	773 (B)	755	750 (B)

DISCUSSION

The characteristic frequency 1600 cm^{-1} remains almost the same except that it gets broadened up more as compared to that in free ligand. Some of the frequencies are also modified and we get broad bands indicating that complextion has taken place from ring nitrogen atom.[4] The ligands contain another centre of complexation, that is, free amino group in the ring. This gives an equal probability of co-ordinating this nitrogen to the metal. The NH_2 group in complexes shows a frequency band in the vicinity of 3474, 3450 and 3490 cm^{-1} while the non-coordinated- NH_2 group has the absorption spectra at 3478, 3454 and 3492 cm^{-1} in 2-aminopyridine, 3-aminopyridine and 4-aminopyridine respectively. The negative shift in the position of the band is due to the co-ordination of the -NH_2 group of the ligand to the metals but we find the bands at the same position. It is, therefore, evident that it is the nitrogen of the ring and not the nitrogen from free amino group, that takes part in complexation. The co-ordinated water is indicated by the M-O bonding frequencies at 870, 850 and 870 cm^{-1}.

REFERENCES

1. P. Pfeiffer; Ber. deut. chem. Ges. 39, 1864 (1906)

2. Plumb, Martell and Bersworth; J. Phys. Colloid Chem. 54, 1208 (1950)

3. Schwar Zenbech and Bildermann; Helv. Chim. Acta. 31, 331 (1948)

4. S. Guru and D. V. Ramana Rao; J. I. C. S. 45, 160 (1968)

5. C. L. Angyal and R. W. Werner; J. Chem. Soc. 2911 (1952)

6. Modern co-ordination chemistry by Lewis and Wilkinson, Chap. IV.

7. Infra-red spectra of inorganic and co-ordination compounds by Kazuo Nakamoto. John Wile & Sons., Inc.; New York

THE NATURE OF MOLYBDENUM(III) SPECIES IN AQUEOUS SOLUTIONS

S. R. Sagi and P. R. Mohan Rao
Chemistry Department, Andhra University, Waltair

INTRODUCTION

In view of the conflicting views expressed in the literature[1, 2, 3] on the species of trivalent molybdenum obtained by electrolytic reduction of molybdenum trioxide in hydrochloric acid medium, we have attempted a study of these species by reducing ammonium molybdate in hydrochloric and sulphuric acid media with metallic and amalgamated metal reductors.

EXPERIMENTS AND RESULTS

Reagents

A 0.05 M molybdenum(VI) solution is prepared by dissolving A. R. ammonium molybdate in water and standardising it, after reduction in a mercury reductor[4], against standard cerium(IV) sulphate using rhodamine-6G as a fluorescent indicator[5]. Hydrochloric acid, sulphuric acid and other metals used are of reagent quality.

Reduction of Molybdenum(VI)

10 ml of 0.02M molybdenum(VI) solution in XN. acid is shaken in a conical flask under carbon dioxide atmosphere with 1 gm. of metallic powder, or granules, or amalgamated granules for 2 - 3 minutes. The extent of reduction is checked after decanting the ferrous formed. The results obtained, together with the standard oxidation potentials[6] of the metals used, show that only powerful reducing agents like aluminium and zinc are capable of reducing molybdenum(VI) to the green molybdenum(III) when the acid concentration is below 4M and to orange-red molybdenum(III) when the acid concentration is 5 M and above. The remaining metals either alone or when amalgamated reduce the molybdenum(VI) to orange-red molybdenum(III) alone irrespective of the acid concentration.

Absorption Spectra of Molybdenum(III) Solutions

The absorption spectra of the green and orange-red of molybdenum(III) in 2N hydrochloric acid medium show that the green variety has a major peak at 370 mμ and a minor peak at 630 mμ while orange-red variety absorbs mainly at 390 mμ with a smaller peak at 470 mμ.

Further, it has been observed that the optical density values of the orange red form are quite stable while those of the green form decrease with time.

Inter Conversions

The green molybdenum(III) solutions change their colour to orange-red slowly in lower acid media and rapidly in higher ones, while the orange-red variety does not change its colour even when the acid concentration is reduced to 0.5 - 1.0 N and kept over-night under carbon dioxide atmosphere. Thus, it is evident that the conversion of the green form to the orange-red is not reversible. However, it has been observed by us that if the orange-red solution in media of 4N acid, could be converted to the green variety either by adding a little of aluminium powder or by passing it through a Jones reductor.

Ion Exchange Studies

Ion exchange studies with an anion exchanger (Dowex 1X8) and a cation exchanger (Amberlite I.R. 120) have shown that i) the green form is a cationic species ii) the orange-red form is an anionic species and iii) the ion exchange behaviour of these two forms of molybdenum(III) afford a method for the separation of the two species.

Behaviour of Molybdenum(III) Solutions on Oxidation

According to Rius et. al.[7, 8, 9, 10] molybdenum(III) exists in two forms, one at lower temperature and another at higher temperatures. The form that is stable at higher temperatures gives on oxidation molybdenum(IV) and then molybdenum(V), while the other form stable at lower temperatures gets oxidised directly to molybdenum(V). These conclusions were drawn by these authors from the results of their potentiometric titration of molybdenum(III). Since potentials are attained very slowly in the molybdenum systems, we followed the oxidation of molybdenum(III) by various mono, and multi de-electronators by an absorptiometric method. Some of the results obtained are given in Table I. These results show that the green and orange-red varieties of molybdenum(III) follow different paths during oxidation with certain oxidants. The table also shows the existence of species corresponding to the oxidation states of 3.5 and 4.5. These are presumably mixed species of 3 and 4 and 4 and 5 respectively. More than that no serious conclusions can be drawn at this stage about these breaks observed in the absorptio-metric titrations.

DISCUSSION

From the behaviour of the two species of trivalent molybdenum seen above, it is evident that they are not simply the isomeric neutral

species as suggested by Wardlaw et al but the green form is a cationic species and the orange-red form an anionic species. These solutions may be probably given one of the following structures or may possibly be a mixture of them.

Molybdenum (III) (green)

(1) $[Mo(H_2o)_6]^{3+}$ (2) $[Mo(H_2o)_5Cl]^{2+}$

(3) $[Mo(H_2o)_4Cl_2]^{+}$ (4) $[MoO(H_2o)_5]^{+}$

Molybdenum (III) (orange-red)

(1) $[MoCl_6]^{3-}$ (2) $[MoCl_5H_2o]^{2-}$

(3) $[MoCl_4(H_2o)]^{-}$ (4) $[MoOCl_5]^{2-}$

(5) $[MoOCl_4.\ H_2o]^{3-}$ (6) $[MoOCl_3(H_2o)_2]^{2-}$

(6) $[MoOCl_2(H_2o)_3]^{-}$

All these structures are in conformity with the octahedral nature of molybdenum(III), which is exhibited in its known compounds[2, 11, 12, 13].

The slow conversion of the green variety to the orange-red which is catalysed by hydrogen ions may be due to the gradual replacement of the water molecules and, or, the oxygen atom by the chloride ligands. The lability of the green variety for substitution and the inertness of the orange-red variety for the reversal of the reaction might indicate that the chloro-complexes are more stable and probably also that these complexes are more symmetrical than the other. In this connection similar work done on chromium(III) and chromium(II) may be referred[14-17].

The fact that simple reduction in acid strength does not convert the orange-red form to the green form, while the addition of a powerful reductant like aluminium or amalgamated zinc does, suggest that probably the transfer is being effected through the formation of traces of molybdenum(II). Molybdenum(II) by virtue of its t_{2g}^4 electronic configuration, might give rise to an unsymmetrical ligand field, and hence an unsymmetrical complex. This on electron exchange with molybdenum(III) (orange-red) gets oxidised to an unsymmetrical molybdenum(III) species, possibly the green form.

REFERENCES

1. Chilesotti; Z. Elektrochem. 12, 173 (1906)

2. F. Foerstar and E. Fricke; Z. Angew. Chem. 36, 458 (1923)

3. W. Wardlaw and R. L. Wormell; J. Chem. Soc. 130 (1927)

4. N. H. Furman and W. M. Murray; J. Amer. Chem. Soc. 58, 1689(1936)

5. S. R. Sagi and G. G. Rao; Z. Anal. Chem. 189, 229 (1962)

6. W. M. Latimer; The oxidation states of the elements and their potentials in aqueous solutions, 2nd edition., Prentice Hall, New York (1952)

7. A. Rius and J. R. Iranzo; Anales Real. Soc. Espan. Fis. Quim. (Madrid) 41, 994 (1945)

8. A. Rius and J. R. Iranzo; ibid. 42, 761 (1946)

9. A. Rius and C. A. Diaz-Flores; ibid. 46B, 289 (1950)

10. A. Rius and M. Martini; ibid. 43, 897 (1947)

11. W. Wardlaw and R. L. Wormell; J. Chem. Soc. 1087 (1927)

12. G. Carobbi; Gaz. 58, 35 (1928)

13. N. V. Sidwick; "The Chemical Elements and their Compounds" 2nd Edn., Oxford, (1950)

14. H. Taube; J. Chem. Ed. 45, 452 (1968)

15. C. W. Merrideth and R. E. Connick; UCRL-11704 (1965)

16. J. P. Hunt and H. Taube; J. Chem. Phys. 19, 603 (1951)

17. R. A. Plane and J. P. Hunt; J. Am. Chem. Soc. 76, 5960 (1954)

TABLE I

OXIDATION OF MOLYBDENUM(III) SOLUTIONS WITH VARIOUS OXIDANTS AND THE TRANSITIONS CORRESPONDING TO THE BREAKS IN ABSORPTIOMETRIC TITRATIONS IN HYDROCHLORIC ACID MEDIUM

Nature of oxidant	Orange-red form			Green form		
	Concentration of acid (M)			Concentration of acid (M)		
	1	2	3	1	2	3
Ce(IV) :	Mo(III) → Mo(V) → Mo(VI)	Mo(III) → Mo(V) → Mo(V) → Mo(VI)	Mo(III) → $Mo^{+3.5}$ → Mo(IV) → Mo(V) → Mo(VI)	Mo(III) → Mo(IV) → Mo(VI)	Mo(III) → Mo(IV) → Mo(V) → Mo(VI)	
Fe(III) :	Mo(III) → Mo(V) → Mo(VI)	-	Mo(III) → Mo(IV) → Mo(V) → Mo(VI)	Mo(III) → $Mo^{+3.5}$ → Mo(IV) → Mo(V) → Mo(VI)	-	Mo(III) → $Mo^{+3.5}$ → Mo(IV) → Mo(V) → Mo(VI)
Cr(VI) :	Mo(III) → Mo(V) → Mo(VI)	Mo(III) → Mo(V) → Mo(VI)	Mo(III) → $Mo^{+3.5}$ → Mo(IV) → Mo(V) → Mo(VI)	Mo(III) → Mo(V) → Mo(VI)	Mo(III) → Mo(V) → Mo(VI)	Mo(III) → Mo(V) → Mo(VI)
V(V) :	Mo(III) → Mo(V) → Mo(VI)	Mo(III) → Mo(IV) → Mo(V) → Mo(VI)	Mo(III) → $Mo^{+3.5}$ → Mo(IV) → Mo(V) → Mo(VI)	Mo(III) → Mo(VI)	Mo(III) → Mo(VI)	Mo(III) → Mo(VI)
Mn(VII):	Mo(III) → Mo(IV) → Mo(V) → Mo(VI)	Mo(III) → $Mo^{+3.5}$ → Mo(IV) → Mo(V) → Mo(VI)	Mo(III) → Mo(IV) → Mo(V) → Mo(VI)	Mo(III) → $Mo^{+3.5}$ → Mo(IV) → Mo(V) → Mo(VI)	Mo(III) → $Mo^{+3.5}$ → Mo(IV) → Mo(V) → Mo(VI)	Mo(III) → $Mo^{+3.5}$ → Mo(IV) → Mo(V) → Mo(VI)
Mo(VI)	Mo(III) → Mo(IV) → $Mo^{+4.5}$	-	Mo(III) → Mo(IV) → $Mo^{+4.5}$	Mo(III) → Mo(V)	-	Mo(III) → Mo(V)

SUBSTITUTED MOLYBDENUM CARBONYL COMPLEXES WITH NITROGEN DONOR LIGANDS

S. C. Tripathi, S. C. Srivastava and R. D. Pandey
Department of Chemistry
University of Gorakhpur, Gorakhpur (U. P)

Ethylamine, isopropylamine, butylamine, benzylamine and cyclohexylamine react with molybdenum hexacarbonyl to give simple substituted products $[L_xMo(CO)_{6-x}]$, where x = 1, 2 and 3. Diisopropylamine, quinoline and α-picoline yield only monosubstituted derivatives, $[LMo(CO)_5]$ Piperazine gives a novel compound bis (Piperazine) molybdenum tricarbonyl and 2, 2'-diquinolyl replaces only two CO molecules from molybdenum hexacarbonyl under all conditions of reactions. The infra-red spectra have been measured and proper assignments have been made.

In the complexes of the type, $LMo(CO)_5$, Table I each I. R. spectrum showed normally four bands in the carbonyl region. A single weak band (1) arising from the A_1 mode of the trans pair of carbonyl groups. Band (2) could be assigned due to B_1 mode, which was only Raman active. It gained some infra-red intensity because the molecules did not possess perfect C_{4v} symmetry due to the structure of the ligands. Band (3) may be due to the E mode and band (4) due to A_1 mode from cis carbonyls, which was just visible as a shoulder or weak peak. In $[(\alpha\text{-picoline})\ Mo(CO)_5]$ and $[(quinoline)\ Mo(CO)_5]$, it was observed that the two modes E and A_1 of lower frequency were accidentally degenerate or so nearly degenerate due to which the bands were entirely unresolved.

The bands in the infra-red spectra of complexes of the type $[L_2Mo(CO)_4]$ Table II having C_{2v} symmetry agreed well with the assignment made for cis configuration. Band (1) might be due to mode A_1 which mainly involved trans carbonyl groups. Band (2), (3) and (4) might be assigned to modes B_1 A_1 and B_2 respectively.

Infra-red spectra of complexes of the type $[L_3Mo(CO)_3]$ Table III suggested to be the cis derivatives having C_{3v} symmetry. Bands (1) and (2) were assigned to A_1 and E modes respectively.

TABLE I

CO Stretching Frequencies for $LMo(CO)_5$ Complexes

Complex	Band	Frequency	Mode
	1	2062(w)	A_1
	2	1972(sh)	B_1
$(C_2H_5NH_2)Mo(CO)_5$	3	1923(s)	E
	4	1887(sh)	A_1
	1	2062(w)	A_1
	2	1961(sh)	B_1
$(iso\text{-}C_3H_7NH_2)Mo(CO)_5$	3	1923(s)	E
	4	1887(w)	A_1
	1	2062(w)	A_1
	2	1961(m)	B_1
$\{(CH_3)_2CH\}_2NH\ Mo(CO)_5$	3	1923(s)	E
	4	1887(sh)	A_1
	1	2062(w)	A_1
	2	1961(m)	B_1
$(C_4H_9NH_2)Mo(CO)_5$	3	1923(s)	E
	4	1887(sh)	A_1

TABLE II

CO Stretching Frequencies for cis-$L_2Mo(CO)_4$ Complexes

Complex	Band	Frequency	Mode
$(C_2H_5NH_2)_2Mo(CO)_4$	1	2000(w)	A_1
	2	1923(sh)	B_1
	3	1869(m)	A_1
	4	1818(m)	B_2
$(iso\text{-}C_3H_7NH_2)_2Mo(CO)_4$	1	2012(w)	A_1
	2	-	-
	3	1862(s)	A_1
	4	1818(w)	B_2
$(C_4H_9NH_2)_2Mo(CO)_4$	1	2000(w)	A_1
	2	1923(sh)	B_1
	3	1869(m)	A_1
	4	1825(m)	B_2
$(C_7H_7NH_2)_2Mo(CO)_4$	1	2000(w)	A_1
	2	1894(s)	B_1
	3	1818(m)	A_1
	4	1770(s)	B_2
$(C_6H_{11}NH_2)_2Mo(CO)_4$	1	2000(w)	A_1
	2	1869(s)	B_1
	3	1818(m)	A_1
	4	1779(s)	B_2

TABLE III

CO Stretching Frequencies for cis-$L_3Mo(CO)_3$ Complexes

Complex	Band	Frequency	Mode
$(C_2H_5NH_2)_3Mo(CO)_3$	1	1862(s)	A_1
	2	1709(s)	E
$(iso\text{-}C_3H_7NH_2)_3Mo(CO)_3$	1	1862(s)	A_1
	2	1709(s)	E
$(C_4H_9NH_2)_3Mo(CO)_3$	1	1869(s)	A_1
	2	1718(s)	E
$(C_7H_7NH_2)_3Mo(CO)_3$	1	1887(s)	A_1
	2	1724(s)	E
$(C_6H_{11}NH_2)_3Mo(CO)_3$	1	1862(s)	A_1
	2	1709(s)	E
$(C_4H_{10}N_2)_2Mo(CO)_3$	1	1880(s)	A_1
	2	1709(s)	E

TABLE IV

Compounds	Methods	Reaction conditions	Characteristics	Yield		Analysis % C	H	N
$(iso\text{-}C_3H_7NH_2)Mo(CO)_5$	Sealed tube	80°C. /6 hrs.	Yellow solid dec. above 62°C.	36.7	C	32.5	3.0	4.7
					F	32.1	2.9	4.6
$(iso\text{-}C_3H_7NH_2)_2Mo(CO)_4$	Sealed tube	125°C. /8 hrs.	Pale yellow solid dec. above 122°C	64.2	C	36.8	5.5	8.5
					F	36.4	5.4	8.4
$(iso\text{-}C_3H_7NH_2)_3Mo(CO)_3$	Sealed tube	155°C. /20hrs	Dirty white	75.8	C	40.4	7.5	11.7
					F	40.1	7.4	11.6
$(C_3H_7)_2NHMo(CO)_5$	U. V. irradiation in tetrahydrofuran.	15 hours	Yellow solid	14.8	C	39.1	4.4	4.1
					F	39.0	3.8	4.0
$(C_4H_9NH_2)\ Mo(CO)_5$	Sealed tube	110°C/6 hrs	Yellow scales m. p. 69°C(d)	38.9	C	34.9	3.5	4.5
					F	34.8	3.4	4.5
$(C_4H_9NH_2)_2Mo(CO)_4$	Reflux in tetrahydrofuran	$1\frac{1}{2}$ hrs.	Yellow scales dec. 132°C	73.1	C	40.6	6.2	7.9
					F	40.6	6.1	7.8
$(C_4H_9NH_2)_3Mo(CO)_3$	Reflux without solvent	3 hrs.	White fibrous solid dec. above 155°C	80.0	C	45.1	8.2	10.5
					F	44.6	8.0	10.4

TABLE IV (Continued)

Compounds	Methods	Reaction conditions	Characteristics	yield %	Analysis %			
						C	H	N
$(C_7H_7NH_2)Mo(CO)_5$	Sealed tube	100°C/4 hrs	Yellow solid m. p. 105°C(d)	45.0	C	41.9	2.6	4.0
					F	41.7	2.2	4.1
$(C_7H_7NH_2)_2Mo(CO)_4$	Sealed tube	155°C/10 hrs	Yellow solid dec. 137°C.	70.4	C	51.1	4.2	6.6
					F	50.6	3.9	6.6
$(C_7H_7NH_2)_3Mo(CO)_3$	Reflux in benzene	3 hrs	White fibrous dec. above 210°C	84.4	C	57.4	5.3	8.3
					F	56.6	5.2	8.3
$(C_6H_{11}NH_2)_2Mo(CO)_4$	Sealed tube	110°C/6hrs	Yellow solid dec. 137°C	68.3	C	47.2	6.4	6.8
					F	46.6	6.6	6.7
$(C_6H_{11}NH_2)_3Mo(CO)_3$	Reflux without solvent	3 hrs	White solid dec. 230°C	79.9	C	52.8	8.1=	8.8
					F	52.6	7.9	8.6
$(\alpha\text{-}C_5H_4NCH_3)Mo(CO)_5$	U.V. irradiation in hexane	40 hrs	Yellow solid	15.0	C	40.1	2.1	4.2
					F	39.8	1.9	4.3
$(C_9H_7N)Mo(CO)_5$	Sealed tube	180°C/4 hrs	Yellow brown solid dec. 159°C	81.0	C	46.0	1.9	3.8
					F	46.0	1.8	3.7
$(C_4H_{10}N_2)_2Mo(CO)_3$	Sealed tube	220°C/18 hrs	Pale yellow dec. 285°C	88.5	C	37.5	5.6	15.9
					F	37.0	4.9	15.8
$(C_{18}H_{12}N_2)Mo(CO)_4$	Reflux in toluene	2 hrs	Greenish black solid	86.8	C	56.8	2.5	6.0
					F	56.4	2.1	6.0

QUADRUPOLE SPLITTING IN SOME MIXED ANION COMPOUNDS OF IRON (III)

A. I. Almaula, M. K. Venkitakrishnan and C. K. Mathews
Radiochemistry Division, Bhabha Atomic Research Centre, Bombay-85

The Mössbauer spectra of high spin ferric compounds are characterized by small quadrupole splitting. The spherically symmetric charge distribution of the ferric ion does not produce any electric field gradient at the nucleus and, therefore, any quadrupole splitting that is observed is attributed to the asymmetric arrangement of ions around the iron atom in the crystal lattice. However, covalent effects have been invoked[1, 2] to explain the quadrupole splitting in some iron(III) complexes. To investigate further the magnitude and origin of the quadrupole splittings in high spin ferric compounds, the Mössbauer spectra of a number of mixed anion compounds were measured. The compounds studied were:

(1) Ferric chlorosulphate [$FeClSO_4$]
(2) Ferric hydroxysulphate [$Fe(OH)SO_4$]
(3) Ferric oxychloride [FeOCl]
(4) Ferric chloroformate hemihydrate [$FeCl(HCOO)_2 . \frac{1}{2}H_2O$]
(5) Ferric arsenate dihydrate [$FeAsO_4 . 2H_2O$]

EXPERIMENTAL

$FeClSO_4$ was prepared by passing chlorine through a slurry of ferrous sulphate heptahydrate in water until most of the solid was dissolved. After filtering off the unreacted ferrous sulphate, the filtrate was allowed to stand overnight, when $FeClSO_4$ slowly crystallized out. $Fe(OH)SO_4$ and $FeCl(HCOO)_2 . \frac{1}{2}H_2O$ were prepared by methods given by Mellor[3]. FeOCl was prepared following the method of Brauer[4] and $FeAsO_4 . 2H_2O$ after Pascal[5]. All these compounds were confirmed by chemical analysis.

The Mössbauer spectra were obtained using a constant velocity spectrometer described elsewhere[6]. The spectra were measured both at room temperature as well as at liquid nitrogen temperature. Typical spectra are shown in Figures 1 and 2.

RESULTS AND DISCUSSION

The Mössbauer parameters are summarized in Table 1. All the compounds studied gave doublet spectra, with the splitting varying from 0.14 mm/sec in $FeCl(HCOO)_2 . \frac{1}{2}H_2O$ to 1.15 mm/sec in $FeClSO_4$. The

individual lines were wide as is characteristic of ionic ferric compounds. The isomer shifts relative to sodium nitroprusside were in the range of 0.6 to 0.8 mm/sec. which is also characteristic of high spin ferric compounds. However, the values of quadrupole splitting in the case of $FeClSO_4$ and $Fe(OH)SO_4$ are outside the range reported for ionic ferric salts.

In ionic ferric compounds, the electric field gradient at the iron nucleus is given by $(1 - \gamma_\infty)q_{lat}$, where q_{lat} is a lattice contribution and γ_∞ is the Sternheimer anti-shielding factor.[7] The spherically symmetric charge distribution of the ferric ion does not contribute to the electric field gradient.

In order to understand the quadrupole splitting in these compounds on the ionic model, one must therefore start from their crystal structure. Ferric oxychloride is orthorhombic[8] and has a layer structure. The nearest neighbours of the iron atom are four oxygen and two chlorine atoms, arranged around the iron in the form of a distorted octahedron. The distortion from the octahedron and the differences in the charges and the polarizations produced by the oxide and chloride ions must be responsible for the observed quadrupole splitting. Considering the fact that Fe-O distances are 1.88 Å and 2.15 Å and the Fe-Cl distance is 2.29 Å, the quadrupole splitting does not appear to be large.

Ferric hydroxysulphate is also orthorhombic[9] with the tetramolecular unit having $a_o = 7.331$ Å, $b_o = 6.419$ Å and $c_o = 7.142$ Å. The iron atom is surrounded by an octahedron of oxygens with Fe-O distances ranging from 1.954 to 2.035 Å; of these the Fe-OH distance is the shortest. The distortion of the octahedron is thus less here than in FeOCl. It is not clear whether the larger quadrupole splitting in $Fe(OH)SO_4$ arises from the contribution from the more distant parts of the lattice or whether some other factors such as covalancy are involved. The temperature dependance of the quadrupole splitting is, however, typical of ionic ferric salts. The crystal structure of $FeClSO_4$ is not known, but similar considerations may apply in this case also.

Ferric chloroformate gives the lowest quadrupole splitting in this series. The crystal structure is not known. The Mossbauer parameters of ferric arsenate dihydrate is included for comparison.

A point-charge lattice-sum-calculation is being attempted to find out whether the quadrupole splitting in these compounds can be explained on the basis of the ionic model.

Small quadrupole splitting has been used by some authors as a criterion to distinguish high spin ferric ions. The large values observed here indicate that such criteria must be used with caution.

ACKNOWLEDGEMENTS

The authors wish to thank Dr. M. V. Ramaniah, Head, Radiochemistry Division, for his interest in this work and encouragement given.

REFERENCES

1. G. M. Bancroft, A. G. Maddock, W. K. Ong, R. H. Prince and A. J. Stone; J. Chem. Soc. (A), 1967 (1966)
2. C. K. Mathews; J. Inorg. Nucl. Chem. 31, 2853 (1969)
3. J. W. Mellor; A Comprehensive Treative on Inorganic and Theoretical Chemistry, 14, 88, 328, Longmans, Green & Co. (1947)
4. G. Brauer; Handbook of Preparative Inorganic Chemistry, Vol. II, 1501, Academic Press (1965)
5. P. Pascal; Nouveau Traite de Chemie Minerale, Vol. XVIII, 147, Masson et cie Paris (1963)
6. C. K. Mathews: Internal Rep., BARC(Radiochem)-75 (1967)
7. R. Ingalls; Phys. Rev. 128, 1155 (1962)
8. S. Goldztaub; Compt. rend. 198, 667 (1934)
9. G. Johansson; Acta Chem. Scand. 16, 1234 (1962)

TABLE I

Mössbauer Parameters

Sl. No.	Compound	Temp °K	Quadrupole splitting (mm/sec)	Isomer shift* (mm/sec)
1	$FeClSO_4$	296	1.12±0.05	0.76±0.05
		78	1.15±0.05	0.84±0.05
2	$Fe(OH)SO_4$	296	1.12±0.05	0.73±0.05
		78	1.04±0.05	0.79±0.04
3	FeOCl	296	0.70±0.04	0.61±0.04
4	$FeCl(HCOO)_2 . \frac{1}{2}H_2O$	296	0.14±0.04	0.66±0.04
5	$FeAsO_4 . 2H_2O$	296	0.39±0.04	0.66±0.04
		78	0.31±0.04	0.79±0.04

* Relative to sodium nitroprusside

SPECTRAL AND MAGNETIC INVESTIGATIONS ON SOME NOVEL PARAMAGNETIC SYSTEMS

P. S. Zacharias and A. Chakravorty
Department of Chemistry, Indian Institute of Technology, Kanpur

Triazene-1-oxides react with metal acetates to give the corresponding metal chelates. When a substituent (X) is put in the ortho-position of the phenyl ring, it has been observed that the metal chelates formed from the ligand exhibit some interesting phenomena in solution.

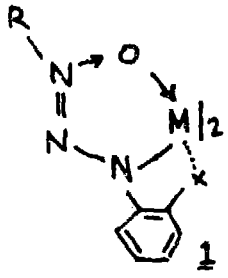

1

M = Ni, Co, Cu, Mn, Zn etc.

X = F, Cl, Br, I, OCH_3, OC_2H_5 SCH_3 etc.

All these compounds can be isolated as crystalline solids.

When M = Ni and X = OCH_3, OC_2H_5 SCH_3 etc., the complexes are fully paramagnetic in solid and solution phases (Table I). The electronic spectra of these compounds are characteristics of an pseudo-octahedral geometry (Table II).

When M = Ni and X = halogen, an intramolecular equilibrium of the type, planar $\rightleftharpoons$ octahedral is obtained. In solid state these complexes

(S = 0) (S = 1)

are diamagnetic, while in solution they become partially paramagnetic (Table I). This type of coordination by the halogen atom is a novel feature in structural chemistry.

The electronic spectra show two transitions at $\sim$ 1095 mμ and $\sim$720 mμ (Table II). From a comparison with the extinction coefficients of the unsubstituted chelates it has been concluded that the population of the planar species is $\sim$60% in solution at 30°C. The $\sim$1095 mμ band in all these nickel (II) chelates is assigned to the $^3A_{2g} \longrightarrow {}^3T_{2g}$ (ν_1) transition assuming an effective octahedral symmetry.

TABLE -I

Magnetic Moments Measurements

R	X	M	Solid	Solution
CH_3	OCH_3	Ni	3.25 B. M.	3.21 B. M.
"	OC_2H_5	"	3.33 "	3.21 "
"	F	"	Diamagnetic	0.86 "
"	Cl	"	"	1.41 "
"	OCH_3	Co	4.85 B. M.	4.78 B. M.
"	OC_2H_5	"	4.90 "	4.80 "
"	Cl	"	4.85 "	4.71 "
"	OCH_3	Mn	6.27 "	-

TABLE-II

Electronic Spectra

R	X	M	Bands λ	ϵ	λ	ϵ
CH_3	OCH_3	Ni	1180	(46.63)	695	(18.37)
"	Cl	"	1090	(12.86)	725	(84.48)
CH_3	OCH_3	Co	1260	(26.54)		
"	Cl	"	1270	(31.54)		

When M = Co, all the complexes are paramagnetic in solid and solution phases irrespective of the substituent at the ortho position.

The magnetic moments for these compounds show that these are octahedral, high spin compounds (Table I). The electronic spectra show a band $\sim$ 1260 mμ (Table II) which can be assigned to $^4T_{1g} \longrightarrow {}^4T_{2g}$ assuming an idealised octahedral geometry.

In the above octahedral complexes, depending on the disposition of the tridentate ligand, the complexes can assume a cis (meridionally span) or trans (facially) geometry. It has been found from the dipole moment measurements (moments less than 1 Debye) that they assume a trans octahedral geometry.

The nmr spectra of these complexes are indicative of the structural features. All the nickel complexes show isotopic contract shifts. Assignments can be made unambiguously based on the well resolved spin-spin splittings of the peaks. Further work is in progress.

DISCUSSION

V. V. Savant : 1) Ni(II) complex which is considered to be octahedral should give three d-d bands. But only 2 bands are shown. What about the third band.

2) If equilibrium occurs in solution, whether solid spectra would have given any information.

P. S. Zacharias : 1) Equilibrium exists.

2) Not recorded.

INFRA-RED ABSORPTION SPECTRA OF METAL COMPLEXES OF SOME SULPHUR CONTAINING LIGANDS

H. L. Nigam, A. N. Kumar and K. B. Pandeya
Department of Chemistry, University of Allahabad, Allahabad

INTRODUCTION

Structure determination of coordination compounds particularly in regard to metal-ligand site attachment[1, 2, 3] has been increasingly pursued in recent years by the study of infra-red absorption spectra of the complexes. The most expedient way of doing so is based on the group-frequency-concept of the observed i. r. bands. However, very little has been achieved even by the application of this method towards understanding the nature of metal-sulphur link, which has aroused considerable interest due to the enigmatic donor properties of sulphur on the one hand and increasing use of these compounds in biology, medicine and industry on the other.

We have, therefore, examined the i. r. spectra of some transition metal complexes involving sulphur-containing ligands, namely, thiovanol, thiosalicylic acid and thiopropionic acid. The ligands have been so chosen that the active sulphydryl-group in each case is present in a different environment. Tables I and II contain relevant data on I. R. bands observed in the spectra of complexes under study.

DISCUSSION

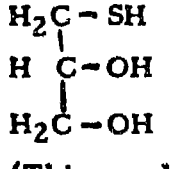

(Thiovanol)

Thiovanol has a propane chain with a sulphydryl group in the α-position and one alcoholic group each in β- and γ-positions and may act, therefore, as a mono-, bi- or tridentate ligand involving either the sulphur or/and oxygen atoms in coordination.

A perusal of the infra-red spectral data (Table I) reveals that the ν_{S-H} band, which appears at 2550 cm^{-1} in the ligand spectrum, disappears in the spectra of the complexes. Further, appearance of additional bands in the 400 - 300 cm^{-1} region, assignable to ν_{M-S}, appears to establish the presence of metal-sulphur link in the complexes. This is also

TABLE I

I.R. Absorption bands (cm^{-1}) of Thiovanol (thin liquid film) and its Complexes (KBr pellets) Recorded on Perkin-Elmer 521 in the Region 4000 cm^{-1} to 300 cm^{-1}

Compounds	ν_{S-H} ref. 4, 5	δ_{O-H} ref. 6	$\nu_{C-O(p)}$ ref. 6	$\nu_{C-O(a)}$ ref. 6	ν_{C-S} ref. 8	ν_{M-O} ref. 9 10, 11	ν_{M-S} ref. 12, 13, 14
$[Co(III)(TV)_3].2H_2O$	-	1392 1320	1080	1015	632	445	340
$[Rh(III)(TV)_3]$	-	1390 1310	1085	1010	-	430	320
$[Ni(II)(TV)_2]_2.16H_2O$	-	1390 1310	1085	1020	-	450	365
$[Pd(II)(TV)_2].2H_2O$	-	1400	1085	1025	-	430	350
$[Pt(II)(TV)_2]$	-	1330 1392 1330	1085	1020	-	460	385 335
$[Cu(I)(TV)]$	-	1400 1320	1085	1010	622	445	365 325
$[Ag(I)(TV)]$	-	1405 1320	1092	1025	632	462	358 328
$[Au((I)(TV)]$	-	1390 1320	1080	1020	632	465	380 350
[Thiovanol (TV)]	2550	1392 1320	1085	1028	635	-	-

TABLE II

I. R. Absorption Bands (cm^{-1}) for Thiosalicylic Acid and its Complexes (all nujoll mull) and Thiopropionic (thin liquid film) and its Complexes (nujoll mull); Perkin-Elmer (3300-700 cm^{-1})

Compounds	ν_{S-H} ref. 4,	ν_{C-O} ref.7	$\nu_{C=O}$ ref. 7	Compounds	ν_{S-H} ref. 4,	ν_{C-O} ref.7	$\nu_{C=O}$ ref. 7
$H[Rh(III)(TSA)_4 2H_2O] \cdot H_2O$	-	1275	1690	$[Rh(III)(TPA)Cl 2H_2O]_2$	-	1241	1712
$H_2[Pt(IV)(TSA)_4Cl_2] \cdot 2H_2O$	-	1275	1695	$[Pt(IV)(TPA)_2Cl_2]$	-	1305	1689
$H_2[Pd(II)(TSA)_2] 2H_2O$	-	1265	1697	$[Pd(II)(TPA)2H_2O]$	-	1266	1712
$[Ni(II)(TSA)_2]_2 2C_2H_5OH$ (Yellowish green)	-	1290	1590	$[Ni(II)(TPA)_2 2H_2O]$ (Green)	-	1316	1587
$H_2[Ni(II)(TSA)_4] 2CH_3COOH$ (Black)	-	1285	1705	$[Ni(II)(TPA)_2]$ (Red)	-	1290	1601
$H[Ni(II)(TSA)_3] 2C_2H_5OH$ H_2O(Muddy Green)	-	1287	1660	$[Cr(III)(TPA)_3]$	-	1290	1575
$H_2[Cu(II)(TSA)_4 2H_2O] \cdot 2H_2O$	-	1275	1690	$[Cu(II)(TPA)_2 2H_2O]$	-	1276	1692
$[Co(II)(TSA) 4H_2O]$	-	1250	1715	$[Co(II)(TPA)_2 2H_2O]$	-	1262	1572
Thiosalicylic acid (TSA)	2570	1275	1695	Thiopropionic acid (TPA)	2577	1250	1712

supported by lowering in the position of ν C-S in the complexes. Bands also appear in the region 500 - 400 cm^{-1} attributable to ν M-O and indicate the presence of metal-oxygen bond in the complexes. Coordination through the oxygen of primary alcoholic group is indicated by the red-shift of the ν C-O (primary alcoholic). Thiovanol, thus, seems to be acting as a mono-negative-bidentate ligand, coordinating through the anionic sulphydryl group and neutral primary alcoholic group.

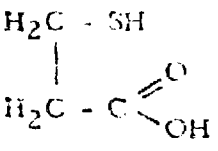

(Thiopropionic acid)

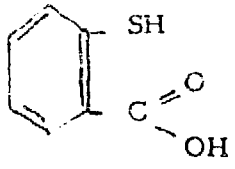

(Thio salicylic acid)

From the structure of the acids it is evident that they may coordinate through the sulphydryl group and/or through the carboxyl group. The νS-H band appearing at 2570 cm^{-1} for thiosalicylic and at 2577 cm^{-1} for thiopropionic acid disappears in the spectra of their complexes, indicating the protonation of the sulphydryl hydrogen followed by the formation of metal-sulphur bond.

As regards coordination through the carboxyl group the acids may show the following three types of behaviour:-

(i) No coordination takes place through the carboxyl group. This type of behaviour is shown by thiosalicylic acid in its complexes with Rh(III), Pt(IV), Ni(II) (violet) and Cu(II), where the position of νC-O and νC=O bands show no considerable change in the spectra of the complexes; the ligand acting as mono-negative mondentate.

(ii) Coordination Takes Place Through the Carbonyl Oxygen of the Carboxyl Group - In the complexes of thiosalicylic acid with Ni(II) muddy green and yellowish green), a red-shift for νC=O band position and a blue-shift for ν C-O band position is observed. Similar shifts for these band positions are also observed in the spectra of the complexes of thiopropionic acid in the complexes with Cr(III), Pt(IV), Ni(II) green, Ni(II) red, Cu(II) and Co(II). The acids in these complexes seem, therefore, to be acting as mono-negative bidentate ligands.

(iii) Coordination Takes Place Through the Hydroxyl Oxygen of the Carboxyl Group: Thiosalicylic acid in its Co(II) and Pd(II) complexes and thiopropionic acid in its Rh(III) and Pd(II) complexes show this type of behaviour, as evidenced by the observed lowering in the position of C-O band.

REFERENCES

1. R. B. Penland, T. T. Lane and J. V. Quagliano; J. Am. Chem. Soc. 78, 887 (1956)

2. R. B. Penland et al; J. Am. Chem. Soc. 79, 1575 (1957)

3. A. Yamaguchi et al.; J. Am. Chem. Soc. 80, 527 (1958)

4. Haines, Helm, Baiky and Ball; J. Phys. Chem. 58, 270 (1954)

5. Wagner, Becher and Kottenhaln; Chem. Ber. 87, 1110 (1956)

6. L. J. Bellamy; The Infra-Red Spectra of Complex Molecules, Methuen& Co. Ltd., London) Ed. II p. 110 (1964)

7. L. J. Bellany; The Infra-Red Spectra of Complex Molecules, Methnen & Co. Ltd.)London) Ed. 11 p. 162 (1964)

8. Sheppard; Trans. Faraday Soc. 46, 429 (1950)

9. Jones Dismukesh and Ballar; J. Phys. Chem. 68, 792 (1961)

10. Djordjevic; Spectrochim. Acta. 17, 448 (1961)

11. Ayres Gilbert, Fredrich and Young; Anal. Chem. 22, 1277-80 (1950)

12. Madan and Goldstein; J. Inorg. Nucl. Chem. 28, 1257 (1966)

13. Madan and Sulich; Inorg. Chem. 5, (10) 1662 (1962)

14. Livingstone, Chaston Lockyer, Pickles and Shannon; Aust. J. Chem. 18, 673 (1962)

SOME COMPLEXES OF RUTHENIUM (II)

M. M. Taqui Khan and S. Vancheesan
Department of Chemistry, Indian Institute of Technology, Madras-36

Tristriphenylphosphine dichlororuthenium(II) and tristriphenyl phosphine hydridochloro-ruthenium(II) have been recently reported by Wilkinson and Coworkers[1, 2] to be very good catalysts for the homogeneous hydrogenation of alkenes. As the part of a programme to study the catalysis by Ru(II) complexes in the homogeneous hydrogenation of alkenes, the following complexes of ruthenium(II) have been prepared.

I. Tristriphenyl arsinedichloro-ruthenium(II)

Triphenylarsine reacts with a methanolic hydrochloric acid solution of aquo-trichloro-ruthenium(III) in nitrogen atmosphere to give a browinsh balck oil which crystallises slowly to a brownish black crystalline solid. (m. p. = 210 - 211°).

Infra-red spectrum of the compound gives a very strong peak at 320 cm^{-1} which can be assigned to Ru-Cl stretching frequency. The assignment of 320 cm^{-1} peak to Ru-Cl stretching is supported by a peak at 315 cm^{-1} in the tristriphenyl-phosphine dichloro-ruthenium(II) complex assigned to Ru-Cl stretch by Hallman et al[2]. The shift in the Ru-Cl frequency in triphenylarsine complex may be explained on the basis of a weaker Ru-As bond as compared to the Ru-P bond. The structure of tristriphenyl arsine dichloro-ruthenium(II) may be similar to the analogous phosphine complex as shown in Figure 1.

II. Bis (1, 2-diphenyl phosphinoethane) dichloro-ruthenium(II)

When an ehanol-benzene solution of 1, 2 bisdiphenyl-phosphionoethane is refluxed with a methanolic hydrochloric acid solution of aquotrichloro-ruthenium(III) in an atmosphere of nitrogen, bis (1, 2-diphenyl phosphinoethane) dichloro-ruthenium(II) (A) separates as a pale yellow amorphous powder. The complex is recrystallised from benzene under nitrogen. (m. p. 295 - 297°).

The infra-red spectrum of A shows absorption at 320 cm^{-1} which may be assigned to Ru-Cl stretching frequency and supports a trans disposition of the coordinated halogens as in the case of triphenyl phosphine complex. Hydrogenation of A has yielded a hydride (B) with Ru-H stretch-

Fig. 1

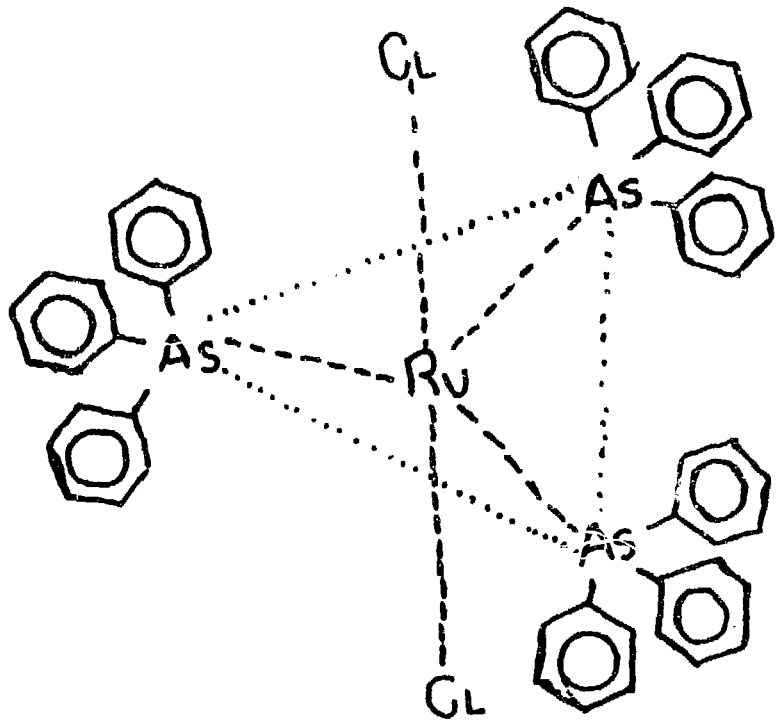

ing at 1615 cm^{-1}. The drastic reduction in M-H stretching frequency in B may be explained on the basis of the formation of a dihydrido complex from the displacement of the two coordinated chloride ions in (A). The assignment of the Ru-H frequency is supported by the work of Chatt et al[3] who has reported a metal-hydrogen stretching frequency of 1615 cm^{-1} for the bis(1,2 dimethyl phosphinoethane) dihydrido-ruthenium(II) complex. The structure of A may be thus represented with a trans disposition of the phosphinoethane and chloride ligands as in Figure 2. The structure of the complex is further supported by a low dipole moment of 0.5 D.

N. M. R. spectrum of the complex at 27° gives a sharp intense peak at τ = 7.21 and a quartet of low intensity centered at τ = 2.8. The intense peak at τ = 7.21 may be assigned to the methylene protons on the phosphinoethane rings. Due to rapid changes in the configuration of the metal-chelate rings in solution, the methylene protons may become equivalent and give rise to a single peak. The quartet of low intensity centred at τ = 2.8 may be assigned to the phenyl protons on the phosphorus atoms. The multiplet may be due to different degrees of rotation of the phenyl groups in solution around the P-C bond.

III. Bis N, N'-diphenylethylenediaminechlorotrichlorostannate-ruthenium(II).

To an boiling solution of aquotrichloro-ruthenium(III) in methanolic-hydrochloric acid, a solution of $SnCl_2$ in HCl (10 times excess) is added in nitrogen atmosphere. On the addition of an aqueous solution of N, N'-diphenylethylene-diamine, an orange red crystalline complex separates. (m. p. 292 - 294°).

The infra-red spectrum of the complex shows a weak peak at 560 cm^{-1} which may be assigned to M-N stretch. A very broad peak is observed from 280-310 cm^{-1} which may be assigned[4] to Ru-$SnCl_3$ and Ru-Cl stretch. The complex may have a cis or trans disposition of chloride and stannous chloride groups and may be a cis or trans isomer. Based on the red colour[5] of the complex it may probably have a cis structure.

A summary of the infra-red peak 700-250 cm^{-1} in the complexes studied are presented in Table I.

TABLE I

Complex	Frequency (700-250 cm^{-1})
$RuCl_2(AsPh_3)_3$	690(s), 465(s), 320(s).
$RuCl_2\{(C_6H_5)_2PCH_2CH_2P(C_6H_5)_2\}_2$	530(v. s.), 505(s), 490(s), 445(s), 420(w), 320(w).
$RuCl\{(C_6H_5)NCH_2\text{-}CH_2N(C_6H_5)\}_2$ $SnCl_3$	560(w), 280-310(broad peak) 270(sh)

EXPERIMENTAL

All the preparations are carried out in an atmosphere of nitrogen freed from oxygen, by passing the gas through a solution of vanadium(II) sulphate.

1) Tristriphenylarsinedichloro-ruthenium(II)

0.2 g of aquotrichloro-ruthenium(III) in 50 ml concentrated HCl and methanol (1:1) mixture is refluxed for an hour. To the hot solution is

added a solution of triphenylarsine (1.2 g) in methanol (20 ml) and refluxed for another 30 minutes. A brownish-black oily liquid separates which slowly turns to a crystalline solid of the same colour. The complex is highly soluble in benzene. The solution of the complex in benzene when exposed to air turns darker due to oxidation of the complex.

Analysis

$RuCl_2 (AsPh_3)_3$

Requires C = 59.45% H = 4.13%

Found C = 57.37% H = 5.12%

ii) Bis(1,2-diphenylphosphinoethane) dichloro-ruthenium (II)

0.2 g of aquotrichloro-ruthenium(III) in 50 ml of concentrated HCl and ethanol (1:1) is heated over a water-bath for one hour. A hot solution of (1,2-bisdiphenylphosphinoethane) (1.2 g) in 15 ml of ethanol-benzene mixture (1:1) is added. A pale yellow amorphous powder is obtained which is recrystallised from benzene.

Analysis

$RuCl_2 \left\{(C_6H_5)_2 PCH_2\text{-}CH_2 P(C_6H_5)_2\right\}_2 . C_6H_6$

Requires C = 66.54% H = 5.14%

Found C = 69.98% H = 6.2%

iii) Bis N, N' diphenylethylenediaminechlorotrichlorostannate ruthenium(II)

0.2 g of aquotrichloro-ruthenium(III) in methanolic-hydrochloric acid solution is refluxed for one hour with $SnCl_2$ in HCl (10 times excess) followed by the addition of 1.2 g of N, N'-diphenylethylenediamine in 15 ml of water. An orange red crystalline complex separates which is recrystallised from hot methanol.

Analysis

$Ru \left\{(C_6H_5) - HCH_2\text{-}CH_2\text{-}N(C_6H_5)\right\}_2 SnCl_3 . Cl$

Requires C' = 43% H = 3.6%

Found C = 39.7% H = 3.9%

ACKNOWLEDGEMENT

The authors thank Prof. C. N. R. Rao, Senior Professor and Dean of Development and Research, I. I. T. (Kanpur), for his valuable aid in getting the far I. R spectra of the complexes in his laboratory. The authors also thank Dr. G. S. Siddhu, Director, R. R. L., Hyderabad, for the n. m. r spectrum of complex A.

REFERENCES

1. D. Evans, J. A. Osborn, F. H. Jardine and G. Wilkinson; Nature 208, 1203-4 (1965)

2. P. S. Hallman, B. R. McGarvey and G. Wilkinson; J. Chem. Soc. (A), 12, 3143 (1968)

3. J. Chatt and J. M. Davidson; J. Chem. Soc. pp. 843 (1965)

4. M. Sakakibara, Y. Takahashi, S. Sakai and Y. Ishii; Inorganic Nuclear Chemistry Letters 427, May (1969)

5. F. Young, D. Gillard and G. Wilkinson; J. Chem. Soc. 5176(1964)

Fig. 2.

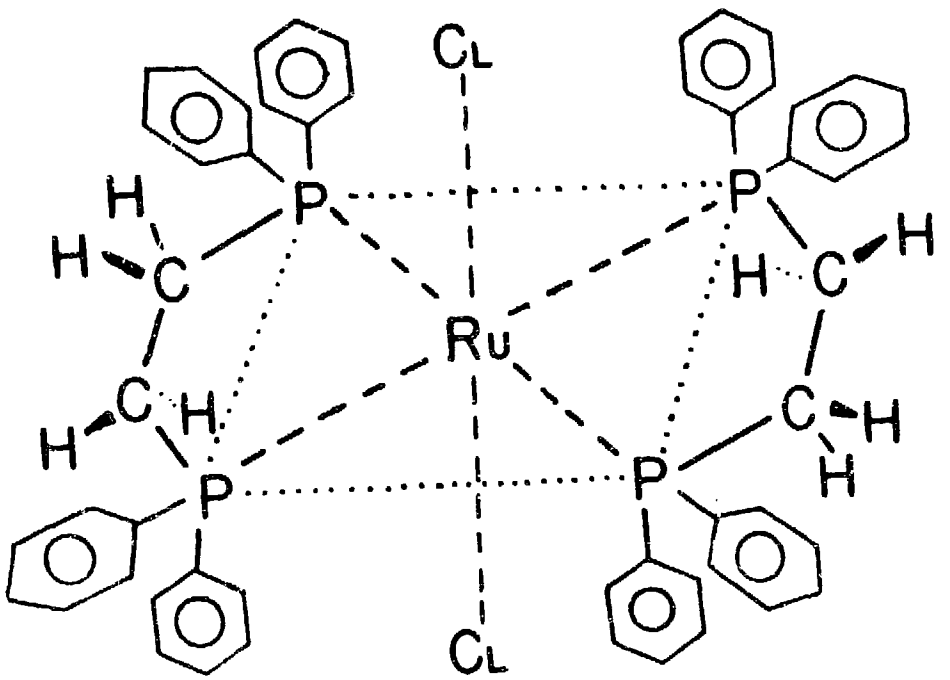

NATURE OF THE SOLUTIONS IN FLUOROSULPHURIC ACID

R. C. Paul, Krishan Kant Paul and K. C. Malhotra
Chemistry Department, Panjab University, Chandigarh-14

A lot of interest has been shown in the solution chemistry of strong protonic acids such as sulphuric[1], fluorosulphuric[2] and disulphuric acids[3, 4] as these are very weak acceptors and, therefore, are capable of stabilizing strongly electrophilic cations of the type I_2^+, Se_4^{2+} and Te_4^{2+} etc. Fluorosulphuric acid has been shown to be even stronger than sulphuric acid[2]. It is, therefore, of some interest to investigate the solution chemistry in this medium. Furthermore, its dielectric constant is even higher than that of water and sulphuric acid; in addition to it, this acid is less viscous than sulphuric acid.

It has been demonstrated by Gillespie and co-workers[5] that the strength of fluorosulphuric acid is further enhanced by the addition of sulphurtrioxide and antimony pentafluoride; the acid formed may ionize as:

$$3SO_3 + SbF_5 \longrightarrow SbF_2(SO_3F)_3$$

$$2HSO_3F + SbF_2(SO_3F)_3 \longrightarrow H_2^+SO_3F + [SbF_2(SO_3F)_4]^-$$

Olah[6] and co-workers have profitably used this medium for the protonation of very weak bases. It has also been shown by Gillespie[7] and co-workers that there is slight protonation of very weakly basic compounds like carbondioxide etc.

Waddington and co-workers[8] have investigated the solution chemistry in liquid hydrochloric acid and a large number of reactions have been explained in terms of the autoionization of the medium as:

$$3HCl \rightleftharpoons H_2^+Cl + HCl_2^-$$

Though a large number of experimental evidence is available for the anionic species HCl_2^-, the literature lacks evidence for the cationic species H_2^+Cl. We have investigated the behaviour of hydrochloric acid (gas) in fluorosulphuric and also in "super acid" to show the existence of acidium hydrochloric acid species.

Hydrochloric gas is only slightly soluble in fluorosulphuric acid. There has been no evidence to show that there has been any loss of sulphur

trioxide as a result of the decomposition of the solvent when hydrochloric gas was passed through fluorosulphuric acid. It has also been found that hydrochloric acid gas obeys Henry's Law when dissolved in fluorosulphuric acid, indicating no interaction between the solvent and he gas. It has further been found that there is no change in the conductance of the solution indicating that it is not protonated in fluorosulphuric acid. The possibility of its behaving as an acid of the system has been ruled out as when potassium fluorosulphate, a strong base of this solvent system is added to the above solution, the slope of the conductance-composition curve is exactly the same as that of pure potassium fluoro-sulphate in fluoro-sulphuric acid indicating that hydrochloric (acid) gas behaves as a nonelectrolyte in fluorosulphuric acid. This seems to be quite reasonable, as sulphuric acid, which is a stronger acid than hydrochloric acid, behaves as a weak base of fluoro-sulphuric acid solvent system.

The behaviour of hydrochloric gas in fluorosulphuric acid has been further confirmed by the behaviour of triphenyl chloromethane which is solvolysed in it. Conductance of the solution has been found to be of the same magnitude as potassium fluorosulphate indicating that triphenyl chloromethane is solvolysed in it as:

$$(C_6H_5)_3CCl + HSO_3F \longrightarrow (C_6H_5)_3C^+ + HCl + SO_3F^-$$

From the value of γ, the number of fluoro-sulphate ions, it is observed that there is no contribution of hydrochloric acid towards the conductance of the solution. The extent of complete solvolysis of triphenyl chloromethane in fluoro-sulphuric acid has been confirmed from the molar extinction coefficient of triphenyl carbonium ion. The observed molar extinction coefficient is comparable to that of reported value in literature[9] indicating the complete solvolysis of triphenyl chloromethane and that hydrochloric (acid) gas is only slightly soluble and behaves as a non-electrolyte in fluoro-sulphuric acid.

However, when hydrochloric (acid) gas is passed in super-acid system $HSO_3F - SbF_5 - SO_3$, it has been found to be fairly soluble. The conductance of the solution steadily decreases as the gas is passed which indicates that hydrochloric acid behaves as a base in super-acid. The decrease in the conductance of the solution by the passage of hydrochloric acid shows the decrease in the concentration of fluoro-sulphuric acidium ion $H_2^+SO_3F$. The reaction may be represented as:

$$2HSO_3F + SbF_5 + 3SO_3 \longrightarrow H_2^+SO_3F + \left[SbF_2(SO_3F)_4\right]^-$$

$$HCl + H_2^+SO_3F + \left[SbF_2(SO_3F)_4\right]^- \longrightarrow H_2^+Cl + \left[SbF_2(SO_3F)_4\right] + HSO_3F.$$

When the complete neutralization of the acid takes place, there is no further increase in the conductance of the solution as HCl is passed. Conducto-

metric titration has been represented graphically. For comparison, conductometric titration between potassium fluoro-sulphate and super-acid has also been reported. Unlike potassium fluoro-sulphate, there is no sharp break in the conductance composition curve in case of hydrochloric acid which suggests that hydrochloric acid is a weak base.

All attempts to isolate a compound of composition $H_2^+Cl.[SbF_2(SO_3F)_4]^-$ have failed because of the high viscosity of the super-acid medium. Proton N. M. R. studies of the solution could not be carried out to characterise the species H_2^+Cl because of the rapid exchange of the proton with the solvent. However, the conductometric titrations definitely indicate the presence of the species H_2^+Cl. Further attempts are being made to characterise the hydrochloric acidium species.

REFERENCES

1. J. Barr, R. J. Gillespie and E. A. Robinson; Can. J. Chem. 39, 1266 (1961)

2. A. A. Woolf; J. Chem. Soc. 433 (1955)

3. R. J. Gillespie and K. C. Malhotra; J. Chem. Soc. 1933 (1967)

4. R. J. Gillespie and K. C. Malhotra; J. Chem. Soc. 1998 (1968)

5. R. C. Thompson, J. Barr, R. J. Gillespie, J. B. Milne and R. A. Rotheenbury; Inorg. Chem. 4, 1641 (1965)

6. G. A. Olah and R. H. Schlosberg; J. Am. Chem. Soc 90, 2726 (1968)

7. R. J. Gillespie and G. P. Pez; Inorg. Chem. 8, 1233 (1969)

8. M. E. Peach and T. C. Waddington; J. Chem. Soc.

9. Gold and Hawes; J. Chem. Soc. 2102 (1951)

DISCUSSION

C. N. R. Rao : Have you examined aromatic hydrocarbons in in flurosulphuric acid? I expect carbonium ions to be formed relatively easily.

K. K. Paul : Aromatic hydrocarbons have not been studied, however, we have studied some diketones and polyketones and there is definite evidence from U.V spectroscopy and conductometry that carbonium ions are formed.

NATURE OF THE COMPLEXES OF SULPHURTRIOXIDE WITH IODINE CHLORIDES

R. C. Paul, C. L. Arora and K. C. Malhotra
Department of Chemistry, Panjab University, Chandigarh

It has recently been established that sulphurtrioxide combines with ionisable chloride ions of metal chlorides to form chloro-sulphates[1-3] which are slightly polymerized through chlorosulphate bridging. Iodine monochloride[4] and trichloride[5] have been shown to be feebly self-ionised which has been illustrated by the solvo acid-base studies in these media by Gutmann and co-workers. It is, therefore, of interest to investigate the nature of the adducts of sulphur trioxide with these chlorides which may be helpful to understand the nature of these chlorides. In the present communication we have isolated compounds of composition $ICl_3.SO_3$, $ICl_3.3SO_3$ and $ICl.SO_3$ and have investigated their behaviour in strongly acidic media.

When excess of sulphur trioxide is added to a cold suspension of iodine trichloride in carbon tetrachloride at 0°C, a yellowish orange crystalline compound of the composition $ICl_3.SO_3$(I) (m. pt. 8°) separates out. Its molar conductance and cryoscopic studies in nitrobenzene indicate it to be a uni-univalent electrolyte. Infra-red spectra of (I) shows the presence of six absorption bands at 1160, 1030, 840, 750, 640 and 560 cm^{-1} which correspond to chlorosulphate group (C_{3v}) and thus conform the presence of chlorosulphate ion[6], which suggests that sulphur-trioxide combines with one chlorine atom of iodine chloride to form mono-chlorosulphate ion.

Iodine dichloridemonochlorosulphate (I) has a high conductance in chloro-sulphuric acid. It may behave as an acid (according to equation 'a') or a base (according to equation 'b') in this medium.

$$ICl_2SO_3Cl + 2HSO_3Cl \longrightarrow H_2^+SO_3Cl + ICl_2(SO_3Cl)_2^- \quad \ldots\ldots \text{(a)}$$

$$ICl_2SO_3Cl \longrightarrow ICl_2^+ + SO_3Cl^- \quad \ldots\ldots\ldots \text{(b)}$$

Acetic acid, a strong base of chloro-sulphuric acid system[7] when added to the solution of (I) in chloro-sulphuric acid causes an increase in the conductance of the same magnitude as would have been produced in the absence of iodine dichloridemonochlorosulphate indicating it to behave according to equation (b) and rules out its behaviour as an acid. It is solvolysed in disulphuric acid like alkali metal chlorosulphates as:

$$ICl_2SO_3Cl + 2H_2S_2O_7 \longrightarrow ICl_2^+ + HSO_3Cl + HS_3O_{10}^- + H_2SO_4$$

ICl_2^+ cation, being a strong electrophile, is quite stable in weakly nucleophilic media. The existence of ICl_2^+ ion in the solid state has already been established by X-ray[8] and infra-red studies[9] of the solid complexes of $ICl_3 . SbCl_5$ and $ICl_3 . Al Cl_3$ which have been found to be ionic in nature.

But, when sulphur trioxide is treated with iodine trichloride at room temperature, an orange coloured compound of composition $ICl_3 . 3SO_3$ is obtained. Infra-red spectrum of the compound shows the presence of chlorosulphate group. Because of the limited transparency of the window used, absence of I-Cl bond could not be observed. Its conductance in chloro-sulpuric acid is quite low (Fig. 1) showing it to be a weak electrolyte. In order to ascertain whether $I(SO_3Cl)_3$ ionizes as an acid or a base, conductivities of the solution obtained by adding successive amounts of acetic acid to $I(SO_3Cl)_3$ solutions were measured. There is no decrease in the conductance of the solution but the slope of the conductivity curve is less than that for acetic acid in HSO_3Cl, indicating that $I(SO_3Cl)_3$ behaves as a weak acid in chlorosulphuric acid as:

$$I(SO_3Cl)_3 + SO_3Cl^- \rightleftharpoons I(SO_3Cl)^-_4$$

The lower values of conductance may be attributed to the removal of SO_3Cl^- ion by $I(SO_3Cl)_3$ as shown in the above equation. Water was also added to the solution of $I(SO_3Cl)_3$ in chlorosulphuric acid. There was no change in the conductance of the solution. By analogy with the reaction of water on iodine trifluorosulphate in fluorosulphuric acid[10], the reaction may be represented as:

$$I(SO_3Cl)_3 + HOH \longrightarrow IO(SO_3Cl) + 2HSO_3Cl.$$

At higher concentration of water, these ions disproportionate and the colour of the solution changes to green. Tri-positive oxidation state of iodine is extensively disproportionated in aqueous solution, however, it has also been found to be quite stable in sulphuric acid[11] and fluoro-sulphuric acid[12].

In case of iodine monochloride, when excess of sulphur-trioxide is removed under vacuum, a viscous deep orange red coloured fuming liquid of composition $ICl . SO_3$ is left behind. Infra-red spectral analysis of the compound shows the presence of chloro-sulphate group, suggesting that sulphur trioxide has not oxidized iodine monochloride, but has combined with chlorine to form mono-chlorosulphate. On exposure to moisture, it develops green colour. It is a thermally stable ionic compound. Its conductivity in chlorosulphuric acid is quite low. It is about one-fourth of that of potassium chlorosulphate. Ultra violet spectrum of the solution shows the presence of I_3^+ cation[13]. From the value of molar extinction coefficient and its conductance in chlorosulphuric acid, the mode of dissociation of iodine monochlorosulphate in chlorosulphuric acid may be represented as:

$$4ISO_3Cl \longrightarrow I_3^+ + I(SO_3Cl)_3 + SO_3Cl^-$$

A slightly lower value of γ (SO_3Cl^- ion is the labile ion in chlorosulphuric acid), than required by the above equation may be due to feeble acidic character of $I(SO_3Cl)_3$. In disulphuric acid iodine monochlorosulphate is solvolysed to form greenish blue solution. Here +1 oxidation state of iodine disproportionates to form I_2^+, I_3^+ and to some extent I^{+3}. Its conductance in disulphuric acid is comparable to that of iodine monochloride in disulphuric acid[14]. Visible spectrum of the solution gives a characteristic spectrum of I_2^+ with a strong band at 640 mμ and weaker bands at 510 and 420 mμ. Here there is also a slight characteristic peak due to I_3^+ ion at 300 mμ. But its concentration is quite low. By analogy with iodine monochloride in disulphuric acid[14], the behaviour of iodine monochlorosulphate in disulphuric acid may be postulated as:

$$5ISO_3Cl + 6H_2S_2O_7 \longrightarrow 2I_2^+ + I^+(HSO_4)_2 + 3HS_3O^-_{10} + 5HSO_3Cl + H_2SO_4.$$

Freezing point and conductance data are in good agreement with the above equation where chlorosulphuric acid behaves as a non-electrolyte[15].

Some of the chlorosulphates are known to be polymeric in character, polymerisation occuring through chlorosulphate bridging. However, in the present case there is no polymerisation because of the absence of d orbitals in iodine. On the other hand, the chlorosulphates ($I.SO_3Cl$, $ICl_2.SO_3Cl$) show ionic character, while $I(SO_3Cl)_3$ acts as weak Lewis acid in chlorosulphuric acid.

REFERENCES

1. R.C. Paul, K.K. Paul and K.C. Malhotra, Chem. Ind. 1227 (1968)

2. R.C. Thompson, J. Barr, R.J. Gillespie; J.B. Milne and R.A. Rothenbury; Inorg. Chem. 4, 1641 (1965)

3. R.C. Paul, K.K. Paul and K.C. Malhotra; Aust. J. Chem. 22, 847 (1969)

4. V. Gutmann; Z. anorg. Chem. 264, 169 (1951)

5. V. Gutmann; Mh. Chem. 82, 473 (1950)

6. T.C. Waddington and F. Klanberg, J. Chem. Soc. 2339 (1960)

7. E.A. Robinson and J.A. Ciruna; J. Am. Chem. Soc. 86, 5677 (1964)

8. K.H. Boswijk and E.H. Wiehenga; Acta. Crys. J. 417 (1954)

9. C. G. Vink and E. H. Wiebenga; Acta. Cryst. 12, 859 (1959)

11. J. Arotsky, H. C. Mishra and M. C. R. Symons; J. Chem. Soc. 2582 (1962)

12. J. Barr, R. J. Gillespie and R. C. Thompson; Inorg. Chem. 3, 1149 (1964)

13. R. J. Gillespie and J. B. Milne; Inorg. Chem. 5, 1577 (1966)

14. R. J. Gillespie and K. C. Malhotra; Inorg. Chem. 8, 1751 (1969)

15. R. J. Gillespie, and K. C. Malhotra; J. Chem. Soc. A, 1994 (1967)

CAPTIONS AND LEGENDS FOR FIGURE-1

Acetic acid.	•
ICl_2SO_3Cl	⊙
ICl_2SO_3	✦
$I(SO_3Cl)_3$	●
Acetic acid in solution of $I(SO_3Cl)_3$	△
Water in solution of $I(SO_3Cl)_3$	⊡

FIG - I

SP. CONDUCTANCES IN CHLOROSULPHURIC ACID.

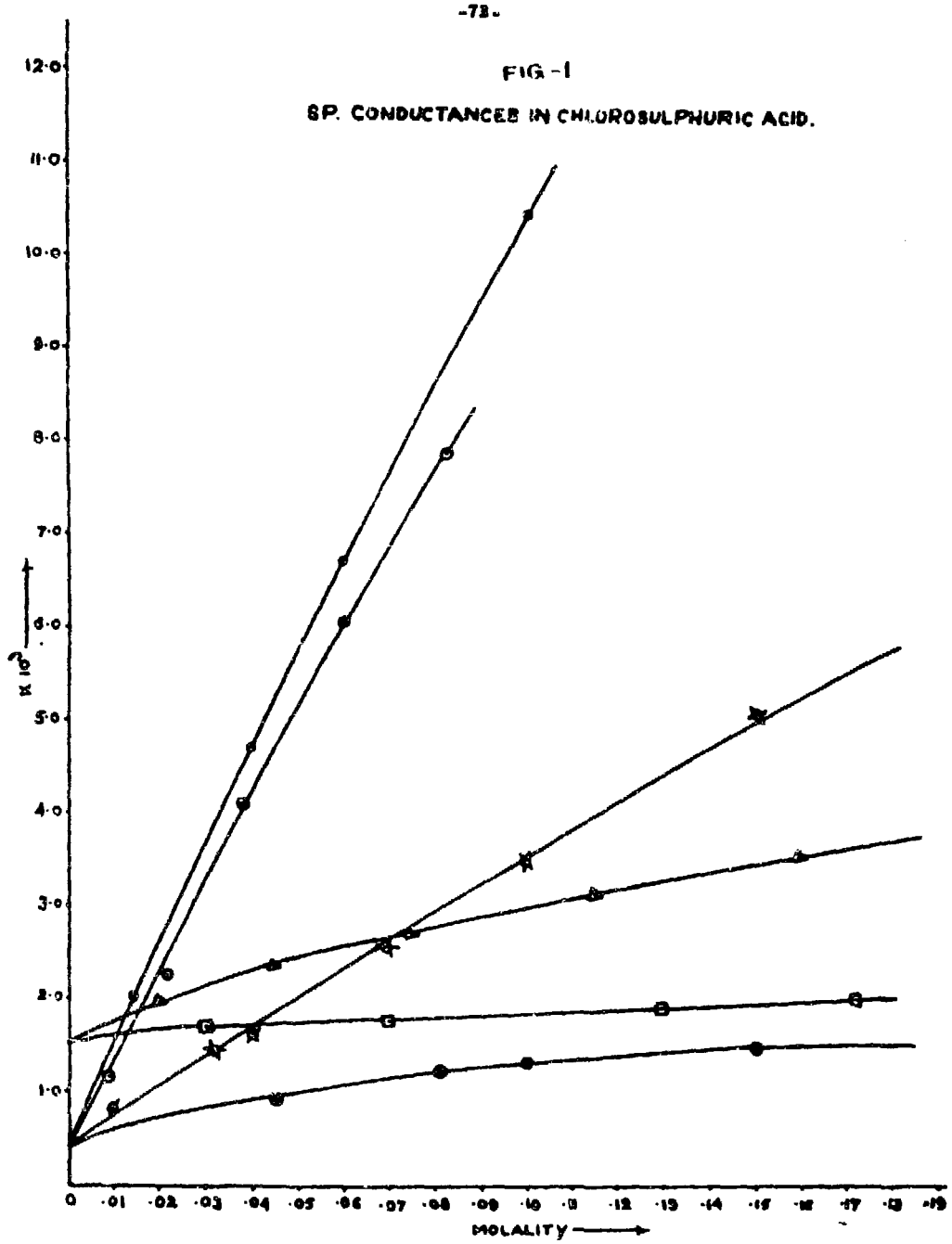

A STUDY IN SOME OUTER SPHERE AND MIXED LIGAND COMPLEXES

D. C. Patel and P. K. Bhattacharya
Chemistry Department, M. S. University of Baroda, Baroda-2

Nickel and copper complexes have received attention of various investigators. Formation of mixed and poly-nuclear complexes have been reported[1-3]. However, study of the exchange of ligand has not been very wide. In a recent communication from this laboratory, the effect of addition of catechol and pyrogallol on bis or tris ethylenediamine nickel complexes was studied. The addition of very small amount of the ligands results in the formation of solids having composition $[Ni(L)_2](enH_2)_2^{+2}$. The compounds have been characterised and it has been argued that catacholate and pyrogallolate ions being more complexing replace the ethylenediamine to the outer sphere even at a high pH. In extension of the work reaction of gallic acid on bis or tris ethylenediamine, nickel dichloride has been investigated. The additon of small amount of the ligand does not result in any reaction. On the addition of excess of the ligand, a solid is obtained. The analysis corresponds to the composition $[Ni(L)_2](enH_2)_2^{+2}$. The same compound is obtained on the addition of ethylenediamine to a mixture of nickel dichloride and gallic acid. This indicates that gallic acid cannot replace ethylenediamine at high pH, but on the addition of excess gallic acid, the pH goes down and the $[Ni(en)_2]^{+2}$ and $[Ni(en)_3]^{+2}$ dissociate. Immediately, there is formation of $[Ni(gallic)_2]^{4-}$ and two enH^{2+} ions come in the outer sphere. The reaction can be represented as follows:

$$[Ni(en)_2]Cl_2 + 2\ (OH)_3C_6H_2COOH \longrightarrow [Ni(C_6H_3O_3COO^-)_2](enH_2)_2^{2+} + 2\ HCl$$

This indicates that coordination takes place from 2-OH groups in the gallic acid. That the solid is a monomer is determined by its amorphous nature and partial solubility in water. The magnetic moment corresponds to two unpaired spin possible in an outer orbital square planar or a distorted octahedral structure. The visible spectrum in the region 400-800 mμ corresponds to a square plannar structure. The IR spectrum shows the absence of M - N stretching frequency confirming that ethylenediamine in the outer sphere.

Similar reaction with protocatechuic acid was tried. The acid decomposes $[Ni(en)_3]Cl_2$ but the formation of the solid does not take place. It is probably because the protocatechuic acid is unstable at low pH. The reactions were repeated with $[Cu(en)_2]SO_4$. Addition of

catechol and pyrogallol results in the formation of greenish and brownish compounds having composition $[Cu(en)(L)]2H_2O$. The compounds are paramagnetic with mμ 1.8. corresponding to one unpaired spin. This indicates the absence of Cu-Cu interaction and thus the absence of polymerisation. The visible spectra of the compounds show peaks corresponding to distorted octahedral structure.

The addition of ethylenediamine to copper catecholate and pyrogallolate solution does not however give the same solids. In case of the former, a very small amount of solid is obtained for which analysis could not be carried out. In the case of latter, a brown compound is obtained corresponding to formula $[Cu(pyrogallol)_2]$ Cu $4H_2O$. Protocatechuic acid and gallic acid under similar condition yield reddish brown and reddish black solids. The colour indicates charge transfer from the ligands to the metal. The compounds on analysis agree with the composition $[Cu(L)_2]$. $Cu_2 \cdot 3H_2O$. They are insoluble in water and also in organic solvents. Their nature is, however, amorphous. They are paramagnetic and hence do not appear to be polymers. Polymeric complexes of Cu with oxy-compounds have been reported[4]. In most cases, however Cu - Cu interaction results in the diamagnetic compounds. Addition of ethylenediamine therefore serves only to increase the pH.

Addition of gallic acid to $[Cu(en)_2]SO_4$ results in the formation of a green compound. The analysis, however, does not correspond to any definite composition. Protocatechuic acid, however, does not yield any solid on addition to $[Cu(en)_2]SO_4$. This is because Cu-protocatechuate is less stable at lower pH. Gallic acid probably forms a mixture of $[Cu(gallic)_2](Cu)_2$ and some mixed ligand complex with ethylenediamine.

Mixed ligand stability constant has been determined in case of copper ethylenediamine with catechol and pyrogallol. Reaction of the type $ML + A \longrightarrow MLA$, where L is phenol and A is ethylenediamine. The formation constant is lower than in case $M + A \longrightarrow MA$ reaction. The coordination of catechol and pyrogallol will reduce the tendency of the M to bind with ethylenediamine. The value is less in catechol and more in pyrogallol. This is in agreement with the fact that metal catecholate being more stable, there is greater accumulation of charge in metal catecholate than in metal pyrogallolate.

EXPERIMENTAL

Catechol (G. R) and pyrogallol (M. B) used were A. R. pure. In order to avoid the complexing tendencies of the anions, metal perchlorate $Cu(ClO_4)_2$ has been prepared and its metal content has been determined. Other reagents used were sodium perchlorate (Fluka), perchloric acid

(B and A.) and ethylenediamine (Riedel). All the solutions have been prepared in conductivity water.

Metrohm pH meter, type E 350A (accuracy ± 0.05), was employed for all pH measurements. The titrations were carried out at 30°C using a constant temperature bath (± 0.1°C).

PROCEDURE

The mixed ligand formation constants were determined by Irving-Rossotti method. The following solution were prepared.

I $HClO_4$ (0.05M, 12 ml.); $NaClO_4$ (1M, 9.4 ml.); conductivity water (28.6 ml.); vol. 50 ml.

II $HClO_4$ (0.05M, 10 ml.); $NaClO_4$ (1M, 9.45 ml.); catechol (0.01M, 5 ml.); copper perchlorate (0.01M, 5 ml.); conductivity water (20.55 ml.) vol. 50 ml.

III $HClO_4$ (0.05M, 10 ml.); $NaClO_4$ (1M, 9.45 ml.); pyrogallol (0.01M 5 ml.); copper perchlorate (0.01M, 5 ml.); conductivity water (20.55 ml.) vol. 50 ml.

The titration cell was a lipless Pyrex beaker fitted with a perspex cover through which were admitted the electrode, burette tip and glass stirrer. The beaker was kept immersed in the thermostat maintained at 30°C for sufficient time and then titrated against standard ethylenediamine (0.2M). The ionic strength was maintained in all cases at 0.2M. The ethylenediamine was added in portions and the above three solutions were titrated. The pH thus observed was plotted against the volume of ethylenediamine added. From the two curves $\bar{n}$ and pL were calculated by using the standard equations.

REFERENCES

1. A. Syamal and R. L. Dutta; J. Ind. Chem. Soc., 45, 1 (1968)

2. N. Ghosh and S. Maulic; J. Ind. Chem. Soc., 46, 675 (1969)

3. E. Martell and Melvin Calvin; Chemistry of the Metal Chelate Compounds (1956) p. 13

4. F. Albert Cotton and G. Wilkinson; Advanced Inorganic Chemistry (1962) p. 757

ACKNOWLEDGEMENT

The authors express their thanks to Prof. S. M. Sethna, Head, Department of Chemistry, for providing laboratory facilities.

TABLE I

Nickel and Copper Compounds were Prepared and Analysed. The Percentages Obtained Correspond with the following Formulae

Substances	% Calculated			% Found out			μ
	Ni	N		Ni	N		
$[Ni(gallic)_2](enH_2)_2$	11.36	10.84		11.21	10.54		2.84
	Cu	N	H_2O	Cu	N	H_2O	
$[(Cu(en)(catechol)]2H_2O$	23.75	10.47	13.47	23.74	10.05	13.37	~1.8
$[Cu(en)(pyrogallol)]2H_2O$	22.42	9.877	12.7	22.25	9.71	12.50	~1.8
$[Cu(pyrogallol)_2]Cu.4H_2O$	28.42	-	16.14	28.25	-	16.28	
$[Cu(gallic)]Cu_2.3H_2O$	32.94	-	9.33	32.90	-	9.12	~1.4
$[Cu(protocatechuc1)]$ $.Cu_2.3H_2O$	34.86	-	9.87	34.51	-	9.97	~1.4

INFRARED AND N. M. R. SPECTRAL STUDIES OF SOME TRANSITION METAL HYDRIDE COMPLEXES

G. K. N. Reddy and E. G. Leelamani
Department of Chemistry, Bangalore University
Central College, Bangalore

Though several complex hydrides of rhodium and iridium stabilized by tertiary phosphines are known[1, 2] corresponding complexes of these metals stabilized by tertiary arsines are comparitively few in number. Such complexes include those containing methyl diphenyl arsine[3], diethyl phenyl arsine[4] and triphenyl-arsine[5]. The authors have recently prepared complex hydrides of rhodium and iridium stabilized by ethyl diphenyl arsine[6]. Some physicochemical investigations on these complexes is being reported here.

RESULTS AND DISCUSSION

The complex hydrides of rhodium and iridium that have been prepared have the general formula $MX_2H(AsEtPh_2)_3$ where X is Cl, Br or I, M is Rh or Ir (Table I). They behave as non-electrolytes in nitrobenzene and monomeric in dichloromethane and show metal-hydrogen bands in the 2000 cm^{-1} region in the infra-red (Some of them also show M-H bending modes around 800 cm^{-1}). Substitution of the hydrioic hydrogen with deuterium produces the metal-deuterium band at the expected position in the infra-red confirming the presence of M-H bond in the complex hydrides. N. M. R. spectral studies with some of the compounds show an M-H peak with very high positive values characteristic of hydrioic hydrogen (Table II). These facts together with the micro-analytical results for some of the elements in the compounds suggest the above mentioned general formula $MX_2H(AsEtPh_2)_3$ for the complexes. Complexes of this formula can exist in the following three isomeric forms.

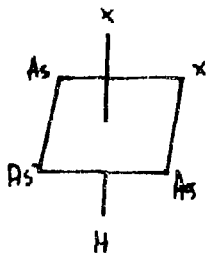

I α

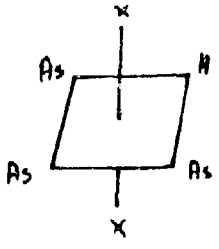

II β

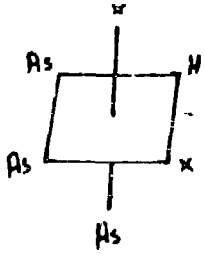

III γ

In several cases (Table I) two isomeric forms α and β have been obtained. These differ in their colour and infra-red and N. M. R. spectra. The α forms are lighter in colour when compared to the β compounds and show M-H bands in the infra-red at a frequency 100 cm^{-1} hig' 'han the corresponding β compounds. It is suggested that the α compounds have structure I, wherein the hydrogen is trans to a halogen, of low trans effect, resulting in a stronger M-H bond and a higher M-H stretching frequency as compared to the β compounds which could have structure II or III with the hydrogen trans to an arsine of stronger trans effect resulting in a weaker M-H bond and a lower M-H stretching frequency. It is likely that the β-compounds will have structure II rather than III on steric grounds. Structure III where in all the arsines are cis to one another would be sterically less stable. A knowledge of the M-X frequencies in the far-infra-red region would perhaps help to fix the correct structure for the β-compounds.

Measurement of the infra-red frequencies in different solvents for the α and β compounds has been carried out (Table III). It is found that the M-H stretching frequency of the α-compounds is solvent sensitive while that of the β-compounds is not. The shifting of the stretching frequency of the M-H bond in α-compounds to higher regions (by 10 to 15 wave numbers) in polar solvents like chloroform as compared to the values in nonpolar solvents like benzene has been attributed to the stronger solvation in chloroform solutions of the halogen trans to the hydrogen. Such a solvation would weaken the M-H bond with a corresponding strengthening of the M-H bond and hence a higher M-H stretching frequency. In the β-compounds the arsenic which is in trans position to the hydrogen is comparatively poorly solvated and hence the nature of the solvent does not have any perceptible influence on the M-H frequency[7]. These results also support the view that the α-compounds have structure I and the β-compounds strucutre II.

Measurements of the chemical shifts due to the hydridic proton in the N. M. R. spectra (Table II) of the compounds further support the above conclusions. It is seen that the α-compounds show higher positive shifts when compared to the β-compounds suggesting a greater screening of the hydridic proton in the α-compounds. This is explained as due to the presence of a halogen with a poor π-bonding capacity trans to the hydrogen in the α compounds as compared to an arsenic with a stronger π bonding capacity in the β-compounds.

EXPERIMENTAL

The infra-red spectra were recorded in a Carl Zeiss UR 10 spectrophotometer. Conductivity measurements were done with a conducti-

vity bridge, Electronics and Electricals model C. B. 102. Molecular weights were determined in dichloromethane by the isopiestic method. The hydride complexes were prepared as reported elsewhere[6].

REFERENCES

1. A. P. Ginsberg; in "Transition Metal Chemistry", Vol. I, R. L. Carlin editor, Marcel Dekkar, Inc., New York (1965)

2. J. Chatt; Proc. Chem. Soc., 318 (1962) and references therin.

3. J. Lewis, R. S. Nyholm and G. K. N. Reddy; Chem. Ind. London 1386 (1960)

4. J. Chatt, R. S. Coffey and B. L. Shaw; J. Chem. Soc. 7391 (1965)

5. G. Canziani and E. Zingales, Rend. Ist. Lombardo Sic. Lettere A 96, 513 (1962)

6. G. K. N. Reddy and E. G. Leelamani; Ind. J. Chem. (under publication)

7. D. M. Adams; Proc. Chem. Soc. 431 (1961)

TABLE I

Complex	Colour	M. P. (°C)	Infra-red bands (cm^{-1})** ν_{M-H}	δ_{M-H}	ν_{M-D}	p*	Molecular Wt Calc.	Molecular Wt Found	Molar conductivity in $ohm^{-1}\ cm^2\ mole^{-1}$
$RhHCl_2(AsEtPh_2)_3$ (α)	Yellow	134 - 136	2077		1490	1.40	949	1005	0.2
,, (β)	Yellow-orange	111 - 114	1980						0.8
$RhHBr_2(AsEtPh_2)_3$ (α)	Orange	141 - 143	2070				1038	919	0.2
,, (β)	Orange-brown	148 - 149	1995						0.9
$IrHCl_2(AsEtPh_2)_3$ (α)	Colourless	194 - 197	2198	779			1038	1150	very low
,, (β)	Yellow	175 - 177	2080	802	1490	1.40			very low
$IrHBr_2(AsEtPh_2)_3$ (α)	Pale-yellow	196 - 198	2194	818			1127	1187	very low
,, (β)	Orange	201 - 202	2088	808	1495	1.40			very low
$IrHI_2(AsEtPh_2)_3$ (α)	Pale-orange	174 - 175	2198	782			1221	1158	very low

p* = ratio of hydride to deuteride. ** Nujol mull

TABLE II

Nuclear Magnetic Resonance Data for Hydrido Iridium (III) Complexes in $CDCl_3$ Solution. Values Relative to $SiMe_4$ as Internal Standard, Measured at 60 M/c on a Varian A60 Instrument at 25°.

Compound		τ
$IrHCl_2(Ph_2EtAs)_3$	(α)	31.62
$IrHBr_2(Ph_2EtAs)_3$	(α)	30.72
$IrHCl_2(Ph_2EtAs)_3$	(β)	25.23

TABLE III

Compound		M-H cm^{-1} in $CHCl_3$	M-H cm^{-1} in C_6H_6	$\Delta\nu = \nu_{M-H}(CHCl_3) - \nu_{M-H}$ cm^{-1}
$IrHCl_2(Ph_2EtAs)_3$	(α)	2194	2180	14
,,	(β)	2112	2110	2
$IrHBr_2(Ph_2EtAs)_3$	(α)	2190	2180	10
,,	(β)	2110	2110	0

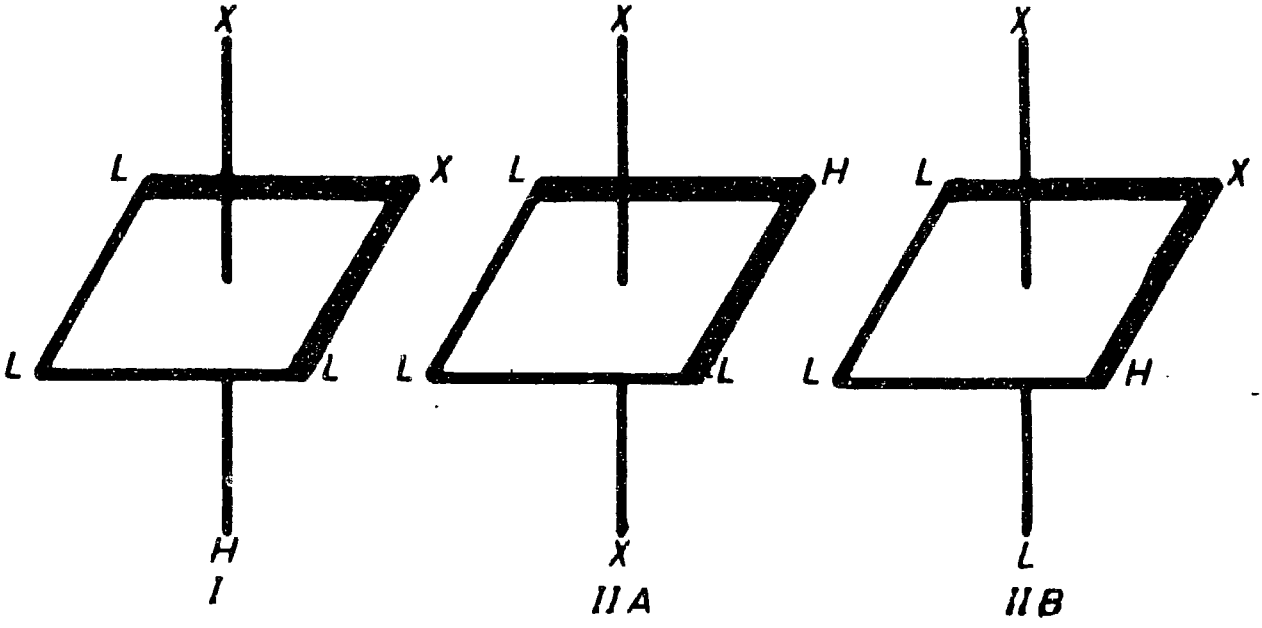
X
L
X
L
L
H
I
X
L
H
L
L
X
IIA
X
L
X
L
H
L
H
L
IIB

DETERMINATION OF NITROGEN IN IRON METEORITES

P. S. Goel
Chemistry Department, Indian Institute of Technology, Kanpur

Not much work has been done on the measurements of nitrogen in iron meteorites (see e.g. Mason's book[1], page 156). The first careful determinations were made by Nash and Baxter[2] in 1947. They determined dissolved nitrogen in a number of iron meteorites and found quite low values for its contents, viz., 0.5 ppm. More extensive and reliable measurements are, however, available for stone meteorites[3, 4, 5].

Urey[6] has pointed out that the nitrides of titanium and silicon might be produced in the formation of meteorites at some stages of the contraction of the gas-spheres postulated in his cosmogony. If molten iron, together with silicon etc, were indeed exposed as "pools" of molten matter on the surface of "primary objects" buried under the pressure of the order of 100 kilobars, it is surprising why the concentration of nitrogen in iron meteorites is so low.

It is desired to have more information on the distribution of nitrogen in iron meteorites since it plays an important role in the early chemistry of meteorites. We undertook its determination by neutron activation analysis taking advantage of the fact that the reaction $N^{14}(n, p)C^{14}$ is exoergic and has high cross section. In addition to its high sensitivity and specificity, the method is reliable for the determination of total nitrogen contents. Excellent methods for the recovery of carbon (C^{14}) from steel exist.[7] The results are given in Table I.

TABLE I

Results from Activation Analysis

Run No.	Meteorite	Mass (g)	C^{14} (10^3 dis $min^{-1} g^{-1}$)	Co^{60} (mc)	Nitrogen (ppm)
2a	Canyon Diablo	1.65	2.26	1.0	340
2b		1.56	1.18	1.0	177
3b	Canyon Diablo	1.46	2.1	1.1	315
3b		1.61	1.64	1.1	246
3c		1.37	0.17	1.1	25
3d		1.52	0.28	1.1	42

contd...)

4a	Odessa	1.11	0.75	1.2	112
4b		1.11	1.06	1.2	162
4c		1.42	1.10	1.1	165
4d		1.68	0.34	1.1	50

Kjeldahl Method

The results of neutron activation indicated a high value of nitrogen contents. It appeared feasible to measure nitrogen using classical methods without serious problems of contamination. Several runs were made following the method described in Furman[8] for the analysis of steel taking appropriate care to use ammonia free reagents. The metal was dissolved in HCl. To the solution was added NaOH solution and NH_3 was distilled in a closed system. The distillate was collected and ammonia in the aqueous solution was determined colorimetrically using Nessler reagent. The results are given in Table II.

TABLE II

Results of Kjeldahl Method

Meteorite	Mass (g)	Nitrogen (ppm)	Blank (ppm)
Odessa	2.02	108	10
	1.73	64	
	1.76	60	
	2.08	77	20
-Inclusion	1.72	40	7
-Incl. powder	0.31	30	7
Canyon Diablo	1.77	26	12
	2.74	28	10

Fusion Method

It has been reported that the Kjeldahl method is not suitable for steels containing titanium because it fails to decompose TiN or other similar compounds. The low results obtained by us using the Kjeldahl technique as compared to those by the neutron activation analysis led us to think on these lines. The metal samples were fused in a platinum boat after the chips had been mixed with NaOH + Na_2CO_3. The fusion was carried out in an atmosphere of H_2 in a combustion furnace made of nickel tube at about

1000°C. The results of fusion analysis are given in Table III.

TABLE III

Results of the Fusion Method

Meteorite	Mass (g)	Nitrogen (ppm)	Blank (ppm)
Odessa	0.51	112	10 to 20
	0.223	180	
	0.105	284	
	0.222	190	
Odessa-inclusion -(Crushed)	0.20	81	5
-(Intact)	0.267	84	5

DISCUSSION

The results by various methods are summarized in Table IV.

TABLE IV

Summary of Nitrogen Results

Method	Nitrogen concentration (ppm)	Blank (ppm)	Remarks
Activation	40 to 340	Low	Large variations, absolute values may be unreliable
Fusion	80 to 300	$\leqslant 10$	Variations verified, triolite inclusions do not give high values
Kjeldahl Distillation	30 to 100	$\leqslant 10$	Variations not large; low values; low values in the inclusions
Mild Dissolution (Nash and Baxter)	0.2 to 1.6 (several meteorites)	-	Gives only dissolved nitrogen

The data show that the nitrogen present in iron meteorites is in the form of more than one compound. The fusion technique decomposes the compounds completely and gives total nitrogen. The same is true for the activation analysis. The most striking result of our work, however, is the finding of large variations in nitrogen contents in samples of the same meteorite taken from nearby regions. Such variations are not found in stone meteorites. Different stone meteorites belonging to one class show[5] remarkably constant value of nitrogen concentrations. The nitrogen minerals in iron meteorites are distributed non-uniformly.

ACKNOWLEDGEMENT

Mr. P. C. B. Gohain carried out the colorimetric analysis and Mr. R. D. Sharma helped me in some activation analyses. I thank Dr. V. K. Iya, Head Isotope Division, Bhabha Atomic Research Centre, for the neutron irradiations. This research was supported in part by a grant from the Department of Atomic Energy, Government of India.

REFERENCES

1. B. Mason; Meteorites, John Wiley and Sons (1962)
2. L. K. Nash and G. P. Baxter; J. Am. Chem. Soc. 69, 2534 (1947)
3. C. B. Lipman; Am. Museum Novitates no. 589 (1932)
4. G. Mueller; Geochim. et Cosmochim. Acta 4, 1 (1953)
5. G. B. Moore and E. K. Gibson; Science 163, 174 (1969)
6. H. C. Urey; Mon. Not. R. Astr. Soc. 131, 199 (1966)
7. P. S. Goel; Cosmogenic Carbon-14 and Chlorine-36 in Meteorites, USAEC Report NYO-8922 (1962)
8. N. H. Furman; Standard Methods of Chemical Analysis, Technical Press, London, Vol. I, pp. 770-772 (1962)

DISCUSSION

R. Tripathi : (1) Why did you prefer to estimate nitrogen only and not other elements?
(2) Did you measure the gradient of concentration of nitrogen compounds in meteorites?

P. S. Goel : (1) For the following three reasons:
a) Nitrogen plays a very important role in the problem of the origin of meteorites
b) Nitrogen has not been studied in iron meteorites so far
c) We had experience in C^{14} measurements and activation analysis could be applied to nitrogen.
(2) The answer is no.

B. M. Shukla : (a) Are the large variations obtained in the nitrogen content of samples furnace and the same meteorites, also shown if samples are taken just from the surface ?.

(b) From your answer to (a), is it not preferable to carry out analysis of various surface samples of the meteorites before it is assumed that it will not show any variations and that it is only the atmospheric nitrogen which will have larger role to play when the meteorite passes through atmosphere ?

P. S. Goel : (a) We have not done analysis on the near surface regions.

(b) The answer is 'no'. Meteorites remain un-affected, thermally, physically and chemically below a few milimeters of surface. The question of atmosphere nitrogen diffusing into the interior does not therefore arise.

K. Rengan : (1) What kind of processing of the sample was done after neutron irradiation ?

(2) What counting system was used ?

P. S. Goel : (1) The metal sample was burnt in a stream of oxygen at 1000°C and CO_2 was recovered as $BaCO_3$ for counting.

(2) We used 1" diameter Sharp Laboratory end-window counter. The background was 0.2 cpm and the sample counting rates ranged from 10 to 100 cpm.

R. K. Dhumwad : What is the nitrogen content in the various types of rocks (earth-bound) ?

P. S. Goel : A thorough work on nitrogen determination in rocks has not been done and we would like to undertake this work in the near future.

STUDIES ON LEAD-210 ACTIVITY IN INDIA

L. U. Joshi, C. Rangarajan and (Smt.) Sarada Gopalakrishnan
Health Physics Division, Bhabha Atomic Research Centre, Bombay 85

INTRODUCTION

Lead-210 is one of the long lived daughter products of radon which diffuses out from the soil. The decay scheme of ^{210}Pb to the stable ^{206}Pb is as given below:

$$^{210}Pb \xrightarrow[21y]{\beta} {}^{210}Bi \xrightarrow[5.0\ d]{\beta} {}^{210}Po \xrightarrow[140\ d]{\alpha} {}^{206}Pb \text{ (Stable)}.$$

The daughter products of radon which contribute a large amount of dose to the population are ^{210}Pb and ^{210}Po.

Measurements of the levels of ^{210}Pb at number of places situated in the latitude band 8°N to 34°N have been carried out. These observations have shown that (a) the winter maxima are prominent at most stations in India, (b) the specific activity of rain water increased at about 30° N and (c) in general, the activity of ^{210}Pb at Gangtok was much higher than at the other stations

SAMPLE COLLECTION

a) Air Filters: Hollingsworth and Vose H-70 filters were used for the collection of samples. Large volumes of air of the order of 5-50 x $10^3 m^3$ were sucked per month using powerful blowers.

b) Surface Deposition Samples: Rain water samples were collected in stainless steel funnels 12" in diameter. These funnels are kept on the polythene vessels. Collections are made every month and these monthly collections are pooled together depending on the amount of rainfall to give detectable activity.

EXPERIMENTAL

The collected samples of (a) air filters and (b) surface deposition are ashed at 400°C prior to chemical analysis. To the ashed samples, 30 mg of lead are added as lead nitrate, digested in aqua regia a number of times and then the residue is dissolved in 1.5M hydrochloric acid. Use is made of anion exchange resin Dowex-1 x 8% (50 - 100 mesh) for the chemical separation of lead. The maximum adsorption of lead is observed at 1.5M hydrochloric acid concentration. The adsorbed lead is eluted with

8M hydrochloric acid. The separated lead is precipitated as lead sulphate and counted in end-window Geiger counters with a background of five counts per minute.[1,2] The samples are counted to an accuracy better than ± 5% s.d.

RESULTS AND DISCUSSIONS

The air concentrations of ^{210}Pb at a number of stations in India are presented in Figures 1 and 2. Figure 3 shows the latitudinal variation of ^{210}Pb in surface air and deposition and Figure 4 gives the location of sampling stations in India.

The significant features of the spatial and seasonal variations of ^{210}Pb are summarised below:

a) Surface air activity shows maximum levels from December to February and minimum values from July to August at almost every station in India although this is not very pronounced at Srinagar. Spring maximum of stratospheric ^{137}Cs was also observed in the month of April each year, but ^{210}Pb levels reduced significantly by April from the peak values observed in mid-winter. This shows that there is no possibility of the presence of significant amount of ^{210}Pb from upper atmosphere in the surface air. Measurements of radon daughters at 9.00 hours in the morning and 15.00 hours in the afternoon at Bombay showed that there is a seasonal variation of radon which closely follows the variation observed in the case of ^{210}Pb. This similarity shows that ^{210}Pb concentrations are mainly dependent on radon levels.

The greater prevalence of inversion conditions during winter is probably the main reason for the winter maximum although part of the summer minimum could be due to the south-west maritime winds in summer.

b) Figure 3 shows the variation of specific activity with latitude. Significant increase of specific activity of rainfall was observed at higher latitude stations. This is due to the difference in the precipitation at high latitudes where the rains during winter season due to "Mediterranean disturbances" are more prominent than the summer monsoon rains. Lower latitude stations have no precipitation in winter when the levels in surface air are maximum.

Measurements of ^{210}Pb at Nainital shows that the winter maximum is not very pronounced at Nainital. It is rather difficult to draw any definite conclusion with the little available data from this station but it is possible that the seasonal cycle for radon may not be effective at high altitudes since inversions phenomenon is confined to surface layers.

c) The Gangtok values, particularly during 1963 and 1964, are higher by a factor of two compared to the other stations. Most probably the high

values in winter result from meteorological conditions. Measurements made by Mishra[3] showed that at Gangtok ^{226}Ra content is higher by 50 to 100% in the soil than at the other stations. However, the fact that higher levels are in winter only, seems to suggest that the cause for the higher concentrations could be the comparatively higher stability of the lower atmosphere at Gangtok. A larger body burden of ^{210}Pb and daughters as a result of this increased levels may be of some radiological significance at Gangtok. This needs to be investigated by the analyses of the autopsy samples of this region.

ACKNOWLEDGEMENTS

The authors are greatful to Dr. A. K. Ganguly, Head, Health Physics Division, and to Dr. K. G. Vohra, Head, Air Monitoring Section, for their guidance and encouragement.

REFERENCES

1. L. U. Joshi and T. N. Mahadevan; Health Physics 15, 67 (1968)
2. L. U. Joshi, C. Rangarajan and (Smt.) Sarada Gopalakrishnan; Tellus XXI, 1 (1969)
3. U. C. Mishra (Unpublished data)

DISCUSSION

P. S. Goel : Did you not try electroplating lead ?

L. U. Joshi : It is not necessary. The samples contained 30 mg of lead as lead nitrate and counted for 1.17 Mev betas of of Bi^{210}.

G. M. Nair : In what form was lead held in the anion exchange column during loading from 1.5 M HCl and in what form is it eluted at 8 M HCl?

L. U. Joshi : Lead is held as $PbCl_4^{=}$ and eluted as H_2PbCl_4.

R. Tripathi : Does the estimation of radon help you in prospecting the uranium ores in the localities where the measurements are being made?

L. U. Joshi : Unless radon levels are unusually high, it may not be of much help in prospecting for uranium since several meteorological factors control radon levels. If Ra^{226}

content of the soil is also high at the places of measurement, then it may be possible that uranium content may be high.

B. M. Shukla : (a) Since you have conclusions based on your study of lead-210 activity in India, could you throw some light whether your results with regard to seasonal and especially latitude studies, in conformity with results obtained elsewhere in the world?

(b) On your reply to (a), is it not correct to say that the study involves a lot of parameters like wind velocity etc., and to make certain conclusions, it will be better to choose place and conditions of experiment so as to keep many parameters constant and vary only one.

L. U. Joshi : (a) Our values are in conformity with those in the U. S. A. and somewhat higher to the values reported in the U. K. This is possibly due to the greater prevalence of maritime air masses over the island of the U. K.

(b) The study of the type reported here does involve a number of parameters, but it is difficult to eliminate any of these parameters by the choice of sample location. In spite of these difficulties, by study of these parameters it is possible to relate the variations in levels to the meteorological conditions.

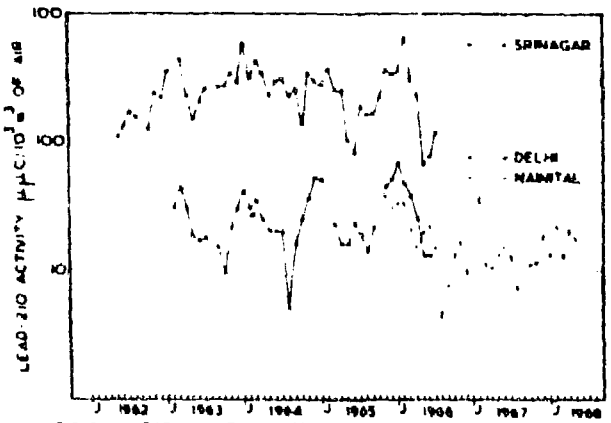

FIGURE 1 LEAD-210 (RaD) ACTIVITY IN GROUND LEVEL AIR AT SRINAGAR DELHI AND NAINITAL

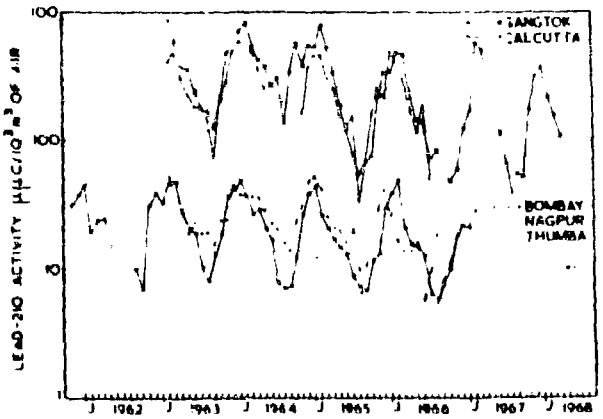

FIGURE 2 LEAD-210 (RaD) ACTIVITY IN GROUND LEVEL AIR AT GANGTOK CALCUTTA BOMBAY NAGPUR AND THUMBA

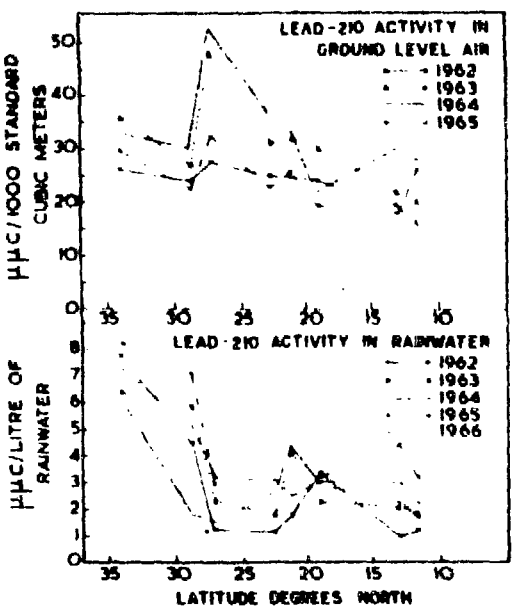

FIGURE 3 LATITUDINAL VARIATION OF LEAD-210 IN RAIN AND GROUND LEVEL AIR IN INDIA

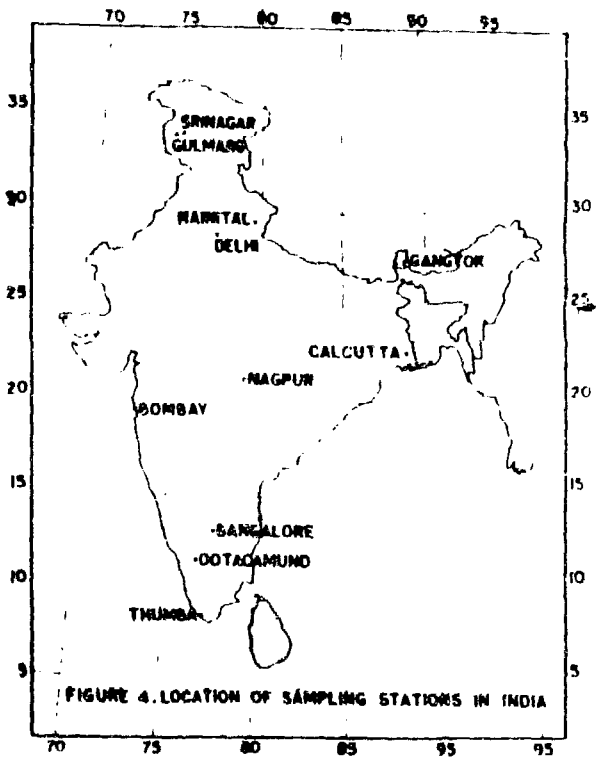

FIGURE 4. LOCATION OF SAMPLING STATIONS IN INDIA

STUDY OF ADSORPTION OF PHOSPHATE IONS ON CERIUM OXIDE

B. M. Shukla and R. S. Tripathi
Nuclear and Physical Chemistry Laboratory,
Banaras Hindu University, Varanasi

INTRODUCTION

Many workers have studied adsorption on oxides. The methods used by earlier workers for studying adsorption of ions on various oxides and metal surface failed to investigate the nature of adsorption at micro and tracer concentrations. Tracer technique has solved this difficulty to a great extent and has given valuable results on adsorption studies. This technique has been successfully used for studying adsorption on crystalline substances[1-2], oxides[3], metals[4-5], glass[6] and other adsorbents . Rutner and coworkers have studied the surface exchange adsorption by this method.

This paper embodies the study of adsorption of phosphate ions on cerium oxide (CeO_2) in aqueous solution at 30.5°C.

EXPERIMENTAL

Cerium oxide (-300 B.S. + 350 B.S.) has been prepared by heating cerium oxalate B.D.H. (A.R.) at 800°C for twenty four hours. Solutions of sodium dihydrogen phosphate $NaH_2PO_4.2H_2O$, B.D.H. (A.R.) of various strengths (10^{-1}M - 10^{-12}M) were prepared in conductivity water. 10 ml of each solution were taken in Jena glass tubes and labelled with carrier free P^{32} obtained from Bhabha Atomic Research Centre, Trombay, and thermostated at 30.5°C for twenty four hours. A drop (~ 0.033 ml.) of each solution was taken with the help of capillary tube in separate aluminium planchet and dried under infra-red lamp. The radio-activity (counts/min) of each sample was recorded with the help of G. M. tube and utility scaler of the type SS 361A (AE. Instruments, India) for zero time. Later, 0.5 gm of cerium oxide was added separately to each of the solutions, stirred gently and thermostated at 30.5°C. At intervals of 5, 10, 15, 20, 30, 60 minutes, the solutions were centrifuged and one drop (~0.033 ml) of the supernatant liquid from each sample was taken in clean aluminium planchets and the activity (counts/min) noted as before. The background (counts/min) was taken prior and was substracted from each observation for different time intervals are recorded in Table I.

RESULTS AND DISCUSSION

Table I shows the amount of phosphate in solution with respect to time for the concentrations 10^{-1}M - 10^{-12}M. A plot of concentration of phosphate versus time (Table I, Fig. 1) indicates that equilibrium is obtained within a period of about twenty minutes for higher concentrations (10^{-1}M - 10^{-2}M) and about fifteen minutes for lower concentrations (10^{-3}M - 10^{-12} M). It has been found that, at higher concentrations, adsorption is followed by desorption, i. e., phosphate ions adsorbed on CeO_2 exchange with the phsophate ions in solution. Hence, the period of equilibrium is less at lower concentrations (10^{-3}M - 10^{-12}M).

From Table I, and Fig. 1, it is clear that adsorption is rapid and drastic. This tremendous adsorption can be attributed to (a) the fineness of oxide, i. e. to the greater surface area of oxide, (b) the presence of active centres on its surface, (c) chemisorption, i. e. formation of compounds. The last one appears to be more effective and is supported by the work of earlier workers on oxide. On the surface of oxide, tetravalent cerium cations form insoluble salt, ceric hydro-orthophosphate, with phosphate anions.

$$4Ce^{4+} + 2H^{+} + 6PO_4^{3-} + 25H_2O \dashrightarrow 2Ce_2H(PO_4)_3.25H_2O$$

Second possibility of formation of cerous phosphate is also there. But as reduction of Ce^{4+} to Ce^{3+} in solution takes place 1-2% in one hour at 20°C according to H. F. Walton and coworkers[7]. Therefore, following reaction

$$Ce^{4+} e^{-} \dashrightarrow Ce^{3+}$$

$$Ce^{3+} + PO_4^{3-} \dashrightarrow CePO_4 \quad \text{(soluble)}$$

takes place in a very small amount, if it occurs.

In the Table II are shown the values of the initial concentration of phosphate, the amount of phosphate adsorbed and the amount of phosphate adsorbed per gram oxide. A plot of log x/m versus log C is a straight line where x/m is the amount of phosphate adsorbed per gram of oxide and C, the initial concentration of phosphate in solution. This shows that adsorption obeys the Freundlich isotherm:

$$x/m = KC^{1/n} \quad \text{where } 1/n = 1$$

in the concentration range 10^{-1}M - 10^{-12}M.

ACKNOWLEDGEMENT

We are thankful to Dr. G. B. Singh, A. M. Ph. D. (Harward), Professor and Head of the Chemistry Department, Banaras Hindu University, Varanasi-5, for providing laboratory facilities and one of us (R. S. Tripathi) to the C. S. I. R. for providing financial assistance for the investigation.

REFERENCES

1. K. R. Kar and M. M. Bhutani; J. Sci. Ind. Res. 21B, 124-6 (1962)
2. R. S. Rai et al.; Radio-chim. Acta 5(1), 30-4 (1966)
3. D. Pavlov and J. Beloni; Compt. rend. 255, 2420-2 (1962)
4. E. Herczynska; Nukleonika 6, 659-65 (1961)
5. B. Genot and et al.; C. R. Acad. Sci. Paris. Ser. C. 265(5), 285-7 (1967)
6. A. J. Arnikar and S. B. Joshi; Proc. Nucl. Radiat. Chem. Symp. Waltair, 327-36 (1966)
7. H. F. Walton; Principles and Methods of Chemical Analysis (Prentice-Hall of India (Private) Ltd., New Delhi, (1966) page 259

TABLE I

ABSORPTION OF PO_4^{3-} IONS ON CeO_2

Volume of solution - 10 ml.
Weight of oxide - 0.5 gm.
Temperature - 30.5°C.

Strength of soln.	10^{-1}M	10^{-2}M	10^{-3}M	10^{-4}M	10^{-5}M	10^{-6}M	10^{-7}M	10^{-8}M	10^{-9}	10^{-10}M	10^{-11}M	10^{-12}M
Amount of Phosphate	gmsx10^{-1}	gmsx10^{-2}	gmsx10^{-3}	gmsx10^{-4}	gmsx10^{-5}	gmsx10^{-6}	gmsx10^{-7}	gmsx10^{-8}	gmsx10^{-9}	gmsx10^{-10}	gmsx10^{-11}	gmsx10^{-12}
Time in minutes												
0	0.9539	0.9539	0.9539	0.9539	0.9539	0.9539	0.9539	0.9539	0.9539	0.9539	0.9539	0.9539
5	0.7324	0.3154	0.1467	0.1582	0.2561	0.1586	0.1940	0.1554	0.1309	0.2121	0.1126	0.1521
10	0.7161	0.1698	0.1113	0.1331	0.2314	0.1559	0.1779	0.1253	0.1278	0.2046	0.0968	0.1427
15	0.6937	0.1458	0.1113	0.1536	0.2578	0.1457	0.1756	0.1207	0.1278	0.1885	0.0933	0.1364
20	0.6826	0.1354	0.1094	0.1484	0.2719	0.1525	0.1802	0.1126	0.1465	0.1848	0.0959	0.1238
30	0.6884	0.1351	0.1127	0.1395	0.2640	0.1529	0.1734	0.1198	0.1464	0.1997	0.1047	0.1154
60	0.6846	0.1389	0.1115	0.1368	0.2457	0.1549	0.1741	0.1228	0.1278	0.1848	0.0933	0.1154

TABLE II

VARIATION OF PO_4^{3-} IONS ADSORPTION ON CeO_2 WITH CONCENTRATION

Volume of solution - 10 ml
Weight of oxide - 0.5 gm
Temperature - 30.5°C

Strength of soln.	'C' Initial Amount of PO_4^{3-} in gm	Log C	Equilibrium amounts of PO_4^{3-} in gms.	Total amounts adsorbed in gms.	'x/m' Amount adsorbed per gram oxide	Log x/m
10^{-1}M	0.9539×10^{-1}	$\bar{2}.9795$	0.6846×10^{-1}	0.2693×10^{-1}	0.5286×10^{-1}	$\bar{2}.7231$
10^{-2}M	0.9539×10^{-2}	$\bar{3}.9795$	0.1339×10^{-2}	0.8200×10^{-2}	0.6400×10^{-2}	$\bar{2}.2148$
10^{-3}M	0.9539×10^{-3}	$\bar{4}.9795$	0.1115×10^{-3}	0.8424×10^{-3}	0.6848×10^{-3}	$\bar{3}.2158$
10^{-4}M	0.9539×10^{-4}	$\bar{5}.9795$	0.1368×10^{-4}	0.8171×10^{-4}	1.6342×10^{-4}	$\bar{4}.2133$
10^{-5}M	0.9539×10^{-5}	$\bar{6}.9795$	0.2457×10^{-5}	0.7082×10^{-5}	1.4164×10^{-5}	$\bar{5}.1461$
10^{-6}M	0.9539×10^{-6}	$\bar{7}.9795$	0.1549×10^{-6}	0.7990×10^{-6}	1.5980×10^{-6}	$\bar{6}.2038$
10^{-7}M	0.9539×10^{-7}	$\bar{8}.9795$	0.1741×10^{-7}	0.7798×10^{-7}	1.5596×10^{-7}	$\bar{7}.1925$
10^{-8}M	0.9539×10^{-8}	$\bar{9}.9795$	0.1228×10^{-8}	0.8311×10^{-8}	1.6622×10^{-8}	$\bar{8}.2206$
10^{-9}M	0.9539×10^{-9}	$\bar{10}.9795$	0.1278×10^{-9}	0.8261×10^{-9}	1.6522×10^{-9}	$\bar{9}.2180$
10^{-10}M	0.9539×10^{-10}	$\bar{11}.9795$	0.1848×10^{-10}	0.7691×10^{-10}	1.5382×10^{-10}	$\bar{10}.1870$
10^{-11}M	0.9539×10^{-11}	$\bar{12}.9795$	0.0933×10^{-11}	0.8606×10^{-11}	1.7212×10^{-11}	$\bar{11}.2358$
10^{-12}M	0.9539×10^{-12}	$\bar{13}.9795$	0.1154×10^{-12}	0.8385×10^{-12}	1.6770×10^{-12}	$\bar{12}.2245$

FIG TIME VARIATION OF CONCENTRATION OF PO_4^{3-} ION IN SOLN.

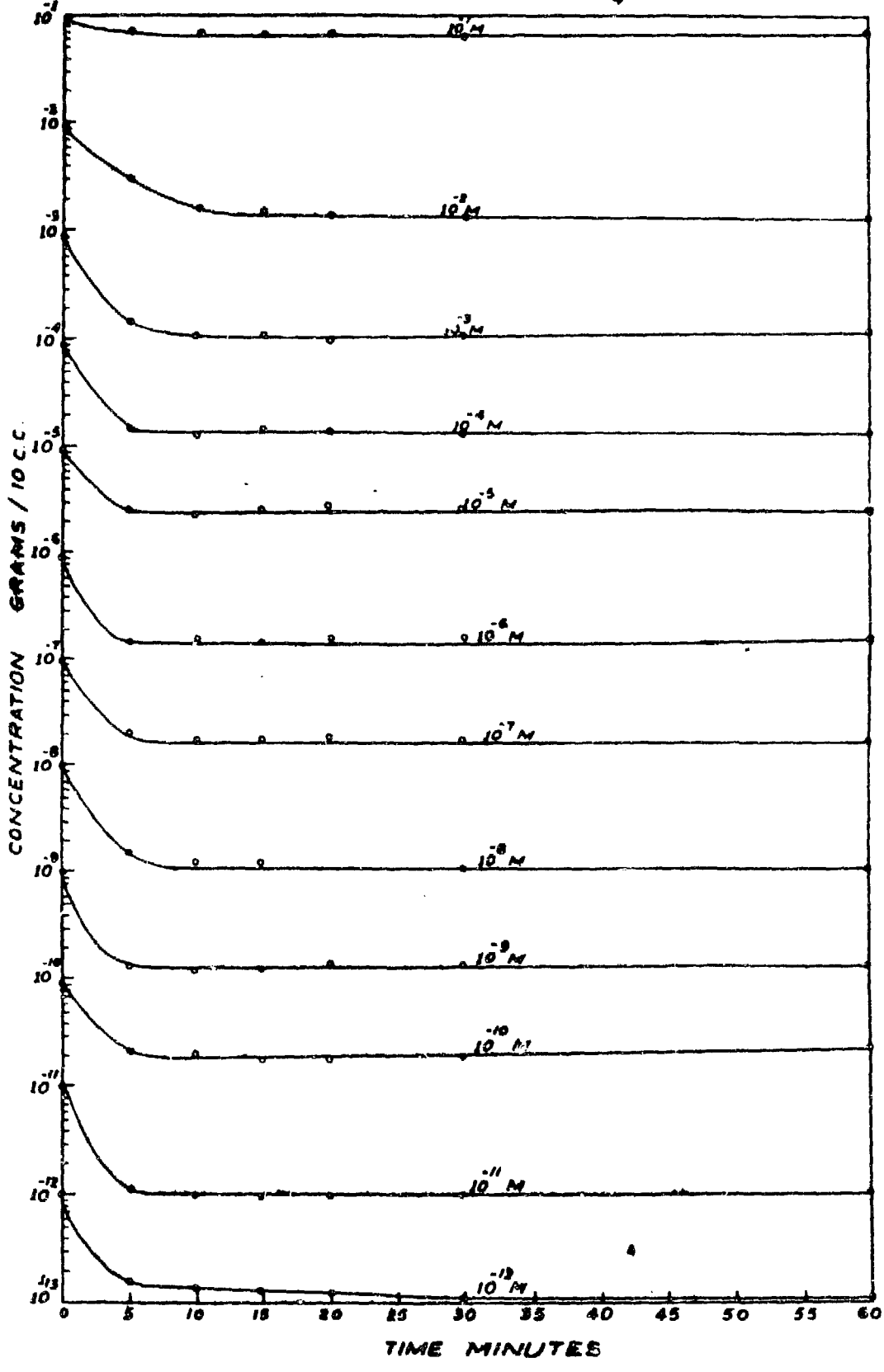

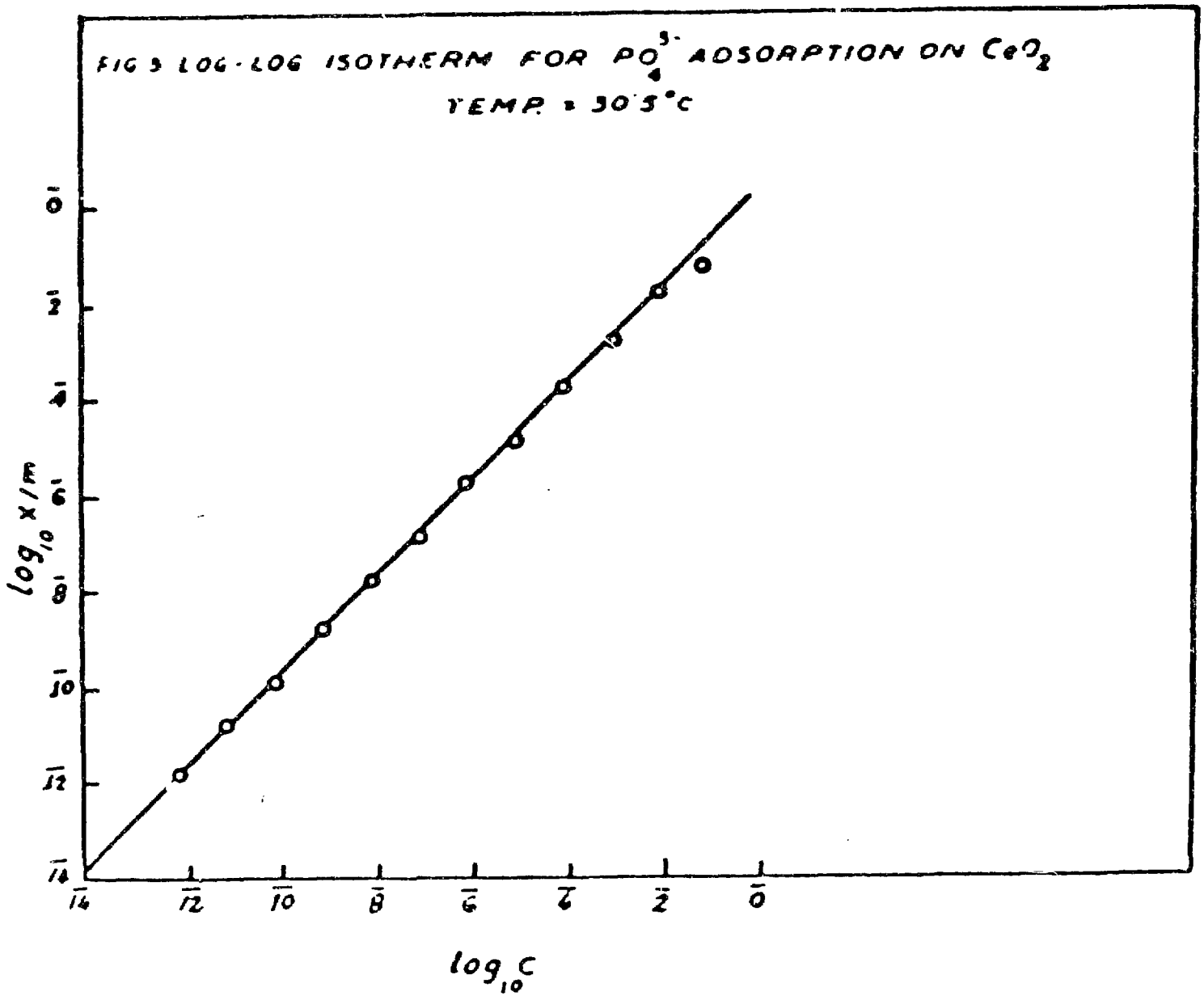
FIG 3 LOG-LOG ISOTHERM FOR PO_4^{3-} ADSORPTION ON CeO_2
TEMP. = 30.5°C
$\log_{10} x/m$
$\log_{10} C$
$\bar{1}$
$\bar{2}$
$\bar{4}$
$\bar{6}$
$\bar{8}$
$\bar{10}$
$\bar{12}$
$\bar{14}$
$\bar{14}$ $\bar{12}$ $\bar{10}$ $\bar{8}$ $\bar{6}$ $\bar{4}$ $\bar{2}$ $\bar{0}$

SEPARATION OF CAESIUM-137 FROM FISSION PRODUCT SOLUTION USING PHOSPHO TUNGSTIC ACID

T. S. Murthy, K. R. Balasubramanian and M. Ananthakrishnan
Isotope Division, Bhabha Atomic Research Centre
Trombay, Bombay-85

High intensity radiation sources of long-lived fission products like caesium-137 and strontium-90 find extensive uses as power sources in SNAP systems, as irradiation sources in large irradiators and teletherapy units[1].

Various methods have been reported in literature for the chemical separation and purification of these isotopes in different countries. These include co-crystallisation[2], solvent extraction[3], ion-exchange on organic resins[4] and precipitation[5] techniques. The choice of a particular method in each country has been greately influenced by the nature and composition of the waste solutions and the operational facilities available.

The precipitation of caesium as the phospho-tungstate and decomposition of the precipitate with baryta had been previously employed at Saclay. In this method reported by Raggenbass et. al[5] caesium was selectively precipitated from 2 M nitric acid solution using phospho-tungstic acid. The precipitate after washing was decomposed with baryta which precipitated the insoluble barium phosphate and tungstate. One of the major disadvantages of the method is that it involves multiple precipitation which complicates the handling. The action of atmospheric carbon dioxide on barium hydroxide also interferes with the complete precipitation necessitating further purification steps.

The subsequent separation of phosphate and tungstate by anion exchange on organic resins (De-acidite FF) has been reported[6]. However, because of the stability of hydrous oxides towards large doses of ionising radiations[7], the possibility of separation on alumina was hence investigated.

EXPERIMENTAL

Reagents : Alumina - Brockman chromatographic grade 100-200 mesh was used fo the experiments. All the other reagents used were of E. Merck (G. R.) grade. Radioactive tracers Cs^{137},

Sr^{85+89}, W^{187}, and Ce^{141} were all available with the Isotope Division, BARC.

Apparatus : Glass columns of dimensions 21 cms. (length) x 1 cm (dia) were used for the ion exchange studies. The spectra of the samples were taken using a 512 channel analyser Type NTA-512 (Hungarian Model).

PROCEDURE

a) Caesium was precipitated as phospho-tungstate in the presence of tracer caesium-137 from solution containing 1.0 mg. of carrier caesium using 0.01 M phospho-tungstic acid. The solution was maintained at 2M with respect to nitric acid in a total volume of 25.0 ml. The precipitate was allowed to settle for about 1 hour. After settling, it was filtered, washed well with water and subsequently dissolved in minimum quantity of 0.1 M sodium hydroxide. About 1 μCi each of tracer phosphorus-32 and tungsten-187 as sodium phosphate and sodium tungstate respectively were added. The pH of the medium was adjusted to about 4 with 0.1 M hydrochloric acid.

This was passed through a column of alumina conditioned with hydrochloric acid at pH 4 and the gamma spectrum of the effluent taken.

b) The interference, if any, in the selective precipitation of caesium using phospho-tungstic acid by other multi-valent ions like Sr, Ce^{+3}, etc. was checked by carrying out the precipitation in the presence of tracer Sr^{85+89} and Ce^{141} and subsequent purification on alumina as above.

c) The above procedure was also tested on simulated fission product solutions having the composition reported by J. M. Fletcher[8] and spiked with tracer Cs^{137}, Sr^{85+89} and Ce^{141}.

RESULTS AND DISCUSSION

Since the published literature did not give complete experimental data for the various factors affecting the precipitation of caesium by phospho-tungstic acid, these were ascertained in detail by a series of experiments.

From the preliminary experiments carried out, it was seen that caesium can be effectively and almost quantitatively precipitated as caesium phospho-tungstate from 2 M nitric acid solution using

61.6 mg. of phospho-tungstic acid for every milli-gram of caesium. At acidities > 1M the precipitate was obtained in a very fine microcrystalline form difficult to filter. However, the precipitate from 2.0-5.0 M solution was easily filterable with an overall yield >95%.

Caesium phospho-tungstate is quite resistant to attack by strong hydrochloric and nitric acids but dissolves in alkali hydroxide forming caesium hydroxide, alkali phosphate and tungstate.[9] To prevent reprecipitation of the phospho-tungstate, the medium should be maintained at pH > 2.

Experiments using tungsten-187 and phosphorus-32 as tracers confirmed almost quantitative uptake of phosphate and tungstate ions in the presence of each other on a column of alumina conditioned with hydrochloric acid at pH 4.

After the precipitation and purification on alumina, the gamma spectrum of the product caesium showed only the presence of 0.66 MeV peak due to ceasium-137. Peaks corresponding to 0.51 MeV Sr^{85} and 0.145 MeV Ce^{141} were absent.

Appendix-I shows a typical spectrum of the product after purification.

CONCLUSION

The precipitation of caesium as caesium phospho-tungstate and subsequent separation of caesium on alumina can be effectively used to separate Cs^{137} from fission product waste solution free from other radioactive impurities. This method is also easily adaptable for remote operations on a plant scale.

ACKNOWLEDGEMENT

The authors are grateful to Dr. V.K. Iya, Head, Isotope Division, for his keen interest and useful discussions during the course of the work and to Shri M.S. Sant, Head, Electronics Section, Isotope Division, for the data on the spectra of samples.

REFERENCES

1. Isotopes and Radiation Technology; 1, (1) 40 (1963)
2. Isotopes and Radiation Technology; 1, (41-42) (1943)
3. L.A. Bray; Solvent extraction process for recovery of Sr, rare earths and caesium from radioactiv solutions, HW-SA-2982(1964)

4. E. J. Wheelwright; et al. Ion exchange separation of Kilocurie quantities of Pm^{147} - BNWL-318 (1966)

5. A. Raggenbass; et al; A pilot unit for the separation of caesium-137. Proceedings of 2nd Geneva Conference on Peaceful Uses of Atomic Energy - P/1179/(1958)

6. K. Saddington; Extraction of individual fission products from chemical process wastes. Conf. UNESCO (Paris); UNESCO/NS/RIC/16 (1957)

7. K. A. Kraus, et al. Proceedings of 2nd Geneva Conference on Peaceful Use of Atomic Energy - P/1832 (1958)

8. J. M. Fletcher; Proceedings of 2nd Geneva Conference on Peaceful Uses of Atomic Energy 20, p. 459-63 (1958)

9. T. V. Healy; Alkali phospho-tungstates - Part I - AERE C/R 2528 (1958)

DISCUSSION

Manohar Lal : Why do you use such a high core of PTA (61.6 mgms) for 1mgm of Cs?

T. S. Murthy : From the reaction experiments carried out we have arrived at this figure for complete precipitation with overall yield averaging $> 95\%$ assuming the formula of the product formed under the conditions to be $Cs_2HPW_{12}O_{40}.2H_2O$.

R. S. Tripathi : Have you tried all three forms of alumina (ie. alkaline, acidic & neutral) for separation of Cs-137?

T. S. Murthy : Only the neutral form was tried and this was given subsequent treatment with 0.1N NH_4OH, H_2O and HCl at pH 4.

P. K. Bhattacharyya: In your method of separation of Cs^{137} could you tell something about decontamination factor from other fission products etc. ?

T. S. Murthy : The interference from other fission products have been checked using respection tracers like Sr^{85+89} and Ce^{141} and the spectrum examined using a S_{12} channel analyser. The spectrum showed the complete absence of other impurities.

S. K. Patil : How γ-emitting Cs^{137} is suitable for isotopic power sources? Usually absence of γ-radiation is desired?

T. S. Murthy : Many of the power sources are in fact γ-emitters like Cs-137 and Ce-144. The particular use depends on the properties like specific power, power density of the sources. In fact even β-emitting sources like Sr^{90} also have associated brehmstrahlung which has to be shielded properly.

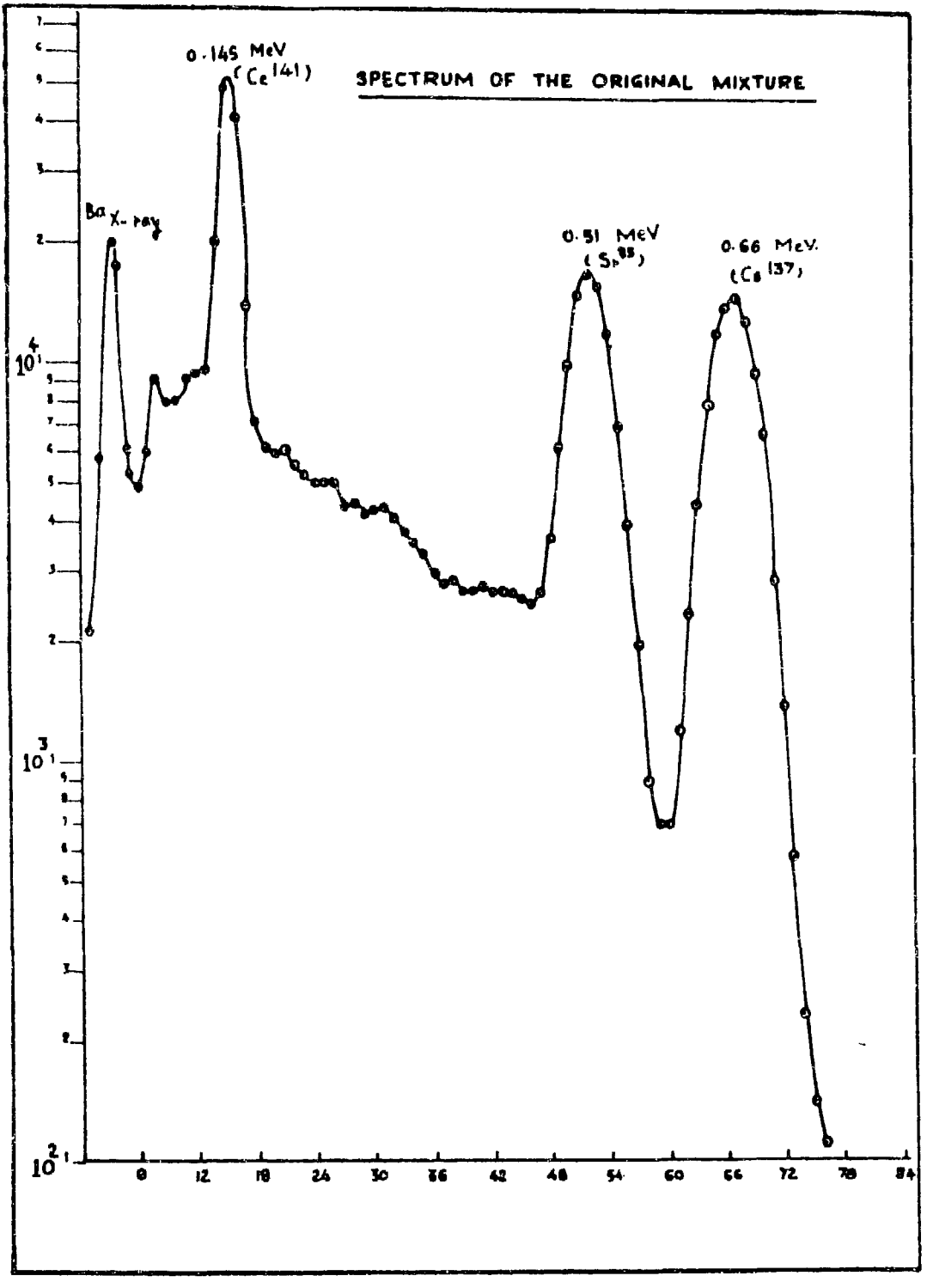
SPECTRUM OF THE ORIGINAL MIXTURE
0.145 MeV
(Ce 141)
Ba X-ray
0.51 MeV
(Sb 85)
0.66 MeV.
(Cs 137)
10 4
10 3
10 2
0
12
18
24
30
36
42
48
54
60
66
72
78
84

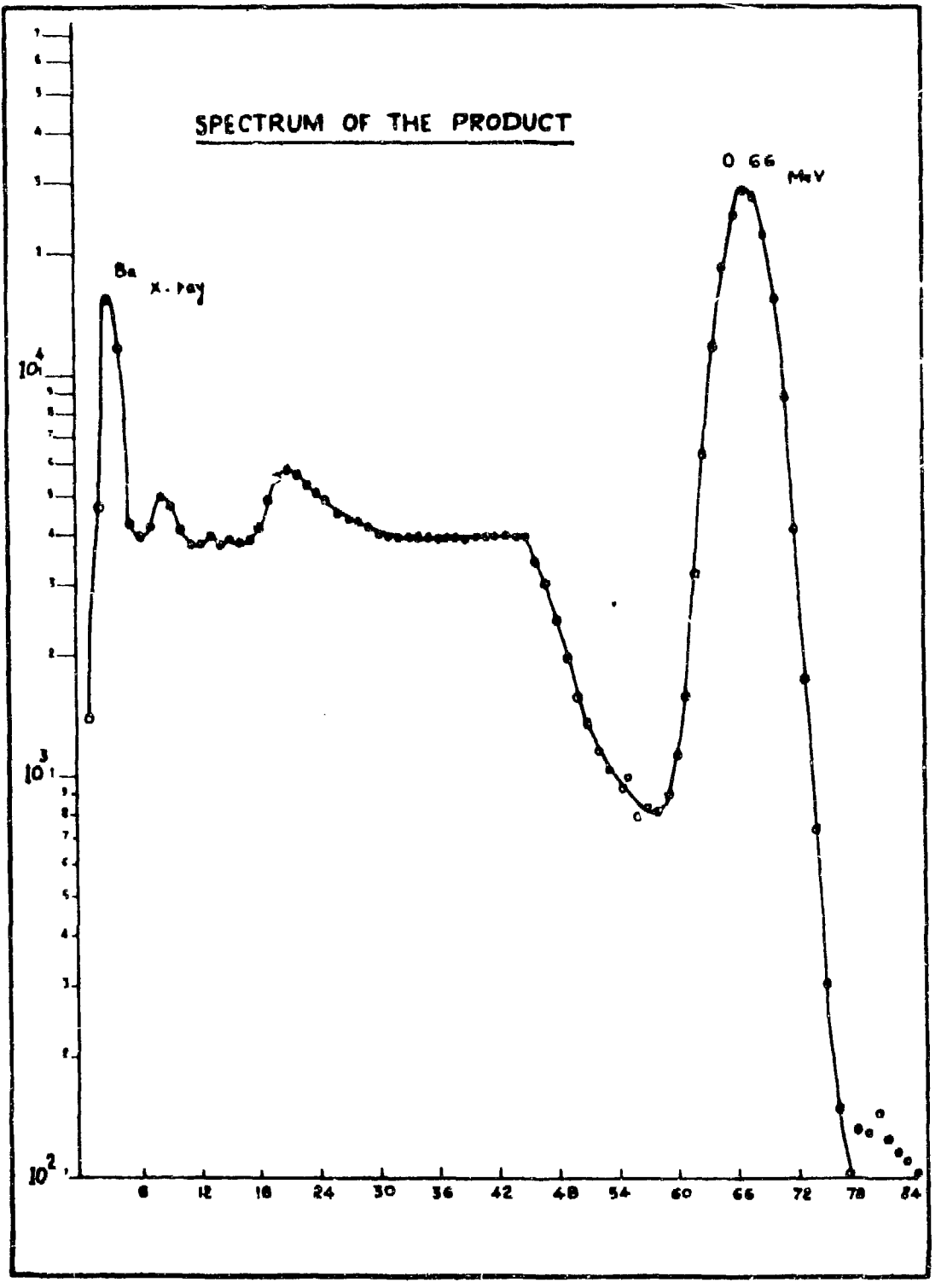
SPECTRUM OF THE PRODUCT
0 66 MeV
Ba X-ray
10^4
10^3
10^2
6
12
18
24
30
36
42
48
54
60
66
72
78
84

SEPARATION OF IODINE-131 FROM NEUTRON IRRADIATED TELLURIUM USING HYDROGEN PEROXIDE

T. S. Murthy, V. C. Nair and S. G. Naik
Isotope Division, Bhabha Atomic Research Centre, Trombay, Bombay-85

INTRODUCTION

Iodine-131 is one of the most widely used radioisotopes in medicine for diagnostic and therapeutic purposes, either directly as sodium iodide or in the form of iodine-131 labelled compounds. Hence, the production of this isotope assumes top priority in any isotope programme. Iodine-131 is produced during nuclear fission or by the pile irradiation of tellurium and its compounds.

$$Te^{130} \xrightarrow{(n,\gamma)} Te^{131} \xrightarrow[24.8\ m]{\beta^-} I^{131} \xrightarrow[8.05\ d]{(\beta^-,\gamma)} Xe^{131} \text{ stable.}$$

When the former method is employed for production, enriched uranium irradiated for 2-3 weeks in the nuclear reactor is dissolved in nitric acid and the iodine-131 is distilled and collected.[1] But separation of iodine-131 from pile irradiated tellurium targets is the most commonly used method of production. The methods of separation varies for different targets. With metal tellurium the target is dissolved in a mixture of sulphuric acid and chromic acid and the iodine is distilled off after reduction with oxalic acid.[2] A dry distillation method is generally used when tellurium dioxide is used as the target.[3,4]. The methods of separation take a little more than a day for completion and it was of interest to develop a speedier method. In the Isotope Laboratory at Trombay, we have developed a new method[5] based on the dissolution of neutron irradiated tellurium in hydrogen peroxide and sodium hydroxide followed by acidification and distillation of the iodine-131. The present paper is an extension of this work in line with a method reported by Gleason[6] wherein tellurium is directly dissolved in hydrogen peroxide and sulphuric acid.

EXPERIMENTAL

E. Merck tellurium and all other reagents of analytical grade were used in the experiments. In the dissolution experiments 5 grams of tellurium and 30 ml. of 100 vol. hydrogen peroxide containing the required amount of sulphuric acid diluted to 100 ml. were refluxed in a round bottom flask. In the distillation studies the total volume of the reaction mixture was maintained at 300 ml. The apparatus consisted of a two necked 1 litre distillation flask and a 3 necked 1 litre receiver flask with an iodine trap, connected by a right-angled bridge having a splash head at one end and a water condenser at

the other end. In the modified version the two limbs of the bridge were replaced by two feet long water condensers. The yield of iodine-131 was estimated by counting the initial and final samples in a well type thallium activated sodium iodide scintillation detector at the 0.36 MeV iodine photopeak and comparing the values after accounting for dilution.

RESULTS AND DISCUSSION

a) Dissolution of Tellurium in Hydrogen Peroxide and Sulphuric Acid

While studying the distillation of iodine-131 from acidified solutions of sodium tellurate prepared by dissolving tellurium in sodium hydroxide and hydrogen peroxide, the effect of adding tellurium was investigated. It was found that tellurium dissolved completely and the yield of iodine-131 remained unaffected so long as there was enough hydrogen peroxide present[5]. Hence, the dissolution of tellurium in hydrogen peroxide at various concentrations of sulphuric acid was studied, with a view to developing it as a method of production. Very little tellurium dissolved when the acid concentration was below 7N. Addition of more hydrogen peroxide, prolonged refluxing or increasing the total volume did not have any effect in bringing the tellurium into solution. In the concentration range of 7-13 N the tellurium dissolved completely in about 10-15 minutes. Above 13 N tellurium did not go into solution. This may be due to the formation of a thin film of telluric acid over the tellurium powder.

b) Distillation of Iodine-131 from the Dissolution Mixture

In our studies reported earlier[5] the distillation of iodine-131 from sulphuric acid solutions of telluric acid containing hydrogen peroxide the yield was found to be independent of the concentration of sulphuric acid beyond 5N. Considering various factors like smooth dissolution of tellurium, time of distillation and acid carried over, the acid strength was fixed at 9N and a few experiments were carried out doing dissolution of tellurium and distillation of iodine-131 simultaneously. The distilled iodine was absorbed in sodium hydroxide. The yield was found to vary from 40-60% for the same 75 minutes distillation period. In view of the fact that nearly 90% of the iodine distilled under identical conditions in the earlier work[5], this result was a little unexpected. The only probable reason that could be attributed to this low fluctuating yield was the carry-over of iodine-131 along with the decomposed oxygen from hydrogen peroxide. This was confirmed by the unusually high iodine-131 activity recovered from the iodine-131 trap over the receiver flask. To counteract this the limbs of the bridge tube were replaced by two 2 feet long water condensers and the mixture was refluxed for about 25 minutes before distillation to ensure complete dissolution of tellurium and decomposition of bulk of the excess hydrogen peroxide. With this modification, an yield of about 88% was obtained for 75 minutes distallation in a series of experiments at 9 N. The distillate took about 5 ml i N sodium hydroxide for adjusting the pH to about 8. The time of distillation can be reduced with increasing acid concentration. But there will be the disadvantage of increased

acid carry-over in the distillate.

Two experiments at production scale were carried out using 25 grams of tellurium. The total volume of the dissolution mixture was maintained at 500 ml. and acid normality 9 N with the volume of 30% hydrogen peroxide added being 150 ml. Here again the yield over a period of 75 minutes distillation was about 85%, with practically very little iodine distilling in the next 15 minutes.

c) Purity of the Product Solution

Distillate from production scale runs were concentrated to about 20 ml. and were analysed for radiochemical purity as well as the presence of other elements. More than 95% of the iodine-131 was found to be in the form of iodide by paper chromatography(7). Spectrographic analysis showed that the elements Al, As, Ag, Be, Mn, Sn, Te, B, Ca, Cs, Cr, Fe, Hg, Ni and Pb were all present in less than 2 ppm. Only silicon was found to be of the order 10 ppm. These purity conditions are satisfactory for its use in medicine for oral administration(8).

ACKNOWLEDGEMENT

The authors are thankful to Dr. V.K. Iya, Head, Isotope Division, BARC, for his keen interest in the work and also to Shri N.G.S. Gopal, Head, Quality Control Section, for the analysis of the samples.

REFERENCES

1. A.F. Rupp; Proceedings of the First International Conference on Peaceful Uses of Atomic Energy, Geneva 14, 68 (1955)
2. V.K. Iya, T.S. Murthy, K.R. Balakrishnan and V.C. Nair; AEET/Radiochem/50 (1964)
3. K. Taugbol and K. Samasahl; JENER/34 (1954)
4. K. Samasahl and K. Taugbol; Proceedings of the First International Conference on Peaceful Uses of Atomic Energy, Geneva 14, 89 (1955)
5. T.S. Murthy and V.C. Nair; Indian J. Chem. 5(7) 337 (1967)
6. G.I. Gleason; U.S. Pat. 3, 107, 155 (to Abbot Labs.) (15th October, 1965)
7. Pharmacopeia of the United States, (Mack Printing Co. Easton, PA) 16, 683 (1955).
8. British Pharmacopeia (The Pharmaceutical Press, London) 751 (1963)

DISCUSSION

B.M. Patel : What is the purity of your starting chemical Te?

V.C. Nair : **Chemically pure tellurium supplied by E. Merck Chemical Company was used for irradiation.**

STUDIES ON THE STABILITY AND SHELF-LIFE OF SOME LABELLED RADIOPHARMACEUTICALS

C. N. Desai, R. S. Mani and T. P. Prabhu
Isotope Division, Bhabha Atomic Research Centre, Trombay, Bombay-85

Radiopharmaceuticals are routinely used in diagnostic nuclear medicine. For this purpose they are required to be of the highest purity and high specific activity. These products, however, undergo decomposition during storage due to self-irradiation and radiolysis. The consequences of this problem are encountered by the radiopharmaceutical manufacturer and also the users. In view of this, stability studies of radiopharmaceuticals are carried out so that the degree of decomposition and preventive measures to minimise the latter are known[1,2].

In the case of radioactive pharmaceuticals, in addition to chemical and pharmaceutical stability, one needs to examine their radiation stability also. This is mainly because radiations are sufficiently energetic to degrade the chemical compounds through their ionizing and oxidising effects which are known as primary and secondary effects. As a consequence of this, radiopharmaceuticals are usually less stable than their non-radioactive counter parts.

The decomposition of labelled compounds depends on the amount of radiation energy absorbed by the compound itself or its environs during its useful life. The percentage decomposition can be correlated with the "G(-M)" values - defined as the molecules permenantly altered or decomposed per 100 ev (energy) of ionizing radiation absorbed. "G(-M)" value of some of the labelled compounds has been determined[3,4]. Generally, high "G(-M)" values indicate less stability.

In addition to radiation, factors such as oxidation, hydrolysis influences chemical decomposition of the labelled compounds, since the latter are often used in very dilute solution. It is also essential to guard against photochemical, microbiological decomposition and also the decomposition caused by inactive impurities. Several of the iodo-organic compounds (Rose Bengal, Hippuran, Hypaque, cholographyn etc.) are sensitive to light, and their labelled preparations should be stored in amber-glass containers to prevent photochemical decomposition[5].

This paper reports the stability studies carried out on radioiodine labelled radiopharmaceuticals such as Tetrachloro-(P)-tetra-iodo-(R)-fluorescein (Rose Bengal), sodium orthoiodo hippurate (Hippuran), Glyceryl-trioleate (Triolein), oleic acid, Human serum albumin (HSA), L-Triiodo-thyronine (TIT), Thyroxine (T_4) and sulfobromophthalein (BSP). Table I

illustrates the specifications and diagnostic use of some of the radiopharmaceuticals supplied by the Isotope Division, Bhabha Atomic Research Centre, Trombay[6].

EXPERIMENTAL

Several lots of the individual radiopharmaceuticals were stored under different conditions of temperature, pH, specific activity and radioactive concentration and examined over a regular interval of time for several weeks.

In a few cases, trace concentration of (i) known metallic impurities and (ii) oxidising agents were added and their effect on radiochemical purity was studied e.g. Rose Bengal, Hippuran, Cholographyn and BSP.

It has been observed that metallic impurities such as silver, copper and cadmium as well as oxidising agents such as H_2O_2 have deteriorating effects when their concentrations exceed the optimum value[7].

The samples of radioactive pharmaceuticals were checked for free iodide by paper electrophoresis using veronal buffer pH 8.6 for 1 hour at 200 volts. The free iodide migrates 10-12 cms from the point of spotting whereas the labelled compounds remain very near the point of spotting. The percentage free iodide was calculated by counting and/or scanning the electrophoretograms.

The integrity of labelling defined by the radiochemical purity was ascertained by ascending paper chromatography using Whatman No. 3 paper, e.g., Rose Bengal I^{131} on paper chromatographic analysis in ethanol: ammonia: water moves with Rf = 0.42 while the lower halogenated fluoresceins have different Rf values[8].

Hippuran-I^{131} has the Rf = 0.5 while the probable impurity O-iodobenzoic acid and free iodide have the Rf values 0.8 and 0.1 respectively in benzene: acetic acid : water (9:1:1)[9].

The absorption spectra of the labelled compounds and the molar absorbance values were determined over a period of storage. This gave some indication of radiation induced decomposition in a few cases e.g. Rose Bengal (λmax 550 mμ) and BSP (λmax 585 mμ).

In the case of labelled iodo-thyronines their radiochemical purity was also determined by thin layer chromatography using silica gel[10] in addition to the paper chromatographic analysis[11]. These techniques reveal the presence of the possible contaminating impurities such as MIT, DIT etc.

Triolein-I^{131}, oleic acid-I^{131} were chromatographed on a standardized silicic acid column and their elution patterns were compared[12].

Radio-iodinated human serum albumin was examined for degraded labelled polypeptides using DEAE sephadex A-50 and DEAE-cellulose columns[13].

In a few specific instances, electivity tests and other suitable biological tests were also carried out to evaluate the presence of biologically unacceptable trace impurities produced by radiolysis e.g., denatured protein in RIHSA and labelled hormones[14].

REMARKS

1. Even under ideal conditions of storage, the labelled radiopharmaceutical formulations show contamination of small percentages of labelled impurities, essentially of an organic nature. However, these are yet to be characterized in detail. Quantivatively speaking the main impurity is free iodide. The latter could be controlled to less than 5% by storing the compounds (i) at 0-2° (ii) by keeping the pH 6-8 (iii) maintaining the radioactive concentration upto 3.0 mCi/ml (iv) having the sp. activity exceeding in many cases 1c/m M during the storage period of 4 weeks for (I-131) and 12 weeks for (I-125) labelled compounds.

2. Stability studies help us (i) to select suitable labelling radio-nuclide for specific biological studies, (ii) to supply and use better radiopharmaceuticals with high purity suitable as genuine tracers, (iii) to assign acceptable shelf-life for the radiopharmaceuticals, However, it must be noted that due to the limited sensitivity of analytical methods and lack of complete knowledge of radiation chemistry of these labelled compounds, the exact nature of the break-down products becomes difficult to be predicted.

3. The shelf-life of iodine labelled radiopharmaceuticals can be prolonged by (i) adding protective agents (e.g., inactive human serum albumin in I^{131} and I^{125} labelled RIHSA (ii) sequestering free iodide using silver salt impregnated silver saddles e.g., I^{131} radio hippuran (iii) continuous removal of free iodide using sterile ion exchange resins enclosed in dialysis membrane [15].

4. Insufficient purification procedures decrease the stability and hence the shelf-life of radioactive pharmaceuticals.

5. I^{125} labelled compounds are more stable than the corresponding I^{131} labelled compounds mainly because of absence of β-emission which indicates that β-rays accelerate the radiation decomposition of labelled compounds.

ACKNOWLEDGEMENTS

The authors wish to thank Dr. V.K. Iya for the keen interest taken by him in this work.

REFERENCES

1. R. J. Bayly and E. A. Evans; J. Labelled Compounds 2, 1 (1966)
2. H. I. Glenn and R. E. Kidwell; Radioactive Pharmaceuticals, U. S. A. E. C. (Proceedings of Symposium) 165 (1966).
3. B. M. Tolbert; Advances in Tracer Methodology (Third Symposium) p. 64 (1959)
4. The Radiochemical Manual; 2nd Edition, published by the R. C. C. Amersham, England (1966).
5. V. K. Iya, R. S. Mani and C. N. Desai; Synthesis of Labelled Molecules (to be published)
6. "Radioisotopes in Medicine"; Catalogue - Isotope Division, BARC, Trombay.
7. R. S. Mani; Ph. D. thesis, University of Bombay (1968)
8. K. B. Taylor; Nature (London) 185, 243 (1960)
9. R. S. Mani; (Unpublished observations)
10. Y. Cohen; Radioactive Pharmaceuticals (Proceedings of the Symposium) U. S. A. E. C. p. 67 (1966)
11. G. I. Gleason, J. Biol. Chem. 213, 857 (1955)
12. G. Lakshminarayana, F. A. Kruger, D. G. Cronwell and J. B. Brown; Arch. Biochem. & Biophys. 88, 318 (1960)
13. R. S. Mani and S. A. Balakrishnan; Isotopanpraxis 7 (1969)
14. K. N. Jeejeebhoy; (personal communication)
15. W. H. Blahd; Nuclear Medicine, McGraw Hill, N. Y. p. 149 (1965)

DISCUSSION

J. P. Mittal : (1) What do you think is the mechanism of free iodide production in the system (i. e., I^-) ?

(2) Do you think I^- is produced via a free radical or ionic mechanism? I am asking this question because, if we know the mecahnism by which I^- is produced, it may be easier for you to develop or find better so called 'preservatives'

(3) If it is due to dissociative electron capture by iodo gp i. e. $RI + e^- \rightarrow R + I^-$, then various electron scavengers can be tried as potential 'protectors'.

C. N. Desai : (1) & (2). It is not possible to say exactly whether it is a free radical or ionic mechanism in the cases we have studied since the radiation chemistry of these compounds has not been adequately studied. But it is quite probable that free radical and/or ionic mechanism must be involved in all the cases.

(3) I agree with you.

Manohar Lal : What is the purpose of using cysteine HCl in your studies?

C. N. Desai : It serves as a preservative, probably by acting as a reducing agent and/or by sequestering the free radicals.

P. N. Moorthy : What is meant by free iodide? Free iodine or inorganic iodide ion?

C. N. Desai : Of course, inorganic iodide.

TABLE I

++ From the date of analysis
** Supplied in sterile, pyrogen-free aqueous buffered solution at pH 6-9 on special request
* Supplied in sterile, pyrogen-free aqueous buffered solution at pH 6-9

S. No.	Product	Chemical & Pharmaceutical form	Sp. Act mCi/mgm	Radioactive concn mCi/ml	Diagnostic use and (Dose in uCi)	Recommended shelf-life++
1.	Rose Bengal-I^{131}	Rose Bengal* I^{131} injection	Upto 5.0	Upto 5.0	Liver function (10-25)	4 weeks at 0-2°C
2.	Hippuran I^{131}	Hippuran* I^{131} injection	Upto 2.0	Upto 2.5	Kidney function (10-50)	4 weeks at 0-2°C
3.	Radioiodinated Human serum albumin	RIHSA* I^{131} injection	Upto 5-10 atoms of iodine/ molecule of protein	Upto 3.0	i) Plasma & blood volume (3-20) ii) Cardiac out put (10-30) iii) Detection & localization of brain tumors (300-500)	4 weeks at 0-2°C
4.	RIHSA-I^{125}	RIHSA* I^{125} injection	-do-	Upto 0.5	-do-	12 weeks at 0-2°C
5.	Triolein-I^{131}	Triolein I^{131} in olive oil (non-injectable)	Upto 20% saturation	Upto 5.0	Fat absorption studies (25-50)	4 weeks at 0-2°C
6.	Oleic acid-I^{131}	Oleic acid I^{131} in oleic acid (non-injectable)	-do-	Upto 5.0	-do-	4 weeks at 0-2°C
7.	Triolein I^{125}	Triolein I^{125} in olive oil (non-injectable)	-do-	Upto 2.5	-do-	12 weeks at 0-2°C
8.	Oleic acid I^{125}	Oleic acid I^{125} in oleic acid (non-injectable)	-do-	Upto 2.5	-do-	12 weeks at 0-2°C
9	L-TIT I^{131}	L-TIT^{131} in 50% aqueous propylene glycol (pH 6-7)	Upto 20	Upto 5.0	Thyroid function studies (less than 1 uCi)	4 weeks at 0-2°C
10.	L-T_4-I^{131}	L-T_4-I^{125}	Upto 20	Upto 5.0	-do- (20-150)	-do-
11.	L-TIT-I^{125}	L-TIT-I^{125} in 50% aqueous propylene glycol (pH 6-7)	Upto 10	Upto 2.0	Thyroid function studies (less than 1 uCi)	12 weeks at 0-2°C
12.	L-T_4-I^{125}	L-T_4-I^{125} in 50% aqueous propylene glycol (pH 6-7)	-do-	-do-	Thyroid function studies (20-150)	12 weeks at 0-2°C
13.	**BSP-I^{131}	BSP*-I^{131}	Upto 2.5	Upto 3.0	Liver function (30-50)	4 weeks at 0-2°C

HIGH SPECIFIC ACTIVITY TRACE LABELLING OF HORMONES AND PROTEINS

R. J. V. Prabhakaran and C. N. Desai
Isotope Division, Bhabha Atomic Research Centre, Trombay, Bombay-85

For thyroid metabolism studies, 3, 5, 3' Triiodo-L-thyronine (TIT) and L-thyroxine (T_4) labelled with I^{131} and I^{125} have been used extensively. Direct synthesis of TIT and T_4 labelled with radioiodine by iodination of di-iodothyronine have been employed[1]. However, methods based on direct exchange between pure non-radioactive TIT and T_4 and radioiodine have been reported.[2, 3, 4] Preparation on a commercial scale of TIT and T_4 labelled with I^{131} and I^{125} with high specific activity and maximum purity are attended with considerable practical difficulties. We have been able to prepare both these hormones with high specific activities in a single preparation by an exchange method involving addition of carrier iodine in trace amounts and purification by gel filtration.

The need for radioiodinated proteins of high specific activity arose from the desire of detecting them at the levels found in blood. The radioimmuno assay technique developed for insulin[5] has been extended to Human Growth Hormone (HGH)[6]. Methods involving iodination under mild conditions are adopted for radioiodination of proteins and hormones so that the biochemical specificity of these sensitive molecules is not altered after labelling. An elegant method using chloramine-T[7], a mild oxidizing agent, for iodination of HGH is now being widely used for a variety of hormones and proteins. After evaluating the published methods in our present study, we have essentially adopted the chloramine-T method[7] for the routine preparation of I^{131} and I^{125} labelled HGH. The same method, suitably modified for I^{131} labelling of acid soluble proteins[8] has been extended for labelling Bovine Serum Albumin (BSA) with I^{131}, which is used as a tracer in protein metabolism studies.

EXPERIMENTAL

a) I^{131} and I^{125} Labelled Thyroid Hormones

To 40-50 mc of reducing agent, free and carrier-free NaI^{131} in a minimum volume is added 200-500 µgm of TIT (sodium salt) in alcoholic ammonia solution. Immediately, tracer amount of carrier iodine in alcohol is added. The reaction mixture is set aside for a few minutes. Then, the solution is directly placed on a column of Sephadex G-25 (1.5 x 30 cms) which has been previously conditioned with dilute alkali. 2.0 ml fractions are collected with dilute alkali as the eluting solution. The elution pattern is as follows: upto 30 ml, unreacted free iodide followed by well separated fractions of TIT-I^{131} and T_4-I^{131}. Finally, pH is adjusted after adding propylene glycol so that the solution is 50% in propylene glycol, the pH 6.0 and

the activity 200-500 μc/ml. A similar procedure is adopted for the preparation of I^{125} labelled TIT and T_4.

The radiochemical purity of the final products is confirmed by paper electrophoresis, paper and thin layer chromatography. The unbound iodine-I^{131} activity is estimated by paper electrophoresis in 0.07 M barbitone buffer, pH 8.6 at 200 volts for 1-2 hr. The labelled individual thyroid hormones are determined by ascending paper chromatography with t-amyl alcohol-2 N. ammonia (1:1) as the developing solvent and thin layer chromatographic separations on silica gel coated plates with isopropanol-ethylacetate-acetone-ammonia (35:30:25:20) as the developing solvent. The radiochemical purity of the products are >95% with specific activity 30-40 mc/mg. The specific activities of I^{125} labelled products are 15-20 mc/mg.

b) I^{131} and I^{125} Labelled Human Growth Hormone

To 3-4 mc (20 μl) of reducing agent, free and carrier-free NaI^{131} taken in a small Pyrex tube added one drop of 0.5 M phosphate buffer, pH 7.5 followed by 25 μl of HGH (5-10 μgm). Then, 25 μl of chloramine-T (50 μgm) is added and gently mixed. After 10-15 sec., 100 μgm of sodium metabisulphite in 25 μl are added. The reaction mixture is transferred to a column of Sephadex G-50 (1.5 x 20 cms) previously conditioned with 0.07 M barbitone buffer, pH 8.6 and pre-saturated with human serum albumin. Elution is carried out with the same buffer collecting 1 ml fractions. The labelled HGH fractions are directly collected in 0.5% human serum albumin.

Paper electro-phoresis of the labelled HGH was carried out as mentioned under TIT. Nearly 40-50% of the original activity is recovered as I^{131} labelled HGH with specific activity , 300-400 μc/μgm.

A similar procedure was adopted for the preparation of I^{125} labelled HGH except the HGH content was varried from 10-20 μgm. Specific activity was of the order of 50 μc/μgm.

c) I^{131} Labelled Bovine Serum Albumin (BSA)

The chloramine-T method has been suitably modified for labelling BSA with I^{131}.

To 5-10 mc of Na I^{131}, reducing agent free and carrier-free, in a minimum volume, 0.75 ml of 0.5 M phosphate buffer, pH 7.5, 5-10 mg of BSA, 10-15 mg of chloramine-T in 0.2 ml are added and gently mixed. After 1 mt. 20-25 mgs of sodium metabisulphite in 0.2 ml are added. The whole reaction mixture was dialyzed in a cellophane bag for 4 hrs. against two changes of 2 litres distilled water. The dialyzed sample was placed on a Sephadex G-25 column (1.5 x 30 cms) conditioned with 0.07 M barbitone buffer, pH 8.6. 1.0 ml fractions were collected. Protein fractions were pooled which constituted 80-90% of the original activity.

The final product was analysed by paper electro-phoresis and paper chromatography for free iodide activity. Electro-phoresis was carried out as mentioned under TIT. Less than 1% of the activity was found to be unbound free iodide. Ascending paper chromatography with 85% methanol as the developing solvent showed that more than 98% of the activity stayed at the point of spotting.

REMARKS

a) I^{131} and I^{125} Labelled Thyroid Hormones

Exchange methods reported earlier, though workable at tracer level, offer problems on a preparative scale. By taking advantage of the method using Sephadex gel filtration (9) we have prepared thyroid hormones on large scale in the highest possible state of purity. The method has the following advantages: (1) Less radiation hazard since the whole column can be enclosed in a lead jacket and iodine is always handled at an alkaline pH. (2) It is very simple, rapid and eliminates the use of a rotary film evaporator which is generally required in the earlier reported methods. (3) The levels of organic impurities are reduced to a bare minimum.

ACKNOWLEDGEMENTS

The authors express their thanks to Dr. R.S. Mani for helpful suggestions and to Dr. V.K. Iya, Head of the Isotope Division, BARC, for his keen interest.

REFERENCES

1. J. Roche et.al.; Bull. Soc. Chim. Biol. 37, 819 (1955)
2. G.I. Gleason, J. Biol. Chem. 213, 837 (1955)
3. L.J. Anghileri; Int. J. Appl. Radn. & Isotopes 14, 328 (1963)
4. Hoye Åge; Acta Chimica Scandinavica 22, Part 2, 695 (1968)
5. R.S. Yalow, S.A. Berson; J. C. Invest. 39, 1157 (1960)
6. W.M. Hunter and F.C. Greenwood; Biochem. J. 91, 43 (1964)
7. F.C. Greenwood, W.M. Hunter and J.C. Glover; Biochem. J. 89, 114 (1963)
8. Moscarello et. al.; Canad. J. Biochem. 46, 235 (1968)
9. E.H. Mougey and J.W. Mason; Anal. Biochem. 6, 223 (1963)

PRODUCTION OF TRITIUM TARGETS AND SOURCES

R. N. Indra and B. A. Kulkarni
Isotope Division, Bhabha Atomic Research Centre, Trombay, Bombay-85

INTRODUCTION

Tritium, absorbed in thin metallic layers deposited on suitable backings, can provide radiation sources, and targets for accelerated deuterons to produce monoenergetic neutrons.

Various authors[1, 2, 3, 4, 5, 6] have reported the preparation of these targets. The procedure, in general, consists of vacuum evaporation of zirconium or titanium on discs of metals like Cu, Au, Pt, Ta, Mo, W, stainless steel, etc.; and subsequently heating the discs in the atmosphere of tritium to achieve its impregnation in the coated layers. The details of procedure are important for obtaining satisfactory targets.

Such targets have so far been imported in India. This paper reports the work undertaken to develop the production of these targets indigenously with copper as substrate and zirconium as coating material. Difficulties arising due to use of conventional vacuum material, and imperfect degassing and cleaning are discussed.

DESCRIPTION OF EQUIPMENT

Vacuum Evaporation Unit : Figure 1 shows the main features of the unit (EPR-001, SR-2), built by the Technical Physics Division of BARC, which wa obtained for this work.

Our subsequent modifications to this unit are: replacement of the neoprene 'L' gasket with the one of 'Viton'; replacement of neoprene gaskets and insulators for the lead-in heating electrodes with silicone rubber and teflon respectively, modification of the heating electrodes to provide water cooling; addition of copper baffle to the liquid N_2 trap; and the provision of an assembly to introduce air into the bell jar or alternatively flush it with argon.

The pivoted cage (Fig. 4) to hold the discs for degassing, the cage (Fig. 6) to hold the discs for vapour deposition and the reflector (Fig. 5) were designed and added to the unit.

Impregnation Unit: Fig. 7 shows the glass line used for impregnation. The impregnator (Fig, 8), excepting the glass joints on the upper part, is made of transparent quartz.

The line is evacuated by a silicone-oil diffusion pump backed by a rotary pump. A ceramic crucible, wound with nichrome wire and housed in

a metallic can with asbestos packing, serves as heater for the U-H^3 trap. The heater for impregnation is a resistance-tape wound mica sheet, sandwitched between two 'Syndanyo' (hard compressed asbestos) plates with a clear hole in the upper plate to accommodate the bottom of the impregnator.

PROCEDURE

Vapour Deposition: Two or three tungsten strands, each 40 mil thick and 6 cm. long, held in close contact with each other between two s. s. holders mounted on water-cooled heating electrodes, form the filament. At a pressure less than 10^{-3} torr a heavy current is passed through the filament, for a few seconds, to clean the tungsten surface.

Eight or ten copper discs,(Fig. 2),cleaned and polished with fine grade emery, degreased with trichlorethylene and washed with distilled alcohol, and pegged on to the pivoted cage,are now introduced into the bell jar. This cage is so positioned that any disc brought against the filament is 12-15 mm away from it. The advantage of this cage is, that rotated with magnets held out side the jar, it permits bringing discs, one by one, against the filament without breaking the vacuum. A reflector (Fig. 5) made from 1.5 mm thick and 35 mm wide s. s. strip, is placed on the other side of the filament, to reinforce radiations on the disc facing the filament.

At pressures less than 3×10^{-5} torr, degassing of the discs,as well as of the filament,is started raising filament upto 2500°C. Each disc is heated for $2\frac{1}{2}$ hrs. But, to prevent over-heating of the bell jar and the base plate, heating at a time is limited to a maximum of 30 minutes followed by an allowance for cooling of the same duration.

With all the discs and the filament well degassed, the rate of pressure rise, in the chamber,isolated from the pumps, is 1×10^{-5} torr/20 seconds or even less.

Argon is now let into the chamber to open it. A piece of Zr foil, 5 mil thick and weighing about 300 mg. is folded at an angle and gently put on the filament. The rotating cage and the reflector are removed. The degassed discs are weighed and loaded with masking rings (Fig. 3) on the hemispherical s. s. cage. The cage is so positioned over the filament that each masked disc has its exposed central part about 5 cm. away from the filament fully viewing the foil loaded on it.

The bell jar is re-placed and the pumping started. During the initial stages of pumping, the chamber is flushed with argon. When the chamber vacuum reaches 10^{-5} torr range, currents in gradually increasing steps are passed, to degas the foil. As earlier, the heating is intermittent to prevent over-heating of the system. After 4-5 hours of heating with increasing currents, eventually a stage is reached when the chamber pressure is in 10^{-6} torr range and does not rise with further increase in current, indicating

thorough degassing of the foil. Finally, the current is slowly raised till Zr melts and evaporation commences. The chamber pressure falls due to the initial clean up by Zr vapours. Most of the metal evaporates off within 10-15 mins. When the evaporation is over, the system is allowed to cool for 2 hours under continuous pumping. Then, the chamber is isolated from the pumps and argon admitted to open it. The discs are removed and re-weighed to determine the quantity deposited on each.

Impregnation: Temperature versus applied voltage calibrations, for the U-H^3 trap and the impregnator heaters, are obtained using thermocouple pyrometers.

H^3 is trapped in finely divided uranium contained in T (Fig. 7) by the usual process[7, 8]. The impregnator, holding a disc with the deposit facing upwards, is connected to the vacuum line. The whole line, including the impregnator and the U-H^3 trap, is evacuated for a couple of hours. Then, raising the impregnator heater to 400°C, the disc is degassed for one hour. After switching off this heater and closing valves 1 and 2, T is heated to release H^3 into the line. Valve 5 is closed and the trap heater switched off, as soon as the manometer M_1 indicates a pressure of 25 cms of Hg. Allowing cooling of the released H^3, the steady pressure in M_1 is noted and the valve 2 opened. Pressures in M_1 and M_2 are noted when they become steady. Then valve 2 is closed and the H^3 left over in the line is allowed to return to the trap by opening valve 5.

Now, the impregnator heater is switched on and its temperature slowly raised. As indicated by M_2, the gas pressure rises with temperature, but at heater temperature around 500°C, the rate of pressure rise suddenly diminishes or even becomes negative, indicating the commencement of impregnation. Heating is continued at this temperature for 15-20 mts. and then the heater is switched off. When the pressure indicated by M_2 drops down to a steady value, it is noted and the valve 2 opened to allow the unused H^3 to return to the trap. After retrapping is completed, valve 2 is closed and the impregnator opened at room temperature to take out the impregnated disc.

The quantity of H^3 impregnated is calculated from the known internal volume of the impregnator and the difference in steady pressures noted in M_2 before and after the heating.

RESULTS

Very shiny and adherent Zr deposits of thickness around 1.3 mg/cm^2 have been obtained in single evaporations, using the procedure described above. Reducing the disc to filament distance to 2.5 cm has, at times, given nice deposits slightly more than 2 mg/cm^2 thick. But, this is rare and in most cases the deposit surface has cloudy or blistery appearance.

Zr to H^3 atomic uptake ratio in impregnation varies from disc to disc. It is around 1:1, though some times, much better ratios are observed. The best ratio observed so far is 1:2.

DISCUSSION

i) Most of the troubles are due to high melting point (2127°C) of Zr and its extraordinary gettering properties. Neoprene is stable upto 80°C and if, used for gaskets and insulators, it gives out a lot of vapours at raised temperature due to high electrode currents and intense filament radiations. As evaporation of Zr starts, its vapours chemically combine with vapours from neoprene to give blue powdery deposit which does not let the subsequent metallic deposit to adhere firmly to the metal of the discs. Replacements of neoprene with 'Viton', silicone rubber and teflon and providing water-cooling to the heating electrodes largely eliminated this trouble.

ii) Grey deposits, often occurring on discs while degassing, indicated significant back steaming of silicone oil vapours from the diffusion pump[9]. It was considerably reduced by introducing a copper baffle (Fig. 9a) into the liquid N_2 trap.

iii) Condensation of Zr-vapours considerably heats the disc which, if not degassed well, gives out gases. These gases, reacting with Zr, give coloured, blistery and poorly adherant deposits. Continuous pumping for 5-6 hrs. is necessary before evaporation is commenced; otherwise traces of oxygen, reacting with Zr vapours, give bluish instead of natural coloured pure Zr deposits.

iv) Introducing argon and flushing with it eliminate the possibilities of moisture condensing on discs and of oxidation of their surfaces or of Zr when heated for degassing.

v) The filament, if not degassed well, fuses quickly when Zr melts on it. Gases coming out in bursts from filament, fly off small lumps of molten metal. This effect is also observed, if filament temperature is raised too high above the melting point of Zr, due to burst of Zr vapours formed in immediate contact with the filament.

vi) No satisfactory method exists to estimate H^3 in the discs, once the impregnation is over. This estimation is possible by known volume of gas in the impregnator together with the fall in pressure due to impregnation. The impregnator is designed to hold less than 50 ml of gas to enable significant fall in pressure to be observed and yet to keep the greased joints away from the heater below. There is a provision for water cooling in case the quartz conical joints tend to get over-heated.

vii) If the discs are not well degassed or if their surfaces contain thin oxide layers under the coating, metal embrittlement[10] may be caused during impregnation, rendering the impregnated Zr film poorly adherent and non-unirofm in appearance.

viii) The exact mechanism involved in impregnation is not well understood. It is not known whether there exists a temperature at which the impregnation is maximum. Quite often, after heating, when the heater is removed, a very rapid fall in pressure is observed. This suggests that heating only breaks down a sort of surface barrier and impregnation actually occurs at much lower temperatures.

ix) Noting the steady pressures in M_1 helps to know and estimate if any impregnation occurs at room temperature on introducting H^3 into the impregnator.

x) Variation in atomic uptake ratio of Zr to H^3 may be due to the variation in texture and purity of the deposit.

REFERENCES

1. E.R. Greaves et. al.; Rev. Sci. Instr. 20, 579 (1949)
2. A.B. Lillie and J.P. Conner; Rev. Sci. Instr. 22, 210 (1951)
3. R.S. Rochlin; Rev. Sci. Instr. 23, 100 (1952)
4. J.P. Conner, T.W. Bonner and J.R. Smith; Phys. Rev. 88, 468 (1952)
5. W.J. Arrot, E.J. Wilson and C. Evans; Report AERE I/R 1135 (1953)
6. B.J. Massey; Report ORNL-2237 (1957)
7. C.H. Johnson and H.E. Banta; Rev. Sci. Instr. 27, 132 (1956)
8. B.J. Massey; Report ORNL-2238 (1957)
9. Dushman; Scientific Foundation of Vacuum Technique, page 254, Wiley, New York (1949)
10. Dushman; Scientific Foundation of Vacuum Technique, Chapter 9, Sec. 15, Wiley, New York (1949)

DISCUSSION

J.P. Mittal : Upto what temperature your targets can be used?

R.N. Indra : Radiochemical Centre, Amersham recommend their targets to be used below 200°C. For our targets, desorption rate studies for various temperatures are still being made.

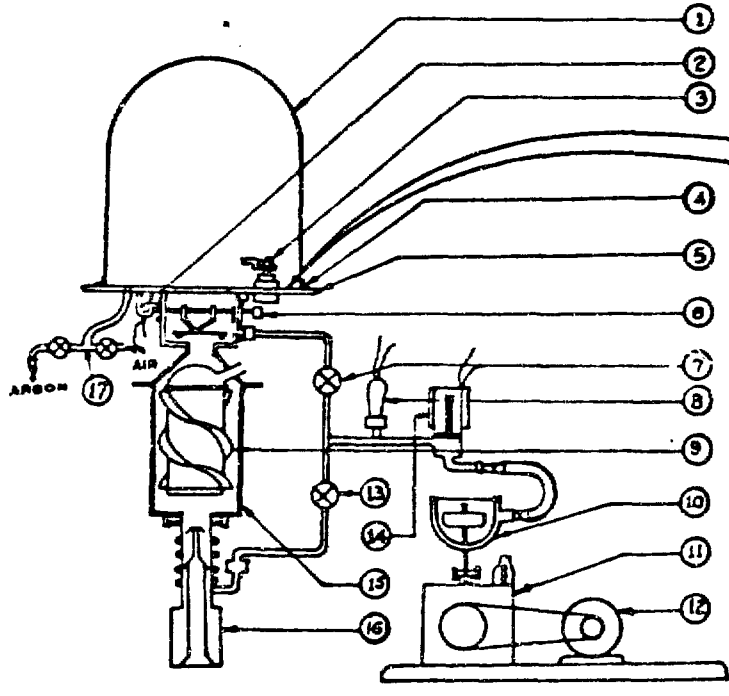

FIG.I. VACUUM EVAPORATION PLANT

1. GLASS BELL JAR (12"ϕ×14")
2. PENNING GAUGE
3. HEATING ELECTRODES
4. 'L' GASKET
5. NICKEL PLATED M.S. BASE PLATE.
6. BAFFLE VALVE
7. ROUGHING VALVE
8. THERMOCOUPLE GAUGE
9. COPPER BAFFLE
10. P_2O_5 TRAP
11. ROTARY PUMP
12. MOTOR
13. FORE-VACUUM VALVE
14. MAGNETIC ISOLATION VALVE
15. LIQUID N_2 TRAP
16. SILICONE OIL DIFFUSION PUMP
17. AIR~ ARGON INLET

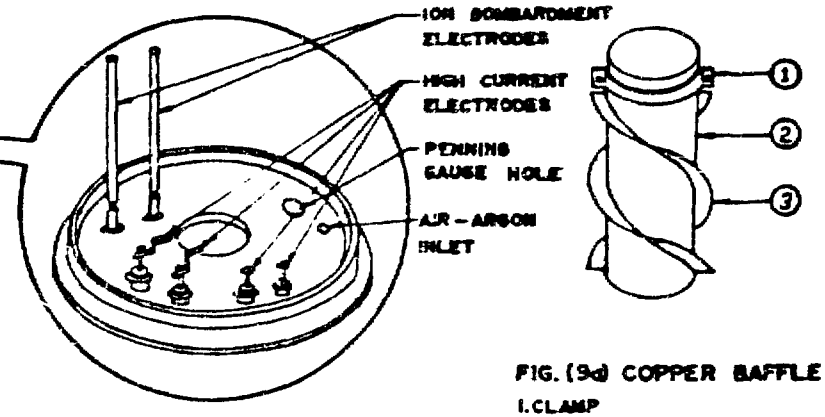

FIG. (3c) COPPER BAFFLE
1. CLAMP
2. COPPER CYLINDER
3. COPPER BAFFLE VANES

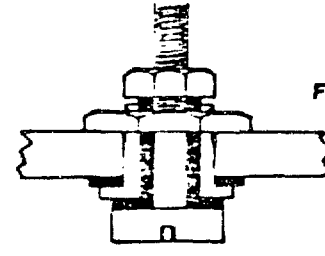

FIG.(3a).
HEATING ELECTRODE ASSEMBLY ORIGINAL

NEOPRENE
METAL

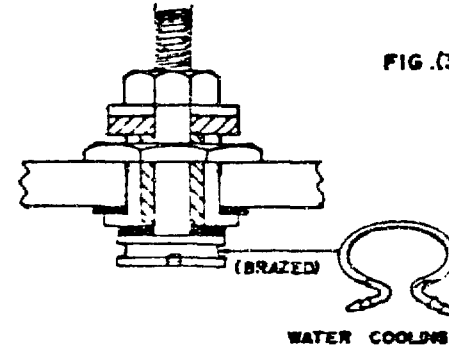

FIG.(3b). HEATING ELECTRODE ASSEMBLY MODIFIED

TEFLON
SILICONE RUBBER
METAL

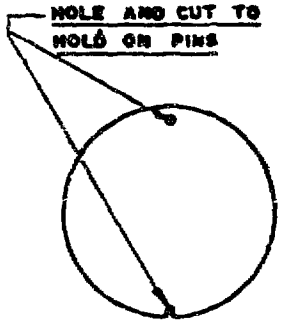

COPPER DISC

10 mil. THICK, 35 mm. DIA.

FIGURE - 2

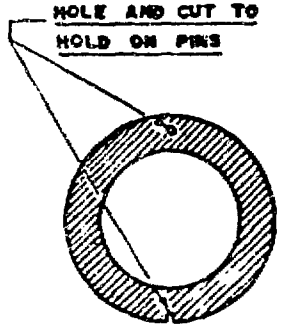

S.S. MASKING RING

35 mm. DIA.

FIGURE - 3

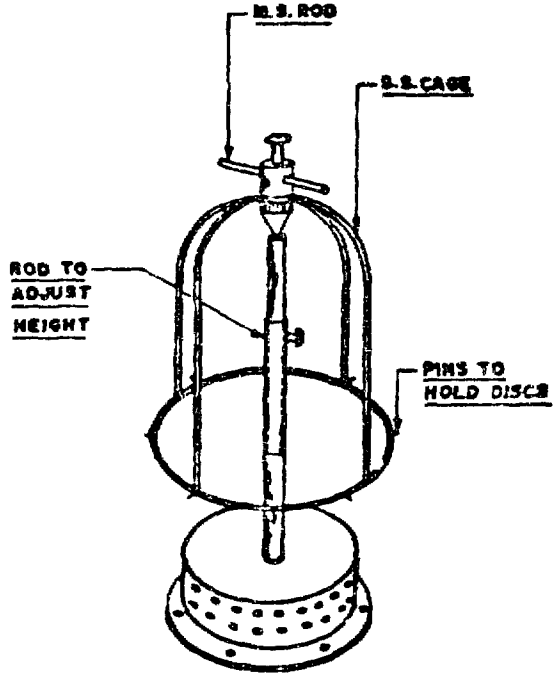

PIVOTED S.S. CAGE

FIGURE - 4

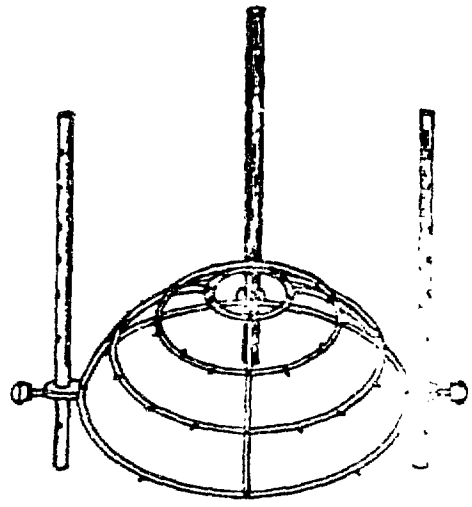

HEMISPHERICAL S.S. CAGE

TO HOLD DISCS FOR VAPOUR DEPOSITION

FIGURE - 6

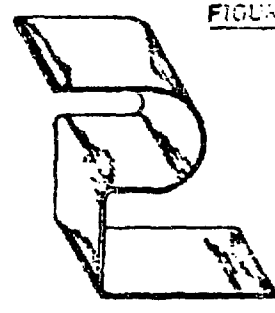

S.S. REFLECTOR

FIGURE - 5

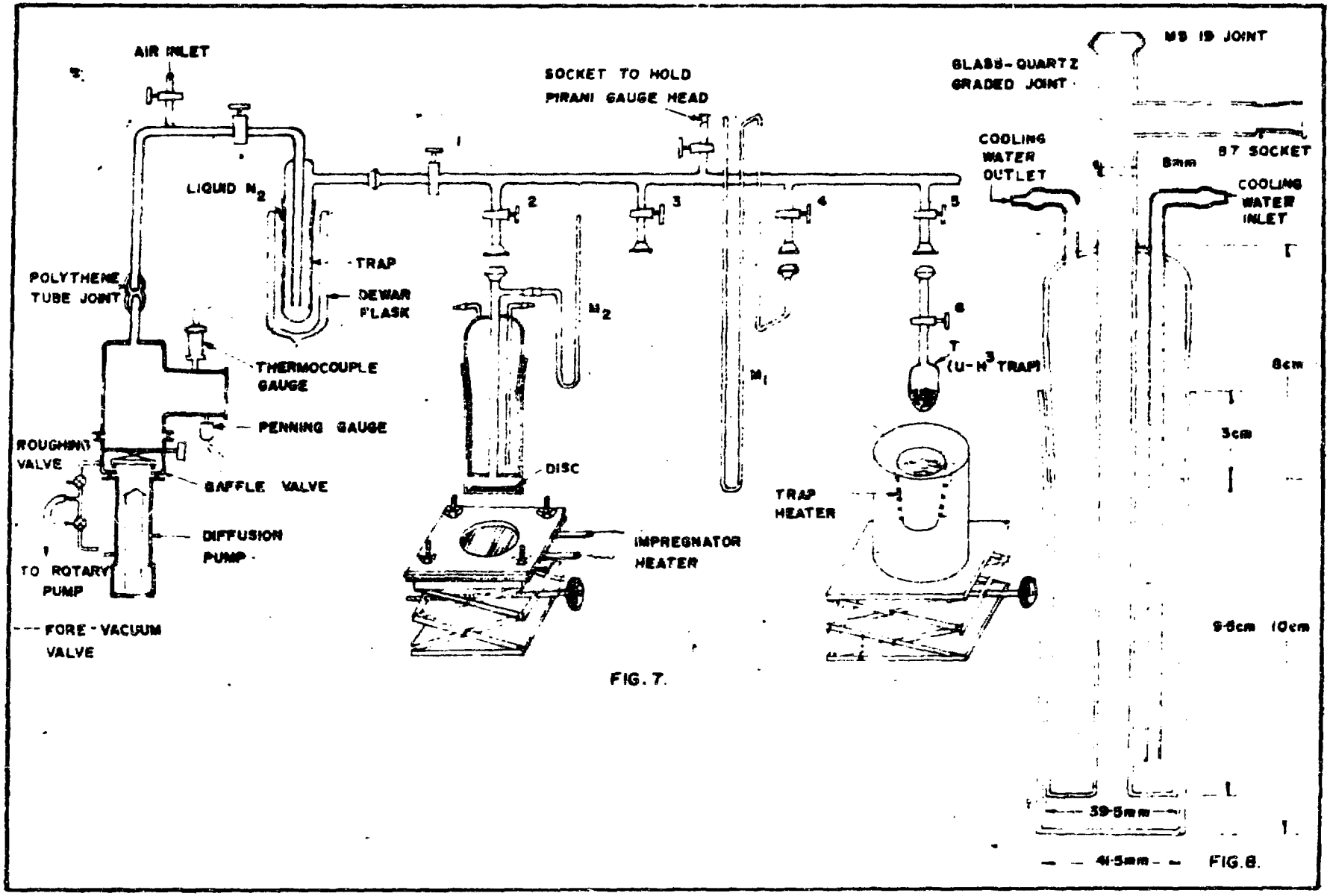
AIR INLET
LIQUID N_2
TRAP
DEWAR FLASK
POLYTHENE TUBE JOINT
THERMOCOUPLE GAUGE
PENNING GAUGE
ROUGHING VALVE
BAFFLE VALVE
DIFFUSION PUMP
TO ROTARY PUMP
FORE-VACUUM VALVE
SOCKET TO HOLD PIRANI GAUGE HEAD
1
2
3
4
5
6
M_2
M_1
DISC
IMPREGNATOR HEATER
TRAP HEATER
T
(U-H^3 TRAP)
COOLING WATER OUTLET
GLASS-QUARTZ GRADED JOINT
MS 19 JOINT
B7 SOCKET
8mm
COOLING WATER INLET
8cm
3cm
9·5cm
10cm
39·5mm
41·5mm

FIG. 7.

FIG. 8.

EMISSION MÖSSBAUER SPECTROSCOPY IN Co^{57} DOPED TRISACETYLACETONE Mn(III)

K. S. Venkateswarlu and V. Ramshesh
Chemistry Division, Bhabha Atomic Research Centre
Trombay, Bombay-85

In 1965 the existence of isotopic exchange in the solid state was shown independently by Collins et al[1] for potassium chromate and by Amar Nath et al[2] for cobalt(III) complexes. This fact has been used by these authors and serveral others to interpret thermal annealing processes following radiative capture of neutrons in these solids. This work was extended by Ramshesh[3] to dilute dispersed systems, where it was shown that if cobalt (Co^{57} or Co^{58}) activity is dispersed on to $Mn(Ac\ Ac)_3$ in the solid state, the activity is found incorporated as $Co(Ac\ Ac)_3$. This clearly shows the existence of atom transfer processes in the solid state.

However, the method of analysis viz., dissolution and separation are destructuve in as much as the identity of species in solid state and in solution may not be the same. It was, therefore, decided to use Mössabauer technique to determine the exact nature of species formed during the exchange of Co^{57} with $Mn(Ac\ Ac)_3$.

EXPERIMENTAL

$Fe(Ac\ Ac)_3$ and $Mn(Ac\ Ac)_3$ were prepared and thoroughly purified by literature methods[4,5]. $Mn(Ac\ Ac)_3$ was doped with Co^{57} as described earlier[3]. A conventional cam drive set-up was used for taking Mössbauer spectra[6]. For low temperatures a glass cryostat with thin mylar windows was used. The gamma rays were counted using a thin NaI(Tl) crystal followed by conventional electronics.

RESULTS AND DISCUSSION

The spectrum of $Fe(Ac\ Ac)_3$ at -196°C against a Co^{57}(Cr) source was taken. A single line absorption curve with a chemical shift of 0.46 ± 0.05 mm/sec was obtained. The emission spectrum of Co^{57} doped $Mn(Ac\ Ac)_3$ (used as a source) at -196°C against an enriched $K_4\ Fe(CN)_6$ absorber at 25°C is shown in Fig. 1. This curve has been drawn as if the substance is used as the absorber. The curve consists of three peaks centred at 0.28 mm/sec, 0.9[illegible] mm/sec and 2.22 mm/sec (± 0.05 mm/sec)

respectively.

To convert this data to Co^{57}(Cr) source we must add 0.15 mm/sec and this gives us the values 0.43 mm/sec, 1.11 mm/sec and 2.37 mm/sec respectively. The identity of the first peak is now obvious and it corresponds to ferric acetylacetonate. Crystallographic data[7] shows that there is not much difference in the cell dimensions for metal-acetylacetonates of Co and Mn and in fact they are isomorphous. The formation of $Co^{57}(Ac\ Ac)_3$ is, thus, accounted for easily.

Wertheim et al[8] have studied the emission spectrum of $Co^{57}(Ac\ Ac)_3$ and our plot is similar to the one obtained by them. The values of chemical shifts are also almost identical (with due corrections for the different source temperatures). They have argued that the other two peaks correspond to the formation of Fe(II) resulting from the Auger ionization during the decay of Co^{57} to Fe^{57} followed by charge stabilization. They have based this conclusion on the fact that no ferrous complexes has so far shown an absorption at 2.37 mm/sec. Recently Herber[9] has interpreted these results on the so called 'pressure effect'. As the unit cell of $Co(Ac\ Ac)_3$ is more compact (density 1.42 g/cm^2) than that of $Fe(Ac\ Ac)_3$ (density 1.33 g/cm^2), the ferric complex as a substitutional impurity is accommodated in a strongly compressed lattice. This compression is comparable to that obtained in the pressure experiments on ferric complexes by Champion et al[10] who showed that under high pressure a Fe(III) complex gives a spectrum similar to the corresponding Fe(III) complex.

Irrespective of the mechanism for Fe(II) formation (either free or complex) there seems to be a preferential stabilization of Co^{57} as Co(III) acetylacetonate. We may, therefore, conclude that an atom transfer exchange takes place, possibly via an exciton mechanism. The dopant and a few molecules of $Mn(Ac\ Ac)_3$ surrounding it are collectively excited and Co^{57} exchanges with Mn of the complex in the excited state.

REFERENCES

1. C.H. Collins, K.E. Collins, Y.F. Ghoos and D.J. Apers; Radiochim. Acta. 4, 211 (1965)

2. A. Nath, S. Khorana, P.K. Mathur and S. Sarup; Ind, J. Chem. 4, 51 (1966)

3. V. Ramshesh; J. Inorg. Nucl. Chem. (In print)

4. R.C. Young; Inorganic Synthesis, Edited by John C. Bailar Jr., Vol. 3, p. 78

5. G.H. Cartledge; Chem. Abst. 46, 1585 (1962)

6. K.S. Venkateswarlu, P.K. Mathur and V. Ramshesh; Indian J. Chem. 7, 915 (1969)

7. Crystal Data Determination Tables, 2nd ed. American Crystallographic Association (1963)

8. G.K. Wertheim, W.R. Kingston and R.H. Herber; J. Chem. Phys. 37, 687 (1962)

9. Y. Hazony and R.H. Herber; J. Inorg. Nucl. Chem. 31, 321 (1969)

10. A.R. Champion, R.W. Vaughan and H.G. Drickamer; J. Chem. Phys. 47, 2583 (1967)

DISCUSSION

A. Chakravarty : You have invoked John-Teller effect in $Mn(acac)_3$. But the detailed crystal structure has been worked out and there is no evidence for J-T effect in the ground state.

K. S. Venkateswarlu : I have been speaking of the distortion of $Mn(ac\ ac)_3$ in its excited state and not in its ground state. John - Teller distortion in the excited state is most probable.

Fig.1

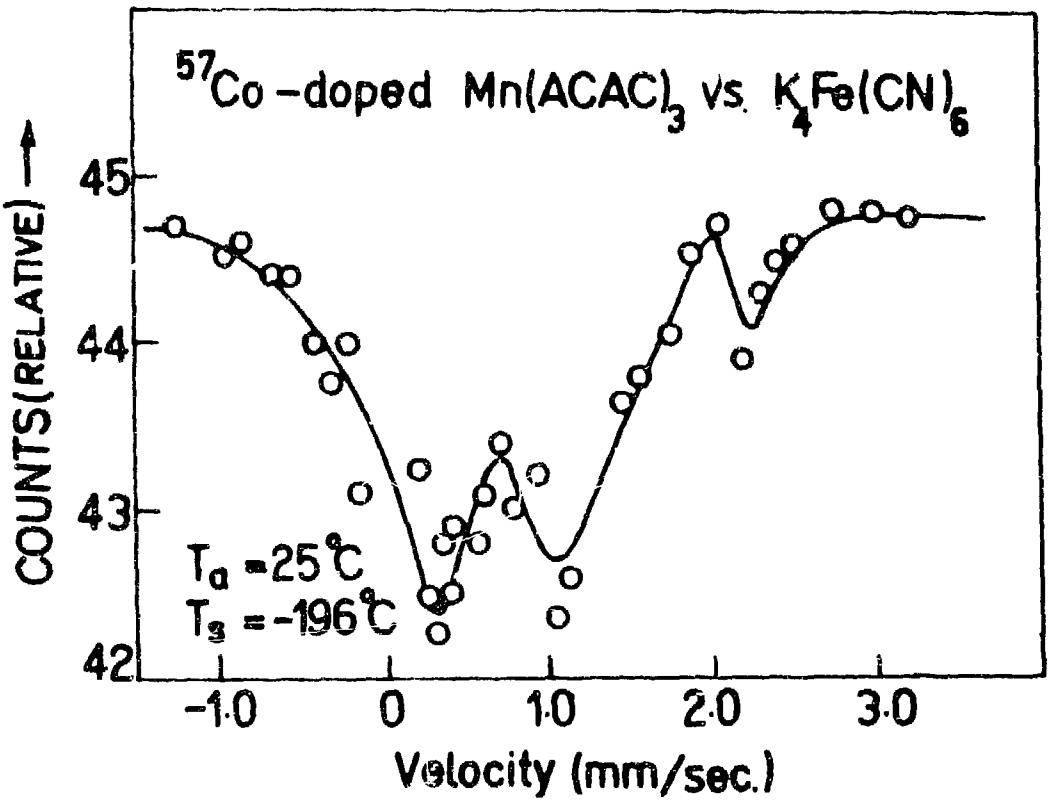
^{57}Co-doped Mn(ACAC)$_3$ vs. K$_4$Fe(CN)$_6$
COUNTS(RELATIVE)
45
44
43
42
T_a = 25°C
T_s = -196°C
-1.0
0
1.0
2.0
3.0
Velocity (mm/sec.)

THERMOLUMINESCENCE OF BARITE

N. M. Gupta and J. M. Luthra
Chemistry Division, Bhabha Atomic Research Centre, Bombay 85

INTRODUCTION

Barite has been reported to be a thermoluminescent material[1, 2], but very little work has been done on its thermoluminescent behaviour. Moore[3] and Medlin[4, 5] have found that glow curves of carbonates sulphates of calcium and barium are markedly affected by the impurities in the solution from which the material is precipitated. The present studies were carried out to find the role of different impurities in the thermoluminescent behaviour of $BaSO_4$. In the present communication we have described the thermoluminescence of $BaSO_4$ samples doped with Ag^+, Mn^{++}, Mg^{++}, Pb^{++}, Co^{++} and Zn^{++} prepared in oxygenated nitrogen atmosphere.

EXPERIMENTAL

(A) The thermoluminescence set-up was essentially the same as described in previous paper[6]. It was modified to achieve different linear heating rates, by introducing a 0-260 volts variac in the primary of the step-down transformer and driving it contineously with the help of a 2rpm motor and a set of suitable gears. Arrangement was made to take the glow curves in different gaseous ambients. A fixed amount of samples was taken for studies with the help of a powder dispenser which dispenses 1.2 mgms of powder with an accuracy of 3-4%.

(B) PREPARATION OF SAMPLES

The impurity doped samples were prepared by co-precipitating various concentrations (from 0.001 mole % to 1 mole %) of each impurity with a fixed amount of $BaSO_4$. The required amount of impurity was volumetrically added to weighed amount of $BaCl_2.2H_2O$ (From E. Merck. A.G., Darmstadt; Pro analysi purity) solution and then 5 cc of 50% H_2SO_4 (S. Merck) were added. The solution was thoroughly shaken and kept over a water-bath to drive off the water. The excess of sulphuric acid was removed by heating at 300 - 350°C. The samples were ground and fired for 2 hours at 900°C and then left in the furnace for slow cooling.

Different samples were prepared in oxygen contaminated nitrogen atmosphere. The powers were sieved through a 100 mesh Endecotts sieve to get the particle size of less than 150μ.

All samples were exposed to X-rays for 10 min from Raymax unit with Cu(K_α) tube operated at 30 kv and 9 ma. Glow curves were recorded after 5 to 10 min. of irradiation.

RESULTS

According to the spectrographic semi-quantitative analysis, the concentration of main impurities present in the natural barite sample used for these studies are Ca 200 ppm; Mn, Al, Fe and Ni 10 ppm; Pb, Ag, Cu, Bi & Sn less than 10 ppm and Sm & Ce less than 50 ppm. Natural barite gives a glow peak at 370°C; however when studied in nitrogen atmosphere, its intensity is considerably reduced. X-ray irradiation induces peaks at 80 - 100°, 175° and 210°C in natural barite [Fig. 1]. Low temperature peak decays at room temperature within four days of irradiation. The position of this peak shifts to high temperature side with increasing dose and energy of radiations, suggesting that it is not due to single energy traps. Pre-irradiation annealing at 400°C for 2 hours increases the intensity of this peak by a factor of one and a half while the other peaks are not much affected. The intensity of all the peaks increases with the dose. However, no definite dose-intensity relation could be established. Ratio of intensity of 175° and 210°C peaks increases continuously with the dose of radiation. Peaks at 110 - 115° and 170 - 175°C are observed in the sample in which no additional impurity was added (named as undoped sample) and are present in all the impurity doped samples also with increased intensity. Mn^{++} induced two peaks at 80° and 225° and two other common peaks [Fig. 2]. In Ag^+ doped samples these new peaks are observed at 70° and 230°C [Fig. 3]. With no other impurity studied so far, these peaks were observed. In the case of $BaSO_4(Mn^{++})$, the intensity of glow peaks increases suddenly when concentration of Mn^{++} is more than 100 ppm and increases upto 10000 ppm concentration. With Ag^+ as dopant, the peak intensities are maximum when concentration is 10 ppm, it reduces suddenly when concentration is increased to 100 ppm and then on further increase of concentration the intensity again increases. In glow curves of Pb^{++} and Mg^{++} doped samples the area of 115°C peak is proportional to the logarithm of dopant ion concentration. Glow curves of Pb^{++} doped sample is shown in Fig. 4. Out of all the samples, the intensities of 115°C and 170°C peaks are maximum in Pb^{++} doped samples for the same dose of radiations. In $BaSO_4(Zn^{++})$ samples slight increase in intensity is observed when the concentration of Zn^{++} is more than 1000 ppm. In Co^{++} doped samples, the peak intensity increases when the concentration is 100 ppm and with higher concentration than this, quenching takes place [Fig. 5].

The appearance of low temperature peak at 80° and 70°C and another peak at 230°C in Mn^{++} and Ag^+ doped samples suggests that these two impurities could probably be responsible for thermoluminescence of natural barite, since no other impurity studied so far

introduces these peaks observed in glow curve of natural barite also. The 115°C peak observed in synthetic samples and in undoped sample might be due to some unidentified impurities which are not present in natural barite or otherwise their effect is quenched by the presence of small amount of Ni or Fe. Any definite conclusions regarding role of impurities could be drawn when the study of effect of other impurities is completed.

REFERENCES

1. James D. Dana; System of Mineralogy Vol. II(Seventh revised edition), John Willy & Sons In., N. Y., pp 410

2. Jan Kantor; Geol. Sbornik (Bratislava) 17(1), 35 - 49 (1966)

3. Louise E. Moore; J. Phys. Chem. 61, 636-677 (1957)

4. W. L. Medlin; J. Chem. Phys. 34(II), 672-677 (1961)

5. W. L. Medlin; J. Opt. Soc. Am. 53(II), 1276-85 (1963)

6. J. M. Luthra and N. M. Gupta; Ind. J. Pure & Appl. Phys. 7(4), 287-88, (1969)

DISCUSSIONS

P. S. Goel : Did you see a sample without adding any external impurity ?

N. M. Gupta : Yes.

B. M. Shukla : Only in the case of Co, you mention
(a) that it has a quenching effect at a concentrations above 100 ppm. Could you think of the possible reason for this ?

(b) Based on your answer to (a), may I suggest that one of the important contributions from your work could be a detailed study of the conditions responsible for the quenching effect.

N. M. Gupta : (a) This is what is known as 'concentration quenching' effect which is the decrease in efficiency when the concentration of the 'activator' centre (generally an impurity) increases to a sufficiently high value. We cannot say at this moment why only cobalt shows the 'concentration quenching effect'. It may be possible that 100 p. p. m. concentration in the case of cobalt is threshold for its effect while in other we might have not reached that concentration.

(b) Yes. I agree with your suggestion

LEGENDS

Fig. 1 Glow curves for natural barite samples exposed to different doses of X-rays

Fig. 2 Glow curves for synthetic barite samples containing different concentration of Mn^{++}

Fig. 3 Glow curves for synthetic barite samples containing different concentration of Ag^{+}

Fig. 4 Glow curves for synthetic barite samples containing different concentrations of Pb^{++}

Fig. 5 Glow curves for synthetic barite samples containing different concentrations of Co^{++}

FIG. 1.

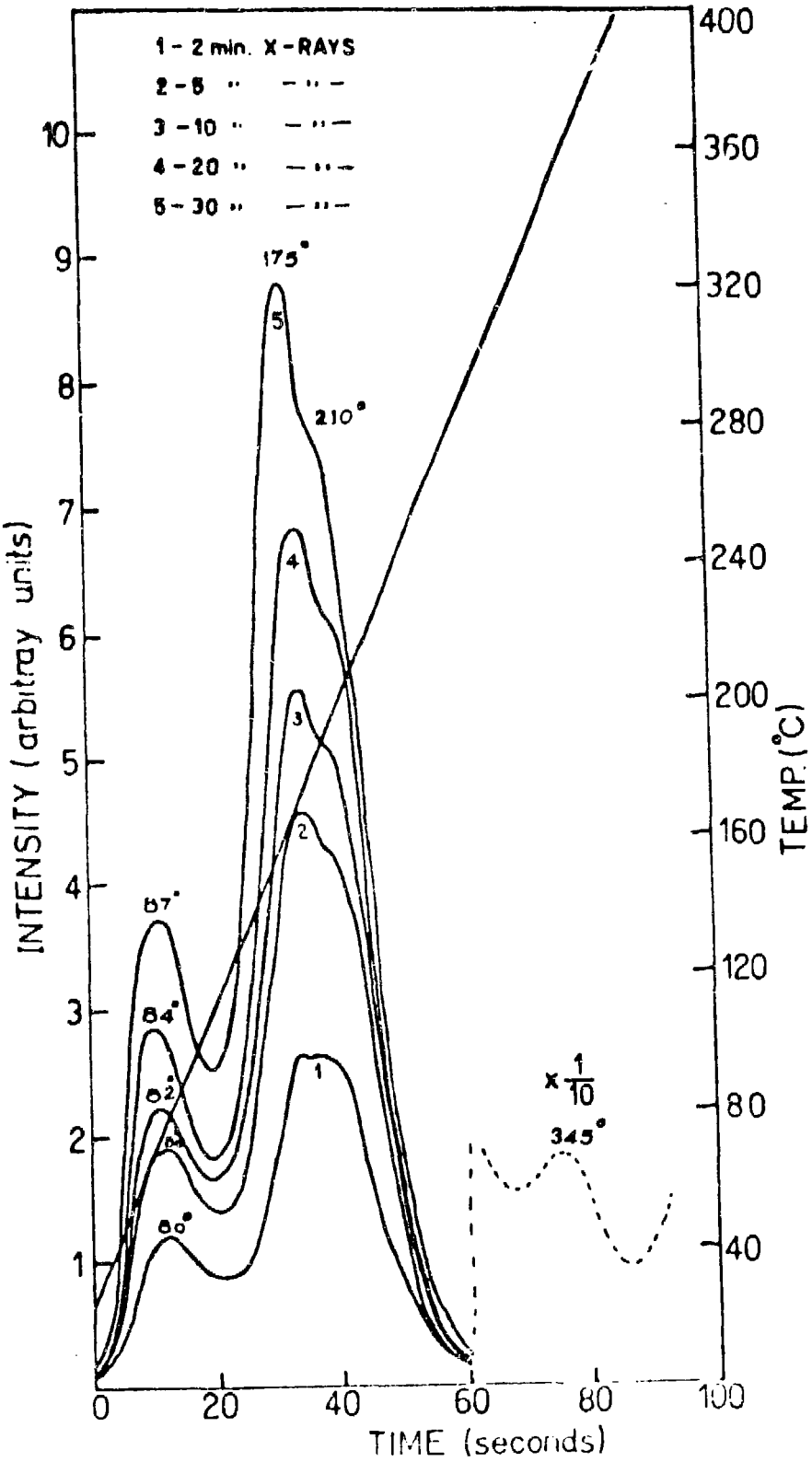
1 - 2 min. X-RAYS
2 - 5 " - " -
3 - 10 " - " -
4 - 20 " - " -
5 - 30 " - " -
175°
210°
87°
84°
82°
80°
345°
x 1/10
INTENSITY (arbitray units)
TEMP.(°C)
TIME (seconds)
0
20
40
60
80
100
1
2
3
4
5
6
7
8
9
10
40
80
120
160
200
240
280
320
360
400

FIG 2.

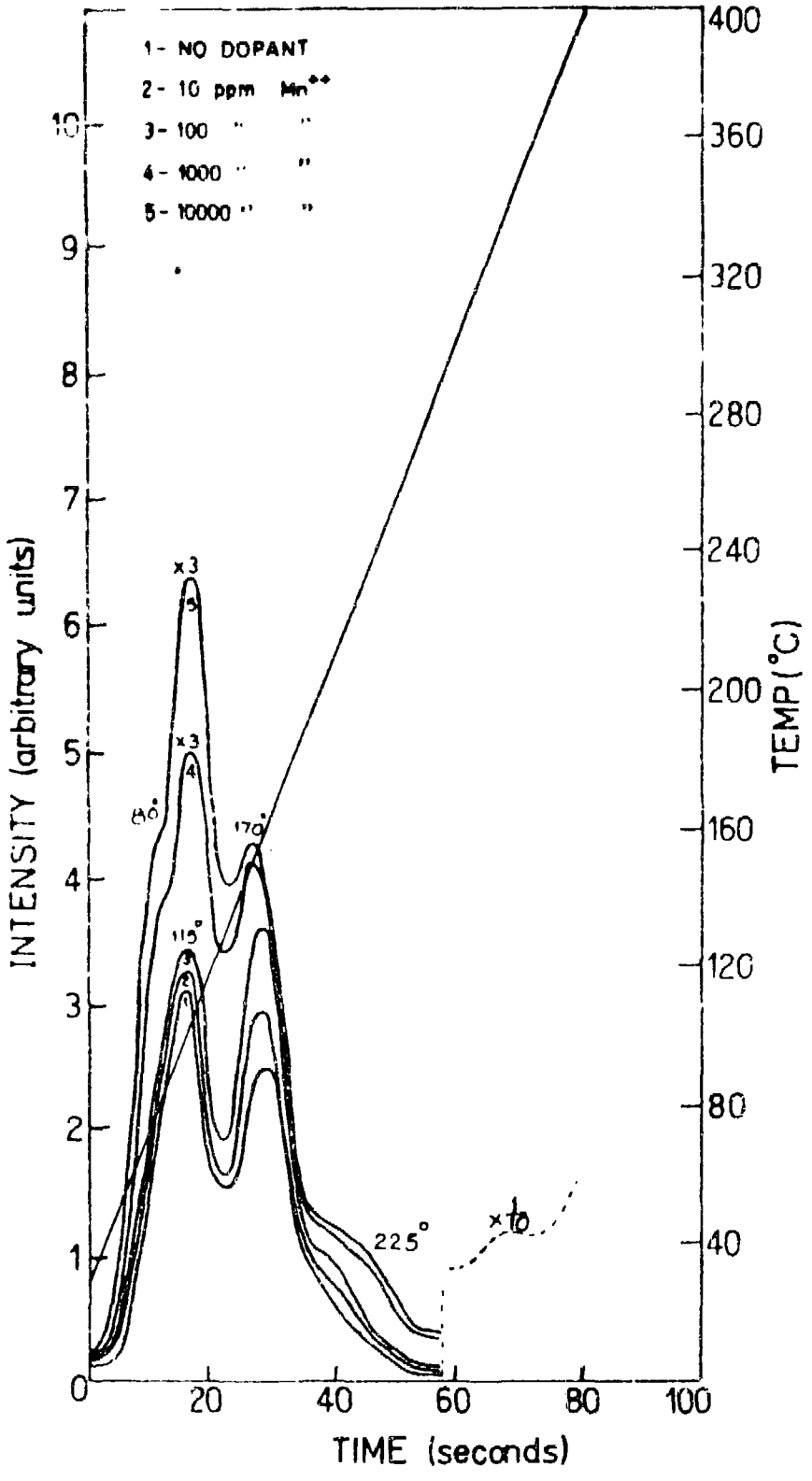
1- NO DOPANT
2- 10 ppm Mn++
3- 100 " "
4- 1000 " "
5- 10000 " "
INTENSITY (arbitrary units)
TEMP(°C)
TIME (seconds)
x3
x3
86°
170°
115°
225°
x10
0
1
2
3
4
5
6
7
8
9
10
20
40
60
80
100
40
80
120
160
200
240
280
320
360
400

FIG. 3.

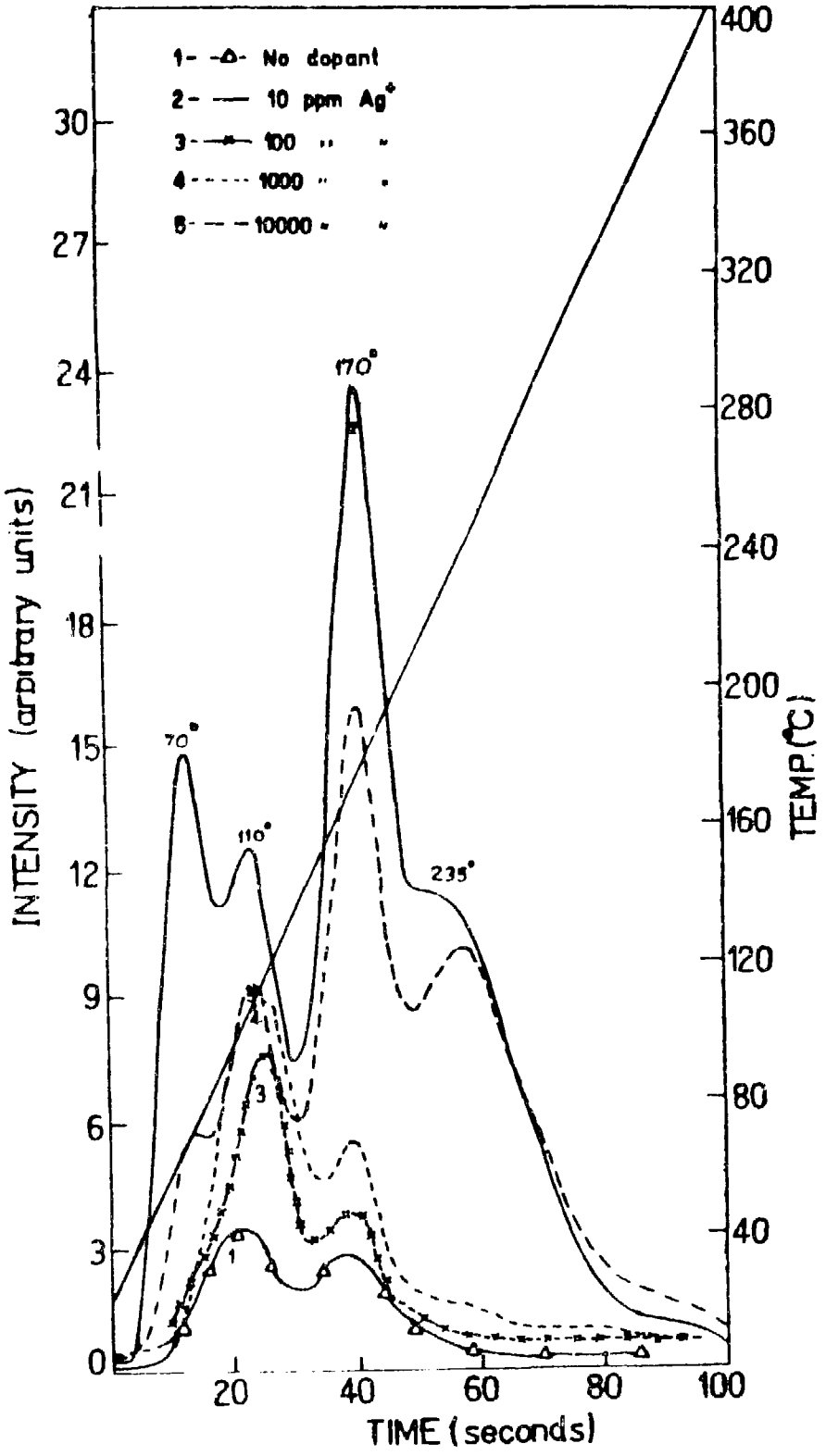
1- -Δ- No dopant
2- — 10 ppm Ag+
3- —×— 100 " "
4- ····· 1000 " "
5- — — 10000 " "
INTENSITY (arbitary units)
TEMP.(°C)
TIME (seconds)
70°
110°
170°
235°
0
3
6
9
12
15
18
21
24
27
30
40
80
120
160
200
240
280
320
360
400
20
40
60
80
100

FIG. 4.

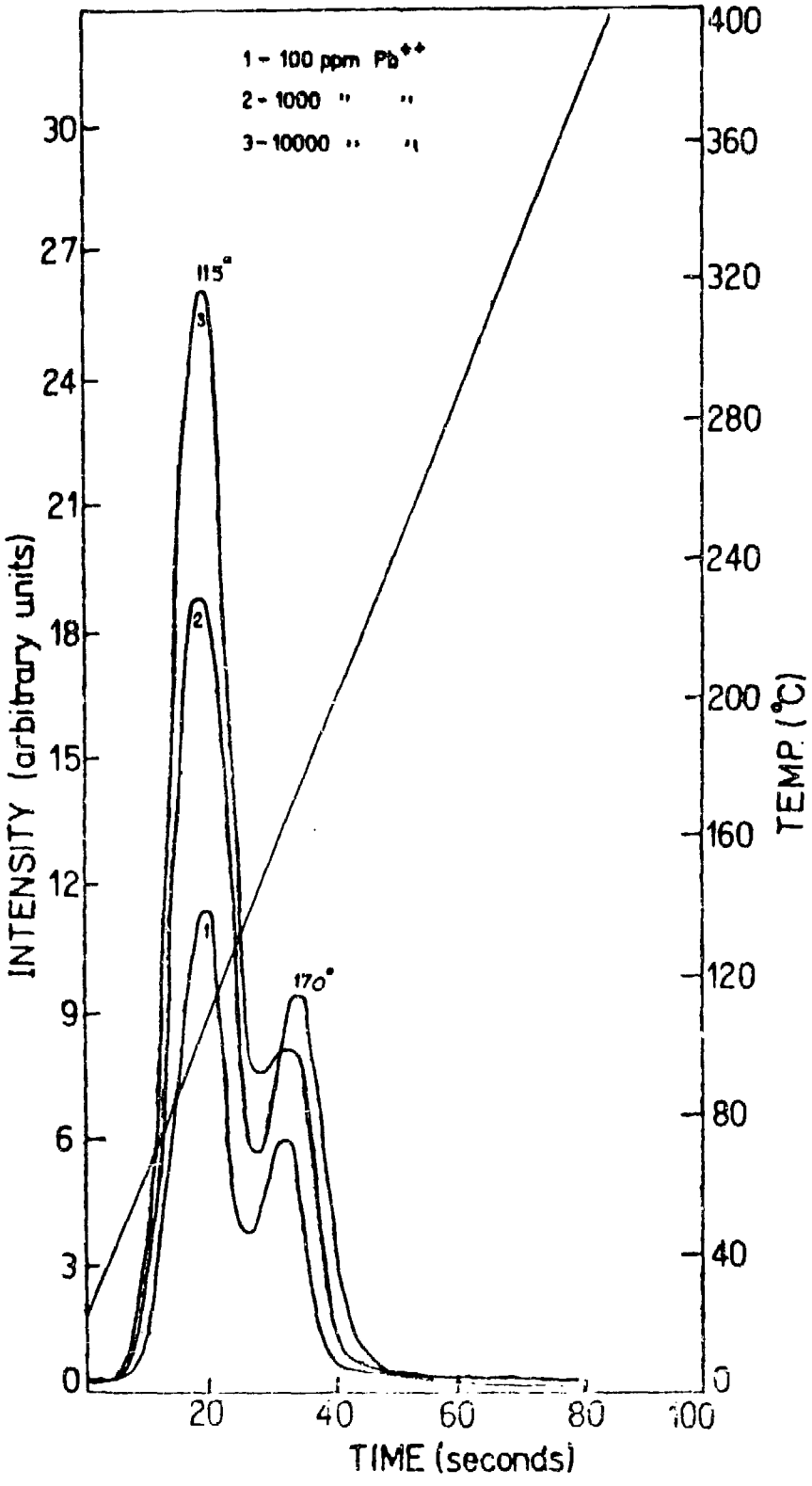
1 - 100 ppm Pb++
2 - 1000 " "
3 - 10000 " "
115°
170°
INTENSITY (arbitrary units)
TEMP. (°C)
TIME (seconds)
0
3
6
9
12
15
18
21
24
27
30
40
80
120
160
200
240
280
320
360
400
20
40
60
80
100

FIG. 5

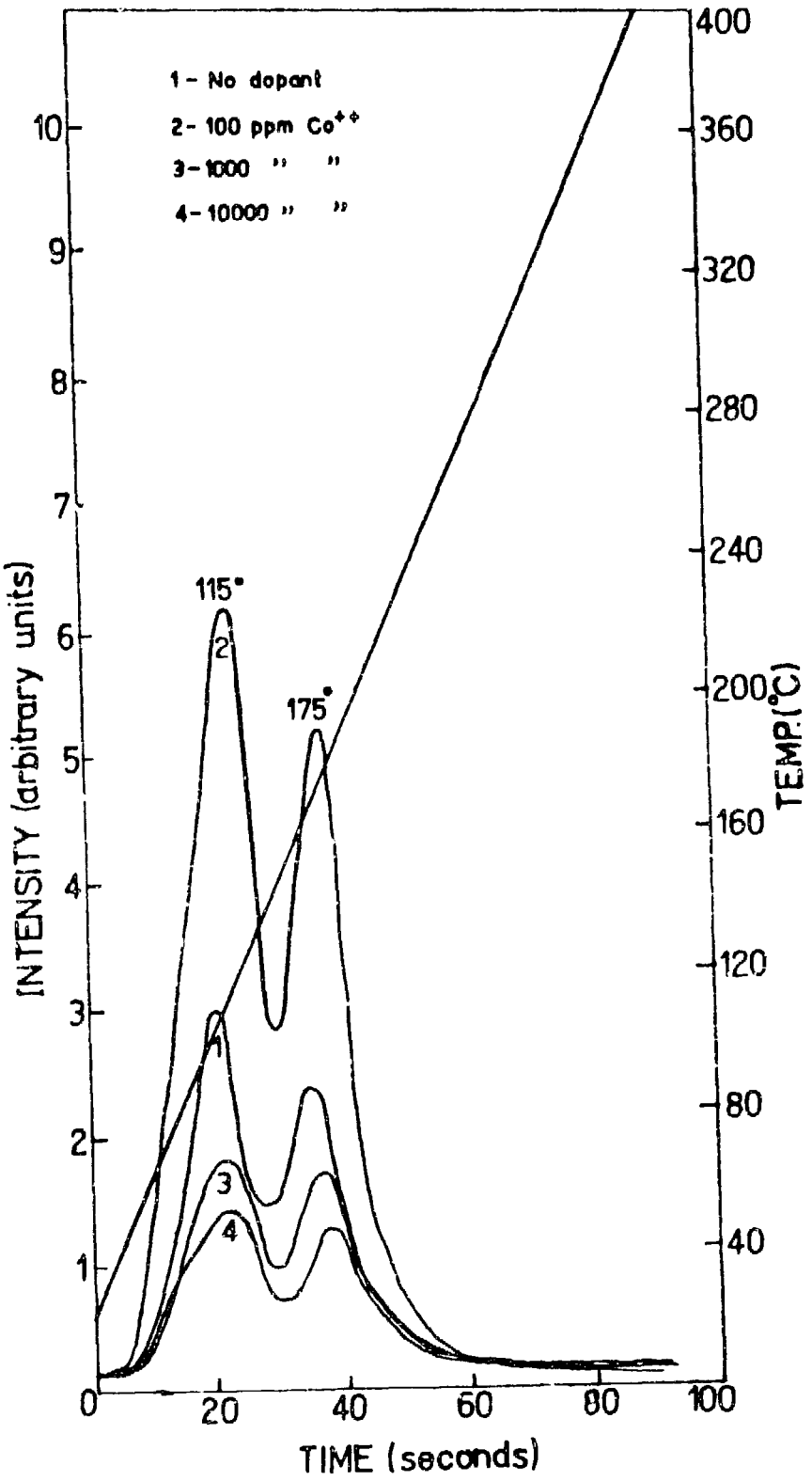
1 - No dopant
2 - 100 ppm Co++
3 - 1000 " "
4 - 10000 " "
115°
175°
INTENSITY (arbitrary units)
TEMP.(°C)
TIME (seconds)
0
20
40
60
80
100
1
2
3
4
5
6
7
8
9
10
40
80
120
160
200
240
280
320
360
400

THE EFFECT OF ELECTRIC FIELD AND IRRADIATION ON THE TRACER DIFFUSION OF ALKALI EARTH IONS THROUGH CALCITE

H. J. Arnikar and B. D. Chaure
Department of Chemistry, University of Poona, Poona-7

INTRODUCTION

It is well established that the defects produced by irradiation may lead to the enhanced diffusion, which is not conclusive always, as irradiation may anneal some pre-existing defects, leading to a decrease in the diffusion rates.[1] These defects may disappear on heating by mutual recombination. In many systems[2, 3] it has been observed that diffusion constant is unaffected by an external electric field. The present study deals with the effect of irradiation and external electric field on diffusion.

EXPERIMENTAL

The tracer technique used here is similar to the one employed by Arnikar and Chemla.[4] The single crystals (spar) were cleaved into rectangular blocks. The isotope layer was sandwitched between two crystals and was kept between two electrodes. Applying a d. c. potential the system was heated at 300°C. After desired time, the samples were sectioned (10 microns) with the microtome and activity was measured with a end window G. M. Counter.

RESULTS AND DISCUSSION

From Table I, it is seen that $D_{Ca} > D_{Sr} > D_{Ba}$ i. e. the diffusion constant decreases with increase in the ionic size. The D-values through irradiated samples show decreasing trend as, during irradiation some interstitial atoms may be deprived of electrons, thus becoming temporarily unstable. This will lose its energy colliding with the neighbours resulting in a localised high temperature region. This thermal spike forces the material to expand into surrounding regions of low thermal stress and can be balanced by self-stress, thus resulting in a loop. As the spike cools, the stress system dies out and the loop contracts again which may be greater than lattice spacing, leading to a decrease in D-values. The unequal expansion coefficients may also be operating simultaneously.[5]

TABLE I

EFFECT OF γ-IRRADIATION ON THE TRACER DIFFUSION OF ALKALI EARTH IONS INTO SINGLE CRYSTALS OF CALCITE AT 300°C

D values in units of 10^{-11} cm^2. sec^{-1}

Ion diffusing	Unirradiated calcite	Irradiated calcite dose: 2.3 M. rads.	Irradiated calcite after annealing
$^{45}Ca^{++}$	4.9	4.0	5.0
$^{90}Sr^{++}$	2.6	2.1	2.5
$^{133}Ba^{++}$	1.1	0.8	0.9

TABLE II

Effect of an electric field

Field applied volts/cm.	D_1, in the field direction	D_2, against the field direction
i Diffusion of $^{45}Ca^{++}$, D without field 4.9		
27	5.5	5.0
40	5.6	4.9
60	5.8	5.0
100	6.3	5.1
ii Diffusion of $^{90}Sr^{++}$, D without field = 2.6		
27	2.9	2.6
40	3.2	2.7
60	3.3	2.7
100	3.6	2.8
iii Diffusion of $^{133}Ba^{++}$, D without field = 1.1		
27	1.6	1.2
40	1.7	1.0
60	1.8	1.1
100	2.0	1.2

D-values, through bleached samples, approach to original values. So it appears that the point defects are destroyed by heat treatment i. e. while bleaching the interstitials move to it's original or near by positions by absorbing the thermal energy, still some of the strain centres remains unbleached.[6]

The results of electro-diffusion (Table II) in and against the field differ (about 10%). The non-Gaussian distribution showed a slight shifting of a scew maximum in the field direction and two D-values are indicated by unequal slopes of the plot of log C versus x^2 which are in marked contrast with those of Redington[7] and Chemla[3] as in their cases D-values are unaffected by an external electric field. In fused salts of nitrates and agar-agar gel media, Arnikar et al[8] had observed $D_2 > D_1$, assigning it as a field induced asymmetry due to unequal charge distribution and relaxation effects. On the basis of Manning's[9] interpretation, it appears that the jump probabilities are disturbed due to external electric field i. e. more in the field direction which were euqal in the absence of the field. The potential energy curve also gets displaced with a non-zero slope. The external electric field may also act as a driving force on each diffusing ion increasing it's drift in the field direction.

This simple interpretation of results on diffusion in crystals where the "ion atmosphere" of oppositely charged ions is rigidly held by lattice forces cannot hold good for ionic diffusion in an electric field - in aqueous media. Here the ion atmosphere retards movement of ion in the field direction as in the well-known relaxation effect in ionic conduction in aqueous solutions. This explains the reverse asymmetry observed by Arnikar et al.

REFERENCES

1. R. D. Johnson and A. B. Martin; J. Appl. Phys. 23, 1245 (1952)
2. R. J. Friauf; J. Appl. Phys. Suppl. 33, 494 (1962)
3. M. Chemla; Ann. Phys. 13 (1) 959 (1956)
4. H. J. Arnikar and M. Chemla; Compt. Rend. 242, 2132 (1956)
5. D. Mapother; J. Chem. Phys. 18, 1231 (1950)
6. R. S. Barnes; Discus. Far. Soc. 31, 38 (1961)
7. R. W. Redington; Phys. Rev. 87, 1066 (1952)
8. i) H. J. Arnikar and R. Tripathi; Ind. J. Chem. 4 (1) (1966);
   ii) H. J. Arnikar and D. K. Sharma; Nature 194, 271 (1962)
9. J. R. Manning; Phys. Rev. 116, 69, 819 (1959); 136, A1413 (1964); 124, 470 (1961)

DISCUSSION

P. K. Bhattacharya : i) How you measure the activity in different lengths of the crystal ?

ii) Are you evacuating the furnace while heating ?

iii) Are you correlating the diffusion with crystal defects ?

H. J. Arnikar : i) Sections of 10 microns in the form of a powder were collected in aluminium planchets and activity of each section was measured with end-window type G. M. counter.

ii) It is not necessary to evacuate the furnace, so the samples were heated in air atmosphere only.

iii) The correlation is only qualitative i. e. if the crystal contains more defects one should expect more diffusion. We have not calculated the defects quantitatively.

FIG. 1

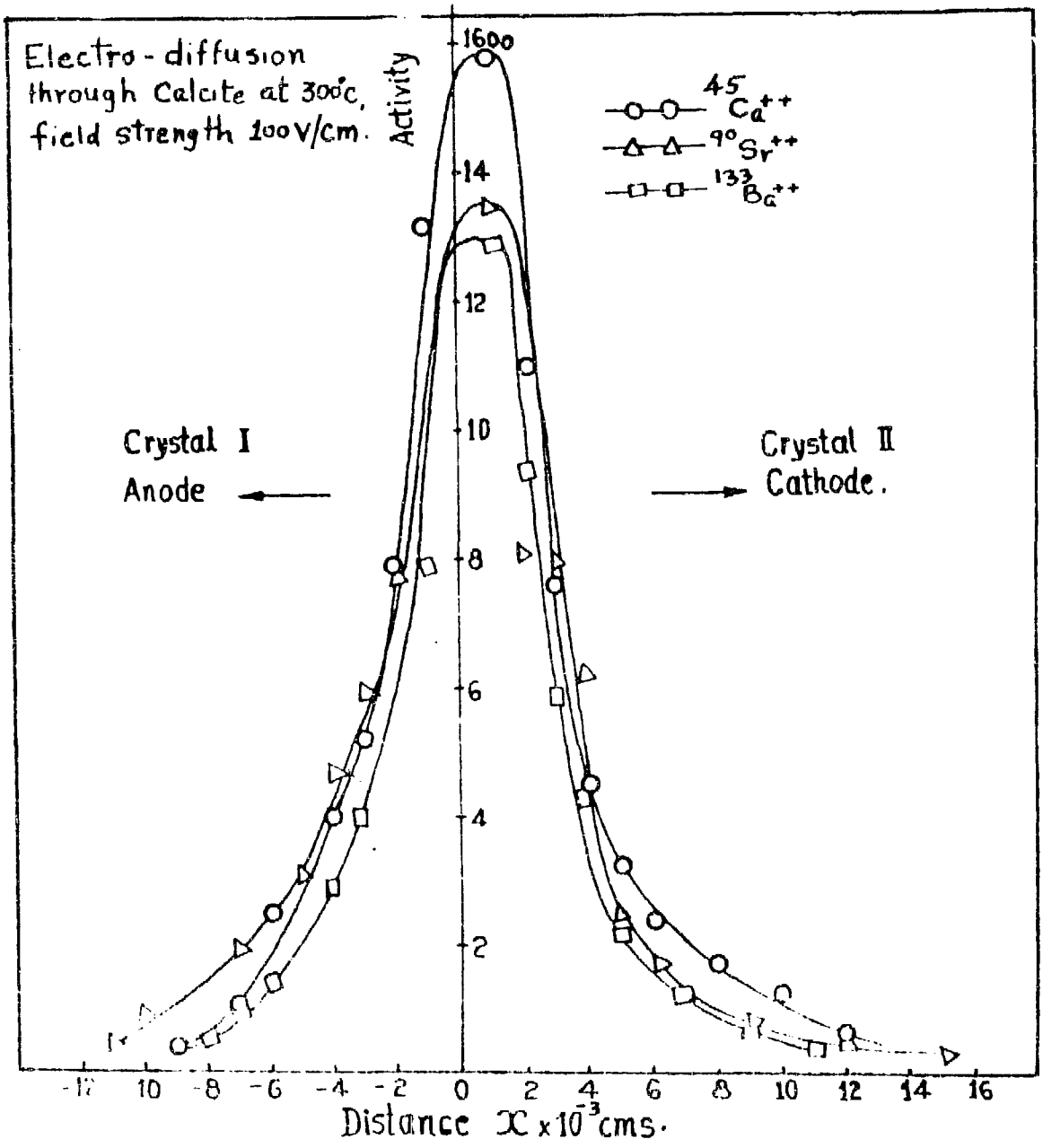
Electro-diffusion through Calcite at 300°C, field strength 100 V/cm.
Activity
1600
14
12
10
8
6
4
2
45 Ca++
90 Sr++
133 Ba++
Crystal I
Anode
Crystal II
Cathode.
-12 10 -8 -6 -4 -2 0 2 4 6 8 10 12 14 16
Distance x x10⁻³ cms.

FIG. 2

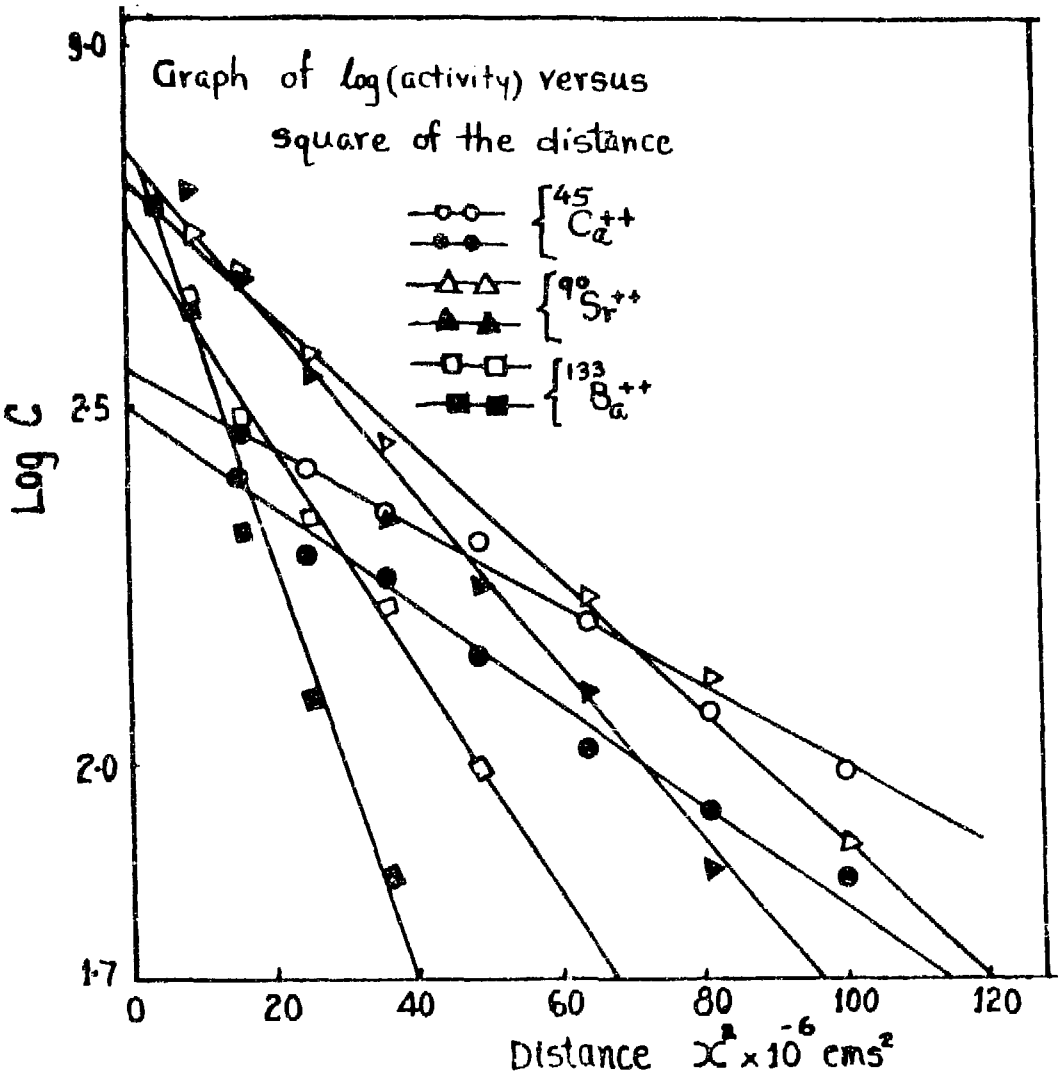
Graph of log(activity) versus
square of the distance
45 Ca++
90 Sr++
133 Ba++
Log C
3·0
2·5
2·0
1·7
0
20
40
60
80
100
120
Distance x² x 10⁻⁶ cms²

SELF-DIFFUSION OF $H_2PO_4^-$ AND SO_4^{-2} IONS IN 2.5 % AGAR GEL AT 35°C

R. Tripathi
Nuclear and Physical Chemistry Laboratory
Banaras Hindu University

INTRODUCTION

For the study of diffusion mainly capillary[1,2] and porous diaphragm[3-6] methods under the boundary conditions of 'front' diffusion have been employed by earlier workers. Agar-agar gel by immobilizing the diffusion medium in a three dimensional gel net-work[7] of semi-rigid form seems to provide and ideal stationary phase for studying self-diffusion by Fick's[8] II Law. Slade[9], Felicetta et al[10], Lauffer[11], Marignan[12] and others have used gels to study the self-diffusion of ions where diffusion proceeded from solution to gel. Here we report the results on the self-diffusion of $H_2PO_4^-$ and SO_4^{-2} ions at various molar concentrations of Na_2HPO_4 and $(NH_4)_2\ SO_4$ respectively, the solution being immobilized in 2.5 % agar gel. The effects of concentration variation of the supporting electrolytes and that of gel net-work on the coefficient of self-diffusion of these ions are discussed.

EXPERIMENTAL

2.5 % agar gel containing Na_2HPO_4 (3.33×10^{-6} to 0.1666 M) and $(NH_4)_2\ SO_4$ (10^{-6} to 1.0 M) solutions was allowed to set in 30 cm long Pyrex tubes of 1.0 cm diameter. A thin 'zone' (0.1 cm) containing either the labelled $H_2\ ^{32}PO_4^-$ or $^{35}SO_4^{-2}$ ions was deposited at the middle of the gel column having the respective electrolyte solution and the tube was thermostated at 35°C. At the end of 24 hours, the tube was taken out and the gel column was carefully sliced into 0.5 cm samples. These samples were accurately weighed and determined their exact lengths by comparing their weights with 10.0 cm long gel column of identical dimensions and composition. Radioactivity (a) in each of the dried samples was measured by an end-window G. M. counter. A plot of radioactivity (a) vs distance from the origin (x) gives a symmetric Gaussian distribution fitting to the Fick's II law integral,

$$a_{(x,t)} = \frac{a_o}{\sqrt{4\pi Dt}}\, e^{-x^2/4Dt} \qquad \ldots(1)$$

under the conditions of the experiment. The typical plots of the distribution of radioactivity in the self-diffusion of $H_2PO_4^-$ and SO_4^{-2} ions are given in Fig. 1.

From the slope of the plots (log a) vs x^2 self-diffusion coefficients of $H_2PO_4^-$ and SO_4^{-2} ions in aqueous Na_2HPO_4 and $(NH_4)_2\ SO_4$ are calculated at the concentrations studied. The slope is given by the following equation,

$$\text{slope} = \frac{1}{2.303 \times 4\ Dt} \qquad \ldots(2)$$

where D is the coefficient of self-diffusion and 't' the period of diffusion. Fig. 2 represents the plots of (log a) vs x^2 for Fig. 1.

RESULTS AND DISCUSSION

Self-diffusion coefficients of tracer amounts of $H_2{}^{32}PO_4^-$ and $^{35}SO_4^{-2}$ ions in purely aqueous gel (containing no electrolyte) are 1.28×10^{-5} and 1.33×10^{-5} $cm^2\ sec^{-1}$ respectively but in the concentration ranges 5.00×10^{-6} to 6.25×10^{-5}M Na_2HPO_4 and 5×10^{-6} to 5×10^{-5} M $(NH_4)_2\ SO_4$ solutions in gel phase, the observed coefficients of self-diffusions for both the ions are higher than the corresponding theoretical values (Tables I and II). The theoretical values of diffusion coefficients of these ions were calculated from Gosting's[13] equation obtained from Onsager-Fuoss[14, 15] theory,

$$D = \frac{RT\lambda_j^\circ}{|z_j|F^2} - \frac{\lambda_j^\circ |z_j| F}{3N\pi\eta} \times 2.694 \times 10^{16} \sqrt{\frac{4\pi}{\varepsilon_f RT}} \left[1 - \sqrt{d(w_j)}\right] \times \sqrt{\sum c_i z_i^2} \qquad \ldots(3)$$

$$d(w_j) = \frac{1}{\sum c_i z_i^2} \sum \frac{c_i |z_i| \lambda_i^\circ}{\frac{\lambda_j^\circ}{|z_j|} + \frac{\lambda_i^\circ}{|z_i|}} \qquad \ldots(4)$$

The symbols in these equations have their usual significance and on substituting the values of these terms, equation (3) reduces to

$$D = 1.10 \times 10^{-5} - 2.849 \times 10^{-6} \sqrt{c}$$

and $$D = 1.320 \times 10^{-5} - 9.13 \times 10^{-6} \sqrt{c}$$

for $H_2PO_4^-$ and SO_4^{-2} ions respectively. A comparision of the theoretical and experimental diffusion coefficients of $H_2PO_4^-$ and SO_4^{-2} ions over the concentration ranges 6.66×10^{-5} to 6.66×10^{-3}M Na_2HPO_4 and 6.25×10^{-5} to 10^{-3} M $(NH_4)_2\ SO_4$ solutions, shows a quantitative agreement (Tables III and IV, Fig. 3 and 4). It is clearly seen from Tables I and II that at relatively low concentrations, self-diffusion coefficients increase with it contrary to Onsager-Fuoss $\sqrt{c}$ law and also to the results of Slade[9] and Lauffer[11] who showed a definite obstruction

effect of the gel on diffusion rates whereas Felicetta[10] reported an absence of gel effect on the diffusion of even bigger dye molecules in agar gel.

Agar-agar gel is a polysaccharide carrying polar sulphonyl group in its molecules. It immobilies[16, 17] more than 55 % of water in its network by H-bonding, sorption, adsorption and dipole - dipole interaction. This is called 'bound' water and the remaining 'free' water is mechanically held up. This loose gel-water structure at different concentrations of the supporting electrolytes is melted to different extents and the states of varying magnitudes of distorted structure of lower viscosity are obtained with increasing concentrations of these electrolytes at least in this range. This clearly shows that the gel structure enhances the diffusion rate contrary to the results of earlier workers. The partial desolvation effect of the gel is inappreciable in these cases.

The above envisaged gel-water structure is completely melted at relatively higher concentrations of Na_2HPO_4 and $(NH_4)_2\ SO_4$ and the diffusion medium, in both the cases, returns to normal state. This is confirmed by the quantitative agreement between the theoretical and experimental diffusion coefficients of $H_2PO_4^-$ and SO_4^{2-} ions (Tables III and IV; Figs. 3 and 4).

At concentrations higher than 6.66×10^{-2} M of Na_2HPO_4 and 10^{-3} M of $(NH_4)_2\ SO_4$ solutions, the observed self-diffusion coefficients are higher than the respective theoretical values. The self-diffusion of $H_2PO_4^-$ ions could not be studied beyond 1.66×10^{-1} M of Na_2HPO_4 because the gel starts degelling and similarly for $(NH_4)_2\ SO_4$ the maximum permissible concentration in the gel is found to be 1.0 M. The plots of D vs $\sqrt{c}$ for both the ions show the validity of Onsager-Fuoss equation at dilute concentrations of the supporting electrolytes and at moderate concentrations a clear divergence from the theory is noticed. In both the cases D vs $\sqrt{c}$ plots show a rise at higher concentrations. The hump in D vs $\sqrt{c}$ plot (Fig. 4) of SO_4^{2-} ions is similar to the effects of concentrations on the self-diffusion of Na^+ in NaCl reported by Wang and coworkers[18, 19] and K^+ in KI by Mills[18], using capillary method and was found absent in self-diffusion of Rb^+ in RbCl[20, 21]. Diaphragm method showed an absence of this hump in D vs $\sqrt{c}$ plot for Na^+ and Cl^- ions in NaCl[18, 19]. Mills and co-workers attributed this to be the characteristic of the capillary method. Present data on the self-diffusion of SO_4^{2-} in $(NH_4)_2\ SO_4$ solutions of various concentrations by a different experimental technique show that the 'hump' is the characteristic of the ionic properties rather than the experimental errors as suggested by Mills. In concentrated solutions, microscopic 'ice-berge' structure due to water dipole interaction is destroyed by the intense ionic fields and also the solvent molecules are dielectrically saturated at about 2.0 N electrolyte solutions. This decreases the viscosity of the solutions and

by decreasing the dielectric constant of the medium, increases the self-energy of the ions. These two effects due to the increase in ionic concentrations enhance self-diffusion where as ion-atmosphere relaxation force ($\propto \sqrt{c}$) always retards it. From the plot D vs $\sqrt{c}$, it is obvious that in the concentration ranges 6.66×10^{-2} to 1.66×10^{-1} M Na_2HPO_4 and 10^{-3} to 10^{-1} M $(NH_4)_2$-SO_4 the acceleration effects increase more rapidly than the retardation. This satisfactorily explains the rise in the diffusion rates of these ions at moderately higher concentrations of electrolytes. But with further increase in the ionic concentration, relaxation force seems to dominate the retardation as is indicated by the fall of diffusion rates of SO_4^{-2} beyond 0.1 M $(NH_4)_2$ SO_4. This implies that the changes in dielectric constant and water structure reaches either a saturation value or are comparatively smaller than the retarding forces. This provides a qualitative explanation of the 'hump' in the concentration dependence of coefficient of self-diffusion of SO_4^{-2} ions at relatively higher concentrations.

However, the effects of concentration variation on the self-diffusion coefficients of ions in concentrated solutions are very complicated and far from clear. Moreover there is no theory which takes into account the changes in dielectric constant and viscosity of the medium at higher molar concentrations. A correction for ion size parameter 'a' and viscosity of the medium was made by Stokes et al[22] and Mills[20] in the self-diffusion of I^- ions in alkali metals iodides and chlorides, and this resulted in satisfactory agreement with the theoretical values at high concentrations of the electrolytes.

TABLE I

Self-diffusion of $H_2PO_4^-$ Ions in 2.5 % Agar-agar Gel with and without a Trace of Supporting Electrolyte

Diffusion medium agar-agar gel (2.5%) containing Na_2HPO_4	D x $10^5 cm^2 sec^{-1}$ Experimental	D x $10^5 cm^2 sec^{-1}$ Theoretical
nil	1.28	-
3.33×10^{-6}M	1.43	1.099
6.66×10^{-6}M	1.40	1.099
3.33×10^{-5}M	1.23	1.098
6.66×10^{-5}M	1.11	1.097

TABLE II

Self-diffusion of SO_4^{-2} Ions in 2.5 % Agar-agar Gel with and without a Trace of Supporting Electrolyte

Diffusion medium agar-agar gel (2.5%) containing $(NH_4)_2SO_4$	D x $10^5 cm^2 sec^{-1}$ Experimental	D x $10^5 cm^2 sec^{-1}$ Theoretical
nil	1.33	-
5.00×10^{-6}M	1.48	1.318
5.00×10^{-5}M	1.51	1.314
6.25×10^{-5}M	1.30	1.313

TABLE III

Concentration-dependence of Self-diffusion Coefficients of $H_2PO_4^-$ Ions in Na_2HPO_4 Solutions Immobilized in 2.5 % Agar-agar Gel at 35°C by 'Zone' Diffusion

Concentration moles/litre Na_2HPO_4	D x 10^5 cm^2 sec^{-1} Experimental	D x 10^5 cm^2 sec^{-1} Theoretical
nil	1.28	-
3.33×10^{-6}	1.43	1.099
6.66×10^{-6}	1.40	1.099
3.33×10^{-5}	1.23	1.098
6.66×10^{-5}	1.10	1.097
3.33×10^{-4}	1.09	1.095
6.66×10^{-4}	1.08	1.093
3.33×10^{-3}	1.06	1.083
6.66×10^{-3}	1.08	1.074
3.33×10^{-2}	1.03	1.048
6.66×10^{-2}	1.05	1.026
1.66×10^{-1}	1.14	-

TABLE IV

Concentration-dependence of self-diffusion Coefficients of SO_4^{-2} Ions in $(NH_4)_2SO_4$ Solution Immobilized in 2.5 % Agar-agar Gel at 35°C by 'Zone' Diffusion

Concentration moles/litre $(NH_4)_2SO_4$	D x 10^5 cm^2 sec^{-1} Experimental	D x 10^5 cm^2 sec^{-1} Theoretical
nil	1.33	-
6.25×10^{-5}	1.30	1.313
3.40×10^{-4}	1.28	1.304
1.00×10^{-3}	1.29	1.291
1.25×10^{-3}	1.34	1.288
2.00×10^{-3}	1.39	1.272
2.50×10^{-3}	1.39	1.271
5.00×10^{-3}	1.40	1.255
1.00×10^{-2}	1.54	1.229
1.00×10^{-1}	1.55	-
0.50	1.18	-
1.00	1.17	-

REFERENCES

1. J.S. Anderson and K. Saddington; J. Chem. Soc. 5381 (1949)
2. J.H. Wang; J. Am. Chem. Soc. 73, 510, 4181 (1951)
3. J.H. Northrop and M.L. Anson; J. Gen. Physiol. 12, 543 (1929)
4. J.W. McBain and C.R. Dawson; Proc. Roy. Soc. 148A, 32 (1935)
5. G.S. Hartley and D.F. Runnicles; Proc. Roy. Soc. 168A, 401 (1938)
6. R.H. Stokes; J. Am. Chem. Soc. 72, 763 (1950)
7. H. Hirai; Bull. Inst. Chem. Res. Univ. 33, 21 (1955)
8. A. Fick; Progg. Ann. 94, 59 (1958)
9. A.L. Slade, A.E. Cramers and H.C. Thomas; J. Phys. Chem. 70, 2840 (1966)
10. V.N. Felicetta, A. Markham, Q.P. Peniston and L.J. McArthy; J. Am. Chem. Soc. 71, 2879 (1949)
11. M.A. Lauffer; Biophys. J. 1, 205 (1961)
12. R. Marignan and G. Grouzat-Reynnes; Trav. Soc. Pharm. 16, 17, 79, 171, 176 (1956)
13. L.J. Gosting and H.S. Harned; J. Am. Chem. Soc. 73, 159 (1951)
14. L. Onsager; Ann. N.Y. Acad. Sci. 46, 241 (1945)
15. L. Onsager and R. Fuoss; J. Phys. Chem. 36, 2689 (1932)
16. R.V. Voitsekhovskii; Ukrain, Khim. Zhur 17, 856 (1951)
17. A.V. Dumanskii and E.F. Nekryach; Colloid Zhur. 17, 171 (1955)
18. J.H. Wang; J. Am. Chem. Soc. 74, 1182 (1952); J. Phys. Chem. 58, 680 (1954)
19. J.H. Wang and S. Miller; J. Am. Chem. Soc. 74, 1611 (1952)
20. R. Mills and J.W. Kennedy; J. Am. Chem. Soc. 75, 5696 (1953)
21. R. Mills; J. Phys. Chem. 61, 1631 (1957)
22. R.H. Stokes, L.A. Woolf and R. Mills; J. Phys. Chem. 61, 1634 (1957)

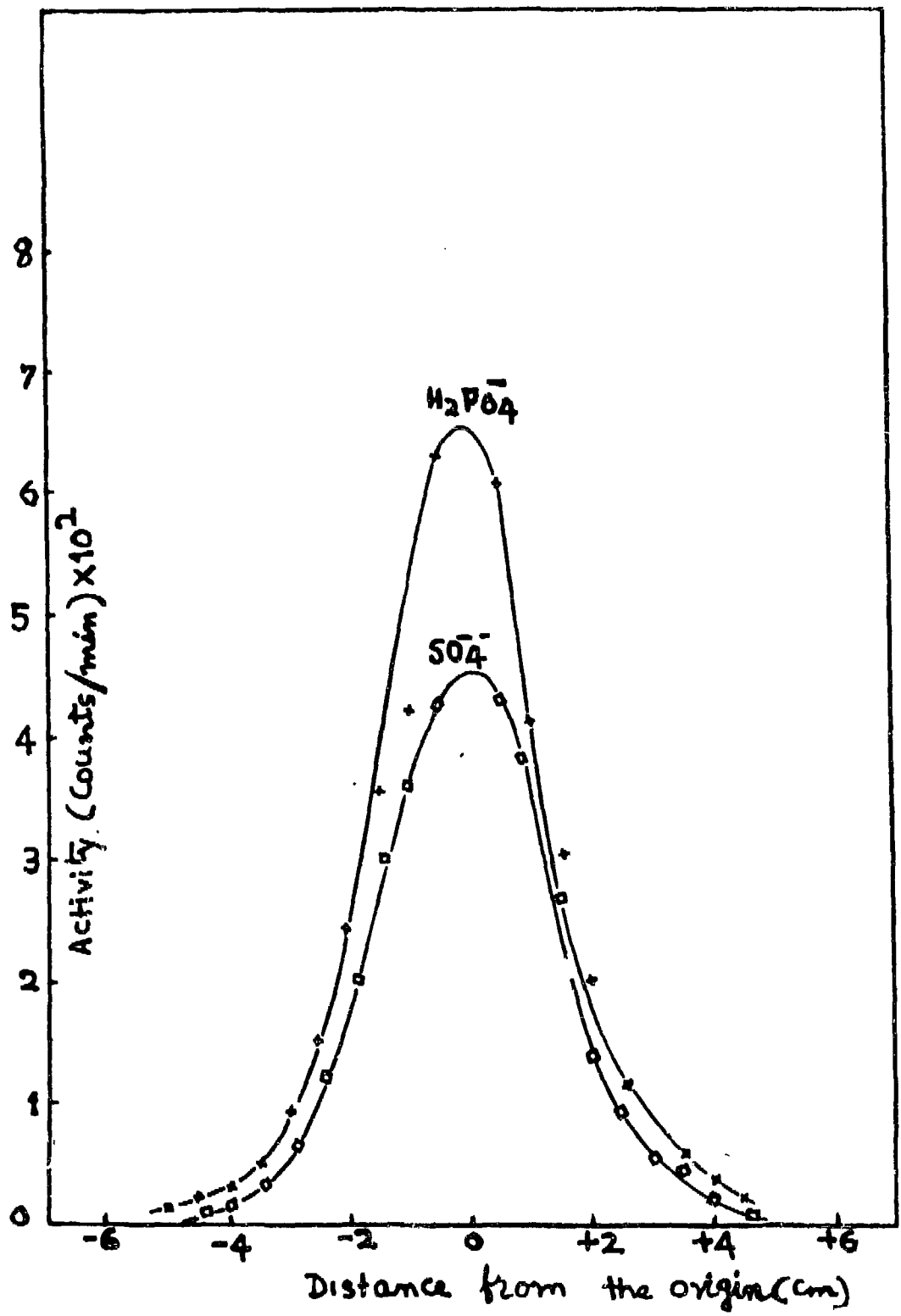

Fig. 1. Distribution of $H_2PO_4^-$ and SO_4^{--} ions after 24 hours of diffusion in 2.5% agar gel containing 10^{-5}N Na_2HPO_4 and 10^{-4}N $(NH_4)_2SO_4$ respectively.

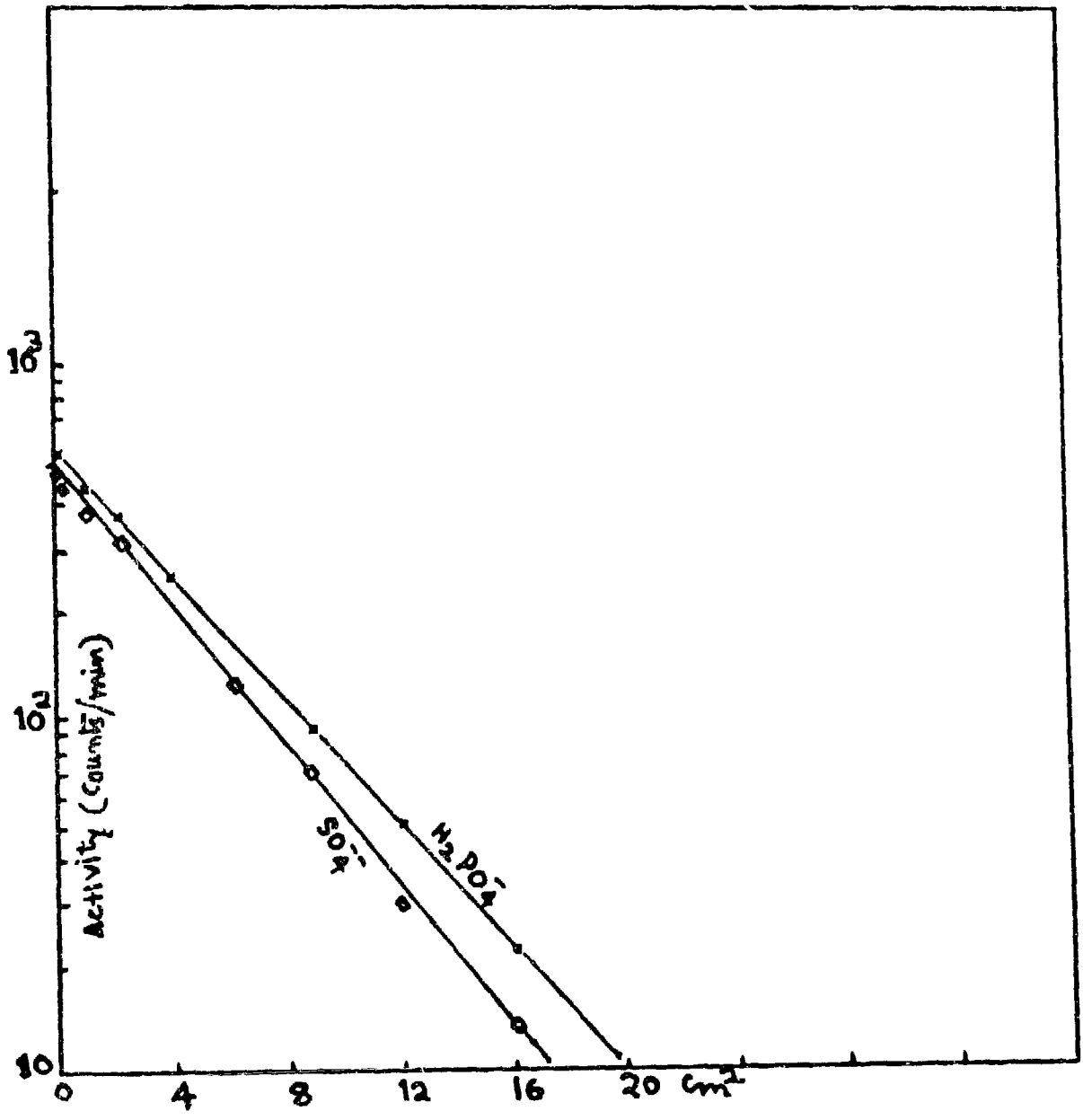

Fig. 2. A plot of log (counts/min.) versus (distance)^2 from the 'zone' for $H_2PO_4^-$ and SO_4^{--} ions corresponding to Fig. 1.

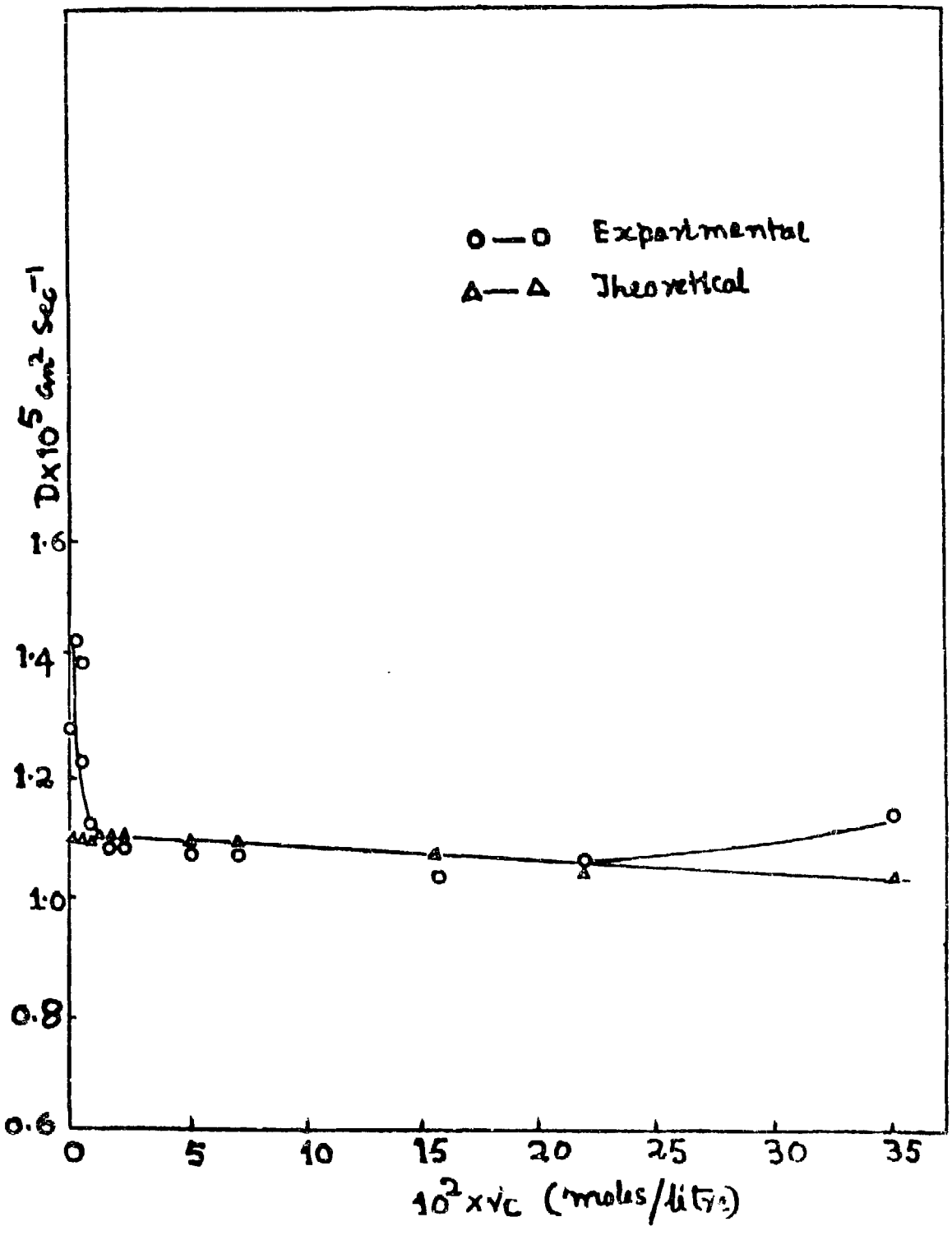

Fig. 3. Concentration variation of self-diffusion coefficient of $H_2PO_4^-$ ion in Na_2HPO_4 solution in 2.5% agar gel at 35°C.

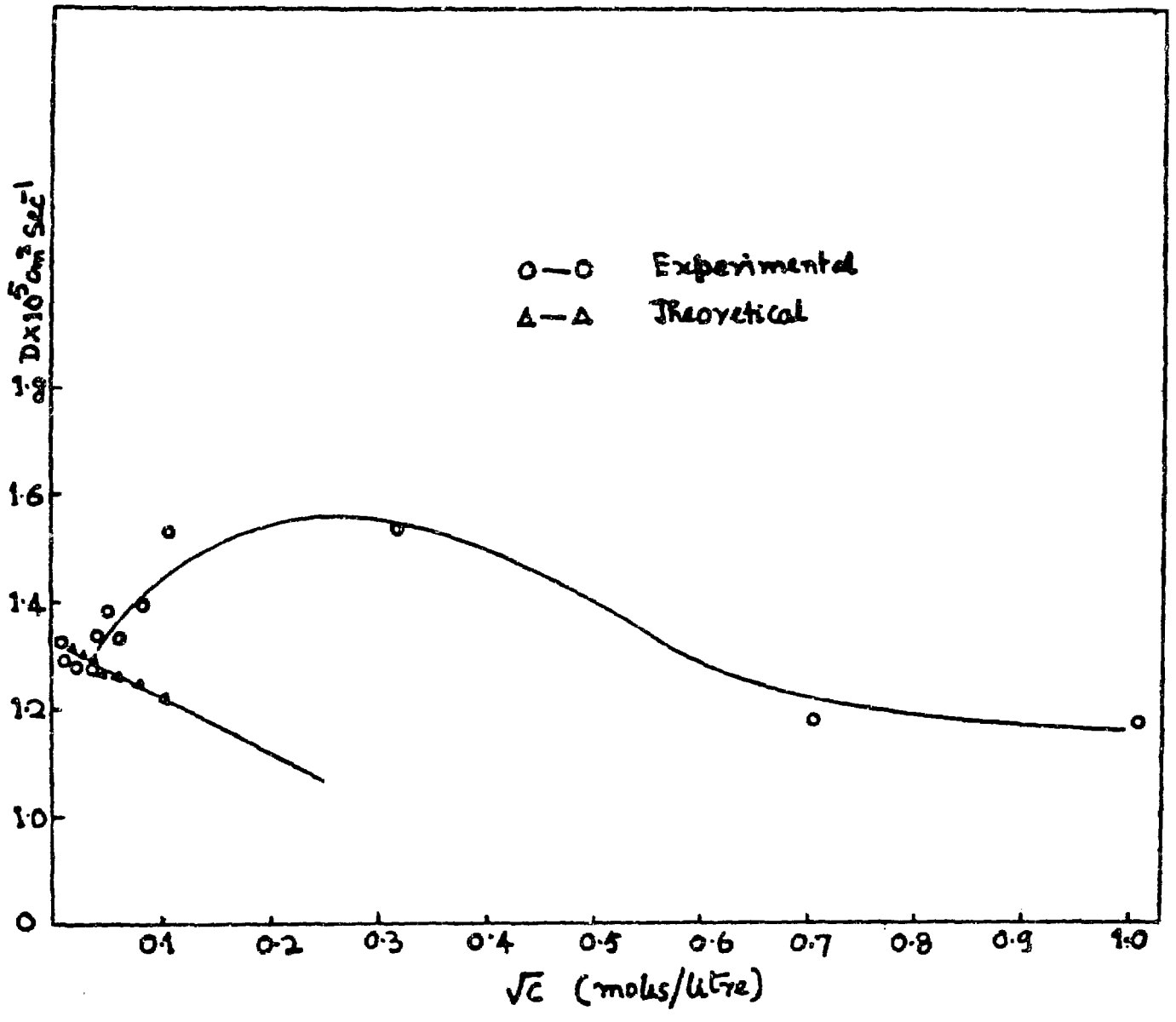

Fig. 4. Concentration variation of self-diffusion coefficient of SO_4^{-2} ion in $(NH_4)_2SO_4$ solution in 2.5% agar gel at 35°C.

TRACER-DIFFUSION OF $H_2{}^{32}PO_4^-$ IONS IN DIFFERENT ELECTROLYTE SOLUTIONS

V. N. Singh, R. K. Tewari and B. M. Shukla
Nuclear and Physical Chemistry Laboratory,
Banaras Hindu University, Varanasi-5

INTRODUCTION

Earlier studies on tracer diffusion of a radioactive ion in salt solutions were carried out mainly by capillary[1, 2] and diaphragm[3-6] cell methods. In these experimental techniques, the diffusion of ions is supposed to take place in stream-lines along with the capillary channels. However, the inherent convection and streaming effects due to the flow of solvent could not be reduced to a satisfactory extent. In our work these effects have been eleminated by using agar-agar gel as diffusion medium. This last has the remarkable property of immobilizing the solvent in a semi-rigid form and provides an ideal stationary medium for studying the tracer diffusion of ions. The present work deals with the studies of tracer-diffusion of $H_2{}^{32}PO_4^-$ ion in LiCl, NaCl and KCl solutions (at various molar concentrations) immobilized in 2.5% agar gel at 30°C. The experimental techniques adopted for these studies are described as under.

EXPERIMENTAL

2.5% agar gel containing the electrolyte (LiCl, NaCl, KCl) at desired concentrations (10^{-6} to 10^{-1} M) was allowed to set in a Pyrex tube of 30 cm. length and of uniform diameter of 1.0 cm. A thin 'zone' (0.1 cm) containing the labelled $H_2{}^{32}PO_4^-$ ions was carefully deposited at the middle of the gel column containing the salt solution. Necessary precautions were taken to exclude air bubbles in the gel column and to maintain a good contact between the diffusing 'zone' and diffusion columns. The tube was then thermostated at 30°C for 24 hours. Thereafter the diffusion column of either side of the central 'zone' was sliced into a series of 0.5 cm. thick samples. These samples were accurately weighed and their exact lengths were determined by comparing their weights with the weight of 10.0 cm. long gel column of identical dimensions and composition. Radioactivity (a) in each of the dried samples was determined by an end-window G. M. counter. Under the conditions of the present experiment, Fick's II law of diffusion takes the form,

$$a_{(x,t)} = \frac{a_o}{\sqrt{4\pi Dt}} e^{-x^2/4Dt} \qquad \ldots(1)$$

$a_{(x,t)}$ is the radioactivity at a distance x from the 'zone' at time t and a_0 is the total activity in the initial 'zone' at t = 0. Experimental values of tracer diffusion coefficients (D) were calculated from the slope of the plot log a vs x^2, where

$$\text{slope} = \frac{1}{2.303 \times 4 \times Dt} \qquad \ldots\ldots(2)$$

RESULTS AND DISCUSSION

Tracer-diffusion coefficient of $H_2PO_4^-$ ion in purely aqueous agar gel (containing no electrolyte) is found to be $1.05 \times 10^{-5} cm^2/sec.$ at 30°C where as in 10^{-6} and 10^{-5} M LiCl, NaCl and KCl solutions immobilized in 2.5% agar gel, the observed values of tracer diffusion coefficients are greater than the corresponding theoretical values (Tables I, II and III and Figs. 1, 2). Further, in the concentration range 10^{-4} to 10^{-2}M of each electrolyte solution, a fair agreement between $D_{expt.}$ and $D_{theo.}$ is observed and at 10^{-1}M a greater divergence between the two values is obtained. The decrease in the values of diffusion coefficients with increasing concentration (10^{-6} to 10^{-2}M) is due to the relaxation effect of ion-atmospheres. The theoretical values of tracer-diffusion coefficients of $H_2{}^{32}PO_4^-$ ions were calculated from Gosting[7] equation obtained from Onsager-Fuoss[8, 9] theory,

$$D = \frac{RT\lambda^0_j}{|z_j|F^2} - \frac{\lambda^0_j |z_j| F}{3N\xi} \times 2.694 \times 10^{16} \sqrt{\frac{4\pi}{\xi RT}} \left[1 - \sqrt{A(w_j)}\right] \times \sqrt{\Sigma c_i z_i^2} \qquad \ldots(3)$$

where

$$A(w_j) = \frac{1}{\Sigma c_i z_i^2} \Sigma \frac{c_i |z_i| \lambda^0_i}{\frac{\lambda^0_j}{|z_j|} + \frac{\lambda^0_i}{|z_i|}} \qquad \ldots\ldots(4)$$

and the other symbols have their usual significance. The equation(3) on substituting the values of all terms, reduces to

$D = 0.990 \times 10^{-5} - 2.106 \times 10^{-6} \sqrt{C}$ for LiCl

$D = 0.990 \times 10^{-5} - 1.914 \times 10^{-6} \sqrt{C}$ for NaCl

and $D = 0.990 \times 10^{-5} - 1.657 \times 10^{-6} \sqrt{C}$ for KCl

It is seen from the results (cf. Tables I - III, Figs. 1 & 2) that the observed tracer diffusion coefficients of $H_2{}^{32}PO_4^-$ ions at all concentrations of the electrolytes studied have the following order.

$$D_{expt.} \text{ in LiCl} < D_{expt.} \text{ in NaCl} < D_{expt.} \text{ in KCl}$$

where as theoretically determined values in LiCl, NaCl and KCl solutions are almost the same. This can be explained on the basis of order producing nature of the ions and electrolytes, being the maximum in case of LiCl and the minimum for KCl. Thus, the presence of LiCl in aqueous agar-gel will increase the viscosity of diffusion medium to a greater extent as compared to that in the presence of NaCl and KCl. The present results show an accelerating effect of the gel on diffusion whereas Slade[10], Allen[11] and Lauffer[12] in their studies have shown that the gel has definitely an obstructing effect on diffusion of the ions contrary to the results of Felicetta and co-workers[13], Friedmann[14] and Eversole et al.[15], who stress that the value of diffusion coefficient is independent of gel concentration. The acceleration effect of the gel in the present work can be explained in the light of partial desolvation effect of the gel. Agar-agar gel immobilizes water molecules in its net-work by H-bonding adsorption and dipole-dipole interactions between the polar sulphonyl groups and water molecules and thus forms a loose gel water structure containing "bound" water and "free" water. This loose gel-water structure is melted to different extents at different concentrations of the electrolytes. Thus, the viscosity of the medium decreases depending upon the degree of distortion. This fact clearly explains the abrupt increase in the tracer diffusion coefficient of $H_2{}^{32}PO_4^-$ ions at 10^{-1}M concentrations of the electrolytes studied. Wang[16] studied the tracer diffusion of Na ion in aqueous KCl solutions and observed that the tracer diffusion coefficient increases above 0.2M concentration of KCl solutions and below this concentration the observed value decreases with the increase of concentration but agrees fairly well with the theory. In the concentration range 10^{-4} to 10^{-2}M of these electrolyte solutions there is a better agreement between the observed and theoretical values of tracer diffusion coefficients of $H_2{}^{32}PO_4^-$ ions, but at concentration 10^{-1}M of the electrolyte solution the observed value is significantly greater than the theoretical value. This can be explained in the light of dielectric polarisation. Dielectric constant fails linearly with concentration upto 2N solution. The decrease in the dielectric constant will increase the relaxation force and consequently the tracer-diffusion coefficient will decrease. But at the same time, the self-energy of the ions increases with the decrease of the dielectric constant which envisages the faster diffusion of the ions at moderate concentration (10^{-1}M) of these electrolyte solutions, where self-energy of the ions dominates the relaxation force.

At very low concentrations of the supporting electrolytes in agar gel, D vs $\sqrt{C}$ plot shows a maximum at 10^{-6}M of these salts. Another finding of interest is that the diffusion coefficients of purely tracer amount of $H_2{}^{32}PO_4^-$ in agar gel containing no electrolyte at all is less than the diffusion coefficient in presence of a tracer amount of the electrolytes in gel. These two findings are explicable in the light of gel-water structure. This loose structure melts to the normal water

structure as concentration of the electrolyte increases from 0.00 to 10^{-6}M which possibly results in the decrease of viscosity of the immobilized system. This causes a faster diffusion rate atleast in this concentration range.

REFERENCES

1. J. S. Anderson and K. Sadington; J. Chem. Soc. 5381 (1949)
2. J. H. Wang; J. Am. Chem. Soc. 73, 510, 4181 (1951)
3. J. H. Northrop and M. L. Anson; J. Gen. Physiol. 12, 543 (1929)
4. J. W. McBain and C. R. Dawson; Proc. Roy. Soc. 148A, 32(1935)
5. G. S. Hartley and D. F. Runnicles; Proc. Roy. Soc. 168A, 401(1938)
6. R. H. Stokes; J. Am. Chem. Soc. 72, 763(1950)
7. L. J. Gosting and H. S. Harned; J. Am. Chem. Soc. 73, 159(1951)
8. L. Onsager; Ann. N. Y. Acad. Sci. 46, 241 (1945)
9. L. Onsager and R. Fuoss; J. Phys. Chem. 36, 2689 (1932)
10. A. L. Slade, A. E. Cremers and H. C. Thomas; J. Phys. Chem. 70, 2840 (1966)
11. G. F. Allen et al.; J. Phys. Chem. 67(7), 1402-7 (1963)
12. M. A. Lauffer; Biophys. J. 1, 205 (1961)
13. F. Vincent et al; J. Am. Chem. Soc. 71, 2879 (1949)
14. L. Friedmann; ibid., 52, 1311 (1930)
15. Eversole et al; J. Phys. Chem. 39, 289 (1935)
16. J. H. Wang; J. Am. Chem. Soc. 74, 1182-86 (1952)

Table I

Concentration Dependence of Tracer-diffusion Coefficients $H_2{}^{32}PO_4^-$ ions in LiCl Solutions Immobilized ion 2.5% Agar Gel at 30°C by "Zone" Diffusion

Concentration mole/litre LiCl	$D_{expt.}$ x10^5 Cm^2/sec.	$D_{theo.}$ x10^5 Cm^2/sec.
0.00 (water)	1.05	----
10^{-6}	1.19	0.989
10^{-5}	1.09	0.989
10^{-4}	1.00	0.988
10^{-3}	0.99	0.983
10^{-2}	0.98	0.969
10^{-1}	1.04	0.924

Table II

Concentration Dependence of Tracer-diffusion Coefficients $H_2{}^{32}PO_4^-$ ions in NaCl Solutions Immobilized in 2.5% Agar Gel at 30°C by "Zone" Diffusion

Concentration moles/litre NaCl	$D_{expt.}$ x10^5 Cm^2/sec.	$D_{theo.}$ x10^5 Cm^2/sec.
0.00 (water)	1.05	----
10^{-6}	1.22	0.989
10^{-5}	1.14	0.989
10^{-4}	1.04	0.988
10^{-3}	1.01	0.984
10^{-2}	0.99	0.971
10^{-1}	1.06	0.930

Table III

Concentration Dependence of Tracer-diffusion Coefficients of $H_2{}^{32}PO_4^-$ ions in KCl Solutions Immobilized in 2.5% Agar Gel, At 30°C by "Zone" Diffusion

Concentration moles/litre KCl	$D_{expt.}$ x $10^5 Cm^2/sec.$	$D_{theo.}$ x $10^5 Cm^2/sec.$
0.00 (water)	1.05	----
10^{-6}	1.25	0.989
10^{-5}	1.18	0.989
10^{-4}	1.07	0.988
10^{-3}	1.03	0.984
10^{-2}	1.00	0.970
10^{-1}	1.08	0.937

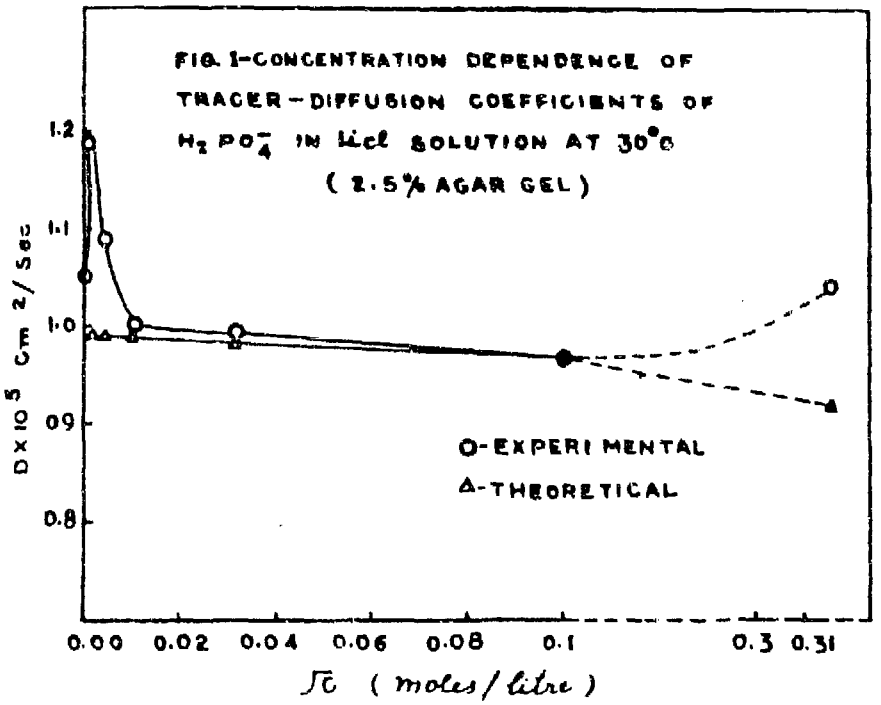
FIG. 1-CONCENTRATION DEPENDENCE OF TRACER-DIFFUSION COEFFICIENTS OF $H_2PO_4^-$ IN LiCl SOLUTION AT 30°C (2.5% AGAR GEL)
D X 10^5 Cm 2/Sec
1.2
1.1
1.0
0.9
0.8
O-EXPERIMENTAL
Δ-THEORETICAL
0.00 0.02 0.04 0.06 0.08 0.1 0.3 0.31
√c (moles/litre)

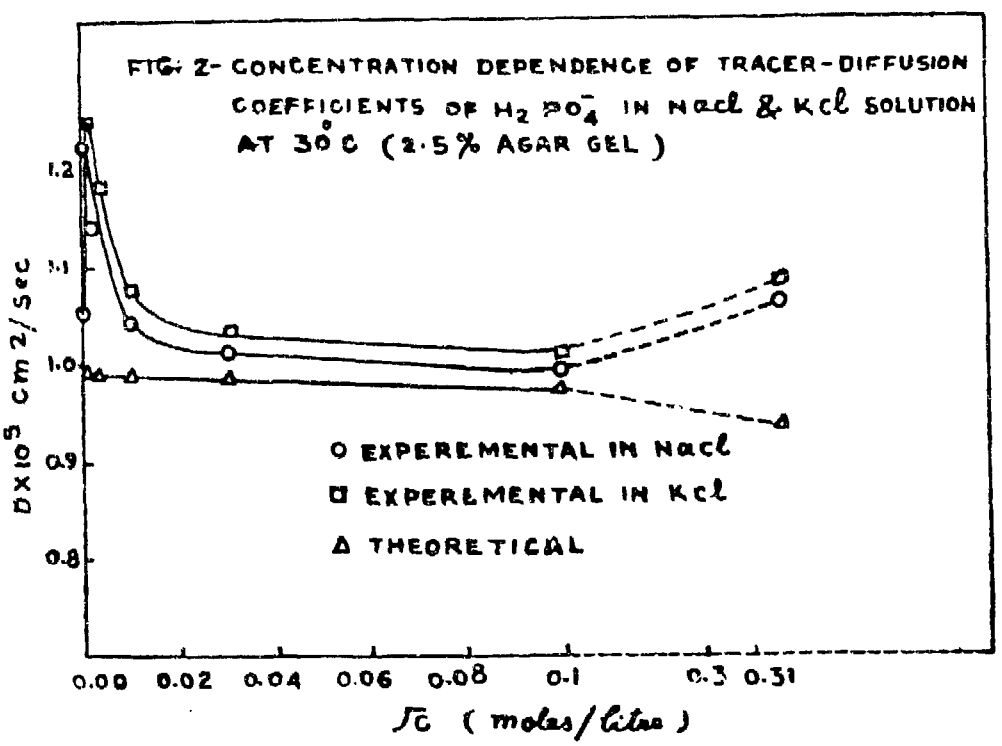
FIG. 2- CONCENTRATION DEPENDENCE OF TRACER-DIFFUSION COEFFICIENTS OF $H_2PO_4^-$ IN NaCl & KCl SOLUTION AT 30°C (2.5% AGAR GEL)
D X 10^5 Cm 2/Sec
1.2
1.1
1.0
0.9
0.8
O EXPERIMENTAL IN NaCl
□ EXPERIMENTAL IN KCl
Δ THEORETICAL
0.00 0.02 0.04 0.06 0.08 0.1 0.3 0.31
√c (moles/litre)

SEPARATION OF $BiPO_4$ CARRIED ACTINIDES BY BiOCl PRECIPITATION

R. S. Iyer and P. R. Kamath
Health Physics Division, Bhabha Atomic Research Centre,
Trombay, Bombay-85

INTRODUCTION

Health monitoring of persons engaged in plutonium processing plants for accumulated body burden is routinely carried out by radio-analysis of body excretions.[1, 2]

Alpha emitters in the process effluents of uranium which has undergone short-term irradiation are predominantly plutonium, uranium and to a minor extent ionium and americium. Long irradiated fuel will contain higher amounts of trans-plutonium elements. The present study was carried out to evolve a rapid determination of uranium, thorium and americium sequentially in a single urine sample. The excretion rates of these heavy elements in urine are of the order of 0.01% (except for uranium) and it is required to take the full volume of urine sample for determination of each element. Sequential analysis avoids repetitive urine collection and processing.

OUTLINE OF METHOD

Measure the volume of urine (16 hours collection). Use 1 ml. for creatinine determination[1].

Add 15.6 ml. HNO_3 (for each 500 ml. urine) to the urine sample and 2 ml. calcium carrier (200 mg). Add 2 ml. H_3PO_4. Heat. Add NH_4OH to precipitate calcium phosphate. Stir well and keep for settling. Centrifuge.

Dissolve the precipitate in 10 ml. 0.5 M.HNO_3. Add 5 ml. 5% NH_2OHCl. . Keep for 10 minutes. Add 1.5 ml H_3PO_4. Heat to boil. Precipitate $BiPO_4$ by adding one ml. Bi carrier (100 mg) drop by drop. Stir and keep for settling. Centrifuge. (Uranium goes in the supernatant, thorium, plutonium and americium remain with the precipitate).

Uranium (supernatant)

Evaporate supernatant; add 0.5 ml. HNO_3, 2 ml. water and 2.5 ml $Fe(NO_3)_3$ (122 mg Fe/ml.). Transfer the solution to a 100 ml. separating funnel. Add 30 ml. ether-nitric acid mixture (100:5) and extract U. Separate, repeat ether extraction. Filter combined ether extracts through a cellulose powder column, soaked previously in ether-nitric

acid mixture, into a beaker and evaporate off the ether. Transfer residue with 1 N. HNO_3 to a platinum planchet for fluorimetric determination of U.[3, 1]

Thorium and Plutonium (precipitate)

Dissolve $BiPO_4$ in 4 ml. HNO_3 and add 3 ml. water and 1 ml. $NaNO_2$ (1 M. solution). Pass through 2.5 gm. of Dowex 1 x 8 anion exchange column conditioned with 8 N. HNO_3. Wash with 20 ml. 8 N. HNO_3. Collect together effluent and washings (containing americium).

Thorium: Elute Th from the column by passing 20 ml. 8 N. HCl. Determine Th (Ionium) by alpha counting in the eluate.[4]

Plutonium: Elute Pu with 1.5 M. NH_2OH HCl in 1 M. HCl. (Eluate is taken up with iron for precipitation and alpha counting[5] or for electrodeposition.[6])

Americium: Evaporate to dryness effluent and washings from 2.2.1. Dissolve residue in 10 ml. 2 N. HCl and add 80 ml. 0.01 N. HCl to hydrolyse. Centrifuge off BiOCl. Evaporate supernatant to dryness and take in 10 ml. 4 N. HCl. Add 1 ml. La carrier and 2 ml. conc. HF. Centrifuge and wash the precipitate.[1] Transfer to a weighed stainless steel planchet, weigh and count for alpha activity.

Table I gives analytical results for urine spiked with different alpha emitters.

TABLE I

Results of Urine Samples Spiked With Different Alpha Emitters

Tracer	Spiked activity (cpm)	Actual recovery* (cpm)	Recovery (%)
Pu	69	58.7	85
Th	16	14.3	89
Am	22	18.3	83
U	392.6 mugm	338.0 mugm	86

* Average of 3 sets of urine samples

$1\sigma = 10\%$

DISCUSSION

The listed references describe methods for the determination of uranium, thorium and plutonium adopted in the laboratory.

The dissolution of $BiPO_4$ and hydrolysis were studied as follows:

$BiPO_4$ precipitate is dissolved in 10 ml. 2 N. HCl and warmed. 80 ml. 0.01 N. HCl are added. The precipitate and supernatant are collected. The precipitate is weighed. Table II gives the recoveries of BiOCl. Supernatant is made upto 100 ml. and divided into two parts for determination of phosphate and bismuth.

The above experiment is repeated with 0.1 M. NH_4Cl and water for hydrolysis. The results obtained for PO_4 $'''$ and Bi content are tabulated below. High $(PO_4)'''$ and low Bi in the supernatant, and high BiOCl recovery are considered most favourable for separation.

TABLE II

Results of Hydrolysis of $BiPO_4$ Using Different Reagents

Reagents used for hydrolysis	Supernatant		Analysis for Bi. in precipitate. Wt. of BiOCl (ppt)
	Phosphate (as Mg NH_4PO_4)	Bi (as $BiPO_4$)	
0.01 N. HCl	42.2 mgm	0.68 mgm	117.5 mgm
0.1 M. NH_4Cl	40.6 mgm	4.4 mgm	114.1 mgm
Water	38.6 mgm	Nil	120.2 mgm

Of the three techniques, 0.01 N. HCl dilution was the most effective and was adopted for final separation. Low$(PO_4)'''$ in the aqueous treatment are likely to result in the hold-back of Am recoveries.

Tracer separation by the hydrolysis method was carried out for $BiPO_4$ carried thorium, plutonium and americium. Results are given in Table III.

TABLE III

Tracer Recovery in Single Precipitation of BiOCl from $BiPO_4$

Tracer	Spiked activity (cpm)present in $BiPO_4$	Tracer in BiOCl precipitate (cpm) (a)	Tracer in supernatant after BiOCl precipitation (cpm) (b)	Total (a) + (b)
Pu	66.7 ± 10%	6.7	60.2	66.9
Am	21.9 ± 10%	0.9	21.3	22.2
Th	24.3 ± 10%	2.7	20.3	23.0

High recoveries indicated that the BiOCl separation technique could be recommended for separation of actinides from bulk carrier bismuth phosphate used in collection of the individual trace element.

REFERENCES

1. P. R. Kamath and S. D. Soman; Bioassay procedures in Trombay Establishment, AEET/HP/1 (Rev) Atomic Energy India Publications (1961)

2. P. R. Kamath, et al. ; Assessment of radioactivity in man, IAEA Publication, 1, 195 (1964)

3. V. M. Matkar; Communication

4. P. R. Kamath, et al. ; Environmental natural radioactivity measurements at Trombay Establishment. The Natural Radiation Environment - Page 957, Rice University Semi-centenial series, University of Chicago Press (1964)

5. Kamala Rudran and P. R. Kamath; Quick methods for radiochemical analysis, IAEA Tech. Series no. 95, p-31 (1969)

6. Kamala Rudran; A comparative study of electro-deposition of actinides from aqueous ammonium sulphate and isopropyl alcohol, AERE-R 5987 (1969)

DISCUSSION

P. S. Goel : Did you observe any difference in the urine of worker in the Uranium and Plutonium plants as compared to non-worker ?

R. S. Iyer : If the questions refer to routine monitoring, there would be hardly any significant variations. If monitoring is done after an incident causing internal exposure, one would see Pu in urine proportional to intake. But such instances are rare and the exposures, if any, have always been very much below the permissible levels. The objective of routine monitoring of urine is to detect any internal exposure which was not as a result of a known incident.

EVEN ELECTRON SPECIES IN THE γ-RADIOLYSIS OF LIQUID HYDROCARBONS

Jai P. Mittal
Chemistry Division, Bhabha Atomic Research Centre, Bombay 85

The radiation chemistry of liquid hydrocarbons has been studied extensively with respect to formation of free radicals and their reactions, but there are few instances in which any attempt has been made to correlate the ultimate products with positive ion precursors[1-4]. Positive ion intermediates in radiation chemistry can be classified into odd and even electron species. Recently, more than 150 radical ionic species have been identified or partly characterised and various ionic processes demonstrated in γ-irradiated organic solids using optical and esr spectroscopy[5,6]. The presence of carbonium ions has been well documented in the mass spectrometric studies[7,8] and reactions such as

$$CH_3^+ + CH_4 \longrightarrow C_2H_5^+ + H_2$$

$$CH_3^+ + CH_4 \longrightarrow C_2H_7^+$$

are well known. The extent of positive ion fragmentation in condensed phase is not known but is presumably small because the process

$$RH^+ \longrightarrow R^+ + H$$

is, in most cases, endothermic for ground state radical ions. On the other hand, the above reaction can occur spontaneously if there is initial ionic excitation. Libby[9] has postulated that carbonium ions are formed by ionizing radiations very readily. Williams[10,11] has given theoretical reasons for expecting the formation of conventional carbonium ions. The main characteristics of the carbonium ion are its strong acidic character and its ability to form salt like complexes. The only earlier measurement of radiation yields of carbonium ions is of Ward & Hamill[12]

$$R^+ + R'OH \longrightarrow ROR' + H^+$$

and found G values of 0.1 - 0.2 for several hydrocarbons (neo-Pentane exception). Some time ago, Burrell[13] reported that an absorption spectra with a maximum of 297 nm could be detected in isobutylene after pulse radiolysis. This spectrum was attributed to the t-butyl cation (trimethyl carbonium ion) on the basis of a previous assignment by Rosenbaum & Symons. However, more recently, Olah and collaborators[14] have definitely shown that the t-butyl cation does not absorb in this region.

In this work, an attempt has been made to count these even electron

positive species (carbonium ions) by derivatising them with suitable negative species X^- produced in situ.

$$RH \rightsquigarrow RH^+ + e^-$$

$$RH^+ \longrightarrow R^+ + H$$

$$e^- + R'X \longrightarrow R' + X^-$$

$$R^+ + X^- \longrightarrow RX$$

RX produced in the presence of a radical scavenger has been taken as a measure of carbonium ions produced in the radiolysis of corresponding hydrocarbons.

EXPERIMENTAL

All saturated hydrocarbons were Phillips pure grade, purified by passing through two 6 foot columns of Fisher 80 - 200 mesh silica gel. VPC analyses on two different columns indicated that unsaturates were less than 10^{-3}M. All other reagents were Fisher certified reagents and were used as received. Iodine used was resublimed J. T. Baker reagent grade.

All samples were outgassed by the freeze, pump and thaw technique.

All irradiations were done by a 10 kCi Co^{60} γ-source. The dose rate was determined by Fricke dosimetry using $G(Fe^{+2}$ to $Fe^{+3})$ = 15.5.

All the gas chromatographic analysis was done on a F & M model 609 - 1 instrument equipped with a flame ionisation detector. A 10 ft column of Silicone Grease on Chromosorb P was used for most of the product analyses. All the samples containing iodine were treated with mercury to remove unreacted iodine before injecting into the gas chromatograph.

RESULTS AND DISCUSSION

On thermochemical grounds, recombination of a positive ion with an electron should lead to decomposition. However, primary reactions of electrons with suitable reagents such as RBr, ROAc etc. can dissipate as much as 3 - 4 ev of this recombination energy, thereby reducing the possibility of a dissociative charge recombination. Even in a low dielectric medium, an additional 2 ev per ion pair will be dissipated by

polarisation of the medium. Columbic energy of the separated ion pair partially converts to kinetic energy during recombination and is expended to overcome viscous drag, dissipating an additional ~2 ev.

On the basis of above consideration, this device of ion - ion recombination has been used to convert the carbonium ions into their stable derivatives. For comparison sake, two saturated alicyclic compounds cyclohexane and cyclopentane along with one heaviiy branched hydrocarbon neo-hexane were tested for the production of carbonium ions. Three different sources for giving the appropriate negative species were used. They were benzyl acetate, carbon tetra chloride and sec. butyl bromide. Organic halides have been shown by Hamill et al[5] to be very efficient electron scavengers utilizing dissociative electron capture. They have been used here to convert electrons into a corresponding negative ions as follows:

$$CCl_4 + e^- \longrightarrow \cdot CCl_3 + Cl^-$$

$$RBr + e^- \longrightarrow R + Br^-$$

The runs with benzyl acetate which gave similar values as other solutes suggest the reactions

$$C_6H_5\ CH_2\ COOCH_3 + e^- \longrightarrow C_6H_5CH_2\cdot + CH_3COO^-$$

$$C_6H_{11}^+ + CH_3COO^- \longrightarrow CH_3COOC_6H_{11}$$

The large electron affinity of 3.3 ev for acetoxy radical[15] moderates the energy of recombination. The instability of acetoxy radical precludes the possibility of radical - radical combination. A small amount of iodine was added to every sample to make sure that none of the products came from any radical - radical reactions.

The results are given in Table I. The results clearly indicate that carbonium ions are not very important in the condensed phase radiolysis of saturated normal hydrocarbons. These results agree very well with earlier work of Ward & Hamill[12]. Recently Samuel et al[16] utilising an independent method have also reached to the same conclusion.

In case of neo-hexane, we find a surprisingly higher G value obtained with the help of all the three solutes used. Here, we are counting the tertiary carbonium ions produced. The dominant ion in the mass spectrum of $(CH_3)_4C$ is $C_4H_9^+$, presumed to have the tertiary configuration while the abundance of $C_5H_{12}^+$ is only ca 0.1%.

The higher G value (0.8) is understandable in terms of the general theoram[17] that hyperconjugation effects due to attached methyl groups operate much more strongly in the even electron carbonium ions than in the odd electron parent ion. This gives the maximum stability to t-butyl

carbonium ions. In the production of these from the parent radical ion, dissociation is accompanied by a gain in resonance energy. This gain will obviously be greater the greater the number of alkyl groups attached to the electron deficient carbon atoms. From the rule that the resonance energy of carbonium ions exceeds that of corresponding neutral radical[18] it follows that the dissociation path naturally tends to favour the formation of the most stable carbonium ion from any particular alkane molecular ion.

One very interesting observation is that the trend of the production of these carbonium ions runs parallel to the values recently obtained for "free ions" obtained by conductivity experiments of Schmidt and Allen[19]. It strongly indicates that the explanation of different values (structure dependent) of "free ion" yield may be correlated with their carbonium ion yields obtained from the respective hydrocarbon's γ-radiolysis. It will have very interesting theoretical implications. Further work is in progress, details of which will be published elsewhere.

ACKNOWLEDGEMENTS

Part of the work pertaining to the contents of this paper was performed by the author at the Radiation Laboratory, University of Notre Dame, U.S.A. in collaboration of Prof. W.H. Hamill. The author would like to thank Dr. J. Shankar, Head, Chemistry Division, Bhabha Atomic Research Centre, Trombay, for his keen interest and providing facilities.

REFERENCES

1. S.Z. Toma and W.H. Hamill; J. Am. Chem. Soc. 86, 4761 (1964)
2. F. Williams; Quart. Rev. (London), 13, 101 (1963)
3. P. Ausloos, S.G. Lias and A.A. Scala; Adv. Chem. Ser. No. 58, American Chem. Soc., Washington, D.C., p. 264 (1966)
4. J.A. Ward and W.H. Hamill; J. Am. Chem. Soc. 87, 1853 (1965)
5. W.H. Hamill "Radical Ions"; Ed. L. Kevan & Kaiser, Interscience Publishers, N.Y. (1968)
6. J.P. Mittal and W.H. Hamill; J. Am. Chem. Soc. 89, 5749 (1967)
7. F.H. Field, J.L. Franklin and F.W. Lampe; J. Am. Chem. Soc. 79, 2419 (1957)
8. S. Wexler and N. Jesse; J. Am. Chem. Soc. 84, 3425 (1962)
9. W.F. Libby; J. Chem. Physics 35, 1714 (1961)
10. T.F. Williams; Trans. Faraday Soc. 57, 755 (1961)
11. T.F. Williams; Quart. Rev. 17, 101 (1963)
12. J.A. Ward and W.H. Hamill; J. Am. Chem. Soc. 89, 5116 (1967)

13. E.J. Burrell, Jr.; J. Phys. Chem. 68, 3895 (1964)
14. G.A. Olah et al; J. Am. Chem. Soc. 88, 1488 (1966)
15. S. Tsuda and W.H. Hamill; Adv. Mass. Spec. 3, 249 (1965)
16. A.H. Samuel and M.A. Golub; TDR-63-4133 (1963)
17. Longuet-Higgins; Chem. Soc. Sp. Publ. 2, 5 (1957)
18. Evans; Disc. Faraday Soc. 10, 109 (1951)
19. W.F. Schmidt and A.O. Allen; Science 160, 302 (1968)

TABLE I

Yields of Ion Recombination Products

Source of X^-	$G(RX)^{a,b}$		
Solutes used[c] (R'X)	Solvents used (RH) Cyclohexane	Cyclopentane	Neo-hexane*
Benzyl acetate	0.21	0.14	0.81
Carbontetrachloride	0.25	0.17	0.84
Sec. butylbromide	0.19	0.12	0.78

a. Dose: 1.52×10^{20} eV/ml; all runs were at room temperature

b. All runs are in the presence of 5×10^{-3} M iodine

c. All solutes used were 2% in concentration (v/v)

* The values are for t-butyl acetate, t-butyl chloride and t-butyl bromide

THE PULSE READIOLYSIS END PRODUCTS IN ALLYL BROMIDE-CYCLOHEXANE SYSTEM

P. K. Bhattacharyya* and E. J. Burrell Jr.
Bhabha Atomic Research Centre, Trombay, Bombay-85

INTRODUCTION

The existence of allyl free radical has been postulated in several radiation chemical reactions[1, 2]. The electronic absorption spectrum of this radical has also been reported by several authors with different absorption maximum values[3, 4, 5]. Recently, the ally radical transient spectrum and the kinetic studies was carried out by us[6] with an absorption maximum of 310 mu. The present investigation was carried out to understand the reaction mechanism of the formation of transient allyl radical and other important radiolysis products in allyl bromide solution in cyclohexane. The pulse radiolysis products were determined by gas liquid partition chromatography. On the basis of the reaction mechanism and the product analysis, the allyl radical molar extinction coefficient at 310 mu was determined.

EXPERIMENTAL

1. Pulse Radiolysis for the Product Analysis

The detailed aspects of experimental set-up of pulse radiolysis and transient studies can be obtained in several publications[6, 7]. A total of 200 pulses of 4.5 u sec duration with maximum current of 150 mA of 13.5 MeV electrons was introduced in the sample solution in a 4 cm cell. To avoid the heating effect and other radiation effects, irradiation was carried out at the rate of one pulse per 20 sec.

2. Sample Preparation for Irradiation

A solution (1.5×10^{-2} M) of allyl bromide was made in cyclohexane (Philips research grade). The solution was degerated by passing pure argon gas for 2 hours through a porous glass frit. The sample was introduced in a 4 cm cell with quartz windows having two openings with teflon plug stopcocks.

---

* This work was carried out at Argonne National Laboratory, Argonne (USA) and was the part of the Ph. D. thesis submitted to the Loyola University, Chicago, in 1967.

3. Gas Chromatographic Analysis

An aliquot of irradiated solution was injected in the preparative gas chromatograph (F & M Scientific Corporation, Model 770). The column used was 20% carbowax 20 M of 12 ft long and 3/4" diameter.

4. Free Radical Scavenging by DPPH

Diphenyl picryl hydrazil obtained from Aldrich Chemical Co. (USA) was dissolved in cyclohexane (7.7×10^{-5}M) by constant shaking for several hours. The solution was deaerated and irradiated by a single electron pulse. The absorption spectrum of DPPH solution before and after irradiation was studied by Cary-14 absorption spectrophotometer. The bleaching of 520 mu band with DPPH(molar extinction coefficient $E = 1.03 \times 10^{4}$)was used for determination of the total radical scavenged by DPPH in cyclohexane.

RESULTS AND DISSCUSSION

The pulse radiolysis of allyl bromide solution in cyclohexane showed an absorption spectrum of the transient with λ_{max} = 310 mμ. The transient was assigned to allyl free radical which was found to decay with second order rate constant[6]. From the DPPH scavenger study, it was found that 4.4×10^{-5}M free radical in cyclohexane was involved per electron pulse. The gas chromatographic results are shown in Tables I and II. The identification of the chromatographic peak was carried out with standard solutions of compounds in cyclohexane. The results are consistent in several experiments. Thus, the quantitative estimation of the products and the decrease of allyl bromide in the irradiated solution along with the knowledge of total radical formation in cyclohexane (i. e. 4.4×10^{-5}M per pulse) helps to propose the following major reaction mechanism involved in the system.

Primary Process

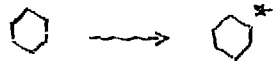
..... (1)

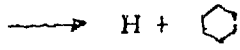
..... (2)

Secondary Process

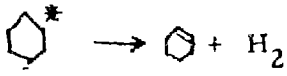
..... (3)

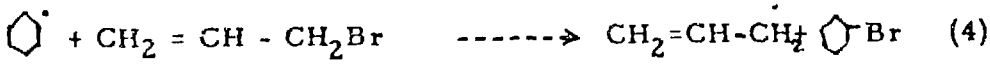
(4)

$$2\ CH_2 = CH - CH_2Br \longrightarrow CH_2=CH-CH_2-CH_2-CH=CH_2 \quad .. (5)$$

$$2\ \bigcirc^{\cdot} \longrightarrow \bigcirc\!\!\bigcirc \quad .....(6)$$

$$2\ H \longrightarrow H_2 \quad .....(7)$$

The reaction (4) was assumed on the basis of formation of $\bigcirc$Br which is comparable to decomposition of allyl bromide (0.89×10^{-5}M) and hence the concentration of allyl radical should be 0.89×10^{-5}M.

Since we determined 0.45×10^{-5}M 1,5-hexadiene, this proves the reaction (5). The consumption of $\bigcirc^{\cdot}$ radical by reaction (4) and (6) account for a total of 2.1×10^{-5}M. If $\bigcirc^{\cdot}$ radical was formed by reaction (2), then we should have 2.1×10^{-5}M, H atom. Thus, the 4.2×10^{-5}M total radical by the primary process was responsible for reaction with DPPH (4.4×10^{-5}M). Since H_2 has been determined by mass spectrometry to be 3.26×10^{-5}M, and the reaction (7) can account for only 1.05×10^{-5}M, the reaction (3) is assumed as molecular dissociation which can give 2.33×10^{-5}M $\bigcirc$ and 2.33×10^{-5}M, H_2. Thus, 3.38×10^{-5}M H_2 is also accounted for. A slight difference of values is possibly due to experimental errors. Thus the product analysis gave a complete understanding of the mechanism of radiolysis of allyl bromide in cyclohexane. From the knowledge of allyl radical concentration with the 16 cm path length[6] and the optical density as determined by the transient spectrum at 310 mu, the molar extinction coefficient was calculated to be $2.93 \times 10^{-3} M^{-1} cm^{-1}$.

REFERENCES

1. E.J. Lawton, J.S. Balwit and R.S. Powel; J. Chem. Phys. 33, 395 (1960)
2. C.A. Heller and A.S. Gordon; J. Chem. Phys. 42, 1262 (1965)
3. H.C. Longuet-Higgins and J.A, Pople; Proc. Phys. Soc. A68, 519 (1955)
4. D.M. Bodily and M. Dole; J. Chem. Phys. 44, 2821 (1966)
5. D.A. Ramsay; J. Chem. Phys. 45, 488 (1966)
6. E.J. Burrell Jr. and P.K. Bhattacharyya; J. Phy. Chem. 71, 774 (1967)
7. J. Rabani, W.A. Mulac and M.S. Matheson; J. Phys. Chem. 69, 53 (1965)

DISCUSSION

Jai P. Mittal : 1) I hope you are aware of the high electron affinity of DPPH and a high rate constt. of the reaction: $DPPH + e^- \rightarrow DPPH^-$

2) Does it not indicate that DPPH should not be used as a solute which is specific only to radicals? DPPH is known to give many times wrong values of G(R)?

P. K. Bhattacharya : 1) I am aware of the fact that DPPH can capture an electron in steady state radiolysis. In pulse radiolysis, the DPPH concentration in cyclohexane solution was $\approx 10^{-5}$M hence electron capture can be neglected. Moreover, it was shown by McLachlan that in pulse radiolysis of cyclohexane is predominant. We have also observed that in allyl halide solution in cyclohexanol (except Allyl Bromide) no allyl radical transient is involved hence

$$e^- + Rx \rightarrow R + x^-$$

reaction are not considered. These indicate that in pulse radiolysis of cyclohexanol electron has very little to do.

2) It is also true that using DPPH correct conclusion can be obtained. It all depends on systems concentration of solutes, Dose and so on.

Since free radical mechanism could explain our results, the use of DPPH in low concentration is justified.

TABLE I

Pulse Radiolysis Product Analysis by GLC

Exptl. Sample after 200 Pulse Irradiation	Standard Compound	Conc. in Cyclohexane	Column Temp	Carrier Flow	Aliquot Injected	Retention Time	Peak Area in mg	Estimated Product Conc. per 200 Pulse	Conc. of Product per Single Pulse	Identified Product
-		1.2×10^{-3}M	150°C	6	2 ml	17.5 min	0.7	-	-	
Allyl Bromide Solution	-	-	150°C	6	2 ml	17.5 min	0.7	1.2×10^{-3}M	0.6×10^{-5}M	
		1.6×10^{-3}M	150°C	6	1 ml	9 min	0.25	-	-	
Allyl Bromide Solution	-	-	150°C	6	1 ml	9 min	0.28	1.76×10^{-3}M	0.88×10^{-5}M	
	Diallyl	1.7×10^{-3}M	75°C	3	1 ml	5 min	1.15			
Allyl Bromide Solution	-	-	75°C	3	1 ml	5 min	0.6	0.9×10^{-3}M	0.45×10^{-5}M	Diallyl
		1×10^{-3}M	75°C	3	1 ml		0.87	1		
Allyl Bromide Solution	-	-	75°C	3	1 ml		0.4	4.67×10^{-3}M	2.33×10^{-5}M	

TABLE II

Decomposition of Allyl Bromide in Pulse Radiolysis by GLC

Condition	Allyl Bromide Solution in Cyclohexane	Column Temp	Carrier Flow	Aliquot Injected	Retention Time	Peak Area in mg	Estimated Conc. of Allyl Br	Conc. of Allyl Br Decomposed 200 Pulse	Decomposition of Allyl Br per Pulse
Before Deseration	1.15×10^{-2} M	75°C	3	1 ml	17 min	7.1			
After Deseration (for 1-2 hr)	-	75°C	3	1 ml	17 min	1.7	2.75×10^{-3} M		
After 200 Pulse	-	75°C	3	1 ml	17 min	0.6	0.97×10^{-3} M	1.78×10^{-3} M	0.89×10^{-5} M

THE NATURE OF THE MOBILE AND TRAPPED SPECIES FORMED DURING THE γ-RADIOLYSIS OF FROZEN SYSTEMS

P. N. Moorthy
Chemistry Division, Bhabha Atomic Research Centre, Bombay 85

INTRODUCTION

The role of ionic processes in the radiation chemistry of both frozen aqueous systems[1, 2] and frozen organic systems[3, 4] is now well established. Investigations of the γ-irradiated frozen systems at temperatures in the region of 77°K by the techniques of electron spin resonance (ESR), light absorption and luminescence have all conclusively shown that the primarily formed chemically signficicant species in these systems are an electron (e^-) and a positive hole (h^+), that these species are mobile even in the frozen matrix at these low temperatures and that they can react with suitable acceptor solutes (scavengers) present as minor components in the system to give product species unambiguously identified as the reaction products of the electron and hole[1, 2, 3, 4]. Besides, the electron has also been identified in its 'trapped' state (T^-) in both frozen aqueous[5, 6] as well as organic[7, 8, 9, 10] systems. In the case of the positive hole, there is proof of its identification in the trapped state (T^+) in photolysed frozen aqueous systems[11]. Hole trapping in γ-irradiated frozen organic systems has also been reported[3, 4]. The purpose of this paper is to propose a model for the physical nature of the electron and hole, both in their mobile and trapped states, and to extend some of these ideas to explain certain aspects of the radiolysis of aqueous solutions.

THE SOLVATED ELECTRON CONCEPT

In the literature, the mobile electron (and some times the trapped electron also) is often referred to as a solvated electron and the hole a positive ion. According to the classical polaron model of the solvated electron developed by Davidov[12] and Diegen[13] and more recently by Jortner[14], the energy necessary for electron binding in a (polar) medium arises as the result of orientation of the pre-existing solvent molecular dipoles around the electron. Can the radiation produced electron and hole be solvated in a frozen matrix? The relaxation time for orientation of H_2O dipoles in ice at -196°C can be calculated to be 10^{+22} sec.[15]. The consequence of such a long relaxation time is that neither the hole nor the electron can polarise the surrounding medium by reorientation of the matrix dipoles which are, so to speak, 'frozen in' and therefore, the concept of solvation by 'self trapping' in a potential well created by oriented H_2O dipoles as in the case of liquid water is not valid for ice. However, polarization of the electronic clouds on the H_2O molecules around the positive hole or electron can still take place as the relaxation time for

such a polarization is very short ($\sim 10^{-15}$ sec) and is independent of temperature. The polaron model of the solvated electron has been recently reconsidered[16] and it is concluded that both in water and ice only the electronic polarization of the medium molecules is of significance in determining the binding energy of the solvated electron, or polaron. Presumably, the same would be the case with the hole also. A picture of the 'solvated' electron is depicted in Fig. 1.

With regard to the other radiolysed frozen systems, some consist of dipolar substances such as the alcohols and the ethers, and others non-polar e.g. the hydrocarbons. For the former, considerations similar to ice would apply. In the case of the non-polar ones, there is no question at all of solvation of the electron or hole by orientation of the matrix dipoles around the radiation produced species. So, for all the frozen systems, our conclusion is that solvation of the electron or hole cannot occur. In both cases only electronic polarisation of the matrix molecules around the charged species is possible.

INTERDEPENDENCE OF ELECTRON AND HOLE REACTIONS

During the course of our study of the radiolysis of frozen aqueous systems, we have found that the reactions of the mobile electrons and holes with the appropriate scavengers are interdependent. That is, no observable reaction takes place when the system contains a scavenger only for either the electron or the hole. Thus, e.g. the electron reacts with the powerful electron scavenger $CrO_4^{=}$ (or $Cr_2O_7^{=}$) only in either an alkaline (e.g. aq. NaOH) or acidic (e.g. aq. H_2SO_4 or H_3PO_4) system wherein the hole can simultaneously react with OH^- or HSO_4^- or $H_2PO_4^-$ ions[1]:

$$e^- + Cr(VI) \longrightarrow Cr(V)$$

$$h^+ + OH^- \longrightarrow OH \xrightarrow{OH^-} O^- + H_2O$$

$$h^+ + HSO_4^- \longrightarrow H^+ + SO_4^-$$

$$h^+ + H_2PO_4^- \longrightarrow HPO_4^-$$

Similarly, alcohols like ethanol and isopropanol, which are good hole acceptors, scavenge that species in the frozen aqueous system only in presence of an acid, in which case the protonated alcohol species (e.g. $CH_3CH_2OH_2.H_2O)^+$ simultaneously acts as the electron scavenger[17].

$$(CH_3CH_2OH_2.H_2O)^+ + e^- \longrightarrow CH_3\dot{C}HOH + H_2O + H_2$$

$$CH_3CH_2OH + h^+ \longrightarrow CH_3CH_2OH^+ \xrightarrow{CH_3CH_2OH} CH_3CHOH + CH_3CH_2OH_2^+$$

In γ-irradiated frozen organic (i.e. non-aqueous) systems also it has been observed[3, 4] that the yield of reaction product of the electrons is enhanced in presence of a hole scavenger and vice versa.

These observations can be explained on the hypothesis that the primarily formed electron and hole are not randomly distributed in the system but instead they move about as correlated electron-hole pairs. Thus, when a scavenger for only one of these species is present, the reaction product will be in such close proximity with the conjugate species as to immediately react with it; as a result no net change is observable:

$$\text{e.g. } X + e^- \longrightarrow X^-;\ X^- + h^+ \longrightarrow X$$

If the electron and hole are in such close proximity to each other, one would expect them to mutually recombine as a result of strong coulombic attraction. What is it that makes trapping in the matrix or chemical reactions with appropriate acceptor solutes possible in preference to such a recombination? One is immediately reminded of the hydrogen atom problem. Here, in the classical (Bohr) picture, the electron does not fall into the nucleus (proton) because the coulombic attraction between the nucleus and electron is balanced by the centrifugal force arising as a result of the motion of the electron in a closed orbit around the nucleus. The same idea can be extended to explain why the electron and hole prefer not to recombine at least over time intervals long enough for chemical reactions with scavengers to take place. Such a species viz., an electron rotating around the hole is known as an exciton in solid state physics.

Depending on their radii (i.e. electron-hole separation) excitons can be broadly classified into three types:

Separation between hole and electron	Resulting species
Very large ($>$ about 100 Bohr radii)	Separate or free hole-electron pair or ionized exciton
Large or intermediate ($\backsim$ 5 - $\backsim$ 100 Bohr radii)	Bound or neutral exciton - Wannier type (weak binding) - Possibility of polarexciton
Small or very small ($<$ 5 Bohr radii)	Lowest bound exciton state - Frenkel type (tight binding) - localized excited molecule - no possibility of polarexciton.

THE RADIATION PRODUCED MOBILE SPECIES

To which category do the excitons formed as primary species during the radiolysis of frozen systems belong? As is apparent from the experimental results mentioned earlier, they are not likely to be

separated or free hole-electron pairs. They are also possibly not of the Frenkel type, for in that case they would be equivalent to excited molecules in which case it would be difficult to explain the observed characteristic reactions of individual electrons and holes. Besides the excited molecule (or Frenkel exciton) concept cannot explain the formation of individual trapped electrons and trapped holes, for, in order to explain this, the excited molecule has to subsequently ionize and it is doubtful whether it will be endowed with enough energy to do so. The Wannier exciton does not meet with these difficulties and we conclude that the radiation produced mobile reactive species in the frozen systems belong to this category. In the case of the Wannier exciton, the electron and hole can individually polarise the matrix - the result being a negative or electron polaron bound to a hole polaron. One may call this a polar-exciton. A picture of this species in frozen systems is depicted in Fig. 2(b).

In the case of ice (and probably also water) one can give a more realistic picture of exciton motion. The dielectric properties of water and ice have been recently explained[18] on the basis of the existence of D- and L- defects in the medium (Fig. 3). An electron can get trapped at a D-defect and a hole at an L-defect (Fig. 4). As the D-and L- defects move about in the medium as correlated pairs so also would the electron-hole pair or the exciton move among pairs of D- and L- defects.

NATURE OF THE TRAPPED SPECIES

The results of thermal and photolytic (i. e. following light absorption) decay of the trapped electron in both the γ -irradiated frozen aqueous and frozen organic systems[3, 4] indicate that majority of the total number of (trapped) electrons are trapped close to the trapped hole. Several different mechanisms have been put forward to explain this trapping process[5, 19, 20]. Without going into the details of these we propose here a mechanism that is immediately obvious from the nature of their precursor mobile species which we consider to be polarexcitons. When the polarexciton encounters a 'trapping site' wherein the matrix molecules exist pre-oriented (forming a sort of cage) the hole undergoes the reaction:

(RH is any molecule in general; not necessarily a hydrocarbon)

$$h^+ + RH \longrightarrow RH^+$$

$$RH^+ + RH(RH)_n \longrightarrow \dot{R} + RH_2^+(RH)_n$$

and the resulting species $RH_2^+(RH)_n$ can trap the electron in an expaned orbital, the positive charge on RH_2^+ inducing electronic polarization of the neighbouring pre-oriented RH molecules in a manner favourable for trapping the electron. This is pictorically depicted in Fig. 5. This picture is rather similar to the one we have proposed[5] to explain the trapped electron in γ -irradiated frozen alkali hydroxide systems and can also account for the effect of glassy phase on electron trapping.

Finally, we would like to mention very briefly our recent finding which suggests that the radiation produced mobile species (polarexcitons) may be triplet excitons. On γ-irradiation of frozen aqueous H_2SO_4 solutions one finds ESR signals attributable to H atoms (product of electron reaction) and SO_4^- ions (product of hole reaction)[1]. But in presence of paramagnetic transition metal ions such as Co^{+2} and Ni^{+2}, both of these signals were not found. It is known[21] that paramagnetic ions can deactivate a triplet excited state by spin exchange. Our experimental result would be explicable if the species formed by the radiation and responsible for the formation of H atoms and SO_4^- ions in the absence of Co^{+2} and Ni^{+2} are triplet excitons.

'SPURS' AND EXCITONS

Does all the radiation energy absorbed by a system give rise to Wannier excitons only? It is possible that in every case all the three types of excitons mentioned above are formed, their relative proportion depending on the physical properties of the system such as state of aggregation, intermolecular interactions etc. What are usually referred to as 'spurs' in radiation chemistry may consist of Frenkel excitons. For example, in water, the interaction between two Frenkel excitons can explain the formation of the 'molecular' products:

$$F + F = H_2O^* + H_2O^* \longrightarrow H_2 + H_2O_2 \text{ (in 'spurs')}$$

On the other hand, the reaction between a Frenkel and a Wannier exciton:

$$F + W = H_2O^* + e^-,\ h^+ \rightarrow \dot{H} + OH^- + h^+ \longrightarrow \dot{H} + \dot{O}H$$

(some distance away from 'spurs')

or that between two Wannier excitons:

$$W + W = e^-,\ h^+ + e^-,\ h^+ \longrightarrow e^-,\ h^+ + h^+,\ e^- \text{ (in 'bulk')}$$

(no change)

would not lead to the 'molecular' products. Wannier excitons, on the other hand, can react with solutes in the 'bulk'.

REFERENCES

1. P. N. Moorthy and J. J. Weiss; Advances in Chemistry Series 50 180 (1965)
2. L. Kevan; "Chemical Reactions of Radiation Produced Electrons in Ice and in Organic Solids" in "Progress in Solid State Chemistry" (Ed. H. Reiss) Vol. I (1964)
3. W. H. Hamill; in "Radical Ions", (Ed. L. Kevan) John Wiley and Sons (1968)

4. J. E. Willard in "Fundamentals of Radiation Chemistry" (Ed. P. Ausulos) , John Wiley and Sons (1968)
5. P. N. Moorthy and J. J. Weiss; Phil. Mag. 10, 659 (1964)
6. K. Eiben and I. A. Taub; Nature 216, 782 (1967)
7. C. Chachaty and E. Hayon; J. Chim Phys. 61, 1115 (1964)
8. B. G. Ershov, P. N. Moorthy and K. V. Lingam; Ind. J. Chem. 4, 494 (1966)
9. D. R. Smith and J. J. Pieroni; Can. J. Chem. 44, 876 (1965)
10. D. W. Skelly and W. H. Hamill; J. Chem. Phys. 44, 2891 (1966)
11. P. N. Moorthy and J. J. Weiss; J. Chem. Phys. 42, 3127 (1865)
12. A. S. Davidov; J. Exptl. and Theoret. Phys., USSR, 18, 913 (1948)
13. M. F. Deigen; ibid. 26, 300 (1954)
14. J. Jortner; J. Chem. Phys. 27, 823 (1957), 30, 839 (1959)
15. R. P. Auty and R. H. Cole; J. Chem. Phys. 20, 1309 (1952)
16. P. N. Moorthy and J. Shanker; Radiation Effects Journal (in press)
17. C. Gopinathan, P. N. Moorthy and K. N. Rao; Ind. J. Chem. 6, 749(1968)
18. L. Onsager and L. K. Runnels; J. Chem. Phys. 50, 1089 (1969)
19. J. Jortner and B. Sharf; J. Chem. Phys. 37, 2506 (1962)
20. M. J. Blandamer, L. Shields and MCR Symons; Nature 199, 902(1963)
21. J. W. T. Spinks and R J. Wood; An Introduction to Radiation Chemistry, John Wiley and Sons, p. 134 (1964)

FIGURES

1. Solvated electron: (a) with orientational polarisation (b) with electronic polarisation, (density of dots indicates electron density).

2. The polarexciton (a) with orientational polarisation (b) with electronic polarisation, (density of dots indicates electron density).

3. D- and L-defects in water and ice.

4. Trapping of electron and hole at D- and L-defects in water and ice.

5. The trapped electron.

DISCUSSION

C. Gopinathan : It is not quite correct to say that H_2O^+ and e^-_s always act as a pair and whenever one is removed you see the reaction of the other. H^+ ions seem to be necessary to see the production of SO_4^- radical; for example, in a frozen Na_2SO_4 solution common electron scavenger like MnO_4^- does not seem to be sufficient to produce SO_4^- ions on gamma irradiation.

P. N. Moorthy : This can be explained on the assumption that it is the HSO_4^- ion (and not $SO_4^=$ ion) that reacts with the holes according to :
$h^+ + HSO_4^- \longrightarrow H^+ + SO_4^-$

J. P. Mittal : (1) If I remember right, did you say that, one never sees solute reactions in the radiolysis if the solute reacts only with one of the transients i. e. either with $\bar{e}_s$ or hole ?
(2) But it does not seem to hold good for organic systems. One example which comes offhand to mind is production of CO_2 anion in 3 methyl pentane.
(3) No, No, ion molecule reaction :

$$RH^+ + RH \longrightarrow RH_2^+ + R.$$

is about 80 kcal/mole endothermic in case of 3 MP or cyclohexane.

P. N. Moorthy : (1) Yes, that is right, at least in the case of frozen aqueous systems studied by us. (2) Here, I guess, the holes are trapped in the matrix itself, and this can be formally considered to be a reaction of the holes with the matrix itself., the electrons react with CO_2. (3) That refers to gas phase, I believe. In a frozen matrix this reaction as depicted in Fig. 5 may not be endothermic.

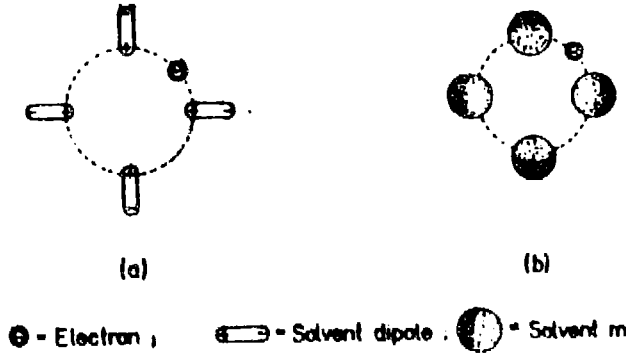
(a)
(b)
⊖ - Electron ;
- Solvent dipole ;
- Solvent molecule

Fig 1

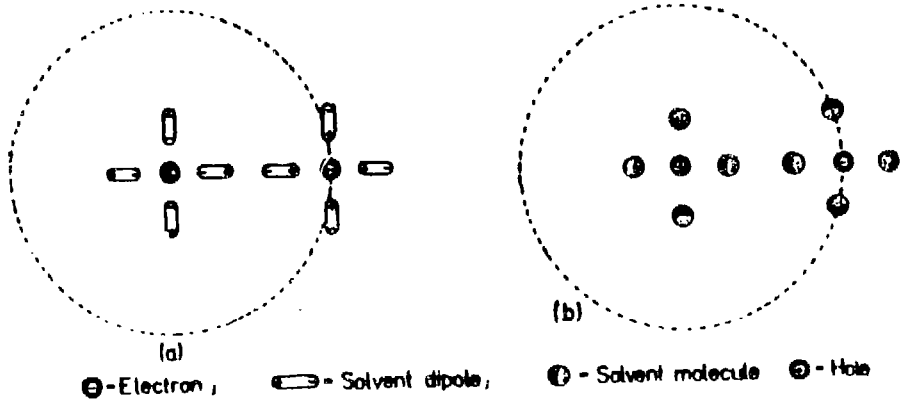
(a)
(b)
⊖ - Electron ;
- Solvent dipole ;
- Solvent molecule
⊕ - Hole

Fig 2

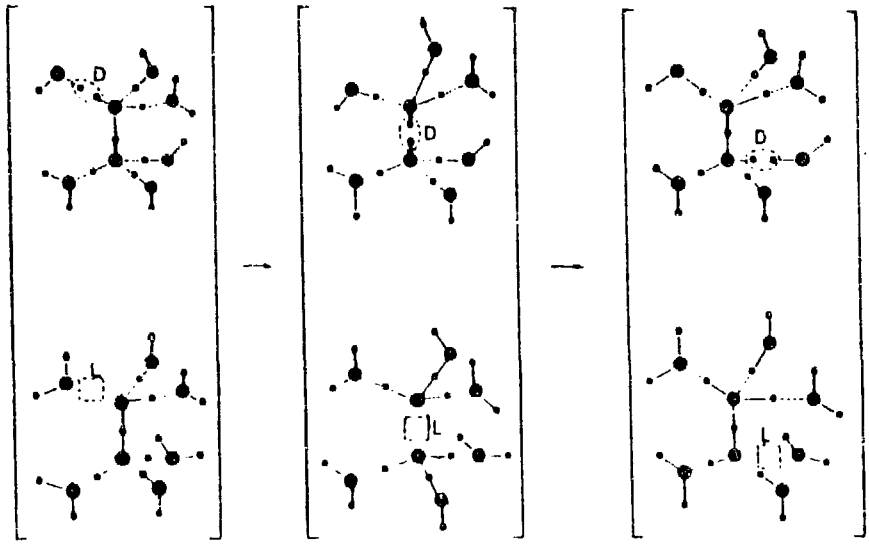

● - Oxygen atom, • - Hydrogen atom
— - Covalent bond, ··· - Hydrogen bond

Fig 3

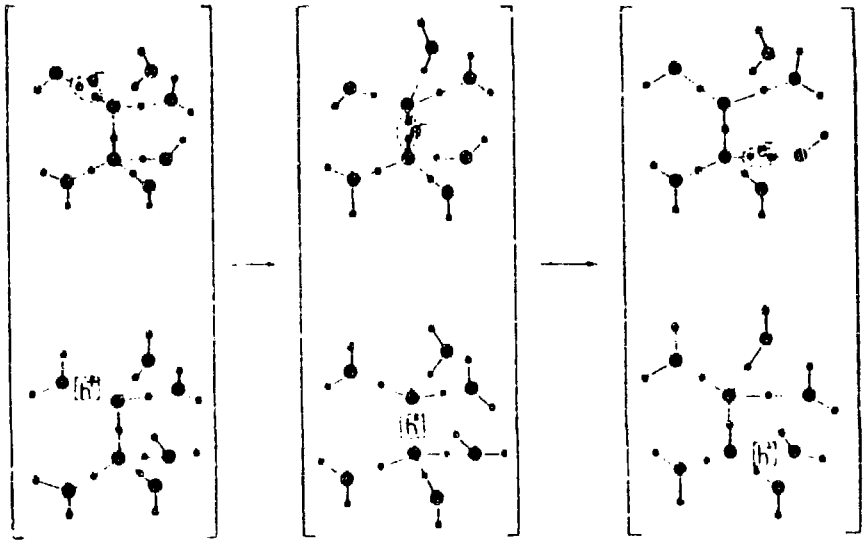

● - Oxygen atom; • - Hydrogen atom
— - Covalent bond; ····· - Hydrogen bond

Fig 4

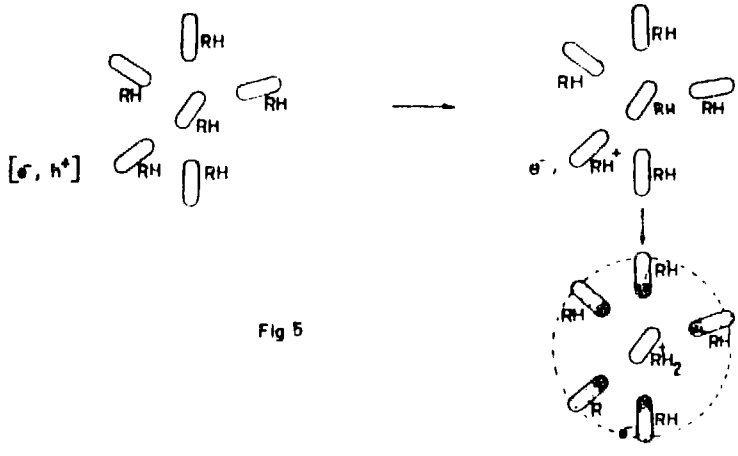

Fig 5

A HOMOGENEOUS KINETICS MODEL OF AQUEOUS RADIOLYSIS

Chakrapany Gopinathan
Chemistry Division, Bhabha Atomic Research Centre, Bombay 85

Until recently, molecular product formation in aqueous radiolysis was explained on the basis that the radicals H and OH diffused out of the initial "spur" - the diffusion kinetics model, originally due to Samuel and Magee. A detailed review of this has been given by Kuppermann[1]. After the discovery of the solvated electron, this was incorporated into the original model by attributing part of the H_2 yield to reactions involving solvated electrons (e.g.)[2].

There has been a considerable amount of critisism recently of the above model. The most important of these is the fact that the effect of solutes on the molecular product yields is not properly explained. This discrepancy has been clearly pointed out by Sworski.[3]

Recent nanosecond pulse radiolysis work[4] also appears to throw some doubt on the existence of spurs, atleast as far as solvated electrons are concerned. After 0.5 nanoseconds, there does not seem to be any decrease in solvated electron concentration. This means that the spur reactions should be over by this time limit.

The diffusion model can also be criticised on the ground that it involves too many "a priori" assumptions. The initial radius of the "spur", for example, has to be about 13Å[2] to get reasonable agreement with the solute results. This should be compared with the de Broglie radius of the thermalised electron of $\sim$60 Å!

Some attempts have been made in recent years[3, 5, 6] to develop a model which does not involve diffusion kinetics. The model being presented here is thought to be an improvement on the earlier models.

The present model involves mobile energy as the main source of molecular products. One well-known way by which energy transfer takes place in ordered solids is the exciton mechanism. The general definition of an exciton is a quantum of mobile electronic excitation. Of the two types of excitons known, only Frenknel, or tight bound excitons are expected to be involved in aqueous radiolysis since the Wannier, as loose bound excitons, would need conduction bands for migration.

Water is a relatively ordered structure because of strong hydrogen bonding. 2/3^{rds} of ice structure is said to persist in liquid water at room temperature. From a short time point of view, water is essentially a crystalline solid with a large number of defects. Therefore, the range of excitons in liquid water is likely to be short. Moreover, their lifetime

will be less than the time needed for rotational relaxation in water, i. e. 10^{-11} seconds.

Molecular product formation is envisaged as follows:

$$\text{exciton} + \text{exciton} \longrightarrow H_2O_2 + H_2$$

It is postulated that two excitons produced close to each other migrate across the ice structure and encounter each other, producing a highly localised concentration of energy resulting in the rearrangement of two neighbouring water molecules to produce H_2 and H_2O_2. If an exciton can be regarded as a periodic wave in an ordered matrix, then the encounter of the two waves can produce a standing wave which is stationery for a sufficiently long period to transfer its energy to the vibrational modes of water molecules close to it, resulting in bond rearrangement.

$$(H_2O + H_2O)^{**} \longrightarrow H_2 + H_2O_2$$

The excitons might arise in three ways. (a) from the simple neutralisation of H_2O^+ by the electron or (b) from the energy released by the fast proton transfer reaction,

$H_2O^+ + H_2O \longrightarrow H_3O^+ + OH$, or from the neutralisation reaction,

$H_3O^+ + OH^- \longrightarrow 2H_2O$. In any case, triplet excited states are likely to be involved rather than singlet excited states because of energy considerations.

The probability of an exciton-exciton encounter will be high only where these are produced close together. Two types of such encounters are envisaged. The first inside the classical "spurs" and second along the track of the ionising particle. This second type of encounter also has to be considered because wherever there is a chain of hydrogen bonded water molecules connecting together two exciton producing events, their encounter becomes possible. Those of the excitons which do not encounter other excitons move on until they encounter a defect in the ice structure when they undergo unimolecular decay by either getting converted into phonons or by fluorescent radiation emission.

The decrease in molecular product yield with increasing solute concentration arises by the scavenging of excitons. This need not necessarily arise only through a transfer of excitation. The presence of a solute provides a 'defect' point in the water structure which enables unimolecular decay to take place. It is easy to see how molecular products can never be completely eliminated by scavengers, while long range encounters (relatively) such as track interactions and those in outer part of the spur can be prevented. Very short range encounters where a high localised deposition of energy has occurred cannot be prevented. Small

localised water structures are likely to exist even in the presence of high concentrations of scavengers.

It is obvious that ejected secondary electrons can have a wide spectrum of energy from hundreds of Kev to a few ev. Recent attempts to remedy this defect in the earlier Samuel-Magee model, tried to split up the electrons into a number of arbitrary groups for purposes of calculations. In the present model only two kinds of electrons are recognised i. e. (i) those which return to the site of creation and (ii) those that do not. The very wide range of energy distribution makes it necessary that such a distinction should exist. The returning electrons give rise to excitons as described earlier. Those that do not, give rise to solvated electrons whose only non-uniformity in distribution is along the tracks.

The net increase in water decomposition at high solute concentrations is caused by exciton + solute reactions, e.g.,

$$h\nu + H_2O + ClCH_2COOH \longrightarrow Cl^- + .CH_2COOH + H^+ + OH$$

A similar reaction in frozen systems has been postulated recently.[7] LET effects are also explainable on the basis of the present model as a merger of track exciton interactions with the spur interactions.

At the moment the model is admittedly semi-quantitative. But by fitting in the necessary parameters, it is hoped that it can be made rigorously quantitative.

REFERENCES

1. A. Kuppermann; in "The Chemical and biological actions of radiations"., Vol. 5, Academic Press, New York (1961)

2. H. A. Schwarz; Radiation Research, Supplement 4, 89 (1964)

3. T. J. Sworski; Advances in Chemistry series 50, 263 (1965)

4. J. K. Thomas; Radiation Research 32, 149 (1967)

5. V. V. Voevodski; Proceedings of the Second All Union Conference on Radiation Chemistry, Translated by Israel Program for scientific Translations p. 103 (1964)

6. W. H. Hamill; J. Chem. Phys. 49, 2446 (1968)

7. F. S. Dainton and C. Gopinathan; Trans. Faraday Soc. 65, 143 (1969)

DISCUSSION

P. N. Moorthy : (i) Do you choose to think that all the excitons in frozen aqueous systems are of the Frenkel type ?

(ii) If so what is your mechanism for the trapped electron formation in frozen aqueous alkali hydroxide ?

Chakrapany Gopinathan: (i) Yes. I have chosen Frenknel excitons and ignored the Wannier excitons because the latter require conduction bands which may not exist in liquid water. Moreover, elegant mathematical treatment is possible with the concept of Frenknel excitons.

(ii) Trapped electrons have nothing to do with excitons. They are formed in the conventional way from the electrons that do not return to the parent site, but get trapped. So, their formation does not affect the model.

RADIATION DECOMPOSITION OF COBALT HEXAMINE NITRATE IN SOLID MATRICES

S. B. Srivastava and A. S. Sarpotdar
Chemistry Division, Bhabha Atomic Research Centre, Bombay 85

INTRODUCTION

Earlier[1, 2] it has been reported that the radiolysis of substances is considerably influenced by the matrix, but so far no quantitative correlation has been shown between the radiation damage produced in the matrix and the sensitised decomposition. The present study attempts to evaluate quantitatively the role of various sensitising species produced in the matrix and measure their yields.

EXPERIMENTAL

Cobalt hexamine nitrate was prepared by known methods. Alkali halide matrices employed were of A. R. quality. Pellets were produced in a die by applying pressure of 200 kg/cm^2 for a few minutes. No measurable decomposition was observed on compression.

Irradiations at 77°K were carried out in Dewar flasks. γ-doses were measured using Fricke dosimeter. Appropriate corrections were applied to calculate the dose absorbed by the sample.

Nitrite yields were estimated by Shinn's method[3] through diazotisation and measurement at 538 nm and Co^{2+} by thiocyanate method[4] in methyl isobutyl ketone at 620 nm.

RESULTS AND DISCUSSION

Nitrite yields obtained on undoped samples and those doped with 99% KBr in powder as well as in pellet form at 300°K are given in Fig. 1. It is seen that the yield vs dose curve is linear upto a dose ~35 Mrads. Also, the relative yields in doped samples are 1 - 2 orders higher than those in undoped samples. When the samples were irradiated in pellet form at 77°K, the nitrite yields in both the undoped and doped samples were 2 - 4 times higher than those at 300°K. Similar studies were also made using KI and KCl matrices in powder form at 300°K. Results are shown in Fig. 2. It would be seen that the efficiency of sensitisation follows the order KCl < KBr < KI. For example, at a dose ~30 Mrads, the corresponding ratios are 1:5·40.

Samples of complex containing variable % of KBr (0-90) were exposed to a fixed dose of 15 Mrads and the $G(NO_2)$ and $G(Co^{2+})$ values were evaluated. These are tabulated in Table I. It is seen that Co^{2+} yield is relatively insensitive to the presence of matrix.

TABLE I

$G(NO_2)$ and $G(Co^{2+})$ in KBr Matrix Irradiated in Powder form to 15 Mrads at 300°K

%KBr in the sample	$G(NO_2)$	$G(Co^{2+})$
0	0.06	2.10
10	0.23	1.63
20	0.39	1.12
30	0.55	0.84
40	0.71	0.58
50	0.74	0.45
60	0.62	0.36
70	0.54	0.30
80	0.47	0.20
90	0.33	0.17

Similarity of kinetics in the doped sample (Fig. 1) observed in the present study to that reported earlier in undoped nitrate[5] suggests similar modes of decomposition. Recent studies[6] have shown that the primary excited species formed in the radiolysis of nitrate are:

$$NO_3^{*} + e \longrightarrow NO_3^{-**} \quad (1)$$

$$\longrightarrow NO_3^{-*} \quad (2)$$

$$e + NO_3^{-} \longrightarrow NO_3^{2-*} \quad (3)$$

where * and ** represent allowed and forbidden states respectively. These on decomposition yield NO and NO_2 which are estimated by Shinn's method as nitrite.

The above mechanism implies that the presence of excess electrons would promote in our system radiolysis of nitrate. Irradiation of alkali halides produces electrons, holes and excitons. In case electrons and holes are captured by impurities, the radiolysis of impurity is promoted. Otherwise, either they are stabilised by defects or else recombine with each other. Since the defect concentration is less in more

ordered systems (pellet form as compared to powder form) more electrons are likely to be available for electron attachment to nitrate anion and hence a higher yield of nitrite is expected in pellet form. Also, Jacckard[7] has shown that NO_3^{2-} yield in halide matrix follows the order KCl < KBr < KI. This again implies that the relative availability of electrons in these matrices also follows the same order. Consequently, NO_2 yield at a fixed dose should follow a parallel order. Fig. 2 confirms this assumption.

Furthermore, if $G(NO_2)$ = G(e) untrapped, the extrapolation of $G(NO_2)$ vs % KBr plot to 100% KBr would yield G(e) untrapped. This value has been found to be ~1.75 (at 300°K).

Cobalt hexamine cation could also react with electrons or holes (present as dihalide anion X_2^- at 77°K) as follows

$$CO(NH_3)_6^{3+} + e \longrightarrow CO(NH_3)_6^{2+} \qquad (4)$$

$$CO(NH_3)_6^{3+} + X_2^- \longrightarrow CO(NH_3)_6^{2+} + X_2 \qquad (5)$$

$$CO(NH_3)_6^{3+} + X_2^- \longrightarrow CO(NH_3)_6^{4+} + 2X^- \qquad (6)$$

Reactions (4) and (5) would yield Co^{2+} whereas reaction (6) would give product which could stabilise as cobaltic hexamine on dissolution. Since the radiolysis of cation has been found to be insensitive to the presence of matrix, reactions (4) and (5) do not seem to occur in this system at 300°K. Localisation of exciton, if at all, also seems to be ineffective.

REFERENCES

1. A. R. Jones; J. Chem. Phys. 35, 751 (1961)
2. Yu. A. Zakharov and V. A. Nevostruev; Russian J. Phys. Chem. 42, (5), 604 (1968)
3. J. Cunningham; J. Phys. Chem. 67, 1772 (1963)
4. D. Katakis and A. O. Allen; J. Phys. Chem. 68, 359 (1864)
5. Chen and Johnson; J. Phys. Chem. 66, 2249 (1962)
6. J. Cunningham; 475 Radical Ions, Edited by E. T. Kaiser and L. Kevan, Interscience Publishers (1968)
7. C. Jaccard; Phys. Rev. 124, 60 (1961)

DISCUSSION

J. P. Mittal : What is the mechanism of energy transfer from major constituent ? Do you consider it can be "F" center from KBr or they are ionic in nature ?

S. B. Srivastava : Energy transfer appears to be through localization of electrons and holes on cobalt hexamine nitrate in preference to their recombination or being trapped on defect centres in the host matrix. The latter is obviously responsible for production of colour centres in alkali halides.

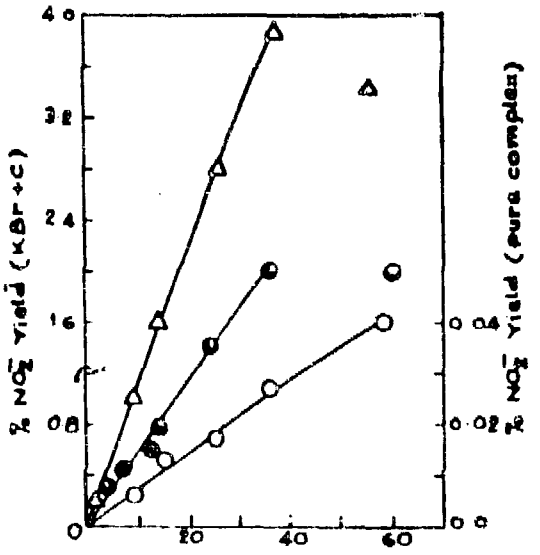

Fig 1 γ-Radiolysis done at 300°K

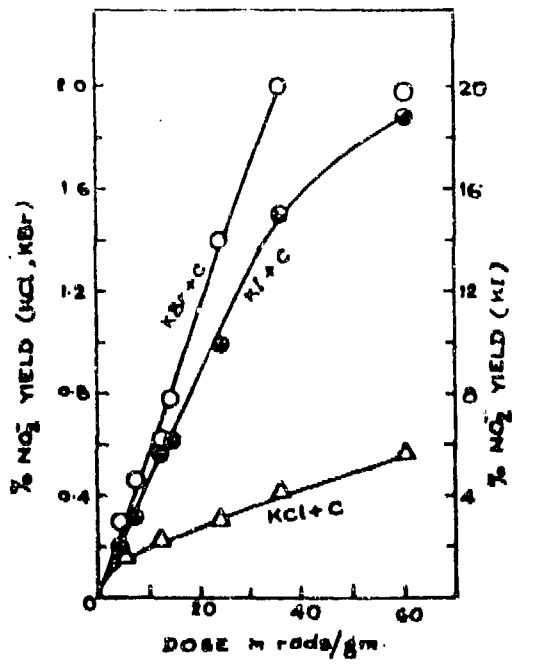

Fig. 2. 1% COMPLEX IN ALKALI HALIDES.
γ-Radiolysis done at 300°K.

RADIOLYSIS OF SOLUTIONS CONTAINING TRIS(ACETYLACETONATO) COBALT(III) IN DIFFERENT SOLVENTS

K. V. S. Rama Rao, A. V. Sapre and L. V. Shastri
Chemistry Division, Bhabha Atomic Research Centre, Bombay 85

INTRODUCTION

On γ-radiolysis, the ionisation of the medium molecules leads to the production of ion-pairs the geminate recombination of which depends, among other influences, on the dielectric constant of the medium and the initial intermediate distance between the components of the pair. The latter does not seem to have a unique value but ranges from a few molecular distances to a few hundred of angstroms. Thermalisation of sub-excitation electrons is not a well understood process below 0.4 ev and probably involves wide angle scattering leading to varying degrees of separated ion-pairs. Conductivity experiments[1] show that ions do escape recombination and the escape probability is satisfactorily given by the Onsager's expression[2] $\exp -r_e/r$. The escape distance r_e is given by $r_e = e^2/\epsilon kT$ where e is the electronic charge and ϵ the dielectric constant of the medium. For a dipolar medium, the static and high frequency values of ϵ are greatly different and the choice of one or the other for defining the free ion formation is not unambiguous. In this paper we will consider the results of radiolysis of solutions of tris-(acetylacetonato) cobalt(III) to experimentally define the problems of ion escape and recombination and attempt to partially answer these questions.

EXPERIMENTAL

Tris-(acetylacetonato) cobalt(III) and Bis (acetylacetonato) cobalt (II) were prepared following standard techniques of synthesis[3]. In this paper, Co(III) complex is implied unless otherwise stated. Triple distilled water, Fluka spectro grade cyclohexane and recrystallised benzene were used. Fluka MTHF was purified by bulb to bulb distillation on sodium mirror and sealed in ampoules which were opened only for purposes of immediate use. A 2-kilo curie cobalt source of 0.4 megarad intensity was used as irradiation source.

RESULTS AND DISCUSSION

Solutions of the cobalt(III) complex in water and cyclohexane are quite stable and the absorption spectra show the characteristic peaks which have been recently characterised[4]. MTHF solutions of the complex are unstable and show shifts in absorption spectra on keeping overnight. The solvent replacement of the ligand is a possible reason. Only

fresh solutions of MTHF were therefore used and the solutions were kept for a maximum cumulative period of 30 minutes at room temperature while degassing by freeze-thaw technique, irradiation and analysis. Unirradiated blanks showed negligible decomposition of the complex during this time. Figure 1 compares the spectra of irradiated and unirradiated solutions of the complex in cyclohexane and the differential spectrum shows an absorption maximum at 280 mμ characteristic of bis (acetylacetonato) cobalt(II) in this solvent.

The total cobaltous has been determined as $G(Co^{++}) = 5.7$ in water[5] and agrees with the relation $G(Co^{++}) = G_{e^-_{aq}} + G_H + G_{OH}$.

$G(Co^{++})$ in the solvents under study are summarised below:

Solvent	$Co(acac)_3$	$G(Co^{++})$	$G(H_2)$
Water pH = 6.5	4.0 to 8.4 x 10^{-4}M	5.7	0.45
50% Water + 50% ethanol	1 x 10^{-3}M	4.5*	2.5 (4.0)
	6 x 10^{-4}M	1.7	3.6
MTHF	1.0 x 10^{-3}M	2.8	(3.8)
	1.7 x 10^{-3}M	**3.5	3.6
Cyclohexane	4 x 10^{-5}M	0.2	5.4 (5.6)
	1 x 10^{-3}M	0.24	5.3
10% MTHF + 90% Cyclohexane	6 x 10^{-4}M	0.29	3.0 (3.6)
Benzene	5 x 10^{-3}M	0.03	0.037 (0.037)

$G(H_2)$ values in bracket refer to those for the solvent.

*Includes contribution from the reduction of the complex by the organic free radical. The electron contribution is estimated as 1.5.

**Includes contribution due to the reduction of the complex by the organic free radical. The electron contribution is estimated as ~0.8 from experiments at 77°K.

The rate constants for the reduction of the complex by e^-_{aq} and H have been evaluated in aqueous solutions as $4.0 \times 10^{10} M^{-1}$ sec^{-1} and $\geq 4 \times 10^9 M^{-1}$ sec^{-1} by competition kinetics[5]. Allowing for the change in the former with the dielectric constant in another solvent we surmise

that the reduction of the complex in both cyclohexane and benzene could only be due to electron reaction since the solvents are quite capable of reacting with all the H in the presence of low concentrations of the complex. The lack of influence of the complex on $G(H_2)$ from benzene is understood because the excited state responsible for H_2 production is different from the one responsible for luminiscence in p-terphenyl solutions of benzene[6]. The precursor of the latter $^1B_{2U}$ state is possibly an ion-pair which is susceptible to an inefficient scavenging by our present solute. The lack of influence of the complex on $G(H_2)$ from MTHF solutions is surprising but conforms to some of our other results with N_2O solutions of MTHF. For cyclohexane solutions $\Delta G(H_2) \geq G(Co^{++})$ and for the mixed solvent system of 10% MTHF + 90% cyclohexane $\Delta G(H_2) \simeq 2G(Co^{++})$. Further, the observed decrease in $G(H_2)$ from 5.6 for pure cyclohexane to 3.6 for 10% MTHF solution is much lower than the expected value of 5.4 for the latter based on electron density considerations and this departure from the expected mean is almost certainly due to

$$C_6H_{12}^+ + MTHF \longrightarrow C_6H_{11} + MTHFH^+ \qquad (1)$$

and verifies Toma and Hamill's[7] proposed reaction

$$C_6H_{12}^+ + e^- \longrightarrow 2H + C_6H_{10} \qquad (2)$$

which is replaced to the extent of reaction (1) by

$$MTHFH^+ + e^- \longrightarrow H + MTHF \qquad (3)$$

Thus the difference 5.4 - 3.6 = 1.8 is G(proton exchange) if all $G(H_2) = 5.6$ in pure cyclohexane arises as a consequence of (2). The observation that $G(e^-)$ is enhanced to its upper limit in 10% MTHF solutions in 3-methyl pentane glass at 77°K[8] supports this view.

The remarkable difference in the degree of electron scavenging by a very efficient solute such as this complex at comparable low concentrations in these solvents clearly indicates a considerable electron escape in dipolar solvents such as water and an efficient geminate recombination in non-polar hydrocarbons. Further, presence of 10% MTHF in cyclohexane is ineffective in markedly enhancing $G(Co^{++})$ although in a frozen glass of 10% MTHF + 90% 3-methylpentane, the immobilisation of proton apparently enhances $G(e^-)$. In liquids, the solute competes very inefficiently with the geminate reaction (3) of the correlated pair. Since the electron contribution to the total reduction of $G(Co^{++}) = 5.7$ is at least 2.8 in water[5], which is the lower limit for the electrons escaping geminate reaction, it appears that the low frequency dielectric constant $\epsilon_s = 80$ should make a significant contribution in evaluating the escape probability using Onsager equation. Since the escape distance r_e for $\epsilon_s = 80$ is 7 Å and for $\epsilon_{op} = 4.9$ is ~ 100 Å, a

significant formation of persistent ion pairs undergoing geminate recombination in presence of solutes would be erroneously predicted if the optical dielectric constant only applies. The basis for using ϵ_{op} is understandably the fact that electron thermalisation ensues within 10^{-13} sec. while the dielectric relaxation time leading to electron solvation is as high as 10^{-11} sec. However, ϵ_{op} leads to an untenable result and does not explain the hydrated electron formation. A recent suggestion from Mozumder[9] is that electron solvation occurs in 10^{-13} sec. Once the electron is solvated, the static dielectric constant needs to be applied. This does not necessarily rule out all geminate reaction as the times for electron return and electron solvation and consequent escape are now comparable. Whether the molecular yields and independent H indeed result from such geminate reaction or correlated ion pair formation[5, 10] is a debatable point but they are the most likely products to have such precursors. An interesting corollary is the trapping of electron as a metastable exciton and there seems to be some justification for such a view for MTHF radiolysis and to a lesser extent for water radiolysis. We may point out that not yet thermalised but relatively hot sub-excitation electrons are particularly susceptible for such trapping as Wannier type excitons if they find themselves at favourable distances from holes where the Couloumb force balances the outward centrifugal force.

ACKNOWLEDGEMENT

The authors take pleasure in thanking Dr. J. Shankar, Head, Chemistry Division, for his keen interest in this work and helpful discussions with him.

REREFENCES

1. A. Hummel and A.O. Allen; J. Chem. Phys. 44, 3426 (1966); K.H. Schmidt and W.L. Buck; Science 151, 70 (1966)

2. L. Onsager; Phys. Rev. 54, 554 (1938)

3. B.E. Bryant and W.C. Fernelius; Inorg. Synth. 5, 188 (1958); R.G. Charles and M.A. Pawlikoushi; J. Phys. Chem. 62, 440 (1958)

4. I. Hanazaki, F. Hanazaki and S. Nagakura; J. Chem. Phys. 50, 265 (1969)

5. K.V.S. Rama Rao, L.V. Shastri and J. Shankar; Radiation Effects (To be published)

6. M. Burton; Z. Electrochem. 64, 975 (1960); J.L. Kropp and M. Burton; J. Chem. Phys. 37, 1752 (1962)

7. S. Z. Toma and W. H. Hamill; J. Am. Chem. Soc. 86, 1478 (1964)
8. J. B. Gallivan and W. H. Hamill; J. Chem. Phys. 44, 2378 (1966)
9. A. Mozumder; J. Chem. Phys. 50, 3153 (1969)
10. W. H. Hamill; J. Chem. Phys. 49, 2446 (1968)

DISCUSSION

J. P. Mittal : I would like to point out that recently we have also obtained strong evidence for reactions like $C_6H_{12}^+ + MTHF \longrightarrow C_6H_{11} + MTHFH^+$. In fact this happens with many bases like ethanol, acetone etc.

Ref: (i) J A C S, 89, 548 (1967) footnote 12.
(ii) J. P. Mittal; Ph. D. Thesis, University of Notre Dame, Sept. 1967.

K. V. S. Rama Rao : The large decrease in $G(H_2)$ observed in 10% MTHF solutions in cyclohexane not only supports the view of proton exchange to bases (Cf. F. Williams, J. Am. Chem. Soc. 86, 3954 (1964)) but also presents evidence for the reaction $C_6H_{12}^+ + e^- \longrightarrow 2H + C_6H_{10}$ which was proposed by Hamill only on the basis of indirect data.

P. N. Moorthy : i) Even in the case where the electron is within a distance of ~ 7 Å from the positive ion, we can still conceive of a Wannier exciton

ii) Perhaps, by way of a general picture, one can assume the presence of all the three types of species, viz. Frenkel and Wannier excitons and randomly distributed free holes and electrons, their relative proportion depending on the physical properties of the medium.

K. V. S. Rama Rao : Neutralisation process of an ion-pair may lead to a Frenkel exciton but more likely to excited molecule. One can conceive of a Wannier exciton formation as the secondary electron thermalises. But whether excitons are actually formed in liquid systems (cf. S. A. Rice and J. Jortner J. Chem. Phys. 44, 4471 (1966)) and whether they have any meaningful life times are highly speculative ideas lacking experimental evidence or firm theoretical basis. As of now, most radiation chemistry seems to be satisfactorily explained by the ion-pair and excited molecule mechanisms.

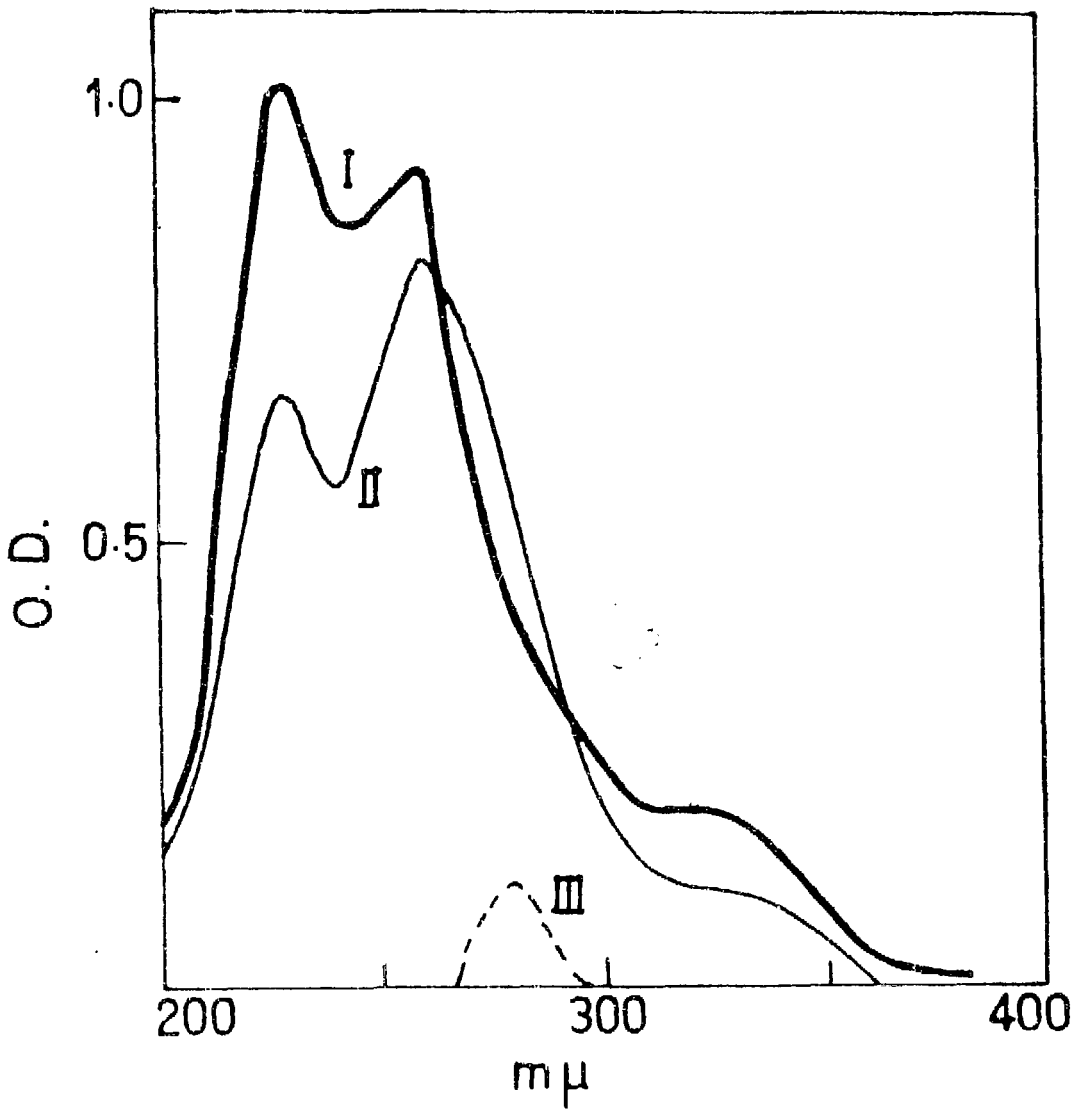

Fig. Absorption spectra in cyclohexane solution.

I —— 4×10^{-5} M $Co(acac)_3$ unirradiated.

II —— 4×10^{-5} M $Co(acac)_3$ irradiated to 4×10^{21} ev/l

III ---- Difference.

OXIDISED PRODUCT YIELDS IN THE GAMMA RADIOLYSIS OF FROZEN GLASSY SULPHURIC ACID

Chakrapany Gopinathan
Chemistry Division
Bhabha Atomic Research Centre, Trombay, Bombay-85

Considerable interest has been shown in recent years in the gamma radiolysis of glassy sulphuric acid at 77°K[1, 2]. This substance shows the remarkable property of being able to transport radiation produced electrons over long distances. Exciton and hole reactions are also possible in frozen sulphuric acid systems under certain conditions[2, 3].

Even though products of electron and H atom reactions have been estimated in frozen, glassy (~5M) sulphuric acid, so far oxidised products of radiolysis such as H_2O_2 and per acids have not been measured. The present work is an attempt to remedy this gap.

EXPERIMENTAL

All chemicals used were of analytical reagent grade. The water used was triply distilled in the normal way. A. R. grade ceric sulphate was dried in a hot air-oven at 80°C for 3 hours before being dissolved in sulphuric acid. The stock solution of Ce^{+4} was kept wrapped in aluminium foil to exclude light. Ce^{+4} concentrations were measured by measuring the O. D. at 315 m u and 320 m u. The difference in the optical densities at these two wave lengths was negligeble.

All irradiations were done at 77°K with the samples immersed inside liquid nitrogen. The dose rate of the Co^{60} source used was measured with a fricke dosimeter and was corrected for electron density and decay. Unless otherwise mentioned, all samples were undegassed.

H_2O_2 was measured by adding a standard Ce^{+4} solution to the melted sample and measuring the decrease of $[Ce^{+4}]$. Per acids were measured by adding a known amount of a standard ferrous ammonium sulphate solution and measuring Fe^{+3} formed, spectrophotometrically, after a minimum period of 1 hr. Per monosulphuric acid reacts very quickly with Fe^{+2}. However, per disulphuric acid reacts only slowly and there is some slight uncertainty whether the

results completely show the per disulpuric yield.

RESULTS

In 5M H_2SO_4 gamma irradiated at 77°K(Dose $\sim$ 1.5×10^{22} ev/l), the H_2O_2 yield was surprisingly small.

In the undegassed system, $G(H_2O_2)$ was ≤ 0.1. In the degassed system, it was somewhat higher with $G(H_2O_2) = 0.19$.

The low yield of H_2O_2 was also confirmed by irradiating these systems in the presence of Ce^{+4}. The results are given in Table I and fig. 1 Each G value is the mean of atleast 3 values with times of irradiation varying from 10 to 40 mts. (Dose rate = 5.3×10^{20} ev/l/min.).

TABLE I

Gamma Radiolysis of 5M H_2SO_4 Containing Ce^{+4} at 77°K

	Initial $[Ce^{+4}]$ M	$G(-Ce^{+4})$
1.	3.05×10^{-3}	0.63
2.	1.85×10^{-3}	0.54
3.	9.6×10^{-5}	0.063

The above G values are based on the initial decrease of $[Ce^{+4}]$.

Obviously, the reduction of Ce^{+4} is strongly concentration dependent. These G values are considerably lower than the G values obtained in similar solutions irradiated at room temperature[4].

Per acid yields, as measured by the production of Fe^{+3} on adding Fe^{+2}, are shown in Table II.

TABLE II

Per-Acid Production in 5M H_2SO_4 Irradiated at 77°K

(Shown as the amount of Fe^{+3} produced on adding Fe^{+2})

Time of irradiation minutes	M $[Fe^{+3}]$ x 10^4	Mean $G(SO_4^-)$
30	1.3	0.68
45	2.7	
60	3.8	
90	4.9	

DISCUSSION

Obviously, the major oxidised products are the per-acids. Not only is the H_2O_2 yield is low, but $G(-Ce^{+4})$ is only about $1/3^{rd}$ the room temperature figure. The reduction of Ce^{+4} probably occurs mostly through electrons and hydrogen atoms. The low yield of H_2O_2 suggests that the OH+OH reaction is almost absent, leading one to suspect whether "spurs" are existent at all in these systems. The rapid mobility of energy might be responsible. The OH radicals probably disappear mostly by reaction with sulphuric acid. The complicated kinetics of Ce^{+4} reduction will be dealt with in a more detailed publication.

ACKNOWLEDGEMENTS

Our grateful thanks are due to Dr. J. Shankar, Head, Chemistry Division, for his interest in the work. I am also grateful to Dr. K. N. Rao for helpful discussions.

REFERENCES

1. F. S. Dainton and F. T. Jones; Rad. Res. 17 (1962) 388

2. F. S. Dainton and C. G pinathan; Trans. Faraday. Soc. 65, 143 (1969)

3. C. Gopinathan, P. N. Moorthy and K. N. Rao; Indian J. Chem. 12, 749 (1968)

4. J. W. Boyle; Rad. Res. 17, 427 (1962)

DISCUSSION

K. V. S. Rama Rao : The fact that low concentrations of electron Scavengers e.g., N_2O do react with electrons in 5M sulfuric acid glass suggests that the molecular H_2O_2 which may have initially been formed is destroyed by electron reaction with the final result your post irradiation analysis shows only a little net H_2O_2. Hence, an apparently low $G(H_2O_2)$ should not been taken any evidence against spurs and does not warrant any postulate of exciton formation or its transport.

C. Gopinathan : The question is, in my humble opinion self-contradictory. If spurs exist and H_2O_2 is formed by OH radicals diffusing and reacting mutually, then H_2O_2 cannot be formed at 77°K since OH radicals are immobile at this temperature. So there is no question of electrons reacting with H_2O_2. Therefore I argue that either spurs do not exist or at least the bimolecular combination of OH does not take place. The exciton mechanism is one way of explaining the small H_2O_2 yield.

Jai P. Mittal

1) I am not at all sure how in 5M H_2SO_4 e^-_{solv} don't react at all in your system?

2) How do you say at one place that (H^+) are absent in 5M H_2SO_4 because of condensation polymer present in 5M H_2SO_4 glass. But on the other hand, you could go back and say that in 0.5 M (H^+) are present in that system.

3) Don't you think this process of e^-_{dry} not reacting with H^+ can be explained on Prof. Hamills idea of portulating a "dry electron" whose rate constant with H^+ is extremely small compared to $e^-_{solv} + H^+$.

C. Gopinathan : 1) Solvated electrons cannot be formed at 77°K The electrons are either mobile electrons, e^-_m or e^-_T, trapped electrons. In acid systems e^-_T is unlikely to be found. Therefore all observed reactions are due to mobile electrons, which make use of conduction pathways such as $SO_3^- \ldots SO_3$ polymer chains.

(2) I say that (H^+) is drastically reduced as a result of condensation polymerisation. I have not quoted any figures for (H^+) since this might vary from system to system. In pure H_2SO_4 glasses and in N_2O containing sulphuric acid glasses, I believe this is very low. Low enough not to be able to compete (effectively) with 10^{-2} M N_2O. In some other systems it may be somewhat higher, in which case higher concentrations of scavengers would be necessary to pick up all the electrons.

(3) No. Some reasons are, (i) If the dry electron cannot react with, or reacts only very slowly with H^+, then the large yields of H atoms at 77°K in frozen acid systems cannot be explained. I do not beiive solvated electrons can be formed at 77°K. (ii) If the dry electron, on the other hand can react readily with scavengers like N_2O, $ClCH_2COOH$ as postulated by Prof. Hamill, why does it take such a large concentration of scavenger in alkaline glasses to significantly reduce trapped electron yield? In fact, in 6 M NaOH glass at 77°K, 10^{-2} μ of scavenger has no effect on $[e^-_T]$. One has to put in about .05 M $ClCH_2COOH$ before significant decrease can be seen.

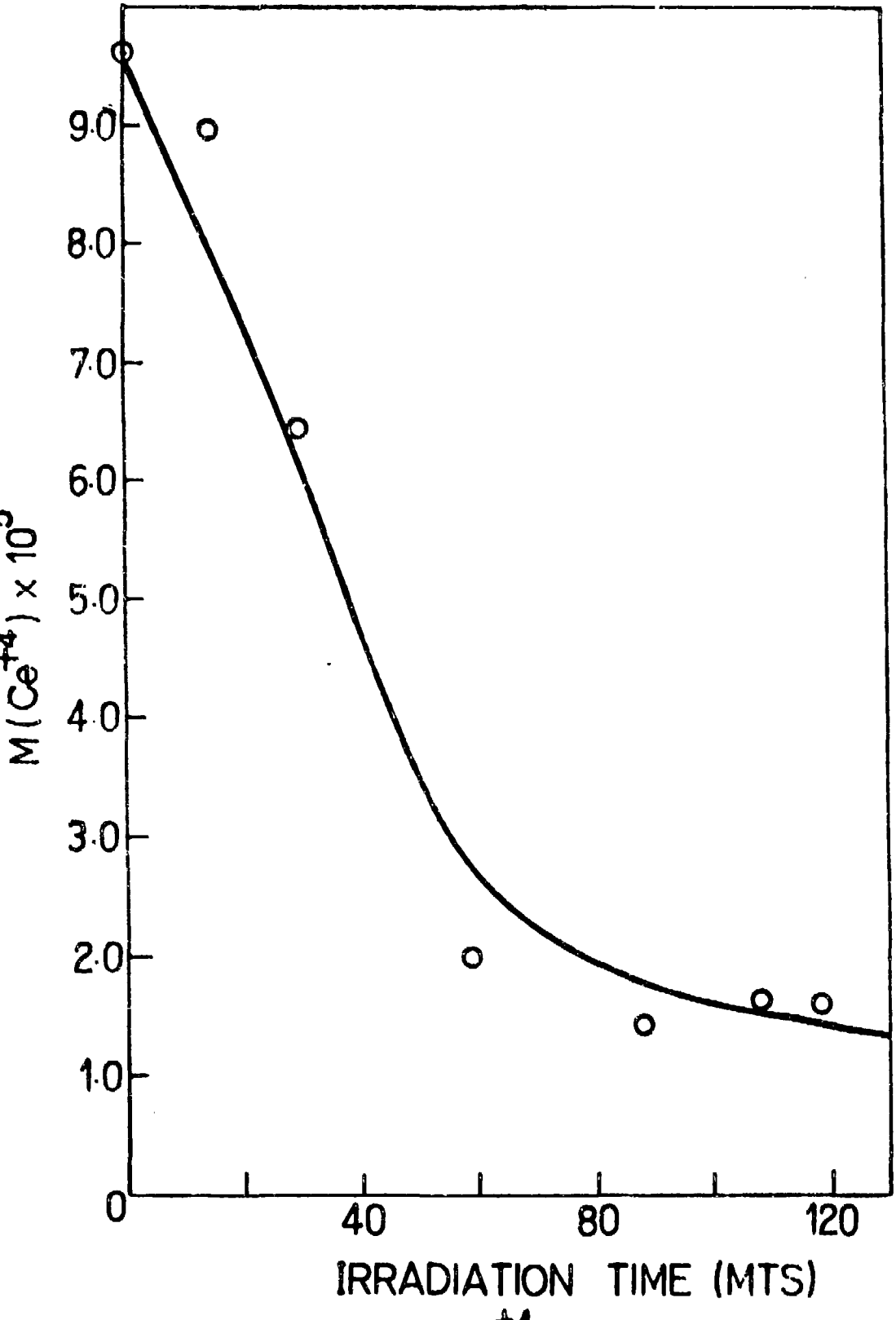

Fig. 1. Reduction of Ce^{+4} in $5M H_2SO_4$ glass.

HYDROGEN PEROXIDE YIELDS IN γ-RADIOLYSIS OF DEAERATED CYSTEINE SOLUTIONS

Manohar Lal
Chemistry Division, Bhabha Atomic Research Centre, Bombay 85

On the basis of the study of radiolysis of an aqueous solution of cysteine El Samahy reported that its reaction with hydrogen peroxide is very fast in neutral solutions.[1] Since our results in a similar study indicated that this reaction is slow, we studied the thermal reaction between air free 10^{-2}M cysteine and 0.9×10^{-4}M hydrogen peroxide in neutral solutions[2] and found that at the end of 24 hours this reaction was only 75 - 80% complete and thereafter proceeded at an imperceptable rate. In view of our results, we allowed all irradiated samples to stand for 24 hours before analysis, and assumed, for practical purposes, that 0.5 ± 0.1 molecules of cystine/100 ev were formed due to reaction (9) in the following reaction scheme, which could explain most of the results in the radiolysis of cysteine[2].

$$CySH + H \longrightarrow CyS + H_2 \quad (1)$$

$$CySH + H \longrightarrow Cy + H_2S \quad (2)$$

$$CySH + OH \longrightarrow CyS + H_2O \quad (3)$$

$$CySH + eaq^- \longrightarrow Cy + SH^- \quad (4)$$

$$SH^- \xrightarrow{H^+} H_2S \quad (5)$$

$$CySH + Cy \longrightarrow CyS + CyH \quad (6)$$

$$H^+ + eaq^- \longrightarrow H \quad (7)$$

$$2\,CyS \longrightarrow (CyS - SCy) \quad (8)$$

$$2\,CySH + H_2O_2 \longrightarrow (CyS - SCy) + 2\,H_2O \quad (9)$$

[In this scheme, CySH, CyH and (CyS - SCy) represent cysteine, alanine, and cystine respectively]

If, however, the air-free cysteine solutions are irradiated at a high dose rate for a short time (10 - 20 m) and the samples analysed for cystine and hydrogen peroxide immediately after irradiation, one would get the hydrogen peroxide yields in acid as well as neutral solutions; since its reaction with cysteine is very slow, we would then get a value of G(CyS - SCy) lower than that reported earlier[2]. This study was undertaken to establish that in irradiated air-free cysteine solutions the reaction (9) is in fact very slow and can be dropped from the above scheme.

The experimental techniques used in this work are the same as described earlier.[2, 3] All irradiations were carried out with a Co^{60} source at a dose rate of $\sim 0.4 \times 10^{18}$ ev. m^{-1} ml^{-1}.

Hydrogen peroxide yields were measured spectrophotometrically at 410 nm by the titanium sulphate method[4] and the cystine yields at 248 nm as reported earlier[3]. Estimations were made immediately after irradiation of the samples.

G values for hydrogen peroxide and cystine as calculated from the slope of the straight lines obtained from yield dose plots are presented in Table 1. For comparison, are shown in brackets the G(cystine) as reported in our earlier papers.[2, 3]

TABLE I

[CySH]	pH	$G(H_2O_2)$	G(CyS - SCy)	
10^{-3}	0.0	0.71	3.2 ± 0.1	(3.1)
10^{-3}	5.4	0.71	3.0 ± 0.1	(2.9)
10^{-2}	0.0	0.675	3.4 ± 0.1	(3.3)
10^{-2}	5.4	0.675	3.0 ± 0.1	(3.4)

Table I shows that the cystine yields (column 4) agree well with those reported earlier for 10^{-3} and 10^{-2} M cysteine at pH 0.0 and for 10^{-3} M at pH = 5.4, indicating that there is no effect of the high dose rate [dose rate of Co^{60} source used earlier = $\sim 6 \times 10^{15}$ ev. m^{-1} ml^{-1}]. However, with 10^{-2} M cysteine at pH 5.4, the present G(CyS - SCy) = 3.0 is significantly lower than that reported earlier (3.4)[2]. The higher G(CyS - SCy) indicates that during the 24 hours of storage, reaction between cysteine (10^{-2}M) and hydrogen peroxide had taken place. The fact that for 10^{-3} M cysteine in neutral solutions the earlier[2] and the present value of G(CyS - SCy) are nearly the same shows that hydrogen peroxide does not react with cysteine at this low concentration. From the present data, it may be concluded that at 10^{-2} M cysteine and under the conditions of this study there is no reaction with hydrogen peroxide.

Further, column 3 of the table shows that for both 10^{-3} M and 10^{-2}M cysteine at pH's 0.0 and 5.4, $G(H_2O_2) = \sim 0.7$. This agrees very well with the hydrogen peroxide yield reported for other systems[5] and confirms that hydrogen peroxide produced has not reacted with cysteine.

The reaction mechanism presented above requires that eaq^-, H and OH. each eventually produce a thiyl radical (CyS). Consequently the total yield of cystine should be given by reaction (8) only [eliminating reaction (9)] and

$$G(CyS - SCy) = \frac{1}{2}\left[G_H + G_{OH} + G_{eaq^-}\right] \qquad (1)$$

Substituting the experimental G(CyS - SCy) = 3.0 in (1), one gets

$$G_H + G_{OH} + G_{eaq^-} = 6.0$$

which agrees reasonably well with our earlier reported[2] total radical yield of 5.8 as well as with other reported values[6]. Subtracting (G_H + G_{eaq^-}) = 3.3 for neutral solutions[2, 6] one gets

$$G_{OH} = 2.7$$

This again is in agreement with many other reported values[6].

The results reported above provide confirmation of the radiolytic mechanism based on reactions 1 to 8 and suggest that it is safe to eleminate reaction (9) from the scheme.

ACKNOWLEDGEMENTS

The author wishes to express his thanks to Dr. J. Shankar, Head, Chemistry Division, for discussions and keen interest in this work.

REFERENCES

1. A. El Samahy; Ph. D thesis, University of Delaware (1964)

2. Verna Gaye Wilkening, Manohar Lal, Meta Arends and D. A. Amstrong; J. Phys. Chem. 72, 185 (1968)

3. Verna Gaye Wilkening, Manohar Lal, Meta Arends and D. A. Amstrong; Can. J. Chem. 45, 1209 (1967)

4. George M. Eisenberg; Ind. Engg. Anal. Ed.; 15, 327 (1943)

5. A. O. Allen; The radiation chemistry of water and aqueous solutions, D. Van Nostrand Co. Inc., (1961)

6(i) Proc. Fifth Informal Conference on the Radiation Chemistry of Water, University of Notre Dame (1966) p. 27 and references cited therein.

6(ii) B. H. J. Bielski and A. O. Allen; INT. J. for Rad. Physics and Chemistry 1, 153 (1969)

"(n,γ) RADIOLYSIS OF SOLID IODIC ACID"

H. J. Arnikar, V. G. Dedgaonkar and Kamal K. Shrestha
Department of Chemistry, University of Poona, Poona-7

INTRODUCTION

Our earlier work on bromates showed an increase in retention from 17 to about 60% on heating the irradiated sample[1]. In iodates however, the initial retention as high as 67% increases to about 90% on thermal annealing [2]. It appeared to be of interest to extend our work on halates[1, 3] to study the distribution of I^{128} activity in neutron irradiated iodic acid and of the effects thereon of thermal annealing and of pre- and post-irradiation by gammas from Co^{60} source.

EXPERIMENTAL

The procedure followed for the irradiation, extraction, correction for observed activities in solid and solution states and subsequent thermal annealing in solid state were in accordance with our earlier work on $LiIO_3$[4]. In case of irradiation at higher temperatures, care was taken for the samples to attain the desired temperature prior to neutron bombardment. In the readiation-annealing experiments, the samples were first exposed to a kilocurie Co^{60} source for varying doses (upto 15 Mrad) both prior and subsequent to (n, γ) irradiation. Each value reported is the average of atleast 3 independent experiments, the reproducibility of individual determination of retention being within 2%.

RESULTS AND DISCUSSION

The following are the major observations in brief:

(i) The retention of crystalline iodic acid at room temperature (31°C) is 67%,

(ii) The saturated retantion values for the samples irradiated at different temperatures but annealed at certain temperature show an appreciable difference, the one irradiated at higher temperature being lower (Fig. 2).

(iii) A minimum constant value of retention appears when the irradiation temperatures is lowered, the retantion decreasing slowly to this constant value (Fig. 3),

(iv) Both pre-and post-iiradiation treatment by intense gammas increase the (n,γ) retention markedly.

(v) Retention increases with the concentration in the case of (n,γ) irradiation of aqueous iodic acid (Fig .4)

It is seen from Fig. 1 that retention approaches almost hundred per cent within the first few minutes of thermal annealing at 90°C, unlike in other iodates[2, 5] suggesting the recombination processes to be very susceptible to annealing temperature. However, at lower temperatures (below -80°C), the initial retention decreases, attaining a minimum value. At these low temperatures, the recombination processes in HIO_3 appear to be independent of thermal annealing and contribute about 53% of the initial retention.

The lower retention value of iodic acid when irradiated and annealed at 70°C (Fig. 2) as compared to irradiation at room temperature and annealing at 75°C is believed to be due to the removal of inherent crystal defects during pre-heating involved in the irradiation at 75°C. The following summary gives comparative retention values due to thermal annealing at different temperatures, the irradiation also being carried out at the same temperatures.

Temperature of annealing (°C)	Irradiation at annealing temp. R_1(%)	Irradiation at 31°C R_2(%)	Difference $R_2 - R_1$(%)
60	76.0	80.5	4.5
75	81.0	90.5	9.5
90	88.0	99.5	11.5

The increase in difference in retention values with the temperature suggests that more crystal defects are eliminated as the temperature is raised. Further, along with the removal of defects, greater recombination also takes place at the elevated temperatures. These two processes have reverse effects on retention; the former tends to decrease retention while the latter tends to increase the same. The maximum difference between these opposing factors is observed to be around 90°C.

Inducing additional defects in HIO_3 by gammas from a Co^{60} prior to the neutron bombardment increases the retention but the results are at variance from those of Maddock et al,[6] on K_2CrO_4 crystals where a decrease in retention was reported. Post-exposure of neutron-irradiated iodic acid to gammas to a dose of about 0.1 Mrad at 31°C has been found to induce a transfer of recoil radio-iodine to iodate by about 3 - 4% in addition to the effects of the thermal annealing at 31°C. Similar results have been reported in alkali metal iodates[2], bromates[7] and other systems[6].

The retention values observed in irradiated aqueous solutions of iodic acid are considerably small. As expected, the nature of the plot in Fig. 4 is very similar to the corresponding one we obtained in the case of lithium iodate[4]. The minimum concentration appears to be around 0.08M giving 30% retention, as suggested by the extrapolation of the curve.

ACKNOWLEDGEMENT

One of us (KKS) is grateful to His Majesty's Govt. of Nepal for the award of Research Fellowship under T. C. S. of Colombo Plan, through the Govt. of India.

REFERENCES

1. H. J. Arnikar, D. K. Sharma and S. F. Patil; Ann. Convention of Ind. Chem. Soc. (1968)

2. W. E. Cleary, W. H. Hamil and R. R. Williams (Jr); J. Am. Chem. Soc. 74, 4675 (1952)

3. H. J. Arnikar, D. K. Sharma and S. F. Patil; Radiochim. Acta. (In press)

4. H. J. Arnikar, V. G. Dedgaonkar and Kamal K. Shrestha; J. Univ. Poona (In press)

5. S. Kaucic and M. Vlatkovic; Croatica Chemica Acta. 35, 305 (1963)

6. A. G. Maddock, F. E. Treloar and J. I. Vargas; Trans. Frarad Soc. 59, 924 (1963)

7. G. E. Boyd and Q. V. Larson; J. Am. Chem. Soc. 90, 254 (1968)

DISCUSSION

Manohar Lal : **Could you tell me the reason for a much lower retention value in aqueous solution as compared to the solid.**

K. K. Shrestha : **In all probability, it may be due to the wide separation of the recoil species, when surrounded by water molecules, so that the possibility of recombination is greatly reduced, as compared in the solid state. The minimum retention value in the lowest concentration irradiated in our work also justifies this probability.**

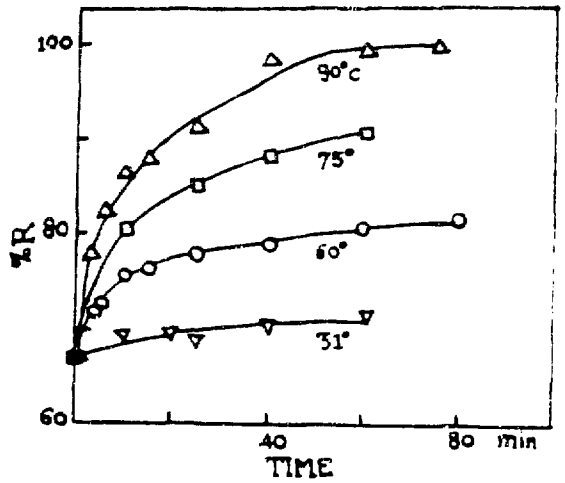

Fig. 1 VARIATION OF % RETENTION IN HIO_3 WITH TIME OF ANNEALING AT DIFFERENT TEMPERATURES

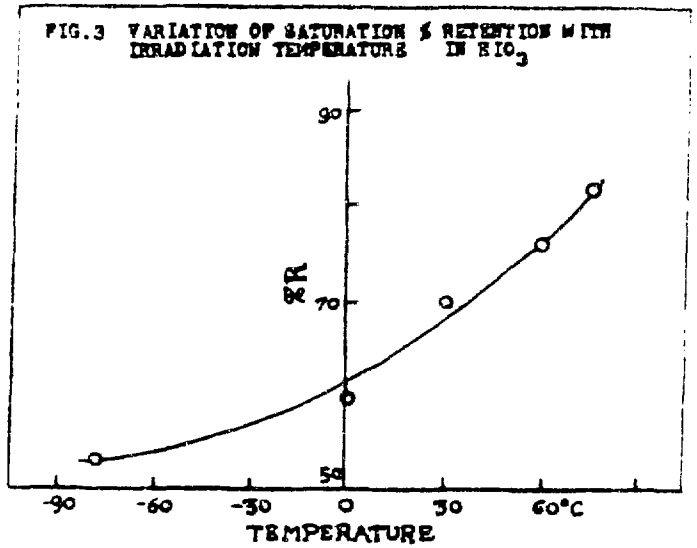

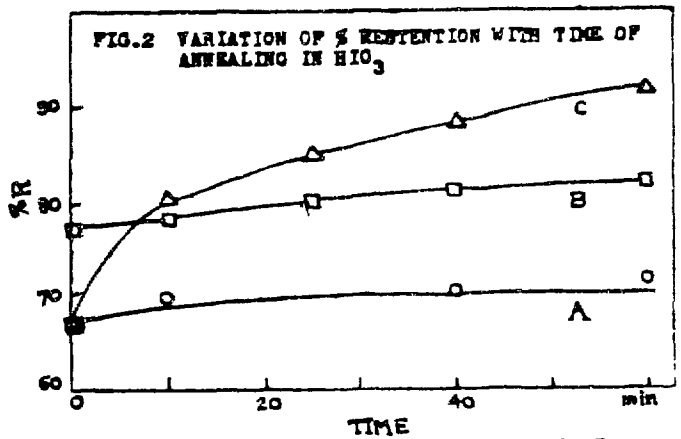

A and B : IRRADIATION AND ANNEALING AT SAME TEMPERATURE (A=31° and B=75°C)

C : IRRADIATION AT 31° AND ANNEALING AT 75°

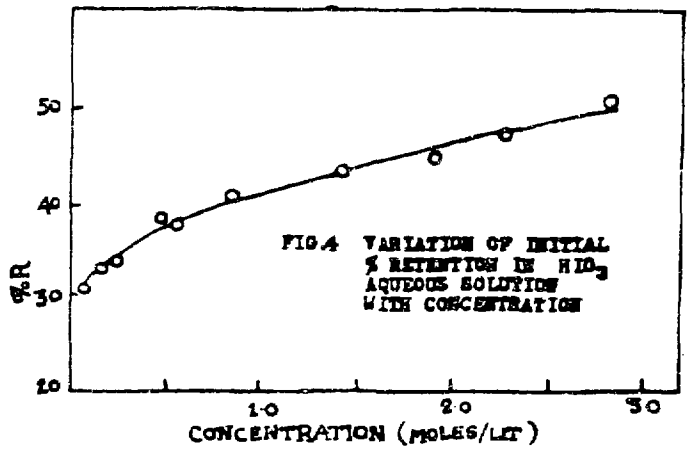

FIG.4 VARIATION OF INITIAL % RETENTION IN HIO_3 AQUEOUS SOLUTION WITH CONCENTRATION

ISOTOPE EFFECT AND SECONDARY REACTIONS OF RECOIL Br-82 AND Br-80m ATOMS UNDER (n, γ) PROCESS IN ALKYLBROMIDES

S. P. Mishra and B. M. Shukla
Nuclear and Physical Chemistry Laboratories
Banaras Hindu University, Varanasi-5.

INTRODUCTION

Studies on chemical effects of nuclear transformations accompanying (n, γ) process have shown that the behaviour of radioactive isotopes of one and the same element in a series of cases is not always the same. Such a difference in the behaviour comes up in the dissimilarity of the degree of retention of each isotope, indicated as 'isotope effect'. A definite effect was first observed between recoil Br^{82} and Br^{80m} atoms in n-irradiated liquid halo-bromomethanes[1-3]. The appearance of ΔR% in pure organic halides containing only one species of the halogen (bromine) has been the subject of many contradictory reports[3-10]. Merrigan, Willard and others[11-16] have recently reported the role of Br^{82m} isomeric transition process for the observed isotope effect.

In view of the earlier works and their controvertial character, it was desirable to search carefully the possibility of an isotope effect between Br^{82m} and Br^{80m} under (n, γ) process in liquid phase of organic compounds containing bromine atom(s) only. The effect was observed in bromobenzene after a series of careful experiments[17]. Experimental success with bromobenzene encouraged the authors to study the effect with other alkylbromides and findings on 1, 2-dibromoethane and ethylbromide have already been reported by us[18, 19]. Similar studies have been extended to other organic bromides and the influence of added diluents (benzene, carbontetrachloride and cyclohexane) on the isotope effect and secondary reactions has also been carried out. The present paper deals with some of the results of our studies on isotope effect and secondary reactions of recoil Br^{82} and Br^{80m} atoms during liquid phase n-irradiation of propylbromides.

EXPERIMENTAL

The experimental technique employed in the present investigations was similar to one reported in our earlier works[17-20]. Pure samples of n-propylbromide (Fluka AG/Whiffen and Sons England) and i-propylbromide (E. Merck) used were purified by main procedure as described by Schuler and McCauley[7]

Ethylbromide (E. Merck/Riedel) used as carrier was purified by main procedures as described by Milman[21]. 1-2-dibromoethane (E. Merck), 1,1-dibromoethane (E. Merck) were purified by a method similar to that of ethylbromide. Methylenebromide (E. Merck) and 1,2-dibromopropane (Fluka AG) were redistilled (98.0°C; 141.0°C respectively).

A. R. quality bromine (E. Merck) used as scavenger was employed as such without further purification.

Tables 1 and 2 represent the results (established on the basis of atleast 3 experiments) on variation of the retentions of recoil Br^{82} and Br^{80m} atoms with added bromine concentration in n-propylbromide and i-propylbromide. The above results are also shown graphically (Figs. 1 and 2).

RESULTS AND DISCUSSION

As can be seen from the results (cf. Tables 1,2 and Figs. 1,2) that isotope effect between recoil Br^{82} and Br^{80m} atoms was observed in n-propylbromide and i-propylbromide with values of 7.4 and 6.4 respectively where no bromine was added initially as scavenger. With the increasing concentration of bromine from 0.00 to 0.03 m. f. $\Delta R\%$ did not change significantly. But as the scavenger concentration increased from 0.03 m. f. to 0.20 m. f. $\Delta R\%$ decreased markedly (Figs. 1 and 2). On further addition of the scavenger (0.20 - 0.50 m. f.) in both the target compounds, a near disappearance of the effect is observed. Present results are similar to those reported earlier in bromobenzene[17], 1,2-dibromoethane[18] and ethylbromide[19].

The marked decrease of isotope effect and its near disappearance at higher concentration of bromine is in conformity with some of the earlier results[1-3, 7, 8, 17-20]. However, it may be mentioned that in the works of some of the earlier authors, not only (n, γ) but (γ, n), (γ, 2n) and (γ, 3n) processes were carried out for obtaining a desired isotope. Further, it has been concluded that the isotope effect is not directly/wholly connected with the initial recoil energy[7, 22, 23].

Recent discovery of Br^{82m} isomer[24, 25] and some works of Merrigan, Willard and others[11-16] show that the enhanced retention of Br^{82} in organic systems may be chiefly due to the secondary interactions of Br^{82} formed as a result of Br^{82m} isomeric transition process. They have further reported that the observed isotope effect between Br^{82} and Br^{80m} atoms is a function of time of irradiation plus the time for which the samples were left in the liquid state while isomeric transition process was occuring. Also, it has been suggested by Willard[10] that higher organic retentions observed for Br^{82} than Br^{80m} in the halo bromo-

methanes, studied by Nesmeyanov, etal may be due to the $Br^{82m} \xrightarrow{I.T.} Br^{82}$ process rather than the Br^{81} (n, γ) Br^{82} activation. Furthermore, it is to be mentioned that (n, γ) activation of bromo-compounds mainly produce Br^{82m} (91%) of which 99.8% decay to the ground state i.e. Br^{82} and only about 9% of Br^{82} is formed by (n, γ) process[24]. Hence most chemical reactions which determine final stabilisation of Br^{82} are induced by I.T. activation rather than (n, γ) process. Chemical effects of the Br^{82m} (I.T.) Br^{82} activation in liquid carbontetrachloride was investigated where substantial amounts of Br^{82} was found organically combined from mixtures of carbontetrachloride and reactor irradiated bromine. The observed isotope effect, in some studies by Mirrigan and others[12, 13] has been indicated as 'pseudo-isotope effect'.

Available evidence indicates that the elastic collision model cannot account for all the high energy organic retention (e.g. H substitution by Br) in the liquid phase[3]. Nesmeyanov etal[3, 26] assumed that recoil Br atoms collide to the struck molecule as a whole, which latter then breaks at a C-H bond as a result of excitation. This should imply that the yield in H-substituted molecule will be a function of the ratio of the mass of the hot bromine atom(s) to the mass of the molecule (M). Fig. 3 (cf. Table 3) shows RH% (the yield in the mono-brominated product by recoil Br^{82} atom) as a function of M/m+M, i.e. as a function of the maximum possible proportion of the energy of the hot Br^{82} atom that can be taken up as excitation energy in an inelastic collision. The yield is clearly a linear function of M/(m+M), which supports the assumption for formation as a result of dissociation in excited molecules. Assuming the C-H bond energy to be 3 eV and using the observation that the substitution starts when M/(m+M) is 0.55, it will mean that the k.e. needed in the bromine atom is 6 eV; this is in good agreement to the hypothesis[3] that epithermal atoms undergo inelastic collisions with the surrounding molecules. Further, the inelastic collision mechanism may result in the formation of many other molecules than H-substituted products e.g. polybrominated products, molecules formed by C-C bond cleavage followed by recoil substitution and even the production of tagged parent molecules.

Figure 4 (cf. Table 4) represents isotope effect as a function of ΔR_D (difference between the diffusion controlled reactions of recoil Br^{82} and Br^{80m} atoms) at zero bromine concentration for propylbromides and other alkylbromides studied by the authors. The nature of the curve shows a direct proportionality between $\Delta R\%$ and ΔR_D. The curve may be assigned the equation of a straight line: $y = mx + c$, where 'x' is abscissa and represents ΔR_D, 'y' is ordinate and designates $\Delta R\%$, 'm' the slope of the line and 'c' the intercept on ordinate. The value of 'c' comes out to be 4 and is closely the same as ΔR_E for all the compounds studied (cf. Table 4). According to the above relationship, it is evident that the observed isotope effect is a linear function of ΔR_D. Thus, the

effect seems to be dependent on ΔR_D and a constant term C (i.e. ΔR_E). The above interpretation is supported from the fact that Br^{82} arising out of Br^{82m} (I. T.) Br^{82} process enters organic combination 50% via hot and 50% via thermal processes[27].

Rack and co-workers[16, 28] have reported that I. T. of Br^{82m} caused much higher organic yields than those produced by (n, γ) processes. In another work[15] from the same laboratory it was found that the Br^{82} organic yields from Br^{82m} (I. T.) Br^{82} activation are generally 1.7 to 1.8 times the yield of Br^{80m}, Br^{82m} and Br^{82} from (n, γ) induced reactions in liquid carbonatetrachloride, cyclohexane and the isomers of hexane at bromine concentration above 0.05 m. f. The organic retentions of Br^{82} reported in the present work are in fact an average of Br^{81} (n, γ) Br^{82} and Br^{82m} (I. T.) Br^{82} processes. The organic retentions of Br^{82} only due to I. T. process will be more than the reported values and in fact in the light of Rack et al's[16] calculation the organic yields of Br^{82} arising only due to I. T. process can be obtained. Table 5 lists the values of $R(Br^{82})/R(Br^{80m})$ in all the studied compounds at lower bromine concentrations. It is clear that the ratio values in all cases are less than 1.7 where in the organic retention values of Br^{82} are the observed one. The ratio values (after correcting Br^{82} retentions for I. T. process only) will come out to be slightly more than the values given in Table 5, but will be less than 1.7. This fact demonstrates that the relative difference in the organic retentions of recoil Br^{82} and Br^{80m} atoms in alkylbromides is less than bromine-hexane systems studied by Merrigan et al[15]. It is quite apparent that in bromine-hexanes there will be only undirectional process of uptake of Br^{82} from inorganically bound Br^{82m} following I. T. process.

The nature of the reactive species, its control, and the possible role of Br^{82m} towards the effect under consideration need extensive study. If a long-lived thermally reactive species is formed as a consequence of I. T. reactions as well as by (n, γ) reactions, the observed pseudo-isotope effect may be due to an increase in the concentration of the species formed by the Br^{82m} I. T. reaction.

Nesmeyanov et al[1-3] confirmed the origin of $\Delta R\%$ in halobromomethanes as a result of high energy processes. In one work[2] they also speculate that an isotope effect may occur during neutron irradiation of alkyl bromides as a result of thermal reactions of recombination diffusion type. The present authors are successful in observing the effect in pure alkylbromides; but effect is not only as a result of diffusive reactions. As has been mentioned earlier, the observed isotope effects are, of course, a function of ΔR_D, but over a constant term C (i.e. ΔR_E). Thus, it may be concluded that observed effect between recoil Br^{82} and Br^{80m} atoms in bromoalkanes is partly due to high energy and partly due to thermal processes regardless of the history of

recoil bromine atoms. In the light of the discovery of Br^{82m} isomer and works of Rack etal[12-16, 27, 28] observations of Nesmeyanov, etal[1-3] may be re-evaluated to get the exact data for Br^{82}, Br^{80m} and Br^{80} arising as a result of (n, γ) process and Br^{82} and Br^{80} coming out purely as a result of I. T. process. It may now be recognised that the observed isotope effect between recoil Br^{82}, and Br^{80m}, atoms are in fact 'pseudo-isotope effect' in the sense that enhanced organic retention of Br^{82} is attributable to Br^{82m} (I. T.) Br^{82} process rather than (n, γ) activation. Thus, it is the type of activation which may give rise to an isotope effect.

ACKNOWLEDGEMENT

The authors are grateful to Dr. G. B. Singh, Professor and Head of the Department of Chemistry, Banaras Hindu University, Varanasi-5, for providing necessary facilities. Our thanks are also due to Dr. Sujan Singh, Mr. B. N. Vohra and Mr. K. N. Vohra, Lecturers, Department of Chemistry for their assistance in the purification of some of the organic compounds used in the present investigation.

REFERENCES

1. A. N. Nesmeyanov, E. S. Filatov, E. A. Borisov, V. I. Kondratenko, C. H. Chang, K. Panek, and B. M. Shukla; Radiokhimiya 1, 712 (1959)
2. A. N. Nesmeyanov and E. S. Filatov; ibid, 3, 601 (1961)
3. A. N. Nesmeyanov, E. S. Filatov, E. A. Borisov, and B. M. Shukla; 'Chemical Effects of Nuclear Transformation,' IAEA, Vienna, 1, 259 (1961)
4. P. C. Capron, etal; Proc. Second Inst. Conf. (Peaceful Uses of Atomic Energy), Geneva; 240 (1958)
5. W. F. Libby; J. Am. Chem. Soc. 69, 2523 (1947)
6. J. M. Miller and R. W. Dodson; J. Chem. Phys. 18, 865 (1950)
7. R. H. Schuler and C. E. McCauley; J. Am. Chem. Soc. 79, 821 (1957)
8. M. Milman, etal.; J. Chem. Phys. 1303-1332 (1957)
9. J. E. Willard; 'Chemical Effects of Nuclear Transformation'. IAEA, Vienna, 1, 215 (1961)
10. J. E. Willard; ibid, IAEA, Vienna, 1, 221 (1965)
11. R. M. Iyer and J. E. Willard; J. Am. Chem. Soc. 87, 2494 (1965)

12. J.A. Merrigan and E.P. Rack; J. Phys. Chem. 69, 2795 (1965)

13. J.A. Merrigan and E.P. Rack; ibid, 69, 2806 (1965)

14. J.A. Merrigan, etal; ibid, 44, 174 (1966)

15. J.A. Merrigan, etal; Radiochim. Acta 6, 94 (1966)

16. J.A. Merrigan, etal; J. Chem. Phys. 44, (1) 174 (1966)

17. B.M. Shukla and S.P. Mishra; Symposium on Chemical and Non-chemical Interactions, UGC-Gorakhpur University, Gorakhpur, Feb. 13-15 (1965)

18. B.M. Shukla and S.P. Mishra; Proc. Symp. 'Nuclear and Radiation Chemistry', Department of Atomic Energy, Govt. of India, Poona, p. 37-48 March (1967)

19. B.M. Shukla and S.P. Mishra; Proc. Indian Science Congress, Varanasi, Jan. (1968)

20. B.M. Shukla, and S.P. Mishra; Proc. Symp. 'Nuclear and Radiation Chemistry', DAE, Govt. of India, Bombay, pp. 128-133, March 16-19 (1964)

21. M. Milman; J. Phys. Chem. 67, 537 (1963)

22. A.E. Richardson and A.F. Viogot; J. Chem. Phys. 28, 854 (1958)

23. F.S. Rowland and W.F. Libby, ibid; 21, 1495 (1953)

24. J.F. Emery; J. Inorg. Nucl. Chem. 27, 903 (1965)

25. O.U. Anders; Phys. Rev. 138, B1 (1965)

26. A.N. Nesmeyanov and E.S. Filstov; Radiokhimiya 3, 614 (1961)

27. J. Blair Nicholes and E.P. Rack; J. Chem. Phys. 48, 4085 (1968)

28. J. A. Merrigan, etal; J. Phys. Chem. 70, 2417 (1966)

29. B.M. Shukla, and S.P. Mishra; (Unpublished data)

TABLE 1

Organic retentions of recoil Br^{82} and Br^{80m} atoms as a function of bromine concentration in liquid n-propylbromide

Mole fraction of bromine (N_{Br})	log N_{Br}	% Organic Retention		Isotope effect (ΔR%)
		R(Br^{82})	R(Br^{80m})	
0.000	-	42.5	35.1	7.4
0.001	3.0000	41.6	34.2	7.4
0.004	3.6021	37.0	30.2	6.8
0.01	2.000	32.5	27.4	5.1
0.03	2.4771	30.2	23.2	7.0
0.04	2.6021	28.1	22.4	5.7
0.10	1.0000	23.1	18.8	4.3
0.20	1.3010	19.1	16.2	3.9
0.30	1.4771	16.4	14.5	1.9
0.40	1.6021	15.0	13.5	1.5

TABLE 2

Organic retentions of recoil Br^{82} and Br^{80m} atoms as a function of bromine concentration in liquid i-propylbromide

Mole fraction of bromine (N_{Br})	log N_{Br}	% Organic Retention		Isotope effect (Δ R%)
		R(Br^{82})	R(br^{80m})	
0.00	-	31.5	25.1	6.4
0.03	2.4771	23.2	17.3	5.9
0.05	2.6990	21.4	15.3	6.1
0.10	1.0000	19.5	13.7	5.8
0.20	1.3010	15.1	10.2	4.9
0.30	1.4771	11.6	8.0	3.6
0.40	1.6021	9.9	7.5	2.4
0.50	1.6990	7.9	6.0	1.9

TABLE 3

Br^{82} recoil yield in monobrominated product (R_H %) as a function of (M/m + M) in alkylbromide targets

Target compound	$\frac{M}{m+M}$	R_H %	References
1. CH_2Br_2	0.6797	11.5	Shukla & Mishra[29]
2. C_2H_5Br	0.5707	1.5	Shukla & Mishra[19]
3. 1,2-$C_2H_4Br_2$	0.6963	13.0	Hilman, Shaw and Simpson[8]
4. n-C_3H_7Br	0.5923	3.9	Present work
5. $CHBr_3$	0.7553	18.0	Nesmeyanov etal[3]

TABLE 4

Organic retentions, R_E, R_D, R_E and R_D for recoil Br^{82} and Br^{80m} atoms in alkyl-bromide targets (N_{Br} = 0.00 mole fraction)

Target Compound	% Organic Retention		ΔR%	ΔR_E		ΔR_D		ΔR_E	ΔR_D
	$R(Br^{82})$	$R(Br^{80m})$		$R_E(Br^{82})$	$R_E(Br^{80m})$	$R_D(Br^{82})$	$R_D(Br^{80m})$		
Methylene bromide	66.1	57.8	8.3	37.2	33.1	28.9	24.7	4.1	4.2
Ethyl bromide	32.2	21.1	11.1	17.5	13.5	14.7	7.6	4.0	7.1
1,2-dibromoethane	34.3	25.2	9.1	22.0	18.5	12.3	6.7	3.5	5.6
n-propyl bromide	42.5	35.1	7.4	23.0	19.5	19.5	15.6	3.5	3.9
i-propyl bromide	31.5	25.1	6.4	15.5	11.5	16.0	13.6	4.0	2.4
n-butyl bromide	40.5	33.4	7.1	25.5	21.5	15.0	11.9	4.0	3.1
Bromobenzene	78.5	69.4	9.1	48.0	44.0	30.5	25.4	4.0	5.1

TABLE 5

Ratios of isotopic yields from n-irradiated organic bromides

Targets	Mole fraction of bromine	$R(Br^{82}) / R(Br^{80m})$		
		0.00	0.05	0.10
CH_2Br_2		1.14	1.25	1.23
C_2H_5Br		1.52	1.26	1.20
l, r-$C_2H_4Br_2$		1.36	1.27[a]	1.16[b]
n-C_3H_7Br		1.21	1.25[c]	1.23
i-C_3H_7Br		1.25	1.40	1.42
n-C_4H_9Br		1.21	1.26	1.22
C_6H_5Br		1.13	1.14	1.10

(a) - at 0.0839 m. f.

(b) - at 0.1239 m. f.

(c) - at 0.04 m. f.

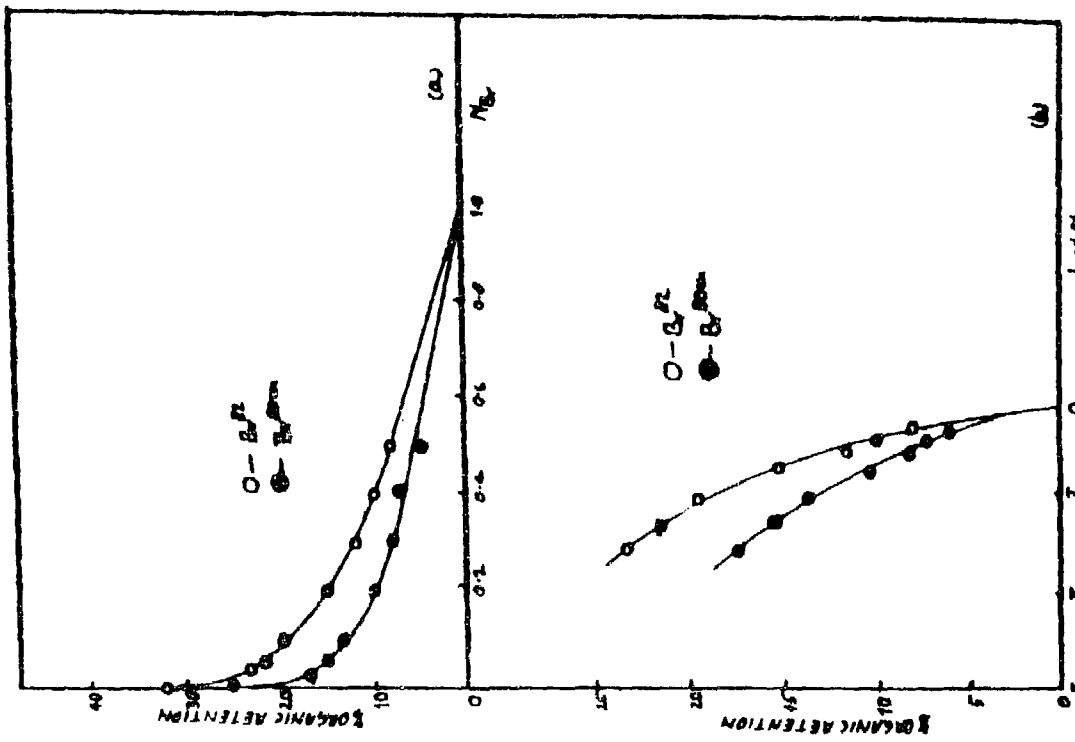

Fig:2. Organic reactions of recoil Br^{82} and Br^{80m} atoms under (n,γ) process in iso-propyl bromide as a function of:
(a) Mole fraction of Bromine (N_{Br})
(b) Log of mole fraction of Bromine ($Log\ N_{Br}$)

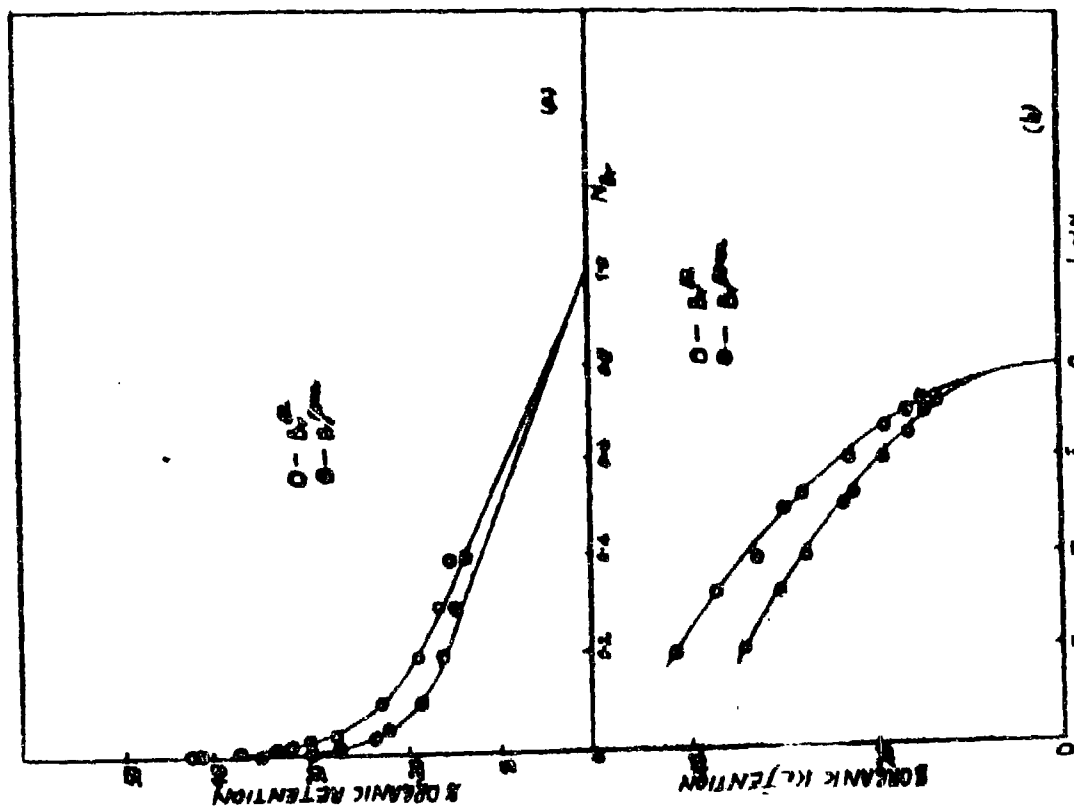

Fig:1. Organic reactions of recoil Br^{82} and Br^{80m} atoms under (n,γ) process in normal propyl bromide as a function of:
(a) Mole fraction of Brumine (N_{Br})
(b) Log of mole fraction of Brumine($Log\ N_{Br}$)

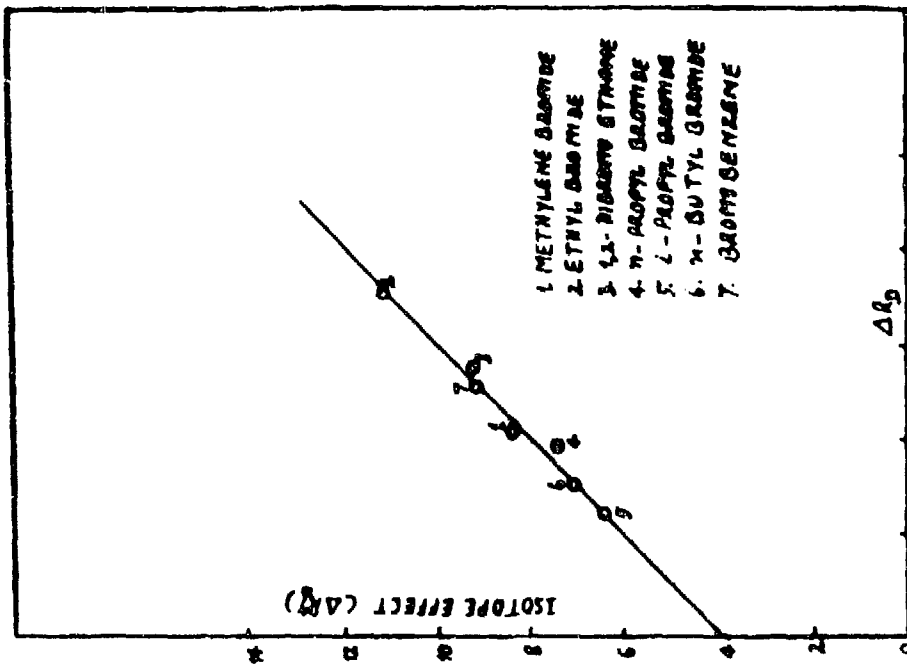

Fig. 4. Organic reactions; R_E, R_D, ΔN_E, ΔR_D for recoil Br^{80m} atoms in Alkylbromide targets (N_{Br}=0.00 m.f.)

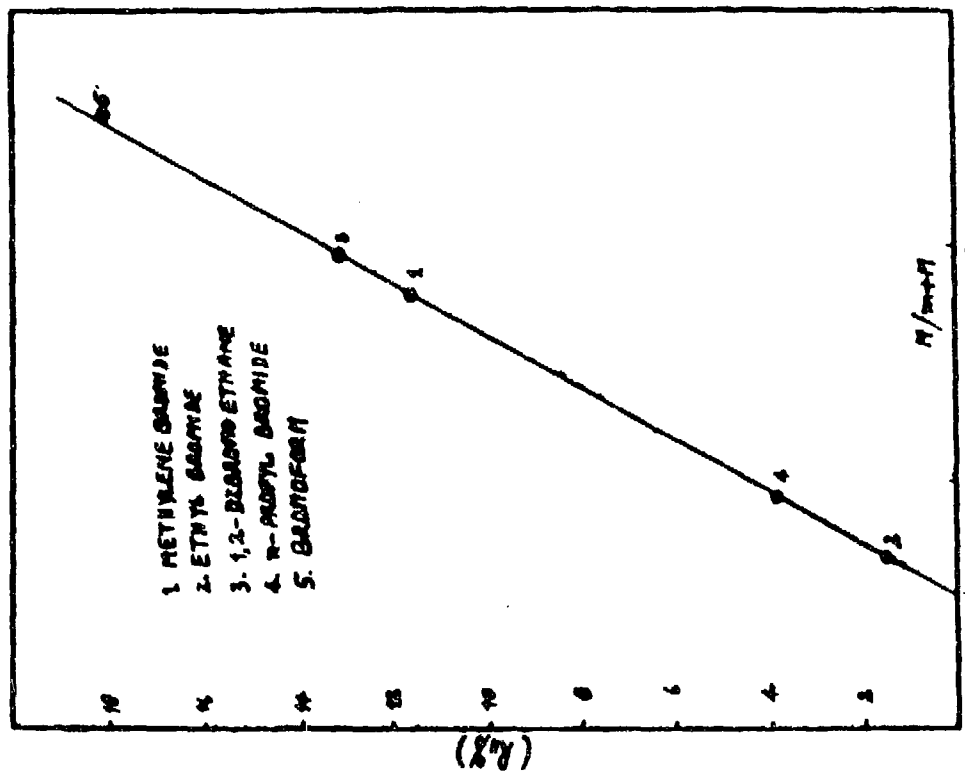

Fig. 3. Yield in monobromosubstituted product (R_H%) as a function of M/(m+M) for recoil Br^{82} atoms.

INVESTIGATIONS ON THE PROCESS CHEMISTRY OF NEPTUNIUM*

N. Srinivasan, M. V. Ramaniah, S. K. Patil, V. V. Ramakrishna,
Rajendra Swarup and Ashok Chadha
Bhabha Atomic Research Centre, Trombay, Bombay-85

I. INTRODUCTION

Neptunium-237 is formed in small but significant amounts during the irradiation of uranium fuel in nuclear reactors. This can be recovered as a by-product during the reprocessing of irradiated fuels. Neptunium-237 serves as a starting material for the production of Pu^{238} which is one of the most suitable isotopes used in isotopic power sources. Kilogram quantities of Np^{237} are produced in power reactors, thus making its recovery a matter of considerable interest. For example, in Tarapur Atomic Power Reactors about 5-8 Kg of Np^{237} may be produced annually[1].

The present work was undertaken with a view of arrive at suitable conditions like feed adjustment, selective extraction of neptunium etc. for the recovery of neptunium along with uranium and plutonium. At Trombay, purex process is used for the reprocessing of irradiated uranium fuel. In the purex process, neptunium accompanies fission products[2], uranium[3] or plutonium[4], or is distributed among the three depending on the chosen or imposed conditions. It was, therefore, found necessary to analyse the purex process solutions at various stages for total neptunium content to know the path of neptunium in the process. It was also considered necessary to investigate some factors which affect the extraction of neptunium by TBP under purex process conditions. In the present work the effect of aqueous nitric acid concentration and organic phase uranium concentration on the extraction of Np(IV) and Np(VI) into 30% TBP has been studied.

2. EXPERIMENTAL

2.1 Analysis of Purex Process Solutions

The TTA extraction method[5] was used for analysing the neptunium content of the purex process solutions. A known volume of the solution to be analysed was initially spiked with a known aliquot of pure Np^{239} to facilitate the chemical yield determination. Normally, three cycle TTA extraction was necessary to get complete decontamination from plutonium. Recovered Np^{237} was measured by alpha counting using alpha proportional counter of known geometry and its radiochemical purity was ascertained by alpha spectrum using 30 mm^2 silicon surface

* Condensed from the report BARC-428

barrier detector and 400 channel analyser. The percentage recovery in each anlysis was obtained by comparing the areas under photopeaks of Np^{239} (228 Kev and 278 Kev) in the recovered sample and the standard Np^{239} sample, obtained by using 3" x 3" NaI (Tl) detector and 400 channel analyser. The calculation of percentage recovery by comparing areas under photopeaks with and without subracting Compton tailing and by beta counting in a few cases was done. For a typical sample, recoveries calculated by all the three methods agreed within a few percent. In the present analysis, however, the efficiencies obtained by comparing the areas under photopeaks without correcting for Compton tail were used.

2.2 Extraction of Np(VI) and Np(IV) with Varying Nitric Acid and Uranium Concentration

2.2.1 Purification of Np^{237}

The neptunium stock solution prepared from $Np^{237}O_2$ obtained from Oak Ridge National Laboratory was purified by TTA extraction[5]. The radiochemical purity of Np^{237} was ascertained by alpha spectrum. The chemical purity was checked by spectrographic analysis using the method given by Wheat[6].

2.2.2 Neptnium-239 Stock Solution

Neptunium-239 was separated, each time, from uranium irradiated either in Apsara or in Cirus, using LaF_3 precipitation followed by TTA extraction. The radiochemical purity of the separated Np^{239} was checked by gamma spectrum and by determining the half-life.

2.2.3 Estimation of Uranium

The concentration of uranium in the stock solution was determined volumetrically by reducing a known aliquot of uranium to U(IV) with Jone's reductor followed by titration with ceric sulphate using Ferroin indicator[7]. The concentration of uranium in the aqueous and organic phase after equilibration with 30% TBP in Shell sol-T was measured spectrophotometrically using thiocyanate method[8, 9].

2.2.4 Extraction of Uranium

Five ml of aqueous solution with known nitric acid and uranium concentration were equilibrated with 5 ml of 30% TBP in Shell sol-T for 10 minutes using a Votex mixer. The two phases were separated after centrifugation and the concentration of uranium in both phases was estimated.

2.2.5 Extraction of Np(IV) and Np(VI)

Neptunium-237 prior to its use was purified from its daughter product Pa^{233} by TTA extraction of the latter from 7 M nitric acid. Neptunium-239 was added to Np^{237} to enable the estimation of neptunium by gamma counting. The initial aqueous concentration of Np^{237} was kept at 1-2 µg/ml. 0.01M $K_2Cr_2O_7$ was used as a holding oxidant in the experiments with Np(VI) and 0.01M ferrous sulphamate was used as a holding reductant for Np(IV).

A suitable aliquot of Np(IV) or Np(VI), as required, was added to 5 ml of aqueous solution of known uranium and nitric acid concentration and was equilibrated for 10 minutes with an equal volume of 30% TBP. The neptunium concentration in both the phase after equilibration was determined by gamma counting. The neptunium count rate was corrected for the contribution from uranium and its decay products.

3. RESULTS AND DISCUSSION

3.1 The Path of Neptunium in the Purex Process

As it was difficult to follow the same feed in the first cycle through all the three cycles, samples were analysed cycle by cycle. The ratio of neptunium to uranium in the feed of the same cycle was found to be roughly constant and hence it was taken as an apprximate measure of neptunium "moving" from one cycle to the next one. The results of the present analyses, though not very quantitative, reveal that in the co-decontamination cycle (1st cycle), neptunium is extracted along with plutonium and uranium, into TBP almost quantitatively while in the partitioning cycle (2nd cycle) the extraction is reduced to about 50%. In the uranium purification cycle (3rd cycle), most of the neptunium follows uranium into TBP as neptunium to uranium ratios in the feed and the product (uranium) of the third cycle are comparable.

In a few cases, for the corresponding samples of the feed and the raffinate in a particular cycle, the volume ratios were available. These volume ratios are approximate as the feed and the raffinate samples were usually not drawn simultaneously. However, these data were used to calculate the percentage extraction of neptunium in each cycle. The extraction of neptunium in the first cycle was around 80-90% while that in the second cycle was about 50%. Less than 20% of neptunium accompanies plutonium stream during partitioning. The extraction of neptunium in the third cycle was about 60% when the neptunium content of the feed and the product were used for calculation while it was 90% when the neptunium content of the feed and the raffinate were used for calculations. The difference in the values calculated by these two methods may be due

to the uncertainties in the volume ratios. Thus, although these results are approximate, the conclusions drawn from them are comparable with those drawn by comparing neptunium to uranium ratios.

3.2 Extraction of Np(IV) and Np(VI)

The distribution coefficients of Np(IV) and Np(VI) were determined at different initial aqueous nitric acid concentrations and uranium saturation of 30% TBP. The results show that for initial aqueous nitric acid concentration ranging from 1 to 4 M, the distribution coefficient (K_d) of both Np(IV) and Np(VI) decrease with increasing saturation of the organic phase with uranium. Similar effect has been observed in the extraction of plutonium[10, 11, 12] and uranium[13, 14, 15], also. The extraction of Np(VI) is higher than that of Np(IV), for the same aqueous acidity and TBP saturation. From the plots of log K_d vs percentage saturation of TBP, it appears that the rate of decrease of log K_d of Pu(IV) and Np(IV) with increasing TBP saturation by uranium is approximately same though the extraction of plutonium is higher than that of neptunium. The same is true for the decrease in the log K_d of U(VI) and Np(VI).

4. CONCLUSIONS

From the data reported here it appears that under the usual loading of 30% TBP with uranium (viz. about 65% saturation) both Np(IV) and Np(VI) get extracted to an appreciable extent, particularly at a nitric acid concentration higher than 2M. At lower nitric acid concentrations, however, very small amounts of Np(IV) may be extracted at 65% saturation or more.

Thus, a flow sheet could be designed either to force neptunium as Np(IV) (or preferably as Np(V)) with raffinate at low nitric acid concentration in the feed and high uranium saturation of TBP or to co-extract neptunium along with uranium and plutonium preferably as Np(VI) at feed acidities greater than 2 M. Mixer-settler experiments using synthetic mixtures containing neptunium, plutonium and uranium and under controlled conditions are planned. The data obtained from such experiments would help to draw more quantitative conclusions, which would be useful in the design of neptunium recovery facility.

5 REFERENCES

1. D. R. Vondy, J.A. Lane and A. T. Gresky; Ind. Engg. Chem. Process Design and Development 3, 293 (1964)

2. W. L. Poe, A. W. Joyce and R. I. Martens; Ibid, 3, 314 (1964)

3. R. E. Issacson and B. F. Judson; Ibid, 3, 296 (1964)

4. J. R. Flanary and G. W. Parker; Progress in Nucl . Energy Series III Process Chemistry 2, 501 (1958)

5. F. L. Moore; Anal. Chem. 29, 1941 (1957)

6. J. A. Wheat; Appl. Spectroscopy 16, 108 (1962)

7. A. I. Vogel; Text- book of Quantitative Inorganic Analysis, 3rd Ed. p. 333 (1961)

8. ORNL Master Analytical Manual; TID-7015, Method No. 1-215212

9. R. T. Chitnis and B. P. Naik; (Unpublished work)

10. H. D. Sharma, M. V. Ramaniah, K. Rengan and K. B. Shah; AEET/Radiochem/4 (1959)

11. J. R. Flannary; Proc. Int. U. N. Conf. Peaceful Uses of Atomic Energy, Geneva 9, p/539, 528 (1955)

12. S. M. Stoller and R. B. Richards (Editors), Reactor Handbook, Vol. II, 2nd Ed. 115 (1961), Interscience Publishers Inc.

13. Ibid, p. 156

14. N. Srinivasan, M. V. Ramaniah, S. K. Patil, V. V. Ramakrishna, R. Swarup and Ashok Chadha, BARC-428

15. H. D. Sharma, M. V. Ramaniah, M. N. Namboodiri, P. K. Bhattacharyya and D. V. Singh; AEET/Radiochem/3 (1959)

ANALYSIS OF PLUTONIUM PART I. CHEMICAL METHODS

R. T. Chitnis, T. S. Laxminarayanan, B. P. Naik, B. V. Prajapathi, R. K. Singh, K. Vijayan, A. V. Jadhav, J. K. Joshi, V. V. Marathe Keshav Chander, G. M. Nair and N. P. Singh
Bhabha Atomic Research Centre, Bombay 85

INTRODUCTION

In order to evolve a suitable method for the accurate estimation of plutonium which does not depend on the isotopic composition of the element a few of the well known chemical methods were taken up for detailed investigation. The techniques chosen for detailed study were the potentiometric, volumetric and coulometric titration procedures making use of the redox reactions of plutonium between its main valency states viz; III, IV and VI. All the studies were carried out on solutions prepared at Fuel Reprocessing Division by dissolving plutonium oxide in HNO_3.

PLUTONIUM SOLUTION

At least 3 samples were taken from each plutonium oxide lot selected for plutonium estimation. For each sample, nearly 500 mg of plutonium oxide, obtained by heating plutonium oxalate at 500°C for several hours, was taken, accurately weighed and dissolved by heating in concentrated HNO_3 containing about 0.15 MHF. The solution was evaporated to a low volume several times with concentrated HNO_3 to remove the HF. This solution after cooling was diluted with 0.5 M HNO_3 and transferred to a calibrated 50 ml flask and made up to the volume with 0.5 M HNO_3. Aliquots of this solution were used for the analysis.

POTENTIOMETRIC ESTIMATION

Procedure

Two methods, one by Milner et al[1] and the other by Drummond and Grant[2], reported in literature were tried and found to be not satisfactory. The procedure given below was developed after introducing some modifications in some of the steps in the reported methods.

500 micro-litres aliquot of plutonium in dilute HNO_3 ($\sim$2M) containing nearly 5 mg of the element were taken in a cylindrical vessel of about 50 ml capacity. This was diluted to about 2 ml with 1 M H_2SO_4

and AgO (prepared by mixing $AgNO_3$ and $K_2S_2O_8$ solutions)[1] was added in small quantities till the solution remained deep brown in colour due to excess oxidant for at least 5 minutes. One ml of 1.5 M sulphamic acid was added to this followed by 10 ml of 1 M H_2SO_4. After a lapse of 5 minutes nearly 20 to 30%, excess of the calculated quantity[3] of 0.2 M ferrous ammonium sulphate in 1 M H_2SO_4 was added to the solution with the help of an Agla micrometer syringe. The excess of Fe(II) was titrated with standard Ce(IV) sulphate solution (0.05 M in 3 M H_2SO_4, taken in an Agla micro-meter syringe) potentiometrically using a platinum indicator electrode and a calomel reference electrode connected through a saturated NH_4NO_3 bridge to avoid the formation of AgCl at its fibre junction. Figure 1 shows the set-up used for the potentiometric titration. A Beckman model G pH meter was used as the millivoltmeter to record the changes in the potential.

The platinum electrode was cleaned after each titration by boiling with concentrated HNO_3, washing with distilled water and heating to red heat in a Bunsen flame. The Fe(II) and Ce(IV) solutions were standardised daily against $K_2Cr_2O_7$ primary standard.

RESULTS

In the analysis of more than 40 plutonium oxide lots following the procedure given above an overall precision of 0.14% was obtained. The accuracy of the estimation procedure was checked by using a standard plutonium solution prepared from pure $Pu(SO_4)_2$. From preliminary studies the accuracy of the estimation was found to be within the precision of the method. More work is in progress for confirming this result.

VOLUMETRIC TITRATION

Procedure

An aliquot of plutonium solution in nitric acid medium containing nearly 2 mg of the element was evaporated to fumes with 1 ml of 15 M H_2SO_4 to remove the nitric acid. After cooling, the solution was diluted with 3 ml of 1% Ag_2SO_4 solution in 1M H_2SO_4. This was then treated with small quantities of AgO till the solution remained dark brown due to excess AgO for at least five minutes. It was then heated to about 85°C till the solution became colourless. The solution was then cooled and about 20% to 50% excess of the calculated quantity of 0.025 M ferrous ammonium sulphate in 0.5 M H_2SO_4 was added to this using a microburette. After diluting to about 10 ml with 0.05M H_2SO_4, the excess Fe(II) was titrated with standard $K_2Cr_2O_7$ (0.02 N) using 5,6 -dimethyl

ferroin as the indicator[4] or with standard Ce(IV) sulphate solution (0.02M in 0.5 M H_2SO_4) using ferroin as the indicator. In both cases the colour change of the indicator at the end point is from pink to pale blue. The blanks for ferrous ammonium sulphate as well as the indicator were determined separately under identical experimental conditions without taking plutonium. The stirring of the solution during the experiments was done using a magnetic stirrer.

RESULTS

From the titration results on a few plutonium samples it was found that the titration with $K_2Cr_2O_7$ using 5,6 -dimethyl ferroin gave sharp end points. The precision obtained was also good (better than 0.1%). However, the titration with Ce(IV) solution using ferroin as the indicator gave less sharp and points. The precision obtained was around 0.3%. Because of the difficulty in procuring 5,6 -dimethyl ferroin indicator, titration using cerium (IV) and ferroin indicator is being followed at present.

COULOMETRIC ESTIMATION

Apparatus

After testing various cells[5, 6, 7] used for coulometric titration of plutonium a combination of the model used by Scott and Peekema[6] at Hanford and the one employed by Shults[5] at Oak Ridge was used in the present work. The diagram of the cell used in this work is shown in figure 2. This cell was used in conjuction with an Automatic Electronic Controlled and Potential Coulometric Titrator[8, 9] of the ORNL Model Q-2005 and a portable precision potentiometer Rubicon No. 2730 supplied by Minneapolis Honeywell Regulator Co., USA.

PROCEDURE

An aliquot of plutonium containing about 2.5 mg of the element was taken in the titration cell and about 20 mg of sulphamic acid was added to it. The solution was stirred with a fractional horse power motor and purified argon gas was passed over the solution to maintain an inert atmosphere. The reduction of plutonium to Pu(III) was carried out at + 0.45v vs saturated calomel electrode (S. C. E.) (or + 0.56v vs S. C. E. if appreciable amount of iron is present) till the current decreased almost to zero. The recording of the readout voltage was continued at two minute intervals to check the completion of the reduction and to correct for background current and amplifier drift. After this the electrolysis was stopped and the integrator was zeroed. Then Pu(III) was oxidised to Pu(IV) at + 0.88v vs S. C. E. until the current again decreased almost to zero. The voltages for controlled

potential reduction and oxidation of plutonium were obtained from a study of the coulograms of plutonium and iron separately for each step. The readout voltage Q corrected for background current and amplifier drift was recorded. From the plutonium factor determined using a standard plutonium solution prepared from pure PuO_2, and the readout voltage Q the quantity of plutonium in the aliquot taken was calculated. Plutonium factor is generally expressed as milligram of plutonium per read out volt.

RESULTS

Controlled potential coulometry as given above was found to be quite fast and higly reproducible when the quantity of plutonium taken was in the range of 2 to 5 mg in each aliquot. Since the plutonium samples analysed were almost free from iron the reduction was done at + 0.45 v vs S.C.E. prior to its oxidation at + 0.88 v vs S.C.E. The precision of the method as calculated from the analysis of more than 40 plutonium oxide lots was 0.18%. The accuracy as determined in a preliminary study using standard $Pu(SO_4)_2$ solution was found to be 0.5% when the quantity of plutonium taken was about 2.5 mg per analysis.

CONCLUSION

Since potentiometric and coulometric titration methods were found to be very simple and gave high precision, these methods were employed for the analysis of a large number of plutonium samples. The volumetric method was also used in analysing many samples. In the potentiometric and volumetric methods employed, impurities such as iron and uranium commonly present in plutonium do not interfere. Though iron, if present in large quantities, interferes in the coulometric estimation, steps can be taken to minimise the error. The results of analysis of the same samples by the three methods showed an agreement within 0.5% as can be seen from Table I which gives the results of analysis of a few typical plutonium oxide samples.

ACKNOWLEDGEMENT

The authors wish to express their sincere thanks to Shri N. Srinivasan, Head, Fuel Reprocessing Division, and to Dr. M. V. Ramaniah, Head, Radiochemistry Division, for their keen interest in this work and to Shri M. N. Nadkarni, Fuel Reprocessing Division, for helpful discussions. Thanks are also due to Shri C. K. Sivaramakrishnan for providing the pure plutonium sulphate used in this work.

REFERENCES

1. G. W. C. Milner, A. J. Wood and G. E. Cassie; AERE-R 4975 (1965)

2. J. L. Drummond and R. A. Grant; Talanta 13, 477 (1966)

3. L. Lindner and A. V. Baeckmann; KFK 701 (1967)

4. R. Belcher and C. L. Wilson; New Methods of Analytical Chemistry, Second Edition, page 30 (1964)

5. W. D. Shults; ORNL-2921 (1960)

6. F. A. Scott and R. M. Peekema; HW-58491

7. G. W. C. Milner and J. W. Edwards; AERE-R3772 (1961)

8. H. C. Jones; ORNL Master Analytical Manual TID-7015 Sec 1, Methods Nos 1003029 and 9003029

9. M. T. Kelley, H. C. Jones and D. J. Fisher; Anal. Chem. 31, 488, 956 (1959)

TABLE I

Results of Analysis of Some Typical Plutonium Samples by Potentiometry, Coulometry and Volumetric Titrations

S. No.	Potentiometry (g/l)	Coulometry (g/l)	Volumetric titrations (g/l)
1.	11.746 ± 0.015	11.738 ± 0.008	*11.700 ± 0.005
2.	6.770 ± 0.007	6.775 ± 0.005	* 6.774 ± 0.002
3	7.588 ± 0.002	7.571 ± 0.005	* 7.569 ± 0.010
4	5.557 ± 0.007	5.532 ± 0.002	@ 5.496 ± 0.012
5	9.472 ± 0.001	9.471 ± 0.015	@ 9.397 ± 0.015
6	8.596 ± 0.017	8.572 ± 0.006	@ 8.642 ± 0.020
7	9.347 ± 0.012	9.348 ± 0.012	@ 9.397 ± 0.005
8	10.458 ± 0.017	10.520 ± 0.012	@ 10.580 ± 0.015
9	7.847 ± 0.016	7.856 ± 0.012	@ 7.825 ± 0.021
10	8.841 ± 0.007	8.793 ± 0.015	@ 8.836 ± 0.018

* Titrations with standard K_2CrO_7 using 5,6 -dimethyl ferroin as internal indicator.

@ Titrations with standard Ce(IV) using ferroin as internal indicator.

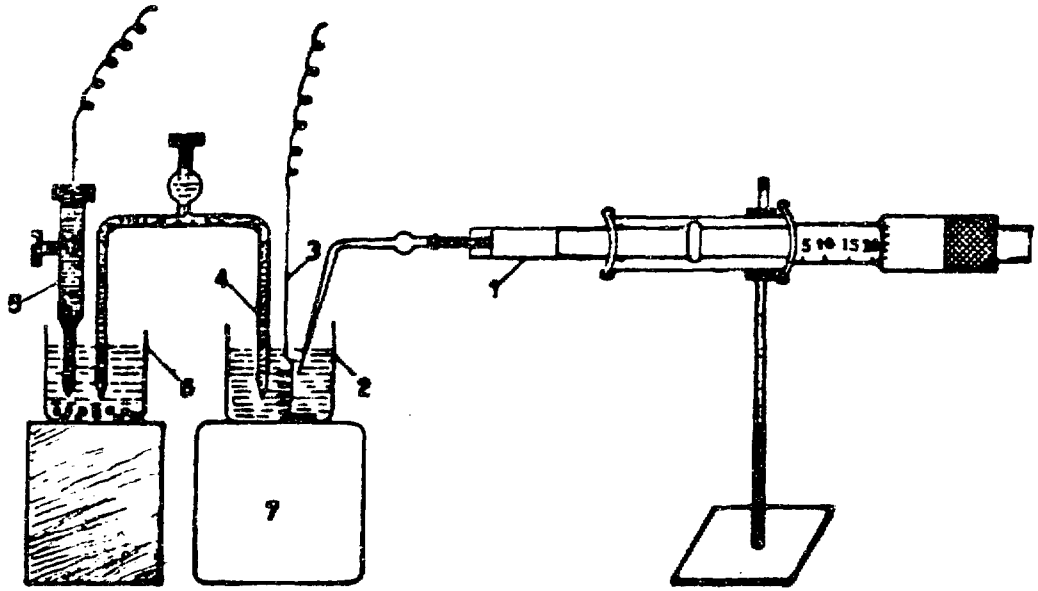

1. AGLA MICROMETER SYRINGE
2. TITRATION VESSEL
3. PLATINUM INDICATOR ELECTRODE
4. AMMONIUM NITRATE BRIDGE
5. REFERENCE ELECTRODE
6. SATURATED NH_4NO_3 SOLUTION
7. MAGNETIC STIRRING MOTOR

Fig.1. POTENTIOMETRIC TITRATION ASSEMBLY

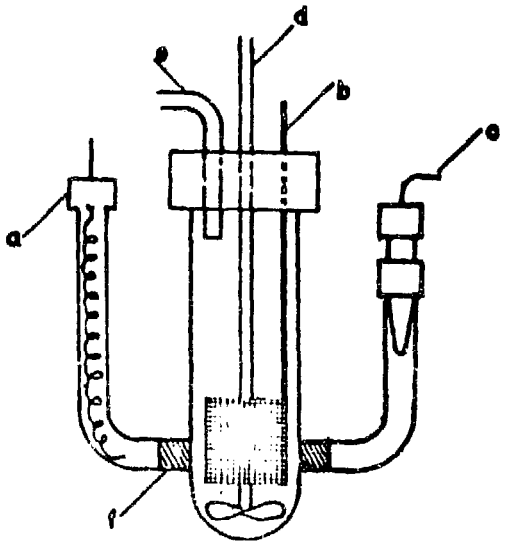

a_ AUXILIARY ELECTRODE

b_ WORKING "

c_ REFERENCE "

d_ STIRRER

e_ ARGON GAS INLET

f_ PORUS GLASS

Fig. 2. COULOMETRIC TITRATION CELL

ANALYSIS OF PLUTONIUM BY CHEMICAL AND RADIOMETRIC METHODS. PART II. DETERMINATION OF SPECIFIC ACTIVITY AND ISOTOPIC COMPOSITION OF PLUTONIUM

N. Srinivasan, M. V. Ramaniah and H. C. Jain
Bhabha Atomic Research Centre, Trombay, Bombay-85

1. INTRODUCTION

This paper describes the details of the method used for determination of specific activity and isotopic composition of plutonium. The isotopic composition of plutonium and the extent of transuranium elements formed, depend on the burn-up and cooling time. A knowledge of the specific activity and isotopic composition of plutonium are of great importance for inventory and accounting of the material and also from the point of its utilisation as a nuclear fuel.

2. EXPERIMENTAL

2.1. Determination of Specific Activity

2.1.1 Sample preparation

The plutonium samples used in this work were obtained after the dissolution of plutonium oxide and plutonium sulphate for which the total plutonium contents was determined as described in Part I. These samples usually had concentration of about 10 mg of plutonium per gram of solution. A dilution factor of 10^4 was necessary to take suitable aliquots for making samples for counting. This was achieved by two dilutions. First dilution was carried out in a glove box on a micro-balance and the second was done using a fumehood and semi-micro Mettler balance. All dilutions and preparation of samples for counting were carried out by weight transfer technique. This avoids pipetting errors and calibration errors of volumetric flasks and micro-pipettes. A 10 ml capacity polythene dropping bottle with a fine long capillary tip, weighing 3 to 4 grams, was used as a weight-burette. All dilutions and samples for counting were made in triplicate or quadruplicate. Reproducibility of better than 0.1% was obtained for about 100 mg weight transfers.

2.1.2 Counting

The samples were counted in an argon-flow proportional counter as well as in an alpha liquid scintillation counter. Accurately weighted samples

(about 100 mg) were either evaporated on electro-polished stainless steel planchets or mixed with 5 ml of liquid scintillator and counted. The composition of the liquid scintillator was dioxane containing 0.03% POPOP 0.7% PPO, and 10% napthalene all measured (W/V) as used by Ihle et al[1].

2.1.3 Counter Efficiency Determination

The efficiencies of the counters were determined using two independent calibrated standards, viz. a ^{241}Am disc source from Harwell and a ^{241}Am solution supplied by the I. A. E. A. The efficiency of the alpha proportional counter was found to be 49.47% with an uncertainty of 0.3% using electro-polished stainless steel planchets and that of alpha liquid scintillation counter to be 100 ± 0.4%.

Total plutonium present in the original solution was estimated as described in Part I.

2.2. Determination of Isotopic Composition

2.2.1 Sample preparation

Thin uniform and weightless sources were prepared for alpha spectrometry by electrodepositing plutonium on electropolished stainless steel or platinum discs. The electrodeposition was carried out either from nitric acid medium[2] or from isopropyl alcohol medium[3].

2.2.2 Alpha Spectrum

The alpha spectrum was obtained using a 400-channel analyser with surface barrier silicon detector in vacuum chamber. The resolution for a 30 mm^2 detector was 20 keV FWHM at about 5 MeV. The alpha spectra were recorded for the two types of electroplated sources, which were prepared from the original plutonium samples and from plutonium, purified through two anion-exchange microcolumns.

2.2.3 Calculation

The alpha spectra of the original plutonium sample (Figure IB) and that of plutonium purified from americium (Figure IC) show two main peaks, namely, 5.15 MeV and 5.50 MeV. The 5.15 MeV peak is due to ^{239}Pu + ^{240}Pu in both cases. In the case of the original plutonium sample

the 5.50 MeV peak is due to alpha particles from ^{238}Pu and ^{241}Am whereas in the case of the purified sample it is due to ^{238}Pu alone. From these data the percentage of ^{238}Pu and ^{241}Am in the sample were calculated. From the specific activity due to $^{239}Pu + ^{240}Pu$ only, the percentage of ^{240}Pu was calculated using the data in Figure 2.

3. RESULTS AND DISCUSSION

Table I gives the specific activity values of plutonium samples. Pure plutonium sulphate refers to the "standard plutonium sulphate" prepared from 2B, 2C, 2D and 2E by standard procedure. The specific activity values from the two independent counting systems (alpha proportional counting and alpha liquid scintillation counting) compare well within 1%. The standard deviation obtained was less than 1%. The accurate determination of specific activity depends on several factors such as counting efficiency, calibration of micro-pipettes and volumetric flasks and determination of the total plutonium content. As described in the 'Experimental', the counting efficiencies were determined using two independent standards and these were found to agree very well within 1% of the values quoted for the standard. Electro-polished or mechanically polished stainless steel planchets, used in this work, gave counting rate which agreed well with the alpha liquid scintillation counting. The efficiency was reproducible using these polished planchets. In case of dull surface of stainless steel the counting rate was always less by about 2% and in the case of platinum it was higher by about 2%. This has also been emphasised by Schneider et. al[4]. The inaccuracies in the volume measurements were avoided by weight transfer technique.

Table I shows the isotopic composition of the plutonium samples. The mass spectrometric method is considered to be more precise for the isotopic analysis, but in the case of ^{238}Pu, the radiometric method is still recommended for the accurate determination[5] since in the mass spectrometric method it is difficult to account for ^{238}U interference and the limitations on the amount which can be used as sample on account of its very high sp. activity (about 300 times than that of ^{239}Pu). In order to check the complete removal of ^{241}Am which will otherwise contribute to ^{238}Pu at 5.50 MeV peak, analysis was carried out on synthetic mixtures of Am^{241} and plutonium at tracer scale in the ratios 1 : 10 and 1 : 100. The alpha spectrum on the sample after anion exchange purification showed that the peak at 5.50 MeV is due to Pu^{238} only. It is advantageous to determine Pu^{240} mass spectrometrically since usually it is present in comparable amount to Pu^{239} and is a direct determination, whereas in radiometric method it involves an indirect determination based on specific activity and the presence of other alpha emitting nuclides. However, the values obtained for Pu^{240} in this work can be checked with that of the mass spectrometric values in due course. An

approximate idea of the burn-up particularly in the case of low burn-up, is obtained from the amount of Pu^{241} present[6], which in turn gives the approximate amount. The direct estimation of Pu^{241} is difficult because of its low energy beta radiation (20 keV). However, effort is being made to standardise the counting efficiency for the low energy beta in the liquid scintillation counter. No detectable amount of Pu^{242} could be observed in the alpha spectrum in the energy region from 4.86 MeV to 4.90 MeV.

4. ACKNOWLEDGEMENT

The authors are grateful to the Atomic Fuels Division for electropolishing the stainless steel planchets, to Dr. K. Rengan and Mr. A. V. Jadhav for helpful discussion and to Mr. K. A. Mathew for his help during the experiments.

5. REFERENCES

1. H. R. Ihle, M. Karayanns and A. P. Murrenhoff; Standardisation of Radionuclides, I. A. E. A., Vienna, 485 (1965)

2. V. G. Khlopin; Radium Institute of the Academy of Sciences of U. S. S. R., AEC - tr (Chemistry) 4497.

3. Procedure Developed in this Laboratory (to be published)

4. R. A. Schneider and K. M. Harmon; Alpha Counting Methods, HW-53368

5. Peter Wolf and Johann Reinhardt; Gaselischaft, mbH, Karlsruhe, KFK-339, July (1965)

6. D. C. Sahni and B. P. Rastogi; AEET/RED/TRP-108.

TABLE I

Sample Number	* Specific activity x 10^{-5} (dpm/μg)		Isotopic composition %				
	Alpha proportional counting	Alpha liquid scintillation counting	Am^{241}	Pu^{238}	Pu^{240}	Pu^{241}	Pu^{239}
I-A	1.5545 ± 0.0094 (7)	1.5499 ± 0.0050 (14)	0.019 [0.88]	0.010 [2.43]	4.2	0.3	95.47
Pure	1.5595 ± 0.0105 (23)	1.5637 ± 0.0092 (23)	0.004 [0.18]	0.012 [2.78]	4.3	0.3	95.38
PuO_2	1.5398 ± 0.0116 (11)	1.5554 ± 0.0042 (12)	0.015 [0.67]	0.011 [2.57]	4.2	0.3	95.47
I-D	1.5440 ± 0.0061 (10)	1.5425 ± 0.0043 (12)	0.016 [0.73]	0.011 [2.56]	4.1	0.3	95.57
2-B	1.5904 ± 0.0087 (15)	1.6159 ± 0.0067 (11)	0.006 [0.25]	0.015 [3.44]	5.1	0.4	94.48
2-C	1.5834 ± 0.0141 (11)	1.6028 ± 0.0069 (12)	0.006 [0.28]	0.014 [3.37]	5.0	0.4	94.58
2-D	1.5827 ± 0.0090 (8)	1.6057 ± 0.0110 (6)	0.004 [0.17]	0.014 [3.27]	5.0	0.4	94.58
2-E	1.5798 ± 0.0177 (8)	1.6105 ± 0.0047 (12)	0.006 [0.26]	0.014 [3.31]	5.0	0.4	94.58
Pure $Pu(SO_4)_2$	1.6090 ± 0.0110 (18)	1.6080 ± 0.0080 (18)					

* Am^{241} contribution has been subtracted.

The number in the parenthesis ( ) indicates the number of independent determinations, i. e. the number of counting samples prepared from various dilutions. The value in the parenthesis [ ] indicates the isotopic composition in terms of the % alpha activity.

OPTICAL, ELECTRICAL TRANSPORT AND DIELECTRIC STUDIES ON RARE EARTH PEROVSKITES

G. V. Subba Rao and C. N. R. Rao
Department of Chemistry, Indian Institute of Technology, Kanpur

The rare earth perovskites of the general formula $LnZO_3$ where Z = Cr, Mn or Fe and Ln is a rare earth element or Y, form a novel series of substances having interesting crystallographic, magnetic, dielectric and electrical transport properties. All the pervoskites except the heavy rare earth manganites are orthorhombic and $LnCrO_3$ and $LnFeO_3$ are anti-ferromagnetic with superimposed weak ferromagnetism. The Neel temperatures, T_N, of $LnCrO_3$ are low (below room temperature) whereas $LnFeO_3$ possess relatively higher values ($\sim$370°C). Although the crystallographic and magnetic properties of these perovskites have been well investigated, only limited information is available on the optical and electrical properties of these materials. In the present study we have carried out a systematic examination of the electronic spectra (in the range 30,000-11,000 cm^{-1}), the infra-red spectra (range 4,000-30 cm^{-1}), electrical conductivity, σ and Seebeck coefficient, β (as a function of temperature and oxygen partial pressure) and dielectric (hysteresis and pyroelectric current) properties of these three series of perovskites in the form of polycrystalline materials (and single crystals in some cases) not only as an aid to supplement the available literature data but also to gain insight into the mechanism of conduction in these solid state materials.

The electronic and infra-red spectra of the rare earth perovskites indicate that they are characteristic of the parent transition metal oxides slightly modified by the presence of the rare earth ion in the lattice. Characteristic variations in the observed spectra have been interpreted in terms of the variation of metal-oxygen covalency effects of Z-O and Ln-O bonds. The covalency of the Z-O bond decreases with increase in the atomic number from Cr to Fe and within the rare earth series the same trend is shown whereas Ln-O covalency seems to increase from La to Lu. There is some indication from the spectra that there is distortion in the ZO_n polyhedra in the heavier rare earth chromites and manganites.

The $LnZO_3$ perovskites (Z = Cr, Mn or Fe) are p - type semiconductors with conductivity in the range exhibited by the parent transition metal oxides (10^{-4} - 10^{-1} ohm^{-1}. cm^{-1}), but considerably higher than the parent rare earth sesquioxides. Among the three series, the orthochromites have the highest conductivity at a given temperature. Within the rare earth series, however, σ decreases with increase in the atomic number of the Ln as in the case of Ln-sesquioxides and the energy of activation for conduction, E_a, increases. La-perovskites possess comparatively higher value of σ than the other Ln-compounds which may be due to the departure from stoichiometry. Small ionic contribution to the total

conductivity seems to be existing in all the perovskites presently examined. Breaks in log σ -1/T plots were noted at known crystallographic and dielectric transtion temperatures. The measured Seebeck coefficients ($\sim$ 0.3 mV/^{o}C and almost independent of temperature), the low E_a values (0.05 - 0.25 eV), the estimated mobilities (10^{-5} - 10^{-3} cm^2/V. sec) and optical spectra (bands characteristic of Z^{3+} ion) all point to the fact that these $LnZO_3$ compounds are narrow band materials exhibiting localized electron behaviour; no intrinsic conduction was encountered upto the maximum temperature investigated ($\sim$ 850^{o}C). For all practical purposes, the d-electrons of the transition element control the optical and electrical properties of these perovskites and Ln plays only a minor role. The conclusions are in accord with the Goodenough scheme proposed recently.

The heavy rare earth manganites which are hexagonal and ferro-electric showed breaks in log σ -1/T plots at the known ferroelectric Curie points. In the heavy rare earth chromites we noted similar breaks at high temperatures ($\sim$ 500^{o}C) which could not be identified as involving crystallographic or magnetic transition; we suspected that these may represent ferroelectric $\rightarrow$ paraelectric transitions and further investigated the dielectric hysteresis loop and pyroelectric current behaviour as a function of temperature. The results lead to the conclusion that these materials are also associated with ferroelectricity just as the manganites. This observation, however, calls for a revision of the reported space group for the heavier rare earth chromites. At present, detailed dielectric hysteresis and pyroelectric current studies on single crystal materials of the orthochromites are in progress in this laboratory.

THERMODYNAMICS AND KINETICS OF OXIDATION OF Pr_2O_3 AND Tb_2O_3

S. Ramdas, K. C. Patil and C. N. R. Rao
Department of Chemistry
Indian Institute of Technology, Kanpur

Praseodymium and terbium oxides form a wide range of non-stoichiometric phases, between 400-1000°C and P_{O_2} = 2 - 200 mm; the compositions ranging from $LnO_{1.5}$ - $LnO_{2.0}$ (where Ln = Pr or Tb). The stable compositions of these oxides can be given by a general formula $Ln_n O_{2n-2}$ ($n \geq 4$) and at a constant temperature they can be expressed as a function of oxygen partial pressure. The Pr_2O_3 exists in two forms C (or ϕ) and A(or θ). A form is a close-packed hexagonal structure and C form has a fluorite derived cubic structure with one fourth of the anion positions vacant.

The oxidation reaction of Pr_2O_3 to the different stable phases can be written as

$$PrO_{1.5} + \nu O_2 \longrightarrow PrO_{1.5+2\nu} \quad \ldots\ldots\ldots (1)$$

Kuznetsov and Rezukhina from their emf measurements base on solid electrolyte cell have reported that ΔS^o = -26 eu/mole or O_2 for reaction (i) with $\nu = 0.167$. For a metal oxidation reaction

$$M^{4u} + \nu O_2 \dashrightarrow MO_{2+\nu} \quad ; \quad \Delta S^o = -44 \text{ eu/mole of } O_2$$

From the plots of $RT\ln p_{O_2}$ versus temperature for each composition we could estimate the standard entropy change and these are found to be roughly 25-30 eu/mole of O_2 for $\nu = 0.105, 0.15, 0.16, 0.165$ and 50 eu/mole of O_2 for $\nu = 0.125, 0.09$. It should be pointed out that the former compositions are stable ordered phases and the latter ones are disordered metastable phases. The increase in entropy must arise from the microstructural behaviour contributing to configurational entropy. In the evaluation of configurational entropy the different phases are derived from PrO_2, with fluorite structure. Because of the varying ratios of Pr^{4+}/Pr^{3+}, the different cations can be arranged in a random manner giving rise to electronic disorder, whose contribution to configurational entropy being ΔS^{conf}_{elec}. Besides, the anion vacancies also contribute ΔS^{conf}_{vac}. In the estimation of these quantities one assumes random distribution of cations and anion vacancies. This is not valid for stable compositions since there is evidence for vacancy ordering. Thus, the

contribution to configurational entropy arise mainly due to electronic disorder and hence ΔS^{o} for reaction (1) with $\nu = 0.165$ can be written as $\Delta S^{o} = \Delta S^{o}_{normal} + \Delta S^{conf}_{elec} = -32$ eu/mole of O_2. But, in the case of the meta-stable phases, where there is only a minor perturbation of the electronic structure from the well-ordered phase of $PrO_{1.71}$, one can expect the normal entropy change of oxidation. Even in the case of wustite and Nb_2O_{5-x}, higher entropy values are reported. Thus, we can conclude that the entropy of oxidation from stoichiometric to non-stoichiometric phases involve configurational factors, especially due to the electronic disorder in such systems.

In order to understand the mechanism of gross oxidation of the sesquioxides, we have carried out the kinetic studies. The kinetic data can be interpreted by assuming that the reaction consists of fast initial oxidation of the reactant, fast nucleation, slow and rate determining propagation of the product phase and fast uniphasic oxidation of the product phase to the equilibrium composition. The rate equation is of the form:

$$(X_{\infty} - X_t)^{1/3} = kt + c \qquad \ldots\ldots\ldots \quad (2)$$

where $k = -R\,(X_{\infty} - X_t)^{1/3}/r$ and $C = (X_{\infty} - X_t)^{1/3}$, X_t and X_{∞} denote the compositions at time t and ∞ respectively, R is the velocity of advancement of the reactant product interphase and r is the particle radius. From our kinetic plots, we find that the activation energy for Pr_2O_3 (C) $\rightarrow Pr_6O_{11}$ is smaller than for Pr_2O_3 (A) $\rightarrow Pr_6O_{11}$; this is what we would expect on the basis of the defect (open) structure of Pr_2O_3(C).

In conclusion we can say that for such grossly non-stoichiometric compounds the configurational factors influence the thermodynamics of reactions and that the rates of ractions are phase boundary controlled.

THE KINETICS OF OXIDATION OF NN-DIMETHYL FORMAMIDE WITH CERICAMMONIUM NITRATE

S. S. Krishnamurthy and S. Soundararajan
Department of Inorganic & Physical Chemistry
Indian Institute of Science, Bangalore-12

The kinetics of oxidation of dimethyl formamide (DMF) with Ce^{iv} in nitric acid medium was studied by the usual titrimetric procedure[1]. When the DMF concentration is in (40-50 times) excess of Ce^{iv}, the disappearance of Ce^{iv} follows a first order rate law. The apparent first order rate constants, k' were determined in this way, varying the concentrations of DMF (0.4-0.7M), acid (0.5-2.0M) and nitrate (1-2M). The results are shown in Table I.

The kinetic data are consistent with the inner sphere mechanism of formation of an intermediate coordination complex between Ce^{iv} and DMF[2]. The observed apparent rate constant k' varied with DMF concentration according as:

$$\frac{1}{k'} = \frac{1}{k} + \frac{1}{k\,K(DMF)^3}$$

where k and K are disproportionation and the equilibrium (formation) constants of the complex[3]. A plot of $\frac{1}{k'}$ vs $1/(DMF)^3$ gives a straight line indicating that a 1:3 complex between Ce^{iv} and DMF is formed as the most predominant species. From this plot the values of K and k were determined.

Keeping (H^+) constant at 1M, increase in the nitrate concentration from 1M to 2M produces no significant change in the quilibrium constant K showing that nitrate ion is not displaced from the coordination sphere of the cerate complex[4]. At the same time the specific rate constant k shows an appreciable change (from 4.35×10^{-4} Sec^{-1} in 1 M NO_3^- to 3.33×10^{-4} Sec^{-1} in 2 M NO_3^-). The retarding effect of added NO_3^- on the rate of reaction shows that a cerate complex richer in nitrate is formed in solutions of higher nitrate ion concentration and this decomposes at a rate slower than that of the cerate complex with lower nitrate content.

At constant nitrate ion concentration (2M) increase of (H^+) from 1.0 to 2.0M increases K by about 1.5 times. Since no nitrate ion is displaced, a reaction such as (A) is indicated:

$$X_5\ Ce(OH) + n\ (DMF) + H^+ \rightleftharpoons X_{6-n}\ Ce(DMF)_n + H_2O \quad \ldots\ldots\ (A)$$

If one OH^- were displaced fr n each molecule of the complex, K would be doubled by increasing $(H^+$ rom 1.0 to 2.0M. Since the increase in K is only 1.5 times, we conclude that more than one cerate species may participate in the rate determining step[4]. The decrease in the disproportionation constant k on increasing acid, is explained on the basis of a higher disproportionation rate for the hydroxy cerate-DMF complex than for the DMF complex with unhydrolysed cerate species.

In summary, the retarding effect of NO_3^- and H^+ on the rate of the reaction enable us to conclude that an hydroxy cerate species $(X_5\ CeOH)^{3+}$ is the most reactive one while the higher nitrate cerate moiety $(X_5\ CeNO_3)^{3+}$ is theleast reactive[3, 5]. (X here represents coordinate NO_3^- or H_2O).

The oxidation process can thus be written as:

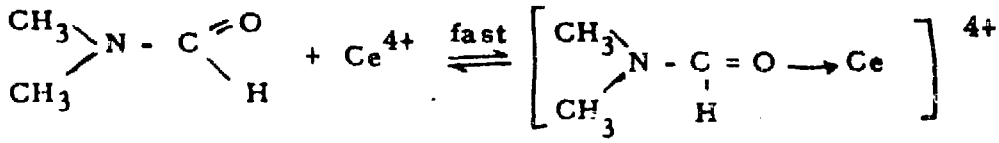

Complex

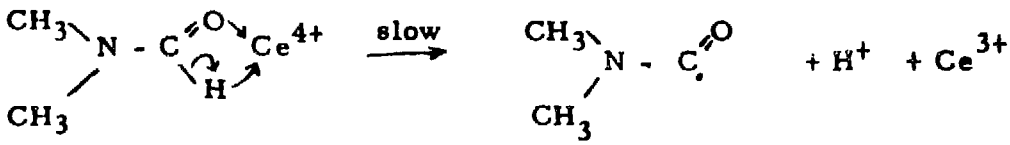

Free-radical

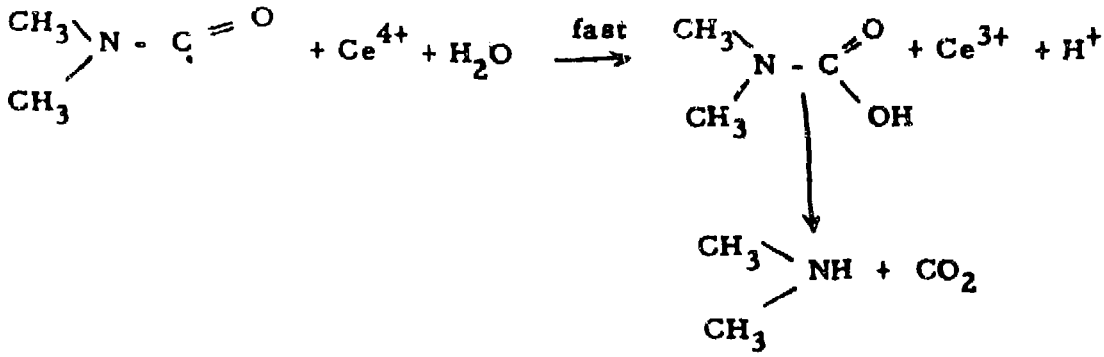

Here for simplicity, the reactive cerate species is represented by Ce^{4+} and coordination of only one DMF is shown.

That a free radical mechanism is involved in Ce^{iv} oxidation of organic substances has been demonstrated by several authors[1, 2]. The low activation energies obtained in the present case (~18.0kcal/mole) support the free radical mechanism[6].

REFERENCES

1. B. Sethuram and S. S. Muhammad; Acta. Chim. Hungary Acad. Sci. 46, 115 (1965)

2. T. A. Turney; "Oxidation Mechanisms", Butterworhts, London, 42 - 46 (1965)

3. M. Ardon; J. Chem. Soc. 1811 (1957); H. Lineweaver and D. Burke, J. Am. Chem. Soc. 56, 658 (1934)

4. F. R. Duke and A. A. Forist; J. Am. Chem. Soc. 71, 2790 (1949)

5. J. Shorter; J. Chem. Soc. 1868 (1962)

6. C. Walling; "Free Radicals in Solution", Wiley, New York p. 39 (1957)

TABLE- I

The Rate Constants in the Oxidation of DMF by Ce^{iv} Under Various Experimental Conditions

(Ce^{iv}) = 0.01M Temp. = 35 ± 0.02°C

H^+	NO_3^-	$k' \times 10^5$ sec^{-1} at various DMF concentrations sec^{-1}				
		0.4M DMF	0.5M DMF	0.55M DMF	0.60M DMF	0.70M DMF
1.0M	1.0M	3.642	6.083	7.693	9.435	13.40
1.0M	2.0M	-	4.976	6.250	7.713	10.75
2.0M	2.0M	-	2.874	3.570	4.255	5.686
1.5M	2.0M	-	-	-	5.206	-
0.5M	2.0M	-	-	-	9.620	-

TABLE- II

The Temperature Dependence of the Rate Constant and the Apparent Activation energy in the Ce^{iv} - DMF system

Ce^{iv} = 0.01M, H^+ = 1.0M, NO_3^- = 1.0M

DMF Concn	$k' \times 10^5$ sec^{-1} at various temps.			Apparent activation energy Kcal/mole
	301.2°K	308.2°K	318.2°K	
0.40M	1.905	3.642	9.210	17.9
0.50M	2.884	6.083	15.35	18.2

INFRARED SPECTRA OF SOME RARE EARTH COMPOUNDS

C. R. Kanekar and V. R. Marathe
Tata Institute of Fundamental Research, Colaba, Bombay-5

and

N. V. Thakur
Chemical Engineering Division
Bhabha Atomic Research Centre
Trombay, Bombay-85

INTRODUCTION

Survey of literature shows that conflicting conclusions regarding bonding in rare earths acetates have been reached from the infrared spectra of these compounds. Edward et al[1] concluded that the type of bonding in these compounds is bidentate. Soundararajan et al[2, 3] recently studied the infra-red data of mono-chloracetates and trichloracetates of some rare earths and also concluded that the type of bonding in these compounds is bidentate. On the other hand Rao et al[4] proposed a monodentate bonding in lanthanum acetate. A systematic study of the infra-red spectra of the acetates, therefore, seemed necessary.

This paper reports the data obtained on the asymmetric and symmetric O-C-O stretching frequencies in the acetates, chloracetates and salicylates of sodium, lanthanum, cerium, gadolinium and ytterbium.

RESULTS AND DISCUSSION

Acetates: In the various acetates studied, the following facts are observed: (Table I). Asymmetric O-C-O stretching frequency increases in the order acetate < monochloracetate < dichloracetate < trichloracetate while symmetric O-C-O stretching frequency decreases in the same order. Four possible structures, as shown below, are possible for acetates

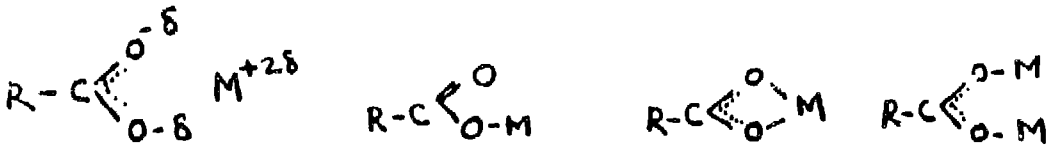

(a) ionic (b) monodentate (c) bidentate (d) bridge type

Following Mehrotra et al[5], the bridge structure need not be considered in the case of rare earths acetates as these species are found to be monomeric. Structures (a) and (c) do not disturb the C_{2v} symmetry of O-C-O group. Hence, any increase in covalency of M-O bond will decrease both the symmetric and asymmetric stretching frequencies for structure (c). On the other hand, in structure (b) C_{2v} symmetry of O-C-O group will be considerably altered on account of the fact that the metal atom is linked to one of the oxygen atoms of the O-C-O group. Hence, as covalency of M-O bond increases, asymmetric frequency should increase while the symmetric frequency should decrease. The data observed for the rare earths acetates, however, show that as covalency of M-O bond increases (from trichloracetates to acetates) asymmetric frequency decreases and symmetric frequency increases. The results indicate a marked increase in symmetry of O-C-O group with increase in covalency of M-O bond. In other, words, ring type structure (c) is favoured with increasing covalency of M-O bond.

The two factors, covalency and symmetry, have opposite effect on symmetric O-C-O stretching frequency and a uni-directional effect on asymmetric O-C-O stretching frequency. Hence, variations in asymmetric frequencies are quite prominent while variations in symmetric frequencies are small and for some of the compounds, random. The trend in symmetric O-C-O stretching frequency from trichloracetates to acetates shows that the "symmetry factor" is more prominent than "covalency factor".

For the acetates of various metals, the asymmetric O-C-O stretching frequency decreases in the order

$$Na^{+} > La^{+3} > Ce^{+3} > Gd^{+3} \sim Yb^{+3}$$

while the symmetric stretching frequencies are not markedly affected.

From the changes in the asymmetric frequency, it may be concluded that the covalency of M-O bond increases in the order

$$Na^{+} < La^{+3} < Ce^{+3} < Gd^{+3} \sim Yb^{+3}$$

Salicylates

The salicylates of lanthanum, cerium and gadolinium are of the type

$$M\ (C_6H_4.OH.COO)_3$$

While ytterbium salicylate has the composition

$$Yb_2\ (C_6H_4.O.COO)_3.4H_2O$$

INFRARED SPECTRA OF SOME RARE EARTH COMPOUNDS

C. R. Kanekar and V. R. Marathe
Tata Institute of Fundamental Research, Colaba, Bombay-5

and

N. V. Thakur
Chemical Engineering Division
Bhabha Atomic Research Centre
Trombay, Bombay-85

INTRODUCTION

Survey of literature shows that conflicting conclusions regarding bonding in rare earths acetates have been reached from the infrared spectra of these compounds. Edward et al[1] concluded that the type of bonding in these compounds is bidentate. Soundararajan et al[2, 3] recently studied the infra-red data of mono-chloracetates and trichloracetates of some rare earths and also concluded that the type of bonding in these compounds is bidentate. On the other hand Rao et al[4] proposed a monodentate bonding in lanthanum acetate. A systematic study of the infra-red spectra of the acetates, therefore, seemed necessary.

This paper reports the data obtained on the asymmetric and symmetric O-C-O stretching frequencies in the acetates, chloracetates and salicylates of sodium, lanthanum, cerium, gadolinium and ytterbium.

RESULTS AND DISCUSSION

Acetates: In the various acetates studied, the following facts are observed: (Table I). Asymmetric O-C-O stretching frequency increases in the order acetate < monochloracetate < dichloracetate < trichloracetate while symmetric O-C-O stretching frequency decreases in the same order. Four possible structures, as shown below, are possible for acetates

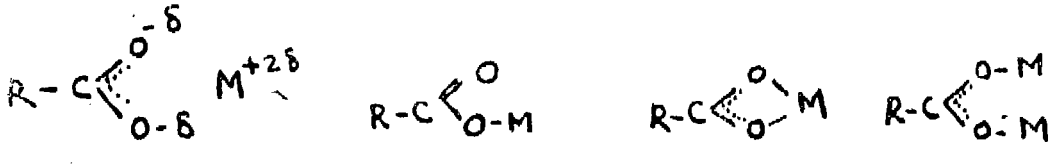

(a) ionic (b) monodentate (c) bidentate (d) bridge type

Following Mehrotra et al[5], the bridge structure need not be considered in the case of rare earths acetates as these species are found to be monomeric. Structures (a) and (c) do not disturb the C_{2v} symmetry of O-C-O group. Hence, any increase in covalency of M-O bond will decrease both the symmetric and asymmetric stretching frequencies for structure (c). On the other hand, in structure (b) C_{2v} symmetry of O-C-O group will be considerably altered on account of the fact that the metal atom is linked to one of the oxygen atoms of the O-C-O group. Hence, as covalency of M-O bond increases, asymmetric frequency should increase while the symmetric frequency should decrease. The data observed for the rare earths acetates, however, show that as covalency of M-O bond increases (from trichloracetates to acetates) asymmetric frequency decreases and symmetric frequency increases. The results indicate a marked increase in symmetry of O-C-O group with increase in covalency of M-O bond. In other, words, ring type structure (c) is favoured with increasing covalency of M-O bond.

The two factors, covalency and symmetry, have opposite effect on symmetric O-C-O stretching frequency and a uni-directional effect on asymmetric O-C-O stretching frequency. Hence, variations in asymmetric frequencies are quite prominent while variations in symmetric frequencies are small and for some of the compounds, random. The trend in symmetric O-C-O stretching frequency from trichloracetates to acetates shows that the "symmetry factor" is more prominent than "covalency factor".

For the acetates of various metals, the asymmetric O-C-O stretching frequency decreases in the order

$$Na^{+} > La^{+3} > Ce^{+3} > Gd^{+3} \sim Yb^{+3}$$

while the symmetric stretching frequencies are not markedly affected.

From the changes in the asymmetric frequency, it may be concluded that the covalency of M-O bond increases in the order

$$Na^{+} < La^{+3} < Ce^{+3} < Gd^{+3} \sim Yb^{+3}$$

Salicylates

The salicylates of lanthanum, cerium and gadolinium are of the type

$$M\ (C_6H_4.OH.COO)_3$$

While ytterbium salicylate has the composition

$$Yb_2\ (C_6H_4.O.COO)_3.4H_2O$$

It is observed that in the case of the salicylates of lanthanum cerium and gadolinium the asymmetric O-C-O stretching frequency is shifted to lower wave number and the symmetric stretching frequency is shifted to higher wave number compared to sodium salicylate (Table II). It appears that the covalency of M-O bond increases appreciably from sodium to lanthanum but thereafter in the rare earths series it remains practically unaltered. The stability constant ($\log k_1$) values also show that the stability of lanthanum and cerium salicylates are very nearly equal, as reported by Cefola et al[6]. (La : $\log k_1 = 2.64$; Ce : $\log k_1 = 2.66$) indicating that M-O bond has nearly the same ionicity.

The O-H stretching frequency has been observed at 3510 cm^{-1} in sodium salicylate; this band shifted to 3330, 3340 and 3290 cm^{-1} in the salicylates of lanthanum, cerium and gadolinium respectively. The shift indicates that the OH group also takes part in bond formation through oxygen. The data thus suggest that salicylic acid acts as a tridentate ligand and it appears that in these complexes, coordination number may be at least nine.

Ytterbium salicylate is formed by replacing H^+ from the - COOH group and the phenolic -OH group. Replacement of the phenolic proton by the metal should result in a strong O - M bond since log k (phenolic H) is quite high (11.72). This would reduce the distance between the metal and the carboxylate oxygen. Consequently, both the asymmetric and symmetric O-C-O stretching frequencies should increase compared to other lanthanide salicylates studied. Exactly this has been observed.

The band observed at 3290 cm^{-1} in ytterbium salicylate may be due to O-H stretching frequency arising from the coordinated water molecules.

REFERENCES

1. D.A. Edwards and R.N. Hayward; Can. J. Chem. 46, 3443 (1968)

2. S.S. Krishnamurthy and S. Soundararajan; J. Less Common Metals 16, 1 (1968)

3. V.N. Krishnamurthy and S. Soundararajan; J. Less Common Metals 13, 263 (1967)

4. K.C. Patil, G.V. Chandrashekhar, M.V. George and C.N.R. Rao; Can. J. Chem. 46, 257 (1968)

5. S.N. Misra, T.N. Misra and R.C. Mehrotra; J. Inorg. Nucl. Chem. 25, 201 (1963)

6. M. Cefola, A.S. Tompa, A.V. Celiano and P.S. Gentile; Inorg. Chem. 1, 290 (1962)

TABLE I

O-C-O Asymmetric Stretching Frequencies (cm^{-1})

	Na(I)	La(III)	Ce(III)	Gd(III)	Yb(III)
Acetate	1560	1562	1560	1550	1548
Monochloracetate	1592	1577	1575	1563	1563
Dichloracetate	1620	1621	1618	1613	1608
Trichloracetate	1675	1669	1653	1631	1631

O-C-O Symmetric Stretching Frequencies (cm^{-1})

	Na(I)	La(III)	Ce(III)	Gd(III)	Yb(III)
Acetate	1408	1399	1400	1416	1410
Monochloracetate	1397	1399	1395	1393	1399
Dichloracetate	1379	1381	1381	1393	1399
Trichloracetate	1351	1351	1359	1389	1389

TABLE II

Infrared Data for Rare Earth Salicylates

	O-C-O stretching Frequency (cm^{-1}) symmetric	O-C-O stretching Frequency (cm^{-1}) symmetric	O-H stretching frequency (cm^{-1})
Sodium salicylate	1575	1370	3510
Lanthanum salicylate	1550	1379	3330
Cerous salicylate	1550	1383	3340
Gadolinium salicylate	1550	1379	3290
ytterbium salicylate	1600	1393	3290*

* Due to water of crystallization.

MULTIDENTATE AZOMETHINE COMPLEXES OF THORIUM (IV)

N. S. Biradar and V. H. Kulkarni
Department of Chemistry, Karnatak University, Dharwar, India

The recent publications on the azomethine complexes of thorium (IV)[1-4] have given an impetus to publish some of our results in this field.

The complexes were prepared by the reaction of a slight excess of azomethine with $ThCl_4$ in absolute ethanol. The mixture was heated at 70-80°C till the solvent vapourised away. The temperature was raised to 180°C and heating was continued till the evolution of HCl gas ceased. The product was cooled, extracted with ethanol, filtered and dried over fused calcium chloride.

The complexes are sparingly soluble in DMF and DMSO. Their limited solubility in the organic solvents did not permit us to determine the molecular weight. The elemental analyses (Table I) correspond to the composition $ThCl_2(L)$ where LH_2 stands for the ligand. The complexes behave as non-electrolytes in DMF. However, in view of the hexa-covalency of Th(IV) these can be regarded as octa-hedral.

Electronic Spectra - The figures I and II show the plots of log ϵ values against wavelength in mμ of the ligands and the complexes.

The intense bands in the region 300-380 mμ (Fig. I) of the ligands are replaced by more complicated bands of varying intensity when they are coordinated with the metal ion (Fig. II). The spectra of the complexes do not resemble the spectra of the ligands. This can be taken as an evidence for the complex formation.

The band in the region 240-260 mμ appearing in the ligands as well as in their complexes can be considered as a π-π^* benzenoid band in view of the assignment made by Chatterjee and Douglas[5].

The spectra of the ligands show an increase in the intensity of absorption as we replace CH_2-CH_2 hydrocarbon bridge successively by phenyl, biphenyl and biphenyl sulphide systems (Fig. I). In the complexes, the same trend is maintained except bis (salicylidene) pp'-diaminodipheny sulphide complex (Fig. II), which falls between bis (salicylidene)-o-phenylinediamine and bis (salicylidene) benzidine complexes. This may be due to the weak coordination of sulphur with thorium.

Infrared Spectra - The important infra-red frequencies and their assignments are given in Table II.

A strong band around ~ 1610 cm^{-1} assigned to the C = N stretch of the free Schiff base[6] is observed in the region 1615-1598 cm^{-1} in the complexes. The slight shift observed in the frequency suggests the coordination through the azomethine-nitrogen.

The broad band in the region 2800-2600 cm^{-1} assignable to the intra-molecular hydrogen bonded -OH[7, 8] is not observed in these complexes. This proves that the hydroxy groups of the ligands have taken part in the complex formation.

600-250 cm^{-1} Region

In this region one would expect to find the vibrational modes due to the M-N, M-O and M-Cl, stretchings. However, the bands appearing due to the ring deformation vibrations complicate the band assignments.

M-N Stretching - In these complexes, two bands appearing in the region 580-550 cm^{-1} are assigned to the M-N stretching vibration. It appears to us that the band appearing between 580-560 cm^{-1} is sensitive to the ligand size.

M-O Stretching - The medium intensity band in the region 450-420 cm^{-1} is assigned to the Th-O stretching vibration in view of the assignments made by the other authors[9-14]. We observe regular increase in the Th-O stretch from bis-(salicylidene) ethylenediamine Th (IV) to bis-(Salicylidene)-pp'-diaminodiphenyl sulphide Th (IV). This change in frequency may be due to the increase in the size of the complex.

M-Cl Stretching - We have assigned a medium intensity band around 360 cm^{-1} to the Th-Cl stretching vibration. This agrees well with the assignment made by others[14-16]. It is obvious from Table II that there is no considerable change in the Th-Cl stretching vibration. This leads us to the conclusion that the oxidation state of the thorium and the coordination number have not been affected.

REFERENCES

1. A.S. Kudravtsev and I.A. Savich; Chem. Abs. 58, 2121b, 8616d (1963) 60:8873a (1964)

2. C.G. Macarovici, E. Perte and E. Motiu; Rev. Roumaine de Chemie. 11, 59 (1966)

3. a. O. A. Osipov, V. I. Minkin, M. I. Knyzhanskii, A. D. Garnovskii, M. I. Gorelov; Chem. Abs. 68, 72545d (1968)

b. P. Prashar and J. P. Tondon; Chem. Abs. 68, 8894u (1968)

c. L. V. Orlova, A. D. Garnovskii, O. A. Osipov, I. I. Kukushkina; Chem. Abs. 69, 113055q (1969)

4. S. N. Poddar and D. K. Biswas, Science and Cutt. 34,117 (1968)

5. K. K. Chatterjee and B. E. Douglas; Spectrochim. Acta. 21, 1625 (1965)

6. J. E. Kovacic; Spectrochim. Acta. 23A, 183 (1967)

7. K. Ueno and A. E. Martell; J. Phs. Chem. 60,1270 (1956)

8. H. H. Freedman; J. Am. Chem. Soc. 83, 2900 (1961)

9. K. Nakamoto and A. E. Martell J. Chem. Phys. 32, 588 (1960)

10. K, Nakamoto, P. J. McCarthy, A. Ruby and A. E. Martell; J. Am. Chem. Soc. 83, 1066 (1961)

11. K. Nakamoto, P. J. McCarthy and A. E, Martell; J. Am. Chem. Soc. 83, 1272 (1961)

12. G. T. Behnke, and K. Nakamoto, Inorg. Chem. 6, 433 (1967)

13. C. Djordjevic; Spectrochim. Acta. 17, 448 (1961)

14. R. C. Fay and T. J. Pinnavia; Inorg. Chem. 7, 508 (1968)

15. A. Buchler, J. B. Berkowitz Muttuck, D. H. Dugre, J. Chem. Phys. 34, 2202 (1961)

16. R. J. H. Clark; Spectrochim. Acta. 21, 955 (1965)

Fig. I

ABSORPTION SPECTRA OF THE LIGANDS

1. BIS (SALICYLIDENE)ETHYLENEDIAMINE.
2. BIS (SALICYLIDENE)-o-PHENYLENEDIAMINE.
3. BIS (SALICYLIDENE)BENZIDINE.
4. BIS (SALICYLIDENE)-pp'-DIAMINODIPHENYL SULPHIDE.

Fig.II

ABSORPTION SPECTRA OF THE COMPLEXES

1. BIS (SALICYLIDENE)ETHYLENEDIAMINATE Th (IV).
2. BIS (SALICYLIDENE)-o-PHENYLENEDIAMINATE Th (IV).
3. BIS (SALICYLIDENE)BENZIDINATE Th (IV).
4. BIS (SALICYLIDENE)-pp'-DIAMINODIPHENYL SULPHIDE Th (IV)

Elemental Analysis	TABLE I						TABLE II			
	% Th		% N		% Cl		Infrared Frequencies (in cm^{-1}) of the Complexes			
	Calc.	Found	Calc.	Found	Calc.	Found	$\nu C=N$,	$\nu Th-N$,	$\nu Th-O$,	$\nu Th-Cl$
1. bis (Salicylidene) Ethylene diaminate Th (IV)	40.70	39.52	4.92	4.56	12.48	12.12	1600 s	560 s.	420 m	360 m. br.
2. bis (Salicylidene) - o-phenylene diaminate Th (IV)	37.60	37.00	4.54	4.61	11.51	10.95	1598 s.	580 s 550 m	430 m.	365 m. br.
3. bis (Salicylidene)- benzidinate Th (IV)	33.48	32.5	4.04	4.15	10.24	9.38	1610 sh. 1600 s.	580 m. 550 m.	435 m.	360 m. br.
4. bis (Salicylidene)- pp'-diamino-diphenyl sulphide Th (IV)	32.01	31.02	3.86	4.05	9.79	9.02	1615 s.	590 s. 570 s.	450 m.	365 m.

ν = stretching. s = strong
m=medium. w = weak
sh = shoulder. br = broad

Fig I

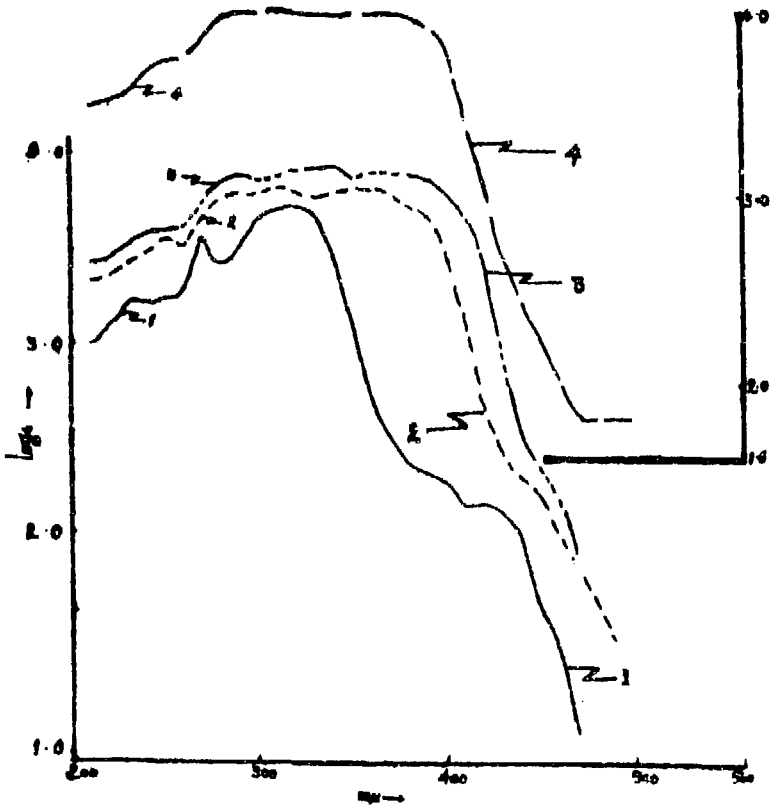

Fig II

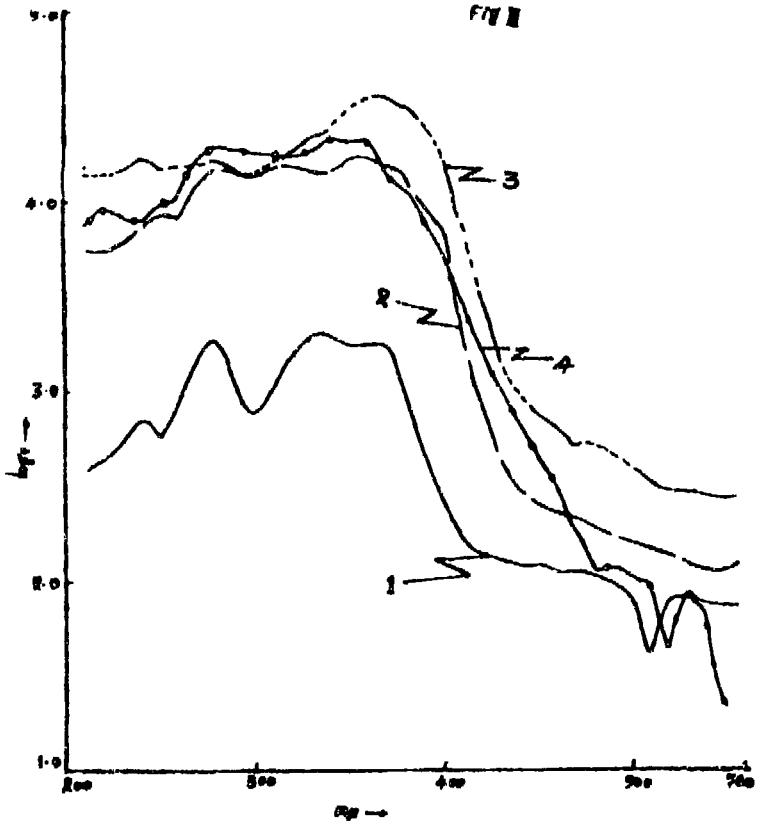

TEMPERATURE DEPENDENCE OF FLUORESCENCE SPECTRUM IN URANYL SOLUTIONS

Hari D. Bist
Department of Physics
Indian Institute iof Technology, Kanpur

The chemistry of uranyl solutions is complex and hence interesting. A number of physio-chemical investigations[1] based on potentiometric and conductometric titrations: pH, ebulioscopic and cryoscopic measurements, and extinctiometric and thermochemical studies have helped in establishing the presence of various anionic complexes (at low pH and high uranyl concentrations) and poly-nuclear hydrolytic species (at high pH and low uranyl concentrations) in these solutions. Pant and Khandelwal[2] have correlated the various spect ral changes in the fluorescence and absorption spectra at room temperature with the ionic 8species present under specific experimental conditions. A close connection has also been established between the room - temperature and snap-frozen liquid-nitrogen temperature absorption and fluorescence spectra of these solutions over a wide range of variations in their pH and concentrations[3, 4].

More detailed quantitative studies were considered necessary to confirm the observations[5] that for a solution of given pH and concentration the spectrum depended not only upon the temperature but also the manner in which the solution was brought to that temperature.

While studying the fluorescence spectra - with a monochromator, 931A photomultiplier and galvanometer arrangement - of the uranyl solutions kept in thin-walled test tubes, a particular temperature could be attained by seven different methods: (1) Snap-freezing from room-temperature (RT = 25°C) to any temperature, Θ, in general and to the liquid nitrogen temperature (LNT = -193°C) in particular, (2) Slow cooling from RT to LNT, (3) Slow warming of a snap-frozen solutions from LNT to RT, (4) Slow warming (upto RT) of a solution previously slowly cooled to LNT, (5) Slow warming of a snap-frozen solution to an intermediate temperature, Θ, and again rapid snap-freezing to LNT, (6) Warming of a slowly cooled solution to an intermediate temperature, Θ, and subsequently, recooling rapidly to LNT, and (7) Slow-cooling to an intermediate temperature, Θ, with subsequent snap-freezing to LNT.

A typical dilute (0.2M) solution of uranyl nitrate hexahydrate (abbreviated UNH hereafter), shows α and γ bands attributed[4] to the UO_2^{++} ion and the species[8] UO_2OH^+, respectively. On raising the temperature, the changes taking place in the spectrum are the following: (a) The overall intensity is associated with the intensities of α and γ

series of bands, (b) The temperature-intensity (T-I) curves for α bands show three peaks - P_1(-75°C), P_2(-20°C) and P_3(-2°C, melting point). (c) The T-I curve for the γ bands also shows three humps - H_1(-120°C), H_2(-60°C) and H_3(-2°C) - but their intensity is vanishingly small in the range -35° to -5°C. The changes for more concentrated solutions are almost similar to those described here.

A curve showing the variation of temperature, T, with time, t, taken during warming of a snap-frozen 3.5M aqueous solution showed three discontinuities: K_1(-3°C), indicating an exothermic change, K_2(-20°C) indicating an endothermic change, and K_3 (-17°C) corresponding to melting in this case. The correspondence between K_1 and the steep fall in γ band intensity and also between K_2 and peak P_2 in α intensity is established.

A snap-frozen UNH melt, which forms transparent glassy mass at LNT, gives prominent α' bands (attributable to $UO_2(NO_3)_3^-$ species) in the absorption spectrum, while in fluorescence it gives β and α bands corresponding to $UO_2NO_3^+$ and UO_2^{++} species respectively. During warming of this sample, the disappearance of β bands, after hump H_2 in T-I curve curve (-60°C), is slower as compared to the disappearance of γ bands in dilute solutions. One extra stage in the spectrum before the exclusive appearance of the α-series of bands is the presence of α' bands even in fluorescence near -30°C. The spectrum of snap-frozen melt is indicative of complex-formation mechanism in UNH for its melting in contrast to the alternative model of crystal-lattice expansion, which may be applicable for molten uranyl perchlorate.

During slow cooling, the intensity rises only after -40°C where an endothermic transformation takes place which could be confirmed by a T-t curve during this process. After this change at -40°C, the spectrum at LNT consists of resolved solid like B-C components[6] along with the prominent γ' bands. During warming of this slowly cooled solution, only the α bands are present in the temperature range -35° to -20°C. The hysteresis type loop for the variation in the intensity of α bands in this temperature range may be associated with the stabilizing action of uranyl ion (well settled in the cavities of large polyhedra formed by layers of tiled pentagonal dodecahedra, each of which is composed of 20 water molecules) in the clathrate hydrate type structure of solid crystalline water. This view seems to be supported by other methods of attaining a particular temperature mentioned in an earlier paragraph.

The author's thanks are due to Prof. D. D. Pant for his keen interest on the problem and to the C. S. I. R. for financial assistance.

REFERENCES

1. E. Rabinowitch and R. L. Belford; Spectroscopy and Photochemistry of Uranyl Compounds (Pergamon Press, Oxford) 1964, Chapters 2 and 3.

2. D. D. Pant and D. P. Khandelwal; Proc. Ind. Acad. Sci. 50 323 (1969); J. S. I. R. 18B, 126 (1959); curr. Sci. 27, 242 (1958)

3. D. D. Papt and D. P. Khandelwal; Proc. Ind. Acad. Sci. 51, 60 (1960)

4. D. D. Pant and H. D. Bist; Ind. J. Pure Appl. Phys. 2 (7), 223 (1964)

5. D. D. Pant, D. P. Khandelwal and H. D. Bist; Curr. Sci. 28, 483 (1959)

6. G. H. Dieke and A. B. F. Duncan; Spectroscopic Properties of Uranyl Compounds (McGraw Hill Book Co. Inc., New York) 1949

7. W. C. Hamolton and J. A. Ibers; Hydrogen Bonding in Solids (W. A. Benjamin, Inc. New York) 1968, p. 198

8. D. L. Cole, E. M. Eyring, D. T. Rampton, A. Silzars and R. F. Jensen; J. Phys. Chem. 71, 2771 (1967)

SOME NEW COMPLEXES OF URANIUM(V) CHLORIDE

Ram Chand Paul, Gurdev Singh and Mangal Singh
Department of Chemistry, Panjab University, Chandigarh-14

A few complexes of uranium(V) chloride with $SOCl_2$, $SOCl_2$[1-4]; PCl_5, $UCl_5.PCl_5$[5-6]; phosphine oxides, $UCl_5.(C_6H_5)_3PO$ and $UCl_5.(C_8H_{17})_3PO$[7] and trichloroacrylylchloride, $UCl_5.CCl_2 = CClCOCl$[3] have been reported in literature. Hexachlorouranate(V) compounds of the type $MUCl_6$ [M = Cs^+, Me_4N^+, $Me_2H_2N^+$, Ph_4As^+, Rb^+ and $(nC_3H_7)_4N^+$] and an octachlorouranate(V) compound, $(Me_4N)_3UCl_8$[3,8] have also been characterised. We report the preparation of nineteen new stable complexes of uranium(V) chloride with nitrogen donor ligands such as pyridine, quinoline, isoquinoline, α-picoline and β-picoline and oxygen donor ligands such as anthrone, benzalanthrone, benzil and dioxone. These complexes have been characterised through the study of their ESR, reflectance and infra-red spectra and magnetic susceptibilities.

A stable solution of uranium(V) chloride in $SOCl_2$, obtained by refluxing UO_3 with $SOCl_2$, was used as the starting material. The compounds of the type $UCl_5$2 nitrogen base and UCl_5. 3 nitrogen base (Table I) have been isolated by the dropwise addition of nitrogen base to an ice-cooled solution of UCl_5 in $SOCl_2$, followed by the addition of dry petroleum ether (40-60°), when solid compounds separated out. In the case of 1:2 compounds, UCl_5 and the base were mixed in the stoichiometric ratio, while for 1:3 compounds a five to ten fold excess of the base, with respect to UCl_5 was added. Since α and β picolines reacted violently with thionyl chloride they were diluted with 50 times their volume of dry CCl_4 before addition to UCl_5 solution. As the UCl_5 compounds are highly susceptible to decomposition by moisture, all the manipulations including filtration and drying, were carried out in completely dry atmosphere.

In the case of oxygen bases reddish brown solid complexes having UCl_5: base molar ratio 1:1 and 1:2 were isolated when ice-cooled thionyl chloride solutions of oxygen bases and uranium(V) chloride in correct stoichiometric quantities were mixed followed by the addition of dry petroleum ether. With dioxane, however, a 1:3 compound was formed (Table I).

All the compounds reported above are stable under anhydrous conditions. However, they disproportionate instantaneously giving rise to greenish yellow solids on exposure to moisture. The complexes

are insoluble in most of the common non-polar organic solvents but are soluble in formamide and dimethylformamide giving organge red solutions which immediately change to greenish yellow due to disproportionation of uranium(V) into uranium(IV) and uranium(VI). Thermogravimetric analyses show that the compounds start decomposing just above room temperature and on heating, continuously lose weight till they are converted to U_3O_8 at about 500-520°C.

Various workers[2, 3, 6, 7, 8, 9, 10] have studied the absorption spectra of uranium(V) complexes in solution. From a study of the absorption spectra of a large number of uranium(V) complexes, Bagnall[7] has concluded that in the range of 16,600 to 11,000 cm^{-1} uranium(V) shows only one characteristic peak (11,500 - 11850 cm^{-1}) for various solutions. The presence of small amounts of uranium(IV) is, therefore, readily detected by the appearance of peaks around 15,000 cm^{-1}. The reflectance spectra of UCl_5. 2 pyridine; UCl_5. 3 pyridine; UCl_5. 2 quinoline; UCl_5. 3 quinoline; UCl_5. 2 isoquinoline; UCl_5. 3 isoquinoline; UCl_5. anthrone; UCl_5. benzil and UCl_5. 3 dioxane show strong absorption-peaks in the region 11,500 to 11,900 cm^{-1}, thus proving unambiguously that the complexes are genuine uranium(V) complexes.

ESR measurements on UCl_5. 2 pyridine; UCl_5. 3 pyridine; UCl_5. 2 quinoline, UCl_5. 3 quinoline, UCl_5. 2 isoquinoline, UCl_5. 3 isoquinoline, UCl_5. benzil and UCl_5. 2 benzanthrone produce extremely broad signals at 5955, 5940, 5915, 5915, 5875, 5970 and 6120-5420 gauss at liquid nitrogen temperature and the 'g' values calculated are 1.124, 1.129, 1.129, 1.130, 1.129, 1.138, 1.122 and (1.11 and 1.25) respectively. These 'g' values may be compared with average 'g' values of 1.1 for powdered samples of $UCl_5.SOCl_2$, $UCl_5.PCl_5$ and $RbUCl_6$[3]. The agreement of the latter values with our experimental values give further support that the compounds are definite uranium(V) complexes and are not equimolar mixture of U(IV) and U(VI) complexes.

The infra-red spectra of uranium(V) chloride complexes with nitrogen bases in the region 400-4,000 cm^{-1} indicate that all the nitrogen atoms of the base molecules are coordinated to uranium atom of UCl_5. Thus, in these complexes uranium atom may be seven or eight coordinated according to the number of base molecules complexing with UCl_5.

A study of the infra-red spectra of the anthrones and their complexes with UCl5 in the region 1700-1500 cm^{-1} shows downward shifts in the carbonyl stretching frequencies, which suggests the coordinate of carbonyl oxygen of the anthrones to the uranium atom of UCl_5.

Magnetic susceptibility measurements on hexachlorouranate(V) complexes[6]. and UCl_5. triphenylphosphine oxide complex[7] have been reported in literature. The compounds show Curie-Weiss dependence with very large values of θ. Magnetic susceptibilities of UCl_5. 2 pyridine, UCl_5. 3 pyridine, UCl_5. 2 quinoline, UCl_5. 3 quinolin, UCl_5. 2 isoquinoline, UCl_5. benzanthrone, UCl_5. 2 benzanthrone and UCl_5. benzil from 86°K to 300°K show Curie-Weiss dependence with large values of the Weiss Constant, θ, namely, -416, -416, -147, -168, -98, -132, -184 and -44 respectively. Magnetic susceptibilities of UCl_5. 2α-picoline, UCl_5. 3 α-picoline, UCl_5. anthrone, UCl_5. methylene anthrone and UCl_5. 3 dioxane were measured at room temperature only, giving $\mu_{(eff)}$ values of 1.703, 1.792, 1.923, 2.182 and 1.658 B. M. respectively. These values of magnetic susceptibilities of uranium(V) ions can be compared with 1.73 B. M. calculated for the spin only paramagnetism, 1.56 B. M. for a $6d^1$ configuration and 2.54 B. M. for a $5f^1$ configuration[4]. Conductometric titrations of solutions of UCl_5 in thionyl chloride against the solution of nitrogen bases in thionyl chloride have also been carried out. The curves show sharp breaks at UCl_5: base molar ratio of 1:1, 1:2 and 1:3 indicating the existence of anionic species UCl_6^-, UCl_7^{2-} and UCl_8^{3-}.

TABLE-I

Uranium(V) Chloride Complexes with Bases

S. No.	Complex	S. No.	Complex
1.	UCl_5. 2 pyridine	11	UCl_5. Anthrone
2.	UCl_5. 2quinoline	12	UCl_5. Benzanthrone
3.	UCl_5. 2 isoquinoline	13	UCl_5. Methyleneanthrone
4.	UCl_5. 2 α-picoline	14.	UCl_5. Benzalanthrone
5.	UCl_5. 2 β-picoline	15.	UCl_5. Benzil
6.	UCl_5. 3 pyridine	16.	UCl_5. 2 Anthrone
7.	UCl_5. 3quinoline	17.	UCl_5. 2 Benzanthron
8.	UCl_5. 3 isoquinoline	18.	UCl_5. 2 Benzil
9.	UCl_5. 3 α-picoline	19.	UCl_5. 3 Dioxane
10.	UCl_5. 3 β-picoline		

REFERENCES

1. H. Hecht, G. Jander and H. Schlapmann; Z. Anorg. Allgem, Chem. 254, 255 (1947); D. C. Bradley, B. N. Chakrawarti and A. K. Chatterjee; J. Inorg. Nucl. Chem, 3, 367 (1957)

2. D.G. Karraker; Inorg. Chem. 3, 1618 (1964)

3. J. Selbin, J. D. Ortego and G. Grisner; Inorg. Chem. 7,976 (1968)

4. D.G. Karrekar, T.H. Siddall and W.E. Stewart; J. Inorg. Nucl. Chem. 31, 711 (1969)

5. A.W. Cronander; Bull, Soc. Chim. France, 19, 500 (1873)

6. R.E. Panzer and J.F. Suttle; J. Inorg. Nucl. Chem. 20, 229 (1961)

7. K.W. Bagnall, D. Brown and J.G.H. Du Preez; J. Chem. Soc. 5217 (1965)

8. K.W. Begnall, D. Brown and J.G.H. Du Preez; J. Chem. Soc. 2603 (1964)

9. R.E. Panzer and J.F. Suttle; J. Inorg. Nucl. Chem. 13, 244 (1960)

10. M.J. Reisfeld and G.A. Crosby; Inorg. Chem. 4, 65 (1965)

LABORATORY INVESTIGATIONS IN NON-AQUEOUS PROCESS CHEMISTRY

A. V. Hariharan, D. D. Sood, S. P. Sood, Rajendra Prasad and R. Sampathkumar
Radiochemistry Division, Bhabha Atomic Research Centre
Trombay, Bombay - 85

1. INTRODUCTION

Halide volatility and pyrochemical methods of fuel reprocessing are being investigated at a number of laboratories for application to a variety of uranium based fuels[1-4]. Chlorination volatility processes have been explored for their application to a variety of fuels, but no complete fuel reprocessing scheme utilising the volatility characteristics of higher chlorides of uranium has been reported. Feasibility of such a scheme has been demonstrated by present laboratory scale investigations on ThO_2-UO_2 and UO_2 - PuO_2 type fuels. Details of this investigation are reported elsewhere[5-8].

Pyrochemical processes consist of high temperature non-aqueous procedures for the decontamination and recovery of fissile and fertile constituents in irradiated reactor fuels. These processes have been used for the reduction of oxides like ThO_2[9] and UO_2[10] and at present a salt-transfer process, for reprocessing UO_2 - PuO_2 type fast reactor fuels is under development[11]. Possibility of reprocessing ThO_2 - UO_2 type fuels by such methods is being investigated and some of results obtained are reported here.

2. PROCESS CHEMISTRY

2.1. Chlorination Volatility Process

ThO_2, UO_2 and PuO_2 can be converted to chlorides at reasonable rates by chlorinating agents like chlorine-carbon tetrachloride gas mixture at 500-600°C. Under such conditions it is expected that most of the constituents of irradiated fuel will be converted to chlorides and the highest chlorides stable at chlorinating temperatures would be present. Large differences in the volatility of these chlorides form the basis of the separation procedure. Boiling points and vapour pressures at 700°C, 500°C and 300°C for some of the pertinent chlorides are presented in Table I[5, 12, 13]. Chlorides having different volatility are separated by use of refractory alumina filter beds maintained at controlled temperatures. Separation of UCl_5 - UCl_6 from fission product chlorides having high volatility has been

achieved by reactions in heated sodium chloride bed. It has been observed that UCl_5 - UCl_6 vapours in the chlorinating gas stream are effectively retained by NaCl bed at 250 - 300°C, in a sharp orange red band, possibly as a binary compound $NaUCL_6$[8]. The orange compound can be converted to a green compound UCl_4. 2 NaCl, by direct reduction with hydrogen or by pyro-hydrolysis and rechlorination. The green compound is highly stable and does not give off any volatile species of uranium upto 600°C even in the presence of strong chlorinating agents. These data have been used for developing the separation procedures.

Chlorination of UO_2 - PuO_2 fuels is complicated by the reaction indicated by equation (1)

$$PuCl_3\ (s) + \tfrac{1}{2} Cl_2\ (g) = PuCl_4\ (g) \quad \ldots\ldots (1)$$

At high chlorinating temperatures an appreciable amount of plutonium is carried by chlorine as $PuCl_4$ and is retained in NaCl bed. Chlorination at a lower temperature, which was possible when UO_2 was converted to U_3O_8, has been used to overcome this problem. As UO_2 - PuO_2 solid solutions having less than 20 wt pct PuO_2, could be easily oxidised to U_3O_8-PuO_2 mixture, further work has been carried out using such mixtures.

2.2. Pyrochemical Processes

For reduction of reactive metal oxides eg. ThO_2[9], UO_2[10] in liquid metalfused salt media, the oxide, suspended in a molten halide flux, is contacted with liquid metal by constant mixing at about 800°C. The liquid metal is normally an alloy of a reductant metal e.g. Mg and a solvent metal e.g. Zn. The reaction for the process is given by the equation (2).

$$UO_2\ (\text{flux}) + 2\ Mg\ (Zn) - U\ (Zn\text{-}Mg) + 2\ MgO\ (\text{flux}) \quad \ldots\ldots\ldots (2)$$

The rate and extent of this reduction depends on the activity and solubility of reduced metal in the liquid alloy, and on the composition of the salt. By suitably selecting the media it may be possible to work out a separation procedure for ThO_2 - UO_2 type fuels. Rare earths and alkaline earths fission products, by virtue of their highly electropositive nature, prefer the salt phase in such a process and can be separated.

Another method for reprocessing oxidic fuel materials could be selective dissolution in certain molten salt media. In the present investigation, chlorination of ThO_2 and UO_2 in $MgCl_2$ - KCl eutectic melt is being

studied.

3. RESULTS AND DISCUSSION

3.1. Chlorination volatility process

A Cl_2 - CCl_4 - N_2 mixture in the ratio of 4:1:1 was found to be an efficient and clean chlorinating gas for oxidic fuel materials. Complete chlorination of ThO_2 - UO_2 was achieved at 700 - 750°C. Chlorinating gases carried the $ThCl_4$ and UCl_5 - UCl_6 vapour onto the filter and sorption beds. $ThCl_4$ could be filtered off by an Al_2O_3 filter bed at 300 - 350°C. Another filter bed at 200 - 250°C prevented any carry over of $ThCl_4$ to NaCl bed. UCl_5 - UCl_6 were quantitatively retained in NaCl bed at 250 - 300°C. Fission product behaviour under similar conditions was studied by chlorination of inactive simulated fission product material tagged with tracer activity. It was observed that rare earths, Ba, Sr etc. remained as residues in the chlorination zone, caesium and ruthenmium clorides were held up in Al_2O_3 filter bed at 300 - 350°C and $ZrCl_4$, $MoCl_5$ and $NbCl_5$ passed through the two Al_2O_3 filter beds, onto the NaCl sorption bed. $MoCl_5$ and $NbCl_5$ were not retained in NaCl bed. In the case of $ZrCl_4$, quantitative sorption took place with the bed at 250°C while at 300°C more than half of $ZrCl_4$ leaked out. Protoactinium behaviour was checked by chlorination of $Pa^{233}O_2$ precipitated with various carriers such as Nb, Zr, Ce, Th and U, under the same experimental conditions. Essentially, all $PaCl_5$ transpired onto the sorption zone and was retained in NaCl bed at 250 - 300°C. Partial hold up of $PaCl_5$ was observed when the filter bed II temperature was less than 250°C.

Based on these observations, experiments with irradiated ThO_2-UO_2 were carried out with chlorination zone at 750°C, Al_2O_3 bed I at 350°C and Al_2O_3 bed II at 250°C and NaCl sorption bed at 250°C. Over 99 pct. $ThCl_4$ collected in filter bed I and more than 90 pct. UCl_5-UCl_6 was absorbed in NaCl bed. Thorium and uranium fractions were subjected to secondary purification. $ThCl_4$ was purified by distillation in a stream of chlorinating gas and use of Al_2O_3 filter beds at 700°C and 500°C. Uranium was purified by converting UCl_5. NaCl to UCl_4. 2NaCl by pyro-hydrolysis at 300°C and rechlorination at 500°C. The decontamination factors are given in Table II.

In the case of U_3O_8-PuO_2, mixtures containing 1 to 17 wt pct PuO_2 were studied with chlorination zone at 350°C, Al_2O_3 filter bed at 200°C and NaCl bed at 300°C. In experiments with irradiated U_3O_8 mixed with PuO_2 and inactive fission product material, all fission products except Nb, Mo and Zr stayed in sample boat with plutonium. $NbCl_5$, $MoCl_5$ and $ZrCl_4$ accompanied UCl_5-UCl_6 onto NaCl sorption bed. Secondary purification of uranium was carried out in the manner described earlier. Recovery and

purification of plutonium fraction was not tried. The decontamination factors for uranium are listed in Table III.

4.2. Pyrochemical Processes

Reduction of U_3O_8 and ThO_2 in $MgCl_2$ - 5 mole pct MgF_2 by Pb - 10 wt pct Mg were carried out in a tilt pour furnace[14]. The experiments indicated very similar reduction behaviour for U_3O_8 and ThO_2. Also, the solubility of uranium and thorium in the alloy was observed to be lower by a factor of four, than in pure lead; and it was felt that this system could not be used for separation procedure. During reduction of ThO_2-10 wt pct U_3O_8 mixture with Zn-10 wt pct Mg alloy using $MgCl_2$-5 mole pct MgF_2, as flux it was observed that 80% U_3O_8 gets reduced in 10 minutes where as only 30% ThO_2 is reduced in the same time. At present the solubility of U + Th in Zn-Mg solutions is being studied, as a function of magnesium concentration, at various temperatures. The data for solubility in Zn-10 wt pct Mg and Zn-20 wt pct Mg is presented in Table IV. It is seen that the solubility of Th in Zn-Mg solutions is higher than that of uranium. Also, the solubility of thorium increases with magnesium concentration whereas the solubility of uranium decreases and it may be possible to preferentially precipitate uranium from these solutions.

In the study of chlorination of oxides in $MgCl_2$ - KCl melts, it was observed that sintered UO_2 and ThO_2 do not dissolve in the salt, to any appreciable degree, at 650°C. Addition of graphite to the salt increased the chlorination rate of sintered UO_2, and upto 40 pct UO_2 could be dissolved in salt in four hours at 650°C. By addition of active charcoal in the salt, melt upto 70 pct UO_2 would be chlorinated in the same time. Dissolution rates of sintered ThO_2 in presence of reducing agents and that of ThO_2-UO_2 solid solutions will be investigated.

5. CONCLUSIONS

Reasonable decontamination factors obtained in laboratory investigations of chlorination volatility process indicate that such a process could be developed. It is expected that the decontamination factors will improve in scaled-up experiments. Preliminary results on pyrochemical investigations show hopeful trend.

6. ACKNOWLEDGEMENT

The authors are grateful to Dr. M. V. Ramaniah, Head, Radiochemistry Division, and Shri N. Srinivasan, Head, Fuel Reprocessing Division, for their interest in the work.

REFERENCES

1. A.A. Jonke; Atomic Energy Review 3 (1) 3 (1965)

2. L. Burris, Jr.; K.M. Harmon, G.E. Brand, E.W. Murbach and R.K. Steunenberg; A/Conf. 28/1 10, 501 (1964)

3. T. Gens: Chemical Engineering Progress Symposium Series 60(47), 57

4. J.H. Goode; USAEC Report ORNL-3977 (1964)

5. D.D. Sood and A.V. Hariharan; BARC Report BARC - 397 (1969)

6. S.P. Sood, P.V. Balakrishnan, Rajendra Prasad and A.V. Hariharan; BARC - 404 (1969)

7. S.P. Sood, D.D. Sood, K. Rengan and A.V. Hariharan; BARC - 405 (1969)

8. Rajendra Prasad, K. Rengan and A.V. Hariharan; BARC - 406 (1969)

9. A.V. Hariharan, J.B. Knighton and R.K. Stuenenberg; USAEC Report ANL - 7058 (1965)

10. J.B. Knighton and R.K. Stuenenberg; USAEC Report ANL - 7057 (1965)

11. W.E. Miller and R.K. Stuenenberg, Reactor Fuel Reprocessing Technology 11 (4) 219 (1968)

12. O. Kubaschewski and E.LL. Evans; "Thermochemical Data", Metallurgical Therochemistry, Pergmon Press, New York (1958) p. 286

13. L. Brewer; "The Fusion and Vaporisation Data of Halides", The Chemistry and Metallurgy of Miscellaneous Materials. Thermodynamics National Nuclear Energy Series IV, 19B McGraw-Hill Book Co. Inc., New York (1950)

14. S.P. Garg, D.D. Sood, C.M. Paul, A.V. Hariharan and R.B. Subramanyam; Transactions of Indian Institute of Metals (To be published)

TABLE I

Vapour Pressure of Chlorides

Chloride	Boiling/sublimation point °C	Vapour Pressure in mm Hg		
		700°C	500°C	300°C
$ThCl_4$	922	10.8	4.0×10^{-3}	5.9×10^{-9}
$PaCl_5$	927	>760	520	4.6
UCl_5	927	>760	518	4.6
UCl_6	277	>760	>760	>760
$PuCl_3$	1730	1.1×10^{-3}	2.0×10^{-8}	7.9×10^{-9}
$ZrCl_4$	331	>760	>760	225
$NbCl_5$	247	>760	>760	>760
$MoCl_5$	268	>760	>760	>760
$InCl_3$	498	760	760	0.11
$CaCl_2$	1300	0.70	2.0×10^{-3}	6.5×10^{-8}
$RuCl_3$	decomposes	0.30	3.1×10^{-5}	3.4×10^{-12}
$RhCl_3$	decomposes	2.0×10^{-4}	3.7×10^{-9}	2.5×10^{-17}
$SrCl_2$	2027	3.5×10^{-7}	2.5×10^{-11}	2.3×10^{-18}
$BaCl_2$	2100	1.5×10^{-5}	1.6×10^{-9}	1.8×10^{-16}
$CeCl_3$	1730	1.7×10^{-4}	6.8×10^{-9}	1.0×10^{-16}
$GdCl_3$	1580	1.7×10^{-3}	1.5×10^{-7}	8.3×10^{-15}

TABLE II

Decontamination Factors for Thorium and Uranium in ThO_2 - UO_2 Processing

Activity	Thorium Fraction		Uranium Fraction	
	Primary Separation	Distillation Purification	Primary Separation	Rechlorination Purification
Gross Gamma	2×10^2	4×10^4	-	34
Gross Beta	20	4×10^3	-	69
Ce	1.6	9×10^2	10^4	10^4
Ba	1×10^2	10^3	10^3	10^4
Ru	1.3	10^3	20	-
Zr	6×10^2	10^4	3.8	3.2×10^2
Nb	3×10^2	10^4	50	10^3
Pa	2×10^2	10^4	1.5	51
U	25	10^3	-	-
Th	-	-	5×10^3	5×10^3

TABLE III

Decontamination Factors for Uranium in U_3O_8-PuO_2 Processing

Activity	Primary Separation	Rechlorination Purification
Gross Gamma	6.7	4.7×10^{-2}
Gross Beta	-	2.8×10^{2}
Zr	14	2.1×10^{3}
Ce	1.4×10^{3}	5.1×10^{3}
Ru	2.7	69
Pu	2.0×10^{3}	2.0×10^{3}

TABLE IV

Solubility of Uranium and Thorium in Zinc-Magnesium Solutions

Mg. Conc. wt pct	Solute	Solubility wt. pct. Temp °C 650	700	750
10	U	0.23	0.31	0.47
	Th	0.31	0.431	2.15
20	U	0.35	0.37	0.38
	Th	2.22	4.74	6.55

SPECTROGRAPHIC DETERMINATION OF SOME LANTHANIDES AND ACTINIDES IN URANIUM AND PLUTONIUM

B. D. Joshi and B. M. Patel
Bhabha Atomic Research Centre, Bombay - 85

INTRODUCTION

Certain rare earths have high capture cross-section for thermal neutrons. The maximum permissible amounts of these in nuclear fuels like uranium and plutonium are in the range 0.04 to 0.1 p.p.m. Emission spectrographic methods are suitable for their estimation in this range.

The spectra of uranium and plutonium are complex and their lines interfere with the weak lines of impurities. Hence in the methods adopted, the rare earths are separated from uranium or plutonium using ion-exchange or solvent extraction methods. The separated rare earths are then estimated by emission spectrographic method using d.c. arc or a.c. spark.

The "Copper-spark" and the "Graphite spark" methods[1,2] have higher sensitivity compared to d.c. arc method. In spark methods sensitivity becomes low and estimation errors become large in the presence of other elements. A "carrier distillation" method reported by Radwan Z. et al.[3], using CsF carrier and d.c. arc gives sensitivity comparable to the spark methods. This paper describes the results obtained with the LiF-AgCl carrier and its use for analysis of rare earths in uranium and plutonium.

PREPARATION OF CARRIER -BUFFER

Specpure LiF, AgCl and graphite powder in the proportion 1:1:2 were ground in an agate mortar. The difficulty in grinding was overcome by moistening the mixture with a small amount of liquid nitrogen. After grinding, the mixture was dried under infra red lamp.

PREPARATION OF STANDARD SOLUTIONS

Specpure rare earth oxides were used for preparation of standard solutions. The rare earth oxides were ignited prior to dissolution in 3M HCl for the preparation of individual stock solutions. Two sets of seven standard solutions were prepared from these in the concentration range 0.01 to 1.0 microgram for 20 microlitres. An aliquot of 20 microlitres of the first set of standard solutions contains varying amounts of rare

earth elements and 0.5 microgram of thulium, which serves as internal standard. An aliquot of 20 microlitres of the second set of standard solutions contains 0.5 mg of lanthanum in addition to the elements mentioned in the first set. The first set of standards is used for plutonium samples. The second set is used for uranium samples.

CHEMICAL SEPARATION PROCEDURE

(a) Preparation of Uranium Sample

2.5 micrograms of thulium internal standard element are added to 5 g uranium solution prior to the separation of rare earth elements using cellulose pulp and ether-nitric acid mixture[2, 4, 5, 6]. The rare earths adsorbed on the cellulose column are isolated and finally precipitated as hydroxides using lanthanum carrier and ignited to oxides. The oxide sample is dissolved in 1 ml con. HCl with addition of a few drops of dilute HF. The sample solution is evaporated to dryness and dissolved in 200 microlitres of 3M HCl.

(b) Preparation of Plutonium Sample

2.5 micrograms of thulium internal standard are added to 100 mg of plutonium solution before separation of lanthanide impurities by anion exchange separation[7, 8], using Dowex 1 x 4 (20-50 mesh) resin and 7.2M HNO_3. The effluent containing rare earths, U and Am is evaporated to dryness and finally dissolved in to 200 microlitres of 3M HCl.

SPECTROGRAPHIC PROCEDURE

An aliquot of 20 microlitres of each standard is loaded on graphite electrode containing 10 mg charge of carrier-buffer in the electrode crater, after wetting it with a drop of ethanol. It is then dried under an infra-red lamp. 40 microlitres of the sample solution are loaded on the graphite electrode already containing 10 mg charge of carrier buffer and dried.

The spectra of standard and samples are photographed on the Hilger 3.4 M Ebert spectrograph with 30,000 lines per inch grating blazed at 1 micron. The spectra are recorded in 3160 - 3500 A region at a dispersion of 0.65 A/mm in the third order, on Kodak B-10 plates. Ultra purity graphite electrodes of diameter 4.8 mm and 3.2 mm are used as sample and counter electrodes respectively. The spectra are photographed with an exposure of 60 seconds and 12 micron slit width using 13 amp current.

RESULTS

The detection limits of the rare earth elements using Li_2CO_3, NaCl and LiF - AgCl carriers are shown in Table I. The sensitivities with the LiF - AgCl - graphite powder carrier - buffer are found to be the highest. The analysis lines of the rare earths, the detection limits and the range of estimation are shown in Table II. Table III shows the detection limits obtained by this method, in comparison with those reported in the literature. It is observed that the detection limits by the present method are lower for the elements Dy, Ho, Er, Yb and Lu compared to copper spark detection limits, which are lowest limits reported. As compared to the detection limits by CsF carrier method, the detection limits by this method are lower for all elements except Sm. The detection limits for Am and U were found to be 0.1 microgram. The standard deviations of the estimations range from 8% to 14%. A typical working curve is shown in Fig. 1.

In the chemical separation methods adopted, it is observed that small amounts of common impurities like Fe, Ca, Al, Mg, Si and U, Pu follow the rare earth elements. Hence, the influence of these impurities on the intensities of rare earth lines was investigated. It is observed that upto 20 micrograms each of uranium and plutonium and 50 micrograms each of other impurities mentioned do not affect the detection limits or the intensity ratios of the analysis lines.

By this method, using only 100 mg of plutonium sample, lanthanides, uranium and americium can be estimated at concentration of 0.5 to 12 p.p.m. Using 5 g of uranium, the lanthanides can be estimated at concentrations of 0.01 to 0.25 p.p.m. Hence, this method is suitable for the estimation of the rare earth elements at the maximum permissible levels in uranium and plutonium, using only 5 g and 100 mg samples respectively.

ACKNOWLEDGEMENT

The authors are grateful to Dr. M.V. Ramaniah, Head, Radiochemistry Division, for his interest in this work.

REFERENCES

1. M. Fred, N.H. Nachtrieb and F. Tomkins; J. Opt. Soc. Am. 37, 279 (1947)

2. C. Feldmann and J. Y. Ellenburg; Anal. Chem. 30, 418 (1958)

3. B. Strzyzewska, Z. Radwan and J. Minczewski; J. Applied Spectroscopy 20, 236 (1966)

4. Ch. A. Berthelot, S. Herrmann, K. F. Lauer and R. A. A. Muzzarelli EUR-587 e (1964)

5. R. T. Chitnis and M. S. Varde; AEET/Anal/16 (1963)

6. B. D. Joshi, R. N. Saxena and B. M. Patel; BARC/Radiochem/76 (1967)

7. A. W. Wenzel and C. E. Pietri; NBL-215 (1964)

8. B. D. Joshi, R. N. Saxena, B. M. Patel, T. R. Bangia and A. G. Page; BARC-383 (1968)

TABLE I

Effect of Different Carriers on Detection Limits of Rare Earth Elements

Amounts in microgram

Element	Lithium carbonate	Sodium chloride	Lithium fluoride and Silver chloride
Cerium	0.5	1.0	0.25
Samarium	0.25	0.5	0.1
Europium	0.1	0.1	0.01
Gadolinium	0.25	0.1	0.01
Dysprosium	0.1	0.1	0.025
Holmium	0.1	-	0.05
Erbium	0.1	0.1	0.01
Lutetium	0.1	0.5	0.05

TABLE II

Analytical Line Pairs, Detection Limits and Estimation Ranges

Element	Analytical Line A	Internal Standard thulium line A	Detection limit in microgram	Estimation range in microgram	Estimation range in p. p. m. *
Cerium	3201.71	3425.63	0.25	0.25 - 1.0	12.5 - 50
Samarium	3321.18	3425.63	0.1	0.1 - 1.0	5 - 50
Europium+	3971.99	4242.15	0.01	0.01 - 0.25	0.5 - 12.5
Gadolinium	3350.48	3425.63	0.01	0.01 - 1.0	0.5 - 50
	3422.47	3425.63	0.01	0.01 - 0.5	0.5 - 25
Dyprosium	3407.80	3425.63	0.025	0.025-1.0	1.25-50
Holmium	3398.98	3425.63	0.05	0.1 - 1.0	5 - 50
	3456.00	3425.63	0.05	0.05 - 0.5	2.5 - 25
Erbium	3264.78	3425.63	0.01	0.01 - 1.0	0.5 - 50
Ytterbium	3289.37	3425.63	0.005	0.01 - 0.05	0.5 - 2.5
Lutetium	3385.50	3425.63	0.05	0.1 - 1.0	5 - 50

* The figures are based on 100 mg of U and Pu

+ Photographed in second order with different range setting

TABLE III

Comparison of the Lowest Detection Limits Obtained by Different Methods

Element	"Copper spark"	"Graphite spark"	"Carrier Distillation"	
			CsF	LiF - AgCl
	Ref. 1.	Ref. 2.	Ref. 3.	Present Investigations
Cerium	0.05	0.2	0.24	0.25
Samarium	0.02	0.2	0.04	0.1
Europium	0.002	0.03	0.04	0.01
Gadolinium	0.05 0.01	0.03	0.16	0.01
Dysprosium	0.05	0.03	0.16	0.025
Holmium	0.1	-	0.04	0.05
Erbium	0.05	-	0.02	0.01
Ytterbium	0.01	-	0.04	0.005
Lutetium	0.2	-	0.04	0.05

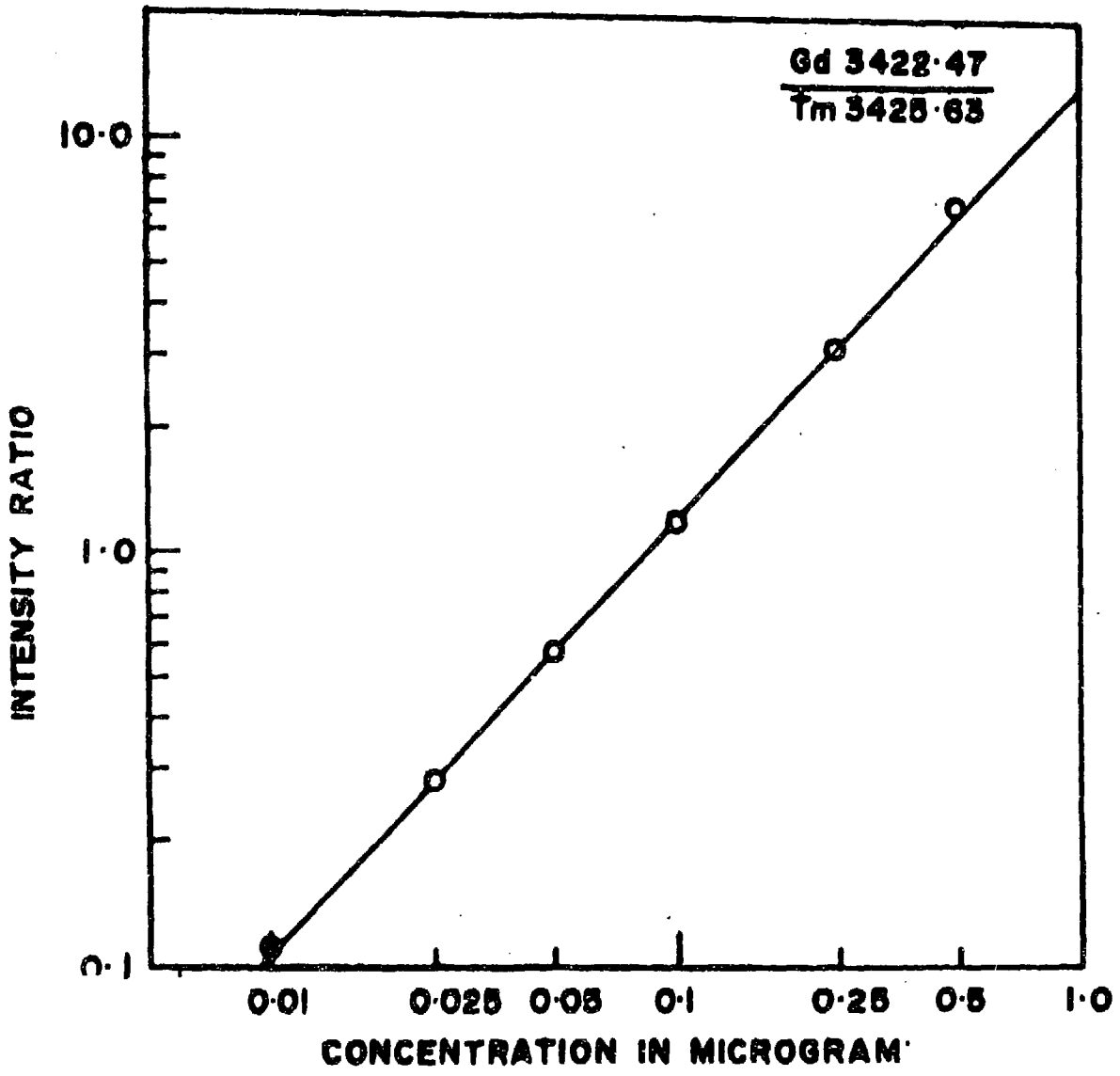

FIGURE-1. WORKING CURVE FOR LINE OF Gd 3422·47 A.

SPECTROGRAPHIC METHOD FOR THE DETERMINATION OF RARE EARTHS IN PLUTONIUM - USE OF TRILAURYL AMINE

R. K. Dhumwad, M. V. Joshi and A. B. Patawardhan
Fuel Reprocessing Division
Bhabha Atomic Research Centre
Trombay, Bombay-85

INTRODUCTION

The spectrochemical determination of impurities in plutonium presents a number of problems. In addition to its spectrum being very complex, it is highly toxic. Impurities are generally separated from the plutonium sample prior to the spectrochemical analysis. For the determination of rare earths in Pu, ion exchange[1, 2] and T. T. A.[3] extraction methods have been used.

This report describes a spectrographic method based on the pre-separation of rare earths by extracting plutonium into trilauryl amine in Shell sol-T and photographing the spectra on a large quartz prism spectrograph by arcing the aqueous phase containing rare earths.

PREPARATION OF STANDARDS AND SAMPLES

Using M/s. Johnson & Matthey spec-pure chemicals, a high concentration composite standard solution (1 ml) containing 1.5 mg Gd, 3 mg each of Sm, Dy and Er, and 6 mg Ce was prepared and by suitable dilutions the lower standards were obtained. An aliquot of 200 micro-litre of rare earth standard solution contained one microgram Sc which was added to serve as internal standard.

An aliquot of the plutonium nitrate sample (containing 100 mg Pu) was evaporated to near dryness and made upto 20 ml by adding 4M nitric acid. Plutonium was kept in the tetravalent state by adding a few drops of hydrogen peroxide and removing the excess by heating. Plutonium was extracted into the organic phase by contacting the sample solution with a 20 ml aliquot of the pre-equilibrated 20% TLA V/V in Shell sol. T. After adding internal standard Sc to the aqueous phase, the volume was reduced to 1 ml and 200 micro-litres of this solution was transferred, dried and arced to obtain the spectra of the rare earths. Each sample was analysed in triplicate.

EXPERIMENTAL

The parameters for spectrographic excitation, recording and photometric analysis are as follows:

Spectrograph	Hilger large quartz and glass prism spectrograph fully automatic E. 478-304.
Slit width	0.020 mm
Emulsion	Kodak B. 10
Wave length range	2850 - 5000 Å
Excitation unit	Hilger and Watts BNF source unit F.S. 131.
Type of excitation	D.C. Arc; 220V; 10A.
Electrodes	Anode; 6.35 mm dia. U.C.P. graphite rod with a cavity 1.5 ± 0.5 mm deep and wall thickness of 0.5 mm.
	Cathode: 3.05 mm dia U.C.P. graphite rod tapered.
Exposure	15 seconds.

RESULTS AND DISCUSSION

The details of the results are given in Table I. The overall standard deviation of the method is 14% at 67% confidence level. The typical working curves are shown in Fig. 1.

Spectrographic analysis of a number of plutonium samples for non-rare earth impurities by another method[4] showed that some of them contained appreciable amounts of Fe and Ca. When such samples were analysed by the present method, these impurities were found to accompany the rare earths in the aqueous phase. A study of the effect of these impurities on the estimation of rare earths has been made which indicates that the present method is applicable to the routine analysis of plutonium samples containing major non-rare earths impurities like Ca and Fe even to the extent of 1000 ppm each (without any subsequent separation of rare earths from these impurities).

ACKNOWLEDGEMENT

The authors wish to thank Shri N. Srinivasan, Head, Fuel Reprocessing Division, for suggesting the use of trilaurylamine in the spectrochemical analysis of plutonium for rare earths and also for his keen interest and encouragement during the progress of the work.

REFERENCES

1. J. P. Faris; U. S. At. Energy Comm., T. I. D. 7655, 193 (1962)

2. B. D. Joshi et al; BARC-383 (1968)

3. H. H. Van Tuyl; General Electric, Hanford Atomic Products Operation, Richland, Wash., Doc. H-W 28530 (1953)

4. R. K. Dhumwad, M. V. Joshi and A. B. Patawardhan; Anal. Chem. Acta. 42, 334-337 (1968)

5. Massachusetts Institute of Technology, Wavelength Tables M. I. T. Press, Cambridge, Mass (1963)

TABLE I

Line Pairs, Concentration Range and Reproducibility

Line Pair[5]		Concentration range Estimation		S. D. at 67% confidence level
Rare Earth	Internal standard	µg on electrode	ppm 100 mg Pu	
Gd 3350.482 Å	Sc 3359.679 Å	0.2 - 2.0	10 - 100	14%
Sm 3382.407 Å	"	1.0 - 4.0	50 - 300	11%
Dy 3385.027 Å	"	0.1 - 2.0	5 - 100	11%
Dy 3388.863 Å	"	0.4 - 4.0	20 - 200	15%
Er 3264.781 Å	"	0.1 - 4.0	5 - 200	14%
Ce 3201.714 Å	"	2.0 - 8.0	100 - 600	18%

µg on electrode : The amount of rare earths in 200 micro-litre deposited on the electrode for spectrographic analysis.

ppm on 100 mg Pu : For a 200 micro-litre aliquot of effluent from 100 mg Pu sample concentrated to 1 ml.

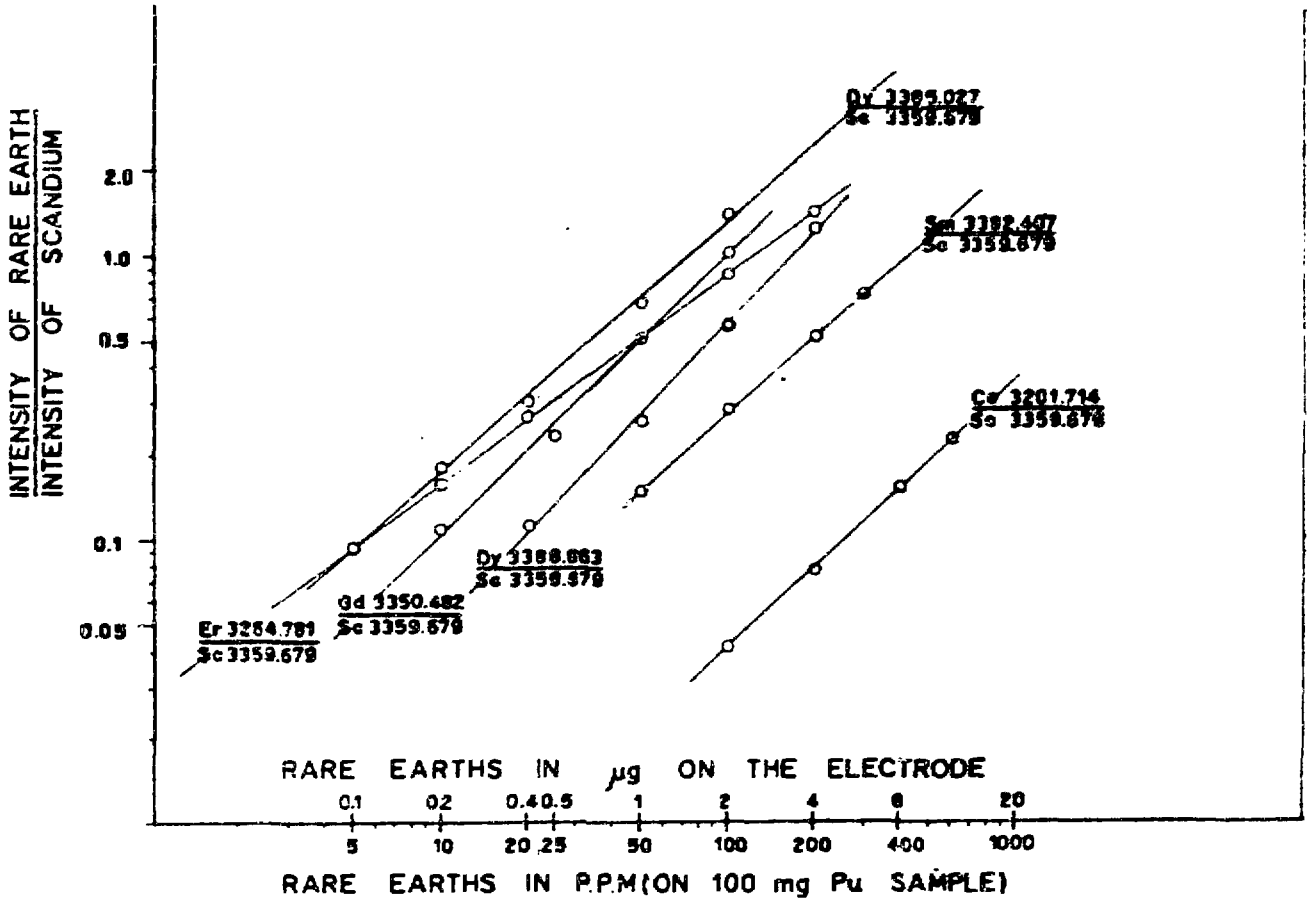
INTENSITY OF RARE EARTH
INTENSITY OF SCANDIUM
2.0
1.0
0.5
0.1
0.05
Dy 3393.027
Sc 3359.679
Sm 3392.447
Sc 3359.679
Ce 3201.714
Sc 3359.679
Dy 3388.863
Sc 3359.679
Gd 3350.482
Sc 3359.679
Er 3264.781
Sc 3359.679
RARE EARTHS IN μg ON THE ELECTRODE
0.1
0.2
0.4
0.5
1
2
4
8
20
5
10
20
25
50
100
200
400
1000
RARE EARTHS IN P.P.M (ON 100 mg Pu SAMPLE)

FIG. 1

STUDIES IN RARE EARTH COMPLEXES OF SOME SUBSTITUTED SALICYLIC ACIDS

D. V. Jahagirdar and D. D. Khanolkar
Department of Chemistry, Marathwada University, Aurangabad

A potentiometric study of formation of lanthanide complexes of salicylic and sulphosalicylic acids is reported in the literature[1]. However, a systematic study of rare earths complexes with various substituted salicylic acids is still lacking. This paper aims at such a study by the Calvin-Bjerrum titration technique with a view to understanding some structural aspects of these complexes.

EXPERIMENTAL

Chemicals: All the chemicals such as sodium hydroxide, sodium perchlorate and perchloric acid were of analytical reagent grade.

Chelating agents: 3-bromo, 3:5-dibromo, 4-hydroxy, 3-nitro, 5-nitro, and 3:5-dinitro salicylic acids (AnalaR grade) were obtained from B. D. H. (India). All the substituted acids were recrystallised and their purity was checked before their use in potentiometric measurements. Rare earths nitrates (AnalaR) obtained from the Bhabha Atomic Research Centre, Bombay, were used for potentiometric study.

All the solutions were prepared in double distilled water.

pH meter: Beckman model H-2 pH meter was used for the measurement of pH. The accuracy of the pH meter is of $\pm$ 0.02 pH unit. It was calibrated by buffer solutions at pH 4.0 and 9.0.

Calvin-Bjerrum Titration: The experimental procedure involved potentiometric titrations of solutions of (i) free $HClO_4$ (3.67×10^{-3} M), (ii) free $HClO_4$ (3.67×10^{-3}M) + reagent (1.0×10^{-3} M), (iii) free $HClO_4$ (3.67×10^{-3} M) + reagent (1.0×10^{-3} M) + rare earths ion (2.0×10^{-4} M) and (iv) free $HClO_4$ (3.67×10^{-3}M) + rare earths ion (2.0×10^{-4} M), against standard sodium hydroxide (0.2 N) added from a microburette. The ionic strength of the solutions was maintained constant at 0.1 M by the addition of 1 M sodium perchlorate solution. The titrations were carried out in an inert atmosphere by bubbling O_2 free nitrogen gas through an assembly containing the electrodes in order to prevent atmospheric oxidation.

Maintenance of temperature at 31°C: The titration vessel of 100 ml capacity was dipped more than two thirds, in water contained in a 4 litre glass beaker. Water at a fixed temperature pumped from ultra-thermostat manufactured by VEB Prufgerate-Werk Medingen/Dresden (Germany), was continuously circulated through the metallic coils immersed in the beaker. The accuracy of temperature regulation was ± 0.02°C.

RESULTS

For all the systems, the deviation of the metal complex titration curve from the reagent curve was observed around pH 4.5. The pH of hydrolysis found from the deviation of metal titration curve from that of acid curve for all the rare earths ions was around pH 7.0 which indicated complex formation in solution.

Values of $\bar{n}_A$ (proton-ligand formation number), and $\bar{n}$ (metal-ligand formation number)were calculated by using the Irving and Rossotti expression[2]. $\bar{n}$ values were calculated upto the pH of precipitation of rear earths ions as observed in metal complex titrations. The highest value of $\bar{n}$ is 1.7. This showed the formation of 1:1 and 1:2 complexes. 3:5-dinitro salicylic acid, however, does not show the formation of a 1:2 complex.

Values of pL = -log [L], where [L] is free ligand concentration, were calculated are various $\bar{n}$ values by employing Irving and Rossotti's expression[2]. Approximate values of log K_1 and log K_2 were obtained by half integral method. The accurate values of log K_1 and log K_2 (Table I) were then calculated by pointwise calculations. In some cases the method of least squares was adopted to determine log K_1 and log K_2 values. The calculated values by this method are given in brackets. It can be seen that the values of log K_1 and log K_2 obtained by the two methods are in good agreement.

DISCUSSION

In the rare earths metal ions the 4f orbitals are effectivyely from interaction with ligand orbitals by electrons in the 5s and 5p orbitals. If hybridisation is to occur, it must involve normally unoccupied higher energy orbitals (e.g. 5d, 6s, 6p) and is expected with the most strongly coordinating ligands. Rare earths, therefore, ordinarily form ionic compounds which should obey the following relationship given by Born for the energy change on complexation of a gaseous ion of charge 'e' and radius 'r' in a medium of dilectric constant D.

$$E = \frac{e^2}{2r} \left(1 - \frac{1}{D}\right)$$

Since the stability constant is related directly to this energy, one expects that the log K values should increase linearly with $\frac{e^2}{r}$. Moeller et al[1] have observed, in general, a regular increase in stability with an increase in atomic number or a decrease in crystal radius from lanthanum to europium and a discontinuity at gadolinium (the gadolinium break).

The plots of log K_1, log K_2 and log K_1K_2 against $\frac{e^2}{r}$ were approximately linear in nature. Values of crystal radii of rare earths ions have been taken from Cotton[3]. The observed gadolinium break in all systems may be related to discontinuity in the crystal radii of rare earths at gadolinium. The decrease in log K_1, log K_2 and log K_1K_2 for complexes of rare earths beyond gadolinium probably arises because of the fact that the progressively smaller radii impose an increasingly greater steric hindrance on the ligands on account of the metal-ligand interaction. This effect should become more pronounced for 1:2 complexes because of formation of two chelate rings. This is borne out by the more pronounced maxima observed in the log K_1K_2 plot than that for the log K_1 plot.

VALIDITY OF LOG K = a pk + b RELATION

The relation, log K = a pk + b first given by Bjerrum[4] has been found to hold for transition metal complexes of a series of closely related ligands by many workers[5-9]. The authors have obtained a linear relation for 1:1 and 1:2 complexes of rare earths. The values of slope 'a' are given below:

	1:1 complex,	1:2 complex
Ce(III)	0.80	0.88
Pr(III)	0.80	0.88
Nd(III)	0.80	0.90
Sm(III)	0.84	1.00
Gd(III)	0.80	1.00
Dy(III)	0.81	1.00

Jones et al[5] suggest on the basis of a purely statistical model that the slope will increase with increasing cationic charge and decreasing distance of separation (equal to the radius of the cation plus a constant). The slope for 1:1 complexes of rare earths was less than that for the corresponding transition metal complexes (the slope values observed by the authors for Cu(II), Ni(II), Co(II), and Zn(II) complexes are, 0.85, 0.95, 1.00 and 1.00 respectively). Though the higher charge on rare earth cations is expected to give a higher value for the slope, the observed lower

value may be explained as due to the higher values of cationic radii of rare earths. The cation-ligand distance is also expected to be greater for the rare earths complexes because of their greater ionic nature.

REFERENCES

1. T. Moeller, D. Martin, L. C. Thompson, G. Friesel and W. J. Randall; Chem. Rev. 65, 22 (1965)

2. Irving and Rossotti; J. Chem. Soc. 2904 (1954)

3. F. A. Cotton; Advanced Inorganic Chemistry, Interscience publishers (1967) p. 1052

4. J. Bjerrum; Chem. Rev. 46, 381 (1950)

5. Jones, Tomkinson, Poole and Williams; J. Chem. Soc. 2001 (1958)

6. D. D. Perrin; Ibid 3125 (1958)

7. M. Calvin and K. Wilson; J. Am. Chem. Soc, 67, 2003 (1945)

8. R. J. Bruehhman and F. H. Verboek; Ibid 70, 1401 (1948)

9. L. G. Van Uitert, W. C. Fernelius and B. E. Douglas; Ibid 75, 457, 2763, 3862 (1953)

TABLE I

Stability Constants of Rare Earth Complexes

	3-brome S.A.		3:5-dibromo S.A.		4-hydroxy S.A.		3-nitro S.A.		5-nitro S.A.		3:5-dinitro S.A.
	log K_1	log K_2	log K_1	log K_2	log K_1	log K_2	log K_1	log K_2	log K_1	log K_2	log K_1
Ce(III)	6.59	5.60	6.65	5.72	5.77	4.26	7.07	5.82	6.64	5.44	4.05
	(6.62)	(5.54)	(6.54)	(5.95)	(5.63)	(4.29)					
Pr(III)	6.46	5.50	6.82	5.82	5.91	4.36	6.80	5.79	6.91	5.50	4.29
	(6.53)	(5.54)	(6.92)	(5.81)	(5.83)	(4.47)					
Nd(III)	6.56	5.58	6.90	5.68	5.67	4.45	6.76	5.92	6.81	5.82	4.44
	(6.62)	(5.54)	(6.93)	(5.70)	(5.69)	(4.69)					
Sm(III)	6.85	5.84	6.91	5.85	6.20	4.69	6.92	5.99	6.92	5.77	4.42
	(6.85)	(5.85)	(6.88)	(5.87)	(6.10)	(4.61)					
Gd(III)	7.36	6.24	7.17	5.97	6.14	4.67	6.88	6.01	6.92	6.01	4.57
	(7.28)	(6.11)	(7.15)	(6.12)	(6.16)	(4.63)					
Dy(III)	7.27	6.01	7.33	6.00	6.10	4.55	7.08	6.07	6.85	5.88	4.54
	(7.23)	(6.10)	(7.15)	(5.98)	(6.10)	(4.59)					

DIPHENYL SULPHOXIDE COMPLEXES OF URANYL AND THORIUM NITRATES

S. K. Ramalingam
Department of Chemistry
Madurai University, Madurai, Tamil Nadu.

INTRODUCTION

Diphenyl sulphoxide complexes of many transition metal salts and of lanthanide perchlorates have been reported[1,2]. DPSO complexes of uranyl and thorium salts are of particular interest in that, the metal ions show better coordinating abilities than the lanthanides and also exhibit large variations in their coordination numbers. The nitrate salts were chosen since these anions have the capacity to bind to metal ions not only as monodentate groups but as bidentate as well, thereby enhancing the coordination number of the metal ion.

PREPARATION OF THE COMPLEXES

A solution of 1 gm. of the hydrated metal nitrate in 5 ml. of methanol was added dropwise to a solution of about 1.2 gm of DPSO in 10 ml of methanol. The solution was stirred well and allowed to crystallise under cold dry conditions. The crystals were filtered, washed with dry benzene and dried in vacuum. The details of analytical techniques employed are given in an earlier work[2].

DISCUSSION

Analytical results show that the complexes have the formulae $UO_2(NO_3)_2.2DPSO$ and $Th(NO_3)_4.3DPSO$. The low molar conductance values for the two complexes in nitrobenzene and acetonitrile which are solvents of poor donors suggest that the complexes have non-electrolytic structures. This means that the nitrato groups are covalently bound to the metal ions and there is no free nitrate ion. The infra-red spectra support these observations. In the spectra of the complexes there are no intense bands in the regions 1350-1390 or 1040-1060 cm^{-1} attributable to vibrations of ionic nitrate[3]. On the otherhand, the strong absorptions occurring at 1527 and 1277 cm^{-1} for the uranyl complex and at 1506 and 1302 cm^{-1} for the thorium complex can be atrributed to the ν_1 and ν_4 vibrations of the covalent nitrate group[4]. If the $\nu_1 - \nu_4$ difference can be taken as an approximate measure of the covalency of the nitrate bonding[4], then in the present cases, values of 250 and 204 cm^{-1} for the

uranyl and thorium complexes suggest strong covalence for the metal nitrate bonding.

A remarkable feature of the I.R.spectra of the complexes is the considerable shift of the S-O stretching frequency towards the lower frequency side. (from 1043 in free ligand to 966 and 971 cm^{-1} in complexes). This clearly indicates that it is the oxygen atom and not sulphur atom of the ligand that is involved in the bonding[2].

The occurrence of asymmetrical stretching vibration (ν_3) of UO_2^{2+} at 925 cm^{-1} as compared to the same vibration occurring above 945 cm^{-1} for the free uranyl ion suggest that the ligand groups presumably lie in a plane nearly perpendicular to the axial O-U-O direction[5, 6]. Also, the absence of a bond around 775 cm^{-1} (sym. stretch of the UO_2 group) indicates the linearity of the O-U-O bond.

Molecular weight data of the complexes in nitrobenzene show them to be monomeric (cf. Table). The possible structure of the complexes assignable from the foregoing arguments will be $UO_2(NO_3)_2 . 2DPSO$ and $Th(NO_3)_4 . 3DPSO$. The coordination number of U and Th would then be 8 and 7 respectively.

The conductivity data in the solvent DMF, however, suggest a 1:1 structure for the U complex and a 1:2 structure for the Th complex (Ref. Table). This means that in the former case, of the two nitrato groups only one is displaceable from the coordination sphere and in the latter, of the four NO_3 groups only two are displaceable. DMF being a monodentate ligand, it can be presumed that the displaced NO_3 groups are monodentate while the undisplaced NO_3 groups are probably bidentate. The coordination number for the U and Th ions would now become 9. From detailed X-ray studies on dioxodinitrobis (triphenylphosphineoxide) uranium (vi)[7] and on $Th_2(OH)_2 (NO_3)_6(H_2O)_8$, it has been clearly shown that the nitrato groups are coordinated to the metal in a bidentate manner in these complexes. It is, however, difficult to find further evidence for bidentate nitrato group from IR spectra on account of their extreme complexity.

Molecular weight studies in the solvent DMSO show that the complexes dissociate almost completely suggesting that DMSO is a better donor than DPSO in respect of the uranium and Thorium metal ions (cf. Table). But the partial charges on oxygen atom of DMSO and DPSO (δ_o) calculated by the method of Sanderson[9] (using stability ratios of atoms) suggest that the two ligands have comparable basicity (δ_o in DMSO is -0.2975 and in DPSO is -0.3073). The experimentally observed lower ligating strength of DPSO must, therefore, be attributed to the resonance interaction of the phenyl rings with S = O bond with a consequent reduction in the electron

availability at the coordination site and also to the steric effect arising out of the greater bulk of the phenyl group compared to the methyl group in DMSO.

ACKNOWLEDGEMENT

The author thanks the Madurai University for the facilities provided and Prof. S. Neelakantan for kind encouragement.

REFERENCES

1. P. W. N. M. Van Leeuwen and W. L. Groeneveld; Recueil 85, 1173 (1966)

2. S. K. Ramalingam and S. Soundararajan; Bull. Chem. Soc. Japan 41, 106 (1968)

3. B. M. Gatehouse, S. E. Livingstone and R. S. Nyholm; J. Chem. Soc. 4222 (1957)

4. C. C. Addison and N. Logan; Advances in Inorganic and Radiochemistry, Vol. 6, Academic Press, London (1964) p. 102

5. A. E. Comyns, B. M. Gatehouse and E. Wait; J. Chem. Soc. 4655 (1958)

6. S. P. Mc. Glynn, J. K. Smith and N. C. Neely; J. Chem. Phys. 35, 105 (1961)

7. C. Panattoni, R. Graziani, U. Groatto, B. Zarli and G. Bomieri; Inorg. Chem. Acta. 1968, 2(1), 43-8 cf CA 69, 22904 Z (1968)

8. G. Johansson; Acta. Chem. Scan. 22, 389 (1968)

9. R. T. Sanderson; Chem. Periodicity' East West Press.

TABLE

Physical, Analytical, Cryoscopic and Conductance Data.

Complex	Colour	M. P. °C	% Metal		% Nitrate		Molar conductance λ_m Ohm^{-1} cm^{-2} $mole^{-1}$			Mol. Wt.		
			Expt.	Calcd.	Expt.	Calcd.	Nitro benzene	Aceto nitrile	DMF	In DMSO	In Nitro benzene	Cald. for monomeric structure
$UO_2(NO_3)_2.2DPSO$	Yellow	152	29.85	29.84	15.17	15.55	3.89	10.65	105.6	175	726	798
$Th(NO_3)_4.3DPSO$	White	175-178	21.77	21.36	22.21	22.84	7.31	23.60	170.5	134	992	1086